The role of neutrophil-derived microvesicles in lung inflammation

Merete Bridget Long

A thesis submitted in partial fulfilment of the requirements for the degree of Doctor of Philosophy

Department of Infection, Immunity and Cardiovascular Disease

School of Medicine

The University of Sheffield

September 2020

Acknowledgements

I would like to express my sincere gratitude to my PhD supervisors, Dr Victoria Ridger and Prof. Alison Condliffe for taking a chance on me and appointing me into this project, and for invaluable guidance over the last years which has shaped me into a Scientist and Academic. In particular, thank you for your support over the past year whilst I've been writing up, your encouragement during this time has been more than appreciated.

Thank you to the collaborators involved in this project, to Dr Helen Marriott, Carl Wright and Jessica Willis for your help with *in vivo* studies, and to Jacob Rudman for the coolest experiments in this thesis and the crazy hours this required. Thank you to Dr Katharine Lodge at Cambridge and Prof. Allan Lawrie in Sheffield for allowing me to work with patient samples and discover the relevance of the work done here, and to Prof. Paul Evans and the group for the helpful lab meetings and feedback which improved this project and my presentation skills. To the MSc and MRes students I had the privilege of working with and who contributed to data in this thesis, I wish you so much success ahead in your very bright futures. Further, thank you to my new lab group in Dundee who have been endlessly supportive whilst I have been writing this thesis.

To everyone in Sheffield in O-, M- and L-floor student offices from the Ridger, Evans, Wilson, Kiss-Toth, Francis, Condliffe, Parker and Fenner groups, you brought sunshine to our windowless rooms, thank you for lending expertise, time and reagents to help me, not to mention the many blood donations that made this project possible. Blanca, Celine and Lindsay, thank you for answering my (many) questions with a smile. Anjana, Daniela and Chiara, thank you for your shared love of caffeine and Falafel King, you've been there at every step, in the early mornings and late nights in the lab, and all the parts in between.

Importantly, thank you to my family, who have always been my rock and an unwavering source of encouragement. I hope that I've made you as proud as you make me. To my friends, old and new, thank you for helping me to do something that didn't involve pipetting. Finally, thank you to my partner, Mircea, for spending weekends in the lab alongside me instead of doing something normal and healthy, and despite working in software development; you've heard much more about microvesicles than I'm sure you would have liked, and I definitely couldn't have done this without you.

Thesis summary

During the pathogenesis of chronic obstructive pulmonary disease (COPD) and in subsequent exacerbations, neutrophilic inflammation predominates and contributes to disease progression. Levels of neutrophil-derived microvesicles (NMVs; small extracellular vesicles formed from membrane blebbing in resting and activated cells) have previously been shown to be elevated in COPD patient sputum and in the circulation during inflammation. Evidence of the pro-inflammatory activity of NMVs in several cell types, along with an ability to increase epithelial monolayer permeability, led to the hypothesis that NMVs are released upon neutrophil activation in the circulation and the inflamed airway environment and are subsequently internalised by lung epithelial cells, inducing their pro-inflammatory activation and dysfunction.

The overall aim of my PhD was to investigate the role of NMVs in lung inflammation. This was firstly done by characterising circulating MVs in COPD patients as both potential disease biomarkers and as mediators of inflammation using stored plasma samples from two COPD patient cohorts. Subsequently, it was crucial to isolate human neutrophils from the peripheral blood of healthy volunteers so as to generate, isolate and characterise a pure population of NMVs from these cells and to investigate the functional effects of these vesicles using the bronchial epithelial cell line BEAS-2B. Finally, to further understand the biological relevance of NMV effects in the lung, C57BL/6 mice were utilised in a series of experiments to explore lung inflammation and NMV fate.

Key findings:

1. Plasma MV matrix metalloproteinase-9 (MMP-9) content is significantly increased in COPD patients compared with age-matched controls, however, numbers of circulating leukocyte-derived MVs are not differential between these groups.

2. NMVs from fMLP-stimulated healthy participant neutrophils contain active MMP-9 and can degrade extracellular matrix proteins, but activated and quiescent neutrophils do not produce differential NMV numbers.

3. NMVs are rapidly taken up by bronchial epithelial cells, likely via an endocytic mechanism, with functional effects of NMVs on epithelial activation, barrier integrity and proliferation.

4. *In vivo* in mice, airway administration of NMVs does not induce or augment lung inflammation, instead, mass uptake and clearance of these NMVs by alveolar macrophages occurs.

In this thesis I have shown that MV-associated protein content is altered in COPD, and investigation of these differences will be important going forward in defining the role of NMVs in chronic lung diseases. Degradation of extracellular matrix shown here and epithelial cell activation and permeability induced by NMVs when applied directly to these cells define key pathological events in COPD and indicate a role of these vesicles in epithelial dysfunction. In contrast, NMV uptake by alveolar macrophages was identified as a mechanism of NMV clearance in healthy lung tissue. Together, these findings provide novel insight into neutrophil interactions and activity in the lungs. This work contributed to our understanding of the processes occurring in inflammation and identified several valuable avenues for future investigation to understand more about complex conditions like COPD.

Awards and prizes:

- UK Cell Adhesion Society (UKCAS) conference 2019 *Birmingham, UK* **Runner-up poster award** and **Travel award**
- ERS Lung Science Conference 2019, *Estoril, Portugal* **Travel award**
- UKCAS 2018 conference *London, UK* **Runner-up poster award** and **Travel award**
- British Association for Lung Research (BALR) summer meeting 2018, *Birmingham, UK* **Commended poster** (public vote), **Commended abstract** and **Travel award**
- The Learned Society funding for travel (2017, 2018, 2019)

Contents

List of figures

List of tables

Abbreviations

ACOS	Asthma-COPD overlap syndrome
ARDS	Acute respiratory distress syndrome
BALF	Bronchoalveolar lavage fluid
BSA	Bovine serum albumin
Cat G	Cathepsin G
COPD	Chronic obstructive pulmonary disease
CSE	Cigarette smoke extract
DAMP	Damage associated molecular pattern
DMSO	Dimethyl sulfoxide
ECM	Extracellular matrix
ER	Endoplasmic reticulum
EV	Extracellular vesicle
F.O.V	Field of View
FCS	Foetal calf serum
FEV1	Forced expiratory volume in 1 second
fMLP	N-Formyl methionine-leucyl-phenylalanine
FMO	Fluorescence minus one
FPR1	Formylated peptide receptor 1
GAPDH	Glyceraldehyde 3-phosphate dehydrogenase
GOLD	Global Initiative for Chronic Obstructive Lung Disease
HR	Hazard ratio
ICAM-1	Intracellular adhesion molecule-1
IL-1, -6, -8	Interleukin-1 beta, -6, -8
LPS	Lipopolysaccharide
LTB4	Leukotriene B4
MCP-1	Monocyte chemotactic protein-1
miR	microRNA
MMP	Matrix metalloproteinase
MPO	Myeloperoxidase
MV	Microvesicle
NADPH	Nicotinamide adenine dinucleotide phosphate

NE	Neutrophil elastase
NFκB	Nuclear factor kappa-B
NMVs	Neutrophil-derived microvesicles
PAMP	Pathogen associated molecular pattern
PBS	Phosphate buffered saline
PCLS	Precision cut lung slices
PFA	Paraformaldehyde
PH	Pulmonary hypertension
PR3	Proteinase C
PS	Phosphatidyl serine
qPCR	Quantitative polymerase chain reaction
ROS	Reactive oxygen species
SI	Separation index
TGF-β	Tumour growth factor beta
TIMP-1	Tissue inhibitor of metalloproteinase-1
TLR	Toll-like receptor
TNF-α	Tumour necrosis factor- alpha
WGA	Wheat germ agglutinin
ZO-1	Zonula occludens-1

<h1 style="text-align:center">Chapter 1: Introduction</h1>

1.1 Chronic Obstructive Pulmonary Disease

1.1.1 Pathogenesis and Pathology

COPD is a debilitating, increasingly common condition characterised by progressive airflow limitation and remodelling of the airways due to a chronic inflammatory response to inhaled noxious particles and gases from sources including cigarette smoke (Vestbo *et al.*, 2013) and biomass fuels (Liu *et al.*, 2007; Zhou *et al.*, 2014). In the UK alone, an estimated 1.2 million people have been diagnosed with COPD, affecting ~2% of the UK population (BLF, 2016). Worldwide, this number stands at 251 million cases (WHO, 2017). The world health organisation previously predicted COPD to be the third leading cause of death globally by 2030 ((WHO), 2008), however this estimate was later reduced to as soon as 2020 (WHO, 2017). Whilst the Global Initiative for Chronic Obstructive Lung Disease (GOLD) defines COPD as a preventable and treatable disease, a rising incidence and current lack of effective treatment able to halt disease progression make COPD a severe problem.

COPD has been described as a complex condition owing to its heterogeneity in both causal exposures and symptomatic and clinical presentations (Mullerova *et al.*, 2012; Vestbo *et al.*, 2008; Agusti *et al.*, 2010). In a small percentage of COPD patients, disease development is markedly accelerated due to severe deficiency of the omnivorous anti-protease α-1 anti-trypsin (Laurell and Eriksson, 2013), a condition associated with mutations in the SERPINA1 gene (Zorzetto *et al.*, 2008). The severe and rapidly progressive disease associated with the deficiency of this anti-protease supports the damaging role of proteases in the lung, emphasising the importance of neutrophils—a major source of proteases—in disease development.

The main pathological processes in COPD airways, illustrated in figure 1.1, include goblet cell hyperplasia (Reid, 1960) and mucus hypersecretion (Kurie *et al.*, 1996; Takeyama *et al.*, 2001), plus thickening of the airway walls—particularly the terminal bronchioles—due to inflammation and fibrosis, resulting in increased resistance and bronchoconstriction (i.e. chronic bronchitis) (Mullen *et al.*, 1985; Yanai *et al.*, 1992; Gelb *et al.*, 1981). Additionally, alveolar cell apoptosis (Tuder *et al.*, 2003) and destruction of the alveolar capillary beds (Kasahara *et al.*, 2001) and lung parenchyma result in reduced numbers of enlarged alveoli with reduced surface available for gas exchange (i.e. emphysema) and subsequent hypoxia (Sharafkhaneh *et al.*, 2008). These events lead to the symptomatic presentations of COPD like shortness of breath (Elbehairy *et al.*, 2015), wheezing and chronic cough with sputum production (Voynow and Rubin, 2009; Theander *et al.*, 2014).
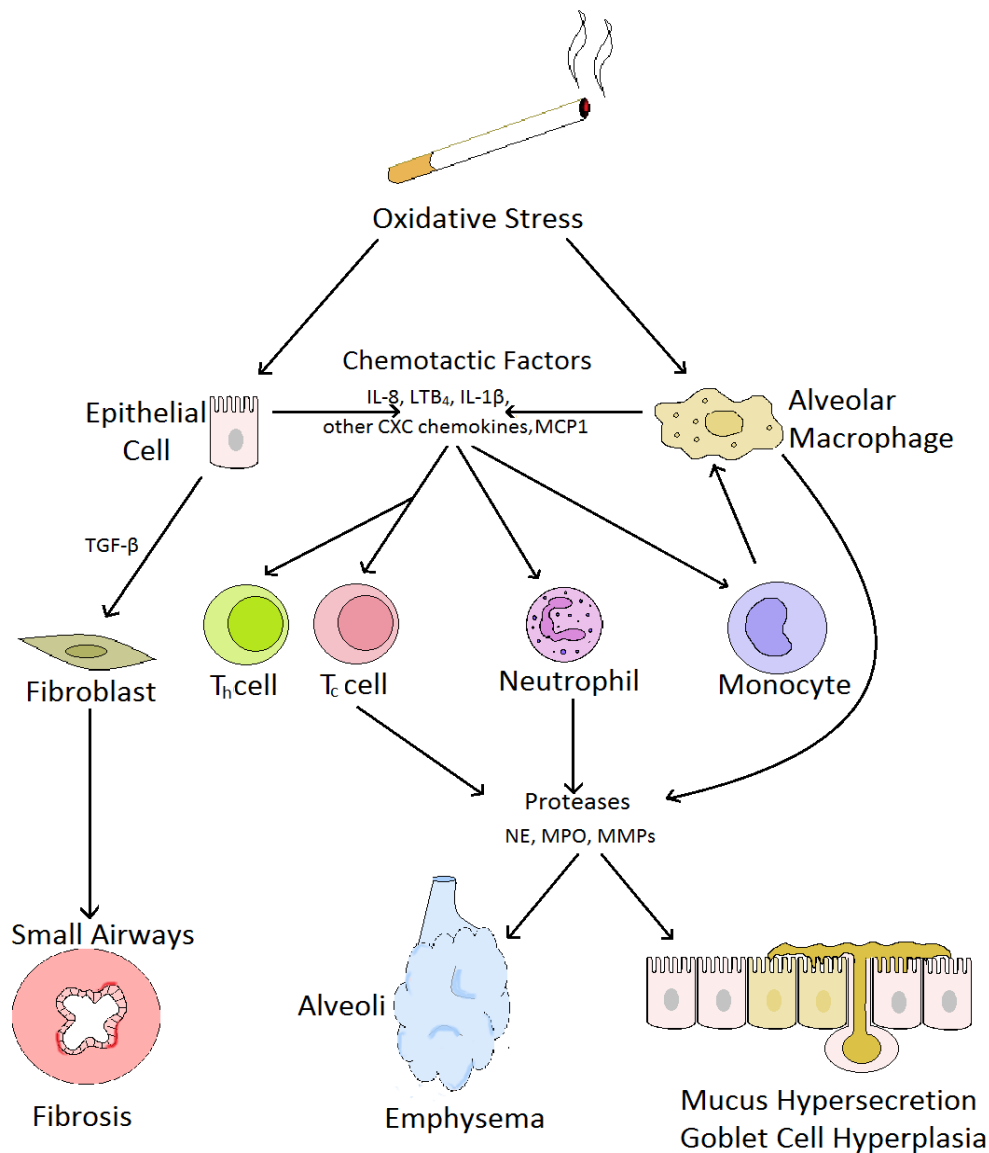
Figure 1.1. Pathogenesis of Chronic Obstructive Pulmonary Disease

Oxidative stress via inhalation of oxidative toxins from sources like cigarette smoke and biomass fuels activate airway epithelial cells and alveolar macrophages to begin producing chemoattractants to recruit T-cells, neutrophils, and monocytes to the site of injury. These cells in turn are activated to release proteases which cause alveolar damage, upregulate mucin production and induce epithelial cell apoptosis along with goblet cell hyperplasia. Activated epithelial cells also secrete tumour growth factor-β (TGF-β) which stimulates fibroblast proliferation and results in fibrosis in the small airways. (Adapted from Barnes et al. (2008))

Abbreviations: IL-8, interleukin-8; LTB_4, leukotriene B4; MCP1, monocyte chemotactic protein 1; NE, neutrophil elastase; MPO, myeloperoxidase; MMPs, matrix metalloproteases.

A characteristic inflammatory cell profile has also been defined in COPD, whereby increased numbers of macrophages, CD4^{+} and CD8^{+} T-cells (Saetta *et al.*, 2000; Saetta *et al.*, 1998) and B cells are found in the airways, along with increasing numbers of neutrophils with increasing disease severity (Hogg *et al.*, 2004). These cells contribute to disease pathogenesis and progression through their activity, particularly through release of pro-inflammatory mediators, as summarised in figure 1.1., and further involvement of neutrophils in particular is discussed later in section 1.2.

1.1.2 Common Comorbidities

Often as a consequence of the systemic inflammation present in COPD, discussed in more detail in section 1.1.3, up to 96% of patients exhibit at least one comorbidity (Schnell *et al.*, 2012), which can make their treatment and disease course more complex (Decramer *et al.*, 2008). Some of the most common of these linked conditions are shown in figure 1.2, along with their hazard ratio (HR) for mortality. The major categories of these diseases include other respiratory diseases (Divo *et al.*, 2012), cardiovascular disease (de Lucas-Ramos *et al.*, 2012)—including pulmonary hypertension (in italics in fig 1.2) which is a subject of experimental investigation in this thesis (chapter 3)—gastrointestinal and liver disease (Tsiligianni *et al.*, 2013) and metabolic syndrome (Marquis *et al.*, 2005). Highlighting the importance of considering these conditions, the leading cause of death in COPD patients is cardiovascular disease, and cardiovascular conditions have been strongly linked to lung function in COPD (Young *et al.*, 2007). Whilst controversial, so-called 'overlap syndromes' of multiple respiratory diseases, particularly asthma–COPD overlap syndrome (ACOS) are also the subject of increasing research to understand the course, impact and treatment for this combination (Barrecheguren *et al.*, 2015).

Not included in this summary but also of high importance is development of anxiety and depression, with occurrence in approximately 10–19% and 24.6% of COPD patients, respectively, and with a HR for mortality of surprisingly 13.76; these conditions are linked to physiological parameters such as exacerbation frequency, which is likely a causative factor along with disease symptoms for these psychological effects (Cleutjens *et al.*, 2014; Negewo *et al.*, 2015; Divo *et al.*, 2012). Estimates of incidence of all of these comorbidities in COPD can be highly variable, likely due to factors including patient cohort and location, method of detection and clinical definitions and classifications of diseases, nevertheless the consistent appearance of these co-morbid conditions indicates an important link with the disease.
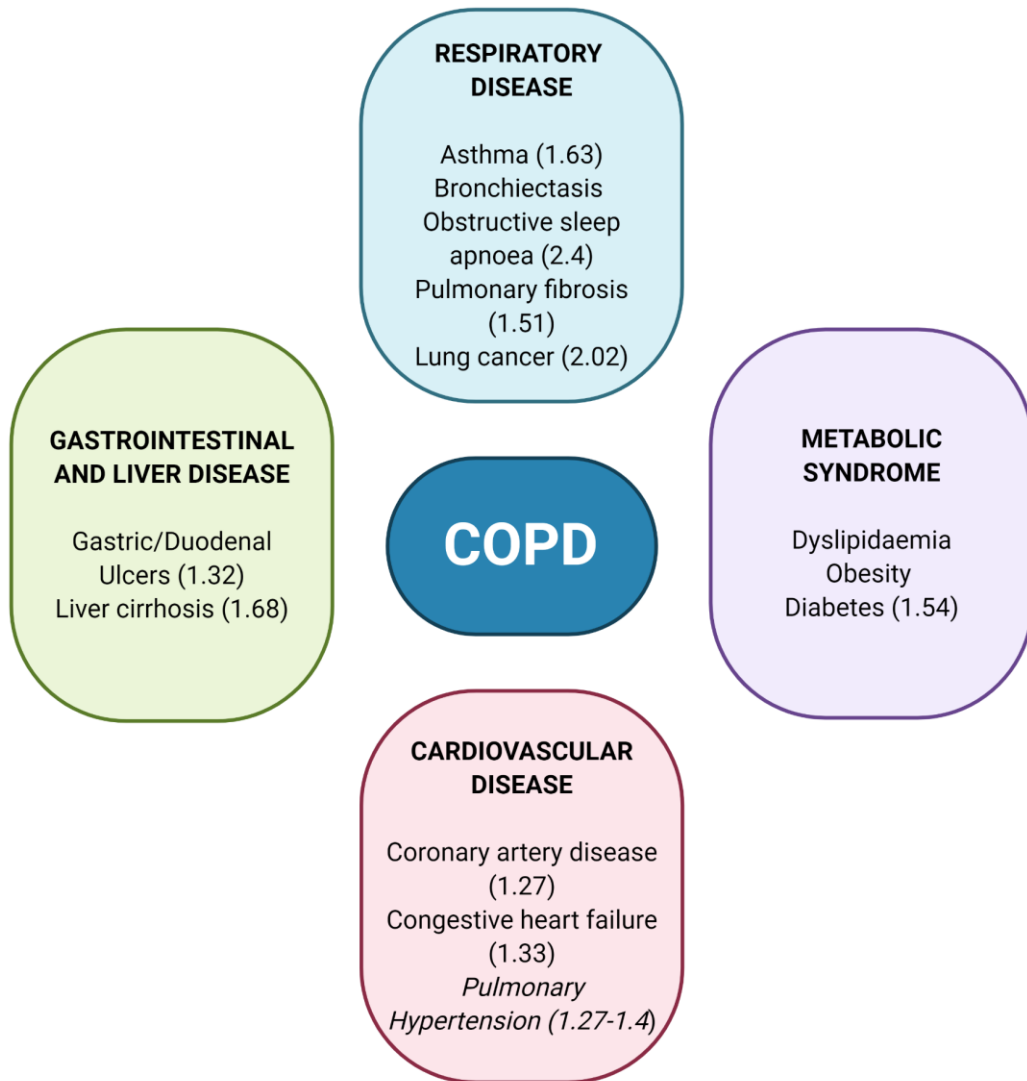
Figure 1.2. Common Comorbidities in Chronic Obstructive Pulmonary Disease

Hazard ratios for mortality taken from Smith and Wrobel (2014), Du et al. (2018), and Divo et al. (2012)

Current GOLD guidelines for COPD treatment—compiled under the guidance of world-leading experts on COPD and designed to improve treatment strategies and outcomes worldwide, as well as highlighting key research areas—include smoking cessation, influenza and pneumococcal vaccination, pulmonary rehabilitation, and a host of pharmacological therapies including bronchodilators, antimuscarinics, antibiotics and glucocorticoids. However, despite the effects of the linked conditions listed above, the GOLD guidelines state that in general, these conditions should not alter the treatment provided for COPD (GOLD, 2018), whilst others make no mention of comorbidities (Neumeier and Keith, 2020). These comorbidities can contribute to patient quality of life (Cecere *et al.*, 2011; Zeki *et al.*, 2011; Rascon-Aguilar *et al.*, 2011), and also treatment costs (Decramer *et al.*, 2008), and it is therefore imperative that these aspects are considered in not only clinical care but also in research focused on this disease.

1.1.3 Systemic Inflammation

COPD is a disease with heterogeneous presentations, made evident by the presence of a diverse range of comorbidities, as described above, and it is increasingly recognised as a systemic disease affecting multiple organs and biological systems. Systemic inflammation in COPD has been well documented, so much so that in their Lancet viewpoint paper, Fabbri and Rabe (2007) proposed the inclusion of chronic systemic inflammatory syndrome to the diagnostic criteria for COPD. Agusti et al. (2012) showed that up to 70% of COPD patients recruited to the large ECLIPSE study had detectable markers of systemic inflammation, and persistence of this inflammatory signal was significantly correlated with poor outcomes. Although this is a recognised element of COPD pathology described in the 2018 GOLD guide for healthcare professionals (GOLD, 2018), more than 10 years after their proposal this feature has not been incorporated into disease diagnosis.

Increased levels of inflammatory cytokines (e.g. TNF-α, IL-1β (Selvarajah *et al.*, 2016), IL-8 (Schols *et al.*, 1996) and IL-6 (Bhowmik *et al.*, 2000a)), leukocyte numbers (Gan *et al.*, 2004) and also systemic oxidative stress (Rahman *et al.*, 1996) have been described and evidenced in COPD. As discussed in chapter 3, increased circulating neutrophil counts in particular have been reported by some authors (Gunay *et al.*, 2014). These processes are associated with COPD comorbidities including cardiovascular disease (Yende *et al.*, 2006) and muscle weakness (Yende *et al.*, 2006) and with disease severity (Selvarajah *et al.*, 2016). Oudijk et al. (2003) speculated that the presence of these systemic cues, particularly elevated cytokine levels, leads to peripheral tissue damage in COPD via induction of aberrant immune cell homing to other sites, as in the case of monocytes in atherosclerotic plaque formation, a cardiovascular comorbidity of COPD, and Lahousse et al. demonstrated that COPD patients with atherosclerosis are more likely to have a vulnerable plaque

(2013). The question of whether such an inflammatory "overspill" effect drives co-morbidity has been postulated by several other authors (Sinden and Stockley, 2010; Barnes, 2016), however the conclusion of these works remains that the evidence to determine a causal link is not yet strong enough to confirm or disprove this hypothesis, and the effects of confounding factors such as cigarette smoking further complicate these investigations (Lowe and Pepys, 2006).

Dysfunctional circulating immune cell activity has been shown in COPD, for example, circulating monocytes exhibit elevated TNF-α expression (de Godoy *et al.*, 1996) and activation marker/adhesion molecule (CD43 and CD11b) expression (Bergmann *et al.*, 1998); it is hypothesised that this leads to greater endothelial activation and monocyte adhesion, contributing to cardiovascular disease development (Sinden and Stockley, 2010). Circulating neutrophils from COPD patients were found to have enhanced ROS generation (Noguera *et al.*, 2001) and to migrate more readily but with lower accuracy in response to chemotactic stimuli; this indirect path during transmigration was postulated to confer greater tissue-destructive potential. These effects were found to be dependent on activation of phosphoinositide 3-kinase (PI3K) signalling, which was increased in COPD and also in aged individuals (Sapey *et al.*, 2011; Burnett *et al.*, 1987; Sapey *et al.*, 2014); raising an important, as yet unanswered question of which event is the initiator: systemic immune cell dysfunction/inflammation or local chronic lung inflammation.

1.1.4 Lung Epithelium in Chronic Obstructive Pulmonary Disease

Epithelial Cell Activation

The potential for epithelial activation to contribute to the pathogenesis and progression of inflammatory lung conditions like COPD was identified almost three decades ago (Cromwell *et al.*, 1992; Devalia and Davies, 1993). Despite this, the processes modulating epithelial cell function in COPD are incompletely understood and have only recently been a subject of in-depth study. The airway epithelium is the first biological barrier to encounter inhaled noxious particles such as those in cigarette smoke, and it is also the first line of defence against infection in the lung (Hiemstra *et al.*, 2015). Increased levels of cytokines which can be associated with epithelial cell activation (e.g. IL-8, TNF-α, IL-6, MCP-1, IL-32) have been shown in sputum and bronchoalveolar lavage (BAL) samples from COPD patients (Kleniewska *et al.*, 2016; Gao *et al.*, 2016; Bhowmik *et al.*, 2000b; Cromwell *et al.*, 1992; Gasiuniene *et al.*, 2016; Traves *et al.*, 2002). These levels are further increased during disease exacerbations (Aaron *et al.*, 2001). More specific epithelial-related proteins detected in COPD patient samples include surfactant protein D, capable of immunomodulatory activity and highly expressed in the distal airways and alveoli (Mori *et al.*, 2002). This protein can be detected in serum samples in COPD and is linked with clinical status (Obeidat *et al.*, 2017), further, deficiency of

surfactant protein D has been shown to result in increased ceramide synthesis upon cigarette smoke exposure, contributing to alveolar cell activation and also death via autophagy and apoptosis (Pilecki *et al.*, 2018).

In further support of the contribution of the epithelium to this inflammatory profile, airway epithelial cells from COPD patients cultured at air–liquid interface have demonstrated increased constitutive cytokine secretion (Comer *et al.*, 2013). However, other authors have shown the reverse effect, with lower levels of cytokine production both at baseline and upon stimulation in COPD airway cells when compared with healthy controls (Patel *et al.*, 2002). One explanation for these differences may be the epithelial cell phenotypes present in harvested samples and the prolonged cell culture methods employed. Overall these *ex vivo* studies suggest permanent and persistent changes in COPD epithelium. Although the utility of these protein levels as biomarkers and their predictive value is debated (Moon *et al.*, 2018), the prevalence of epithelial activation and dysfunction in the disease is clear.

A major consequence of epithelial activation is initiation or perpetuation of an inflammatory response, occurring in part via activation of the mitogen-activated protein kinase (MAPK) and nuclear factor kappa-light-chain-enhancer of activated B cells (NFκB) signalling pathways (Wang *et al.*, 2002b; Fitzgerald *et al.*, 2003). These signals lead to increased pro-inflammatory cytokine production and adhesion molecule expression, immune cell recruitment and activation, and also mucin overproduction which is altered by the NFκB pathway (Fujisawa *et al.*, 2009; Kang *et al.*, 2015). Inhibitors of these pathways or their intermediates have been proposed as therapeutic options in COPD (Shimizu *et al.*, 2012; Newton *et al.*, 2007). However, the diverse role of these signalling cascades in other beneficial processes in both the epithelium and immune cells might suggest a risk of significant adverse effects if such ubiquitous processes are targeted. Other pathways involved in altered epithelial function in COPD include PI3K/protein kinase B (Akt) (Jiang *et al.*, 2018; Noda *et al.*, 2013) and also WNT/β-catenin (Guo *et al.*, 2016; Zou *et al.*, 2013) signalling which induce long term consequences including epithelial-to-mesenchymal transition (EMT), fibrosis and cellular senescence (Houssaini *et al.*, 2018). Indeed, an emerging treatment of increased interest in COPD is senolytic therapy, using drugs which target cellular senescence and ageing (Baker *et al.*, 2020). Additional major triggering events for epithelial activation in COPD, particularly in later disease stages, include recognition of pathogen-associated molecular patterns (PAMPs) via toll-like receptors (TLRs) (Sha *et al.*, 2004), oxidative stress (Dye and Adler, 1994; Rahman and Adcock, 2006) and subsequent responses to the action of resident and recruited immune cells in the lung tissue

(Shao and Nadel, 2005). The contribution of neutrophils to this process is discussed later in this chapter (section 1.2.2) and further investigated experimentally in this thesis (chapter 4).

Epithelial Apoptosis and Barrier Integrity

Cell death describes a myriad of processes which are sub-categorised into mechanisms of programmed cell death such as apoptosis, autophagy and the more recently identified necroptosis, or accidental (e.g. injury-induced) death such as necrosis (Galluzzi *et al.*, 2018). Epithelial apoptosis is investigated experimentally in this thesis (chapter 4), and evidence for increased apoptosis in COPD includes significant detection of apoptotic alveolar epithelial cells in patients with emphysema compared with those in both non-smokers and apparently healthy smokers (Yokohori *et al.*, 2004; Segura-Valdes *et al.*, 2000), along with increased expression of proteins involved in pro-apoptotic signalling pathways such as p53 (Siganaki *et al.*, 2010) and caspase-3 (Imai *et al.*, 2005). Kasahara et al. (2001) also found increased levels of alveolar apoptosis in both epithelial and endothelial cells, along with decreased expression of vascular endothelial growth factor (VEGF). They hypothesised that these events likely contribute to the disappearance and remodelling of alveoli in emphysema. In contrast, other authors found no changes in epithelial apoptosis between patients with emphysema and smoking controls, although apoptosis did correlate with number of cigarettes smoked (Majo *et al.*, 2001). Indeed significant increases detected in other studies are mainly when compared with control groups other than smokers (Imai *et al.*, 2005; Kasahara *et al.*, 2001). It is therefore unclear whether these changes may be mainly due to cigarette smoking or to pathways triggered specifically in COPD. Other inducers of apoptosis include perforin and granzyme B released from infiltrating CD3$^+$ and CD8$^+$ T-cells, which have been shown in greater numbers in the alveolar walls of smokers with emphysema compared with non-smokers and also smokers without emphysema (Segura-Valdez *et al.*, 2000; Majo *et al.*, 2001).

Apoptosis is a homeostatic activity, however, in COPD, clearance of apoptotic cells (efferocytosis) by phagocytic cells particularly alveolar macrophages has also been shown to be defective (Grabiec and Hussell, 2016), resulting in release of damage-associated molecular patterns (DAMPs) from these non-cleared cells, inducing an inflammatory response and promoting alveolar destruction (Vandivier *et al.*, 2006; Gasse *et al.*, 2009; Houghton *et al.*, 2006). Further, these changes can result in increased epithelial permeability due to impaired barrier integrity. In support of this loss of barrier function, changes in epithelial junctional protein expression have been documented in COPD and smoker lung tissue (Heijink *et al.*, 2014; Jones *et al.*, 1980). Cigarette smoking has been shown to activate epidermal growth factor receptor (EGFR) and subsequent ERK signalling and increase ROS and IL-6 production, resulting in deregulation and cleavage of zonula occludens-1 (ZO-1) (Heijink *et al.*, 2012; Petecchia *et al.*, 2009; Olivera *et al.*, 2010). Cigarette smoke was also shown to disrupt E-cadherin

localisation via A-kinase anchoring protein (AKAP)-9 downregulation, (Aghapour *et al.*, 2018). Additionally, ROS-dependent breakdown of epithelial hyaluronan resulted in decreased E-cadherin (Oldenburger *et al.*, 2014; Forteza *et al.*, 2012). Furthermore, *in vitro*, cigarette smoke has been shown to downregulate a multitude of epithelial junctional protein genes including occludin, claudin, junctional adhesion molecule-A (JAM-A) and E-cadherin—which reside in the space between cells, linking them together—and intracellular scaffolding proteins which anchor junctional proteins, such as ZO-1, ultimately leading to increased permeability (Tatsuta *et al.*, 2019). The list of major junctional proteins affected in COPD is illustrated in figure 1.3.

The ultimate consequence of compromised epithelial integrity is increased susceptibility to microbial infection (Soong *et al.*, 2011; Georas and Rezaee, 2014) and dysfunctional cell signalling resulting in inflammation (Heijink *et al.*, 2007), epithelial differentiation and remodelling (Hackett, 2012). The effects of specific neutrophil functions on these phenomena has been investigated experimentally in this thesis (chapter 4).
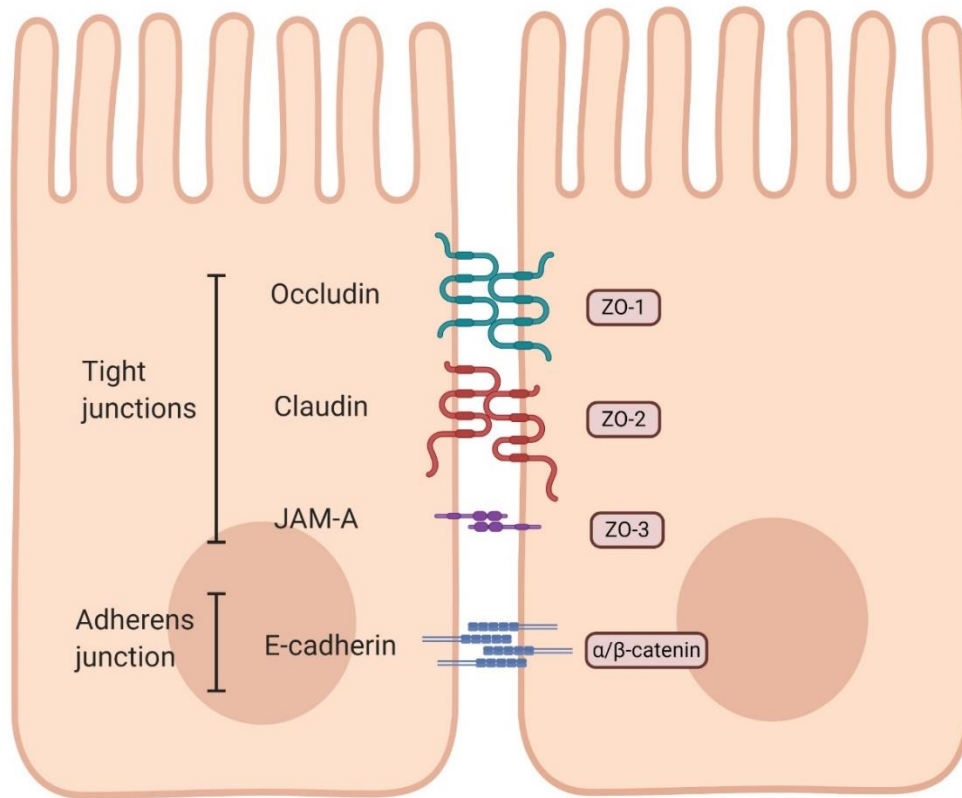
Figure 1.3. Airway epithelial cell junctional proteins

Major junctional proteins shown to be dysregulated in chronic obstructive pulmonary disease are shown (labels on left side). The associated scaffold/anchor proteins linking these to the cytoskeleton are labelled in the right side. Abbreviations; JAM-A: junctional adhesion molecule-A, ZO-: zonula occludens. Adapted from Georas (2014).

1.2 The Neutrophil

Neutrophils, granulocytic leukocytes with a characteristically multi-lobed nucleus, comprise the majority (50–60%) of the circulating white blood cell population. These cells are well-known as first responders to inflammatory signals and microbial invasion (Kruger *et al.*, 2015). In addition to their well-established phagocytic role, cross-talk with and modulation of other immune cells (Silva *et al.*, 1989) along with involvement in tissue damage and potentially also wound healing (Ebaid, 2014; Theilgaard-Monch *et al.*, 2004) has dispelled previous misconceptions that these cells possess only a limited, well-defined role in inflammation. Indeed, even in cell death neutrophils serve an important purpose in the immune response, with apoptotic neutrophil uptake by other immune cells being a method of immunomodulation (Ren *et al.*, 2008), and neutrophil extracellular trap (NET) formation facilitating further antimicrobial action (Brinkmann *et al.*, 2004) but potentially also pathological processes and tissue injury (Toussaint *et al.*, 2017; Wong *et al.*, 2015).

Originating from $CD34^+$ cells in the bone marrow (Kerst *et al.*, 1992), mature neutrophils are deployed into the circulation where they are thought to have a half-life of ~18 h (Lahoz-Beneytez *et al.*, 2016), although both much shorter (Athens *et al.*, 1961) and much longer (Pillay *et al.*, 2010) values have been proposed, reflecting methodological differences. Under normal conditions, there is a homeostatic base level of neutrophils in the circulation (~2–7 × 10^9 cells/L (Hsieh *et al.*, 2007; von Vietinghoff and Ley, 2008). When pro-inflammatory factors are present, including bacterial proteins (Larangeira *et al.*, 2001), DAMPs, cytokines and chemokines (Foxman *et al.*, 1997), neutrophil numbers increase up to 10 times, mainly due to release of the pool of mature or near-mature neutrophils stored in the bone marrow (Furze and Rankin, 2008; Craddock *et al.*, 1960) plus increased granulopoiesis (Cain *et al.*, 2011). Neutrophils are rapidly recruited to sites of inflammation or injury via a chemotactic gradient, where they have diverse, protective roles in the immune response.

Neutrophils have three main functional phenotypes: quiescent, primed and activated. In the circulation of healthy individuals, neutrophils are typically quiescent, being nonmotile with a rounded morphology (Ekpenyong *et al.*, 2015). When a stimulus such as interleukin (IL)-8, tumour necrosis factor (TNF)-α or lipopolysaccharide (LPS) is encountered, neutrophils can become primed and show increased adhesion molecule expression, life span (Murray *et al.*, 1997; Klein *et al.*, 2001; Cowburn *et al.*, 2002) and chemotaxis, along with reduced deformability (Condliffe *et al.*, 1998; Hughes *et al.*, 1997). Priming is reversible and the lungs have been shown to be a major site for this activity, where primed neutrophils are sequestered in the tissue and re-released in a quiescent state into the circulation—a process which is defective following lung injury (Yoshida *et al.*, 2006;

Summers *et al.*, 2010b; Nahum *et al.*, 1991; Summers *et al.*, 2014). Neutrophil activation occurs typically when these cells encounter bacterial-derived stimuli. Along with phagocytosis, release of ROS via nicotinamide adenine dinucleotide phosphate (NADPH) oxidase then ensues along with neutrophil degranulation for maximal antimicrobial activity (Karlsson *et al.*, 1995). Priming of the neutrophils before detecting these activating stimuli enhances the neutrophil response (Guthrie *et al.*, 1984; Rainard *et al.*, 2000).

However, neutrophil activity is not always beneficial and has been shown to contribute significantly to the progression of inflammatory lung conditions. In particular, the pathogenesis and worsening of COPD are inextricably linked with neutrophilic inflammation.

1.2.1 Neutrophils in Health and Disease

This versatile cell has been described as a double-edged sword, playing a crucial role in the removal of pathogens and resolution of infection whilst possessing the capacity to cause significant tissue damage during inappropriate activation (Smith, 1994; Parkos, 2016). Furthermore, neutrophils have been implicated in the pathogenesis of a variety of diseases; the dual role of the neutrophil as 'Jekyll and Hyde' is epitomised in inflammatory lung conditions such as COPD (Hoenderdos *et al.*, 2016) and acute respiratory distress syndrome (ARDS) (Grommes and Soehnlein, 2011). The neutrophilic inflammation characteristic of these conditions is typically initiated in an attempt to clear pathogens and/or harmful particles from the lungs, but an enhanced neutrophil response contributes detrimentally to disease progression. In fact, increased neutrophil numbers in the lungs are associated with worsening of FEV1 (Sparrow *et al.*, 1984) and greater disease severity in COPD patients (Di Stefano *et al.*, 1998). In ARDS, the presence of neutrophilia in the BALF is associated with disease severity and worse patient outcome (Steinberg *et al.*, 1994). An overview of the benefits vs. damage of neutrophil functions and activity is provided in table 1.1.

Whilst neutrophil degranulation and protease release have been studied in detail, much less is known about other mechanisms of neutrophil action such as NET formation and microvesicle (MV) release. Neutrophil-derived MVs (NMVs) are utilised in a novel mechanism of cellular communication (Raposo and Stoorvogel, 2013), can contain cell cytoplasmic and membrane-bound proteins, DNA and RNA (Lee *et al.*, 2012) and are being increasingly studied in inflammatory diseases.

Table 1.1 The role of the neutrophil in inflammation: an overview of benefits vs. damage

Activity	Benefit	Harm from overactivation or failing of the process
Phagocytosis	-Crucial for clearance of pathogens, allows their killing, degradation, and processing -Facilitates immune signalling and transition to adaptive immunity[1]	- Accumulation and activity of neutrophils due to frustrated phagocytosis (i.e. failure to engulf the triggering agent and subsequent release of harmful content)[34]
Degranulation and protease release	-Can be critical to phagocytosis and ROS generation[2] -Killing and degradation of microbes over a wider area -Degradation of ECM[3] and basement membranes, permitting greater neutrophil infiltration when required	-Too much damage to tissue and ECM during wrongful or amplified neutrophil activation[4] -Increased degranulation is associated with chronic inflammatory conditions [5] -Protease activity can affect gene/protein expression of nearby cells detrimentally[6]
Respiratory burst	-Results in production of strong antimicrobial factors, particularly HOCl[7] -Mediates the activation of proteases for greater antimicrobial activity [8,9] -Plays a role in homeostasis, immunomodulation[10], and proliferation/differentiation[11] -Regulates neutrophil apoptosis[12]	-Can degrade host tissue and result in greater protease release, especially during excessive neutrophil activation[13] -Oxidative damage contributes to the progression of many inflammatory conditions[14]

Neutrophil extracellular trap formation (NETosis)	-Highly effective at trapping and killing pathogens[15] -Helps to prevent systemic invasion of bacteria[16]	-Linked with autoantibody production[17], vasculitis development[18], and impaired wound healing when dysregulated[19]
Microvesicle release	-Allows communication between near-by and more distant cells[20] -Antibacterial activity[21] -Method of immunomodulation[22]	-Can reduce endothelial[23] and epithelial cell monolayer integrity[24] -May induce immunosuppression[25] or excessive inflammatory response[26] and atherosclerosis development[27]
Apoptosis	-Allows controlled death and removal of neutrophils without release of harmful intracellular content[28] -Apoptotic neutrophils can recognise and bind pathogen-associated molecular patterns, tagging pathogens for phagocytosis[29]	-Delayed or dysregulated apoptosis prolongs inflammation and contributes to development/progression of chronic inflammatory conditions[30]
Efferocytosis by macrophages	-Has a pro-resolving effect[31] -Clears area of unnecessary neutrophils and associated material[32]	-Can be impaired by factors like cigarette smoke[3], causing prolonged inflammation

[1](Blander, 2018); [2](Hong et al., 2011); [3](Bradley et al., 2012); [4](Stamenkovic, 2003); [5](Wark et al., 2002); [6](Fischer and Voynow, 2002); [7](Weiss, 1989); [8](Weiss et al., 1985); [9](Reeves et al., 2002); [10](Fialkow et al., 2007); [11](Touyz, 2005); [12](Simon et al., 2000b); [13](Travis et al., 1994); [14](Mittal et al., 2014); [15](Brinkmann et al., 2004); [16](Yipp et al., 2012); [17](Kelley et al., 2011); [18](Kessenbrock et al., 2009); [19](Wong et al., 2015); [20](Raposo and Stoorvogel, 2013); [21](Timar et al., 2013); [22](Prakash

et al., 2012); [23](Pitanga et al., 2014a); [24](Butin-Israeli et al., 2016a); [25](Pliyev et al., 2014);

[26](Lacedonia et al., 2016); [27](Chironi et al., 2006); [28](Fox et al., 2010); [29](Ren et al., 2008)

[30](Walmsley et al., 2005); [31](Huynh et al., 2002); [32](Elliott et al., 2009); [33](Noda et al., 2013)

[34](Travis et al., 1994)

1.2.2 The Neutrophil in Chronic Obstructive Pulmonary Disease

Upon exposure to an inflammatory insult, endogenous chemotactic factors such as IL-8/CXCL8, CXCL1 and CXCL2 are released from activated resident alveolar and interstitial macrophages—where toll-like receptor signalling has been shown to be critical in generating a response (Hollingsworth et al., 2005) —as well as the pulmonary endothelium and epithelium. These factors, recognised by neutrophil CXCR-1 and -2 (Sawant et al., 2015; Reutershan et al., 2006), or exogenous cues like bacterial N-formyl-Met-Leu-Phe (fMLP) detected by neutrophil GPCRs, form a chemotactic gradient, and neutrophils are recruited to the lungs, towards the highest concentration of these chemoattractants, subsequently infiltrating the alveoli from the pulmonary capillaries (Downey et al., 1993). The importance of alveolar macrophages (AMs) in particular in orchestrating and also controlling this response has been demonstrated previously, where macrophage depletion led to increased neutrophil influx to the lungs, and AMs were able to suppress alveolar epithelial cell production of chemokines during acute lung injury (Beck-Schimmer et al., 2005).

Typically, neutrophil trafficking into an organ or tissue from the circulation employs a sequence of adhesion molecule interactions facilitating initial tethering and rolling (involving selectin ligands binding to endothelial P- and E-selectin), then slow rolling, arrest and firm adhesion (involving integrins, particularly integrinβ2 binding to endothelial ICAM-1 and VCAM-1), followed by transmigration (reviewed in (Ley et al., 2007)). In contrast to the systemic circulation, the mechanism of adhesion in the pulmonary microcirculation is thought to be selectin and β2-integrin independent, but may instead rely on adhesion molecules such as integrin β1 (Hellewell et al., 1994; Jagels et al., 1995; Kubo et al., 1999; Ridger et al., 2001), although these molecules do seem necessary for the subsequent retention of neutrophils in inflamed pulmonary capillaries (Kuebler et al., 2000), and the β2 integrin CD18 has been shown to be involved in neutrophil influx depending on the type of bacterial challenge, indicating that adhesion cascades may be stimulus-dependent. Interestingly, prolonged neutrophil entrapment in these areas during acute lung injury has been shown to disturb the pulmonary microcirculation, an effect reversible by blocking Mac-1 in mice (Park et al., 2019). Further, priming of circulating neutrophils with GM-CSF or platelet activating factor (PAF) has been shown in humans to further increase transit time (Summers et al., 2014).

One major explanation for this difference in mechanisms of neutrophil migration in the lung compared with other organs is the requirement of circulating, spherical neutrophils to actively deform to transit through the pulmonary capillaries which are narrower than the neutrophil themselves (Kornmann et al., 2015), resulting in longer transit times, whereas these cells reach most tissues via the post-capillary venules requiring rolling on the endothelium and then adhesion (Doerschuk et al., 1993; Gebb et al., 1995; Doerschuk, 2000). It is therefore unsurprising that the lungs contain a marginated pool of neutrophils which may be readily and rapidly recruited.

However, a limitation of many of these studies is the use of murine models which may not necessarily be a true reflection of the human situation. Of note, the accumulation of circulating ^{99m}Technetium (Tc)-labelled neutrophils in the lungs of patients with stable COPD was much greater than in matched healthy volunteers, and was equivalent to that seen in volunteers who inhaled LPS (Tregay et al., 2019), suggesting increased pulmonary neutrophil–endothelial interactions is a constitutive process with COPD, although the mechanisms were not explored in this study.

Persistent airway neutrophilia is a major feature of COPD and correlates with disease severity (Stanescu et al., 1996). Despite this, COPD patients suffer recurrent infection-driven disease exacerbations (Boixeda et al., 2012). On the other hand, blocking of neutrophil migration and activity was investigated as a therapeutic approach in phase-two clinical trials in COPD, utilising a CXCR2 antagonist, but resulted in increased exacerbation incidence (Lazaar et al., 2020), highlighting this complexity of this core neutrophil activity in COPD. Neutrophilic inflammation predominates during COPD exacerbations and high levels of neutrophils are found in the sputum and bronchoalveolar lavage fluid (BALF) of COPD patients (Rutgers et al., 2000; Wen et al., 2010). Several hypotheses of COPD pathogenesis strongly implicate neutrophils. The classical hypothesis is that there is an imbalance of proteases and antiproteases in favour of the former, which are majorly secreted from neutrophil granules, particularly neutrophil elastase (NE), proteinase 3 (PR3), cathepsin G and matrix metalloproteinase-9 (MMP-9) (Travis et al., 1994; Moraes et al., 2003). Neutrophilic protease signatures have been detected in COPD patient sputum and BAL samples (Van Overveld et al., 2006; Ilumets et al., 2007), particularly NE and MMPs, the importance and utility of which in chronic lung disease has recently been highlighted in the investigation of point-of-care devices for protease detection (Shoemark et al., 2019; Thulborn et al., 2020).

An oxidant–antioxidant imbalance is also present, where the secretion of ROS is associated with neutrophil and macrophage accumulation and activity during inflammation (Ahmad et al., 2013). Additionally, neutrophils can display altered properties under hypoxia, a common feature of COPD, including impaired bacterial killing (McGovern et al., 2011), increased NE, MPO and MMP9 release

(Hoenderdos *et al.*, 2016) and prolonged survival promoted by the release of neutrophil survival factors (Mecklenburgh *et al.*, 2002; Walmsley *et al.*, 2005). Therefore, hypoxia in COPD patient lungs may initiate a feedback loop which increases the propensity of the neutrophil for damage whilst decreasing its defensive and pro-resolving qualities, furthering disease progression.

Finally, NMVs have shown immunomodulatory (Eken *et al.*, 2010; Pliyev *et al.*, 2014) and antimicrobial activity (Timar *et al.*, 2013) in addition to likely contribution to inflammatory disease progression (Prakash *et al.*, 2012; Pitanga *et al.*, 2014a; Lacedonia *et al.*, 2016). Importantly, **NMVs can be found at high levels in the induced sputum of COPD patients** (Lacedonia *et al.*, 2016), and their activity shown so far strongly suggests a role for these MVs in lung inflammation.

1.3 Neutrophil-Derived Microvesicles

1.3.1 Definition and Biogenesis

MVs are a type of extracellular vesicle (EV) defined by their formation by membrane budding/blebbing (Stein and Luzio, 1991). Although the size ranges for MVs from specific cell-types are slowly being redefined as techniques and our knowledge advance, in general MVs are considered to reside in the size range of ~100–1000 nm (Raposo and Stoorvogel, 2013). These small parcels are the focus of increasing research attention. First documented by Stein and Luzio (1991) in activated neutrophils, the process of MV formation is termed ectocytosis. Due to this process, MVs have a membrane comprising a lipid bilayer which contains cell-surface markers from their parent cells (Johnson *et al.*, 2014). At sites of inflammation or infection, the normal levels of MVs shift in favour of NMVs, which rapidly become the most common type in these areas, echoing the increased abundance of their parent cells (Guervilly *et al.*, 2011; Prakash *et al.*, 2012). Cells release MVs during activation and apoptosis and can also undergo spontaneous MV release in the absence of any apparent stimulus (Boysen *et al.*, 2016; Johnson *et al.*, 2014). The present study focused primarily on NMVs generated upon cell activation with fMLP, a proven NMV-inducing agonist (Hess *et al.*, 1999; Nolan *et al.*, 2008) which binds to neutrophil G-protein coupled receptors, inducing Ca2+ influx to the cell (fig 1.4) (Becker *et al.*, 1998; Carp, 1982).

Of particular relevance, fMLP is commonly used in models of lung inflammation. A number of other stimuli associated with lung inflammation have also been shown to induce NMV formation, including LPS (Watanabe *et al.*, 2003), C5a (Pliyev *et al.*, 2014) and TNF-α (Johnson *et al.*, 2013). Neutrophil activation with these stimuli results in an increase in the intracellular calcium concentration ($[Ca^{2+}]_i$), triggering the ATP-dependent activity of the translocase floppase and calcium-dependent scramblase. These enzymes translocate phosphatidyl serine (PS) from the inner to the outer mono-

leaflet to create an area of net negative charge (Tuck, 2011; Zwaal *et al.*, 2005). PS presentation has also been suggested to be important for the interaction of NMVs with their target cells (Eken *et al.*, 2008; Fadok *et al.*, 1992).

The increased $[Ca^{2+}]_i$ induces activation of calpain (Pasquet *et al.*, 1996), an enzyme that degrades cytoskeletal talin and activin, and gelsolin, which cleaves actin-capping proteins (Enjeti *et al.*, 2008). These proteolytic enzymes breakdown the cell cytoskeleton and promote separation of the membrane from the cytoskeleton and cytoskeletal reorganisation. After formation, proteolytic cleavage of the vesicle from the membrane occurs via a cascade initiated by ADP-ribosylation factor-6 (Kalra *et al.*, 2016).

It should be noted, however, that despite the initial observation of ectocytosis in neutrophils, platelet-derived MVs were the first to be recognised (Wolf, 1967), and much of our knowledge of MV formation stems from this MV type. Therefore, known mechanisms of ectocytosis should be applied to NMVs with caution and this topic represents a gap in current knowledge.
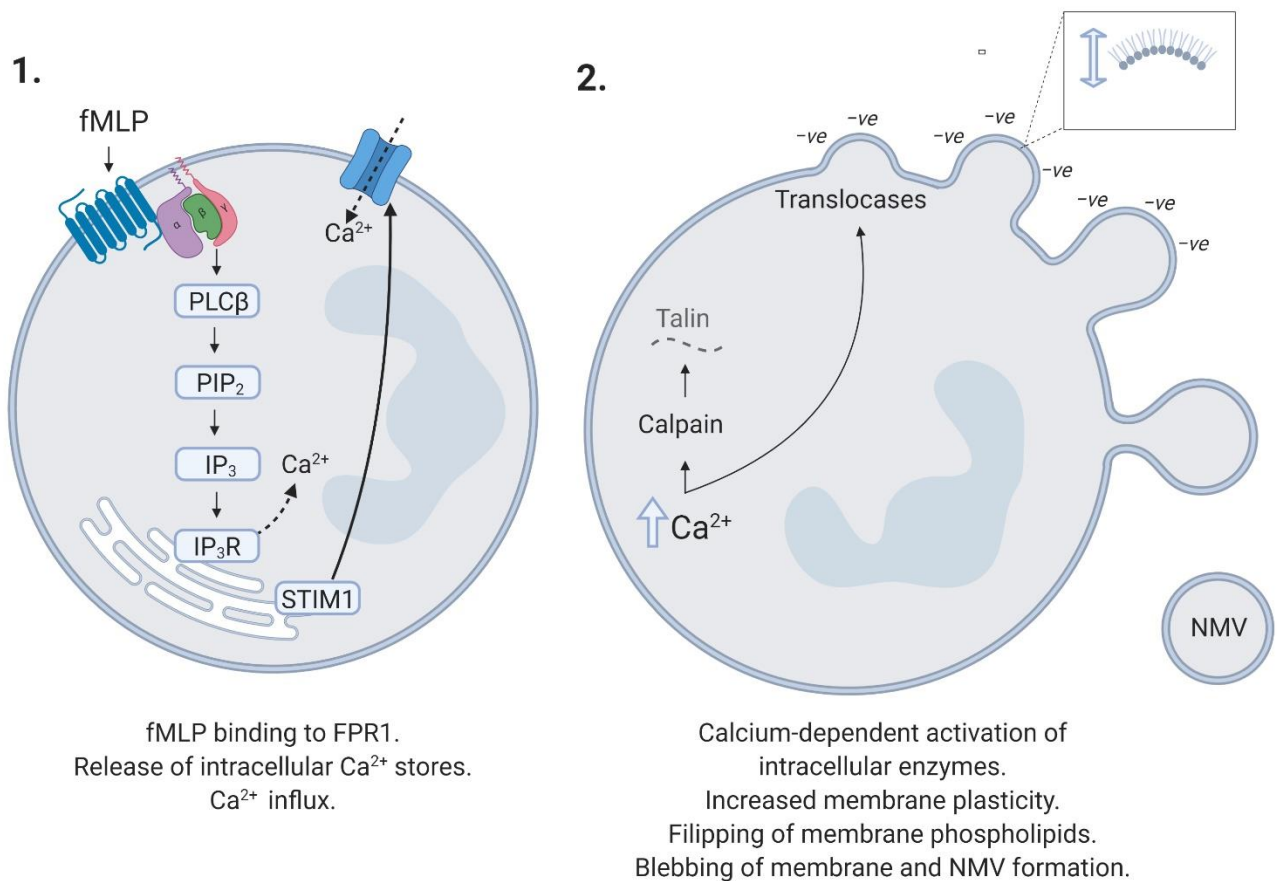
Figure 1.4 Neutrophil-derived vesicle (NMV) formation

*(**1**.) Neutrophil activation with f-met-leu-phe (fMLP), the bacterial peptide used in the present study, via binding to membrane G-protein coupled receptors (mainly formylated peptide receptor 1 [FPR1]) triggers dissociation of the -β and -γ subunits of the G-protein and subsequent binding to phospholipase C-β (PLCβ) initiating a signalling cascade which results in the release of intracellular Ca^{2+} from the endoplasmic reticulum (ER). Upon sensing depletion of these stores, STIM1 from the ER then interacts with membrane calcium release-activated calcium channels to facilitate extracellular Ca^{2+} influx. (**2**.) After this, the Ca^{2+}-dependent activity of calpain, and other enzymes, degrade cytoskeletal components including talin, promoting cytoskeletal reorganisation. The increased intracellular Ca^{2+} concentration also induces the activity of the translocases which flip phosphatidyl serine from the inside to the outside of the cell membrane, generating an area of negative (-ve) charge and promoting membrane plasticity and blebbing. This eventually results in proteolytic cleavage of the blebbing vesicle, to release the newly formed NMV. Adapted from Turturici et al. (2014), Newton and Dixit (2012) and Dorward et al. (2015).*

Abbreviations; PIP_2: Phosphatidylinositol 4,5-bisphosphate, IP_3: Inositol trisphosphate, IP_3R: Inositol trisphosphate receptor, STIM1: Stromal interaction molecule 1.

.

1.3.2 Neutrophil-Derived Microvesicles Protein Content

MVs have been shown to contain cell cytoplasmic and membrane-bound proteins, DNA, RNA and miRNAs (Raposo and Stoorvogel, 2013). Whilst miRNAs are increasingly realised as important for NMV activity and have been shown to act on both inflammatory and cell death pathways in endothelial cells (Gomez *et al.*, 2020; Ajikumar *et al.*, 2019) and intestinal epithelial cells (Butin-Israeli *et al.*, 2019), the present study focused on the role of protein, and particularly protease, content of these NMVs.

A proteomics study by Dalli et al. (2013) provided important information about the protein content of NMVs. NMVs derived from fMLP-stimulated neutrophils were shown to highly express the protease MMP-9 and also MPO, which are critically implicated in lung inflammation. The presence of these proteins in NMVs was supported by research from Gasser et al. (2003) and Butin-Israeli et al. (2016a) who showed by gelatin zymography that NMVs contain highly active MMP9, and Pitanga et al. (2014a) who showed that endothelial cell damage could be induced via NMV-derived MPO activity.

In their proteomic analysis, Timar et al. (2013) found that 28 of the 282 proteins they identified were predominantly granule-associated; NMVs may therefore represent a method of delivery for these proteins to target cells. Interestingly, proteases and other proteins from all three granule types are incorporated into NMVs. However, the location of these proteins in the NMVs has not yet been determined (i.e. membrane-associated or cytoplasmic expression). In addition, these authors showed high levels of the antimicrobial peptide neutrophil defensin-1, supporting the antibacterial activity of NMVs in their study, and identified 26 proteins associated with adhesion. The latter result was reinforced by the work of Dalli et al. (2013), also showing high expression of proteins associated with cell interaction/adhesion and also activation. Specific proteins identified by these authors included lactoferrin, an enzyme with anti-microbial activity, capable of NF-κB activation and associated with prolonged neutrophil survival (Ando *et al.*, 2010; Francis *et al.*, 2011), annexins, myosin, shown to facilitate neutrophil transepithelial migration (Hofman *et al.*, 1999), catalase, shown to protect neutrophils from oxidative damage (Roos *et al.*, 1980), and integrin β2 (a.k.a CD18) and integrin αM (a.k.a. CD11b), which, by interaction with ICAM-1, has been shown in the Ridger group to be a major mechanism of NMV adhesion to endothelial cells (Gomez *et al.*, 2020). The presence of many neutrophil proteins implicated in lung inflammation raises the possibility of a role for NMVs in COPD pathology.

1.3.3 Neutrophil-Derived Microvesicles in Lung Inflammation

In healthy lungs, alveolar macrophage- and epithelial-derived MVs comprise the majority of the endogenous MV population (Soni *et al.*, 2016). However, during lung inflammation, numbers of NMVs greatly increase making them one of the major MV types present. Increased numbers of NMVs positive for the neutrophil/granulocyte markers CD66b and CD11b have been demonstrated in the BALF of ARDS patients within 1 day of onset, as compared to patients undergoing mechanical ventilation for reasons other than a pulmonary condition and patients undergoing a BAL procedure for non-infectious/inflammatory pulmonary disease (Guervilly *et al.*, 2011). These authors also showed that higher levels of $CD45^+$ leukocyte-derived MVs, of which NMVs make up a major part, at day 1 of ARDS onset were correlated with survival in these patients.

Lacedonia et al. (2016) found increased NMV numbers in the induced sputum of COPD patients, however, in contrast to findings in ARDS patients, these authors showed that NMVs expressing CD66b were positively correlated with BODE index (Body-mass index, airflow Obstruction, Dyspnoea, and Exercise capacity, a scoring system used to grade the severity of COPD)—echoing the correlation of sputum neutrophils (Peleman *et al.*, 1999) and neutrophil peptides (Paone *et al.*, 2011) with greater airway obstruction in COPD. Indeed, NMVs have been shown to account for a significant portion of the neutrophil-derived protein content found in biofluids such as BALF (Hamacher *et al.*, 1998; Sadallah *et al.*, 2011). Contrasting evidence for NMV activity exists, and NMVs have been shown to be capable of immunomodulation of diverse cell types including macrophages, dendritic cells and natural killer cells (Table 1.2).

Surprisingly, Lacedonia et al. (2016) found no correlation between the MV and cellular composition of the sputum. The authors suggested that these MVs may therefore not all originate from this area. In agreement with this theory, it has been shown previously in COPD patients that the cellular composition of induced sputum did not correlate with that of BALF or lung biopsy specimens (Rutgers *et al.*, 2000). In normal, healthy lungs, Soni et al. (2016) showed that $CD11b^+/Ly6G^+$ MVs— considered to be NMVs—were present at very low levels in a mice. However, a dramatic increase in these levels occurred 4 hours after LPS instillation, corresponding with the influx of their parent cells into the lungs. Although, a further possibility is pulmonary capillary endothelial barrier disruption by LPS instillation, as has been shown previously in mouse models (Barabutis *et al.*, 2015), and subsequent passive transport of NMVs from the circulation to the lungs without the requirement for neutrophil migration.

Table 1.2. Neutrophil-derived microvesicle (NMV) immunomodulatory activity		
Details	NMV activity	Reference
In vivo, Mouse	Inhibition of neutrophil trafficking in response to interleukin (IL)-1β	(Dalli *et al.*, 2008)
In vitro, Human	Increased tumour growth factor (TGF)-β1 expression from activated macrophages and dendritic cells Reduced pro-inflammatory gene transcription (tumour necrosis factor (TNF)-α, IL-1β, -6, -8, -10 and -12)	(Eken *et al.*, 2010; Eken *et al.*, 2013)
In vitro, Human	Inhibition of immature monocyte-derived dendritic cell (DC) maturation Impaired DC-promotion of T-cell proliferation	(Eken *et al.*, 2008)
In vitro, Human	Increased TGF-β release from IL-1 and -12-stimulated natural killer (NK) cells Inhibited NK-cell interferon-γ and TNF-α release	(Pliyev *et al.*, 2014)
In vitro, Human NMVs isolated from sepsis patients	Enhanced phagocytic ability of macrophages Increased macrophage HLA-DR, CD80 and CD86 expression	(Prakash *et al.*, 2012)
In vitro, Human	Increased ICAM-1, VCAM-1 and E-selectin expression on human microvascular pulmonary endothelial cells co-cultured with PBMCs	(Tirlapur *et al.*, 2016)
In vitro, Human	Increased endothelial cell release of IL-6, IL-8 and MCP-1 Procoagulant activity	(Mesri and Altieri, 1998; Mesri and Altieri, 1999)
In vivo, Human and Mouse	Decreased junctional protein (Dsg-2) expression and increased neutrophil transepithelial migration via MMP-9 activity.	(Butin-Israeli *et al.*, 2016a; Slater *et al.*, 2017; Butin-Israeli *et al.*, 2019)

	Impaired resolution of inflammation via miR-23a and -155 delivery and MPO activity.	
In vitro, Human	Increased brain endothelial monolayer permeability and alteration in gene pathways associated with junctional protein expression and inflammation.	(Ajikumar *et al.*, 2019)
In vivo, Mouse	Increased TGF-β production by chondrocytes via delivery of Annexin A1. Anti-inflammatory effects for arthritis.	(Headland *et al.*, 2015)
In vitro, Human and *In vivo,* Mouse	Increased endothelial adhesion molecule expression and monocyte adhesion via miR-155 delivery.	(Gomez *et al.*, 2020)

It may be postulated that sputum MVs originate from neutrophils in the lung tissue or circulation, indicating an ability to traverse the airways. In fact, NMV migration into areas unreachable by their parental counterparts has been observed in other inflammatory conditions such as rheumatoid arthritis (Headland *et al.*, 2015). On the other hand, it should also be noted that neutrophilia has been shown in the airway lumen and walls of patients with COPD (Saetta *et al.*, 1997). Alternatively, neutrophils may have undergone processes such as NETosis in the airways, as demonstrated previously by high levels of DNA and NET associated complexes in COPD sputum samples (Dicker *et al.*, 2018), and may therefore be no longer detectable whilst NMVs may persist.

Prakash et al. (2012) showed raised CD66b^{+} MV levels in the BALF of patients with suspected pneumonia, a common comorbidity of COPD (Mullerova *et al.*, 2012) and a common cause of ARDS. They also found that that the NMVs isolated from these patients were phagocytosed by macrophages *in vitro*. Combined with the immunomodulatory activity of NMVs described in table 1.2, it may be postulated that these effects occur in the lung *in vivo* upon interaction with resident immune cells.

Evidence of functional impacts of neutrophil EVs in the lung was recently provided by Genschmer et al. (2019). Whilst their biogenesis is distinctly different and these EVs likely have differential functions, these authors found that a single administration of neutrophil-derived exosomes generated from an activating stimulus induced alveolar enlargement and damage via an elastase-dependent mechanism in A/J mice. Surprisingly, this was not accompanied by immune cell

infiltration at any of the time points analysed in their study, highlighting the potential for protease-mediated damage by neutrophil-derived EVs.

In addition, in intestinal epithelial cells, NMVs were shown to facilitate increased neutrophil transepithelial migration by decreasing epithelial cell monolayer integrity (Butin-Israeli *et al.*, 2016a) and also to impair wound healing and resolution of inflammation (Butin-Israeli *et al.*, 2019) via MMP-9 activity and delivery of miRs. Evidence that NMVs activate both human microvascular endothelial cells support a role for NMVs in the pulmonary vasculature (Tirlapur *et al.*, 2016), whilst alveolar epithelial cells have been shown to rapidly internalise MVs from resident immune cells(Schneider *et al.*, 2017). It is therefore likely that similar effects observed in other epithelial or pulmonary cell types may apply to NMV–lung epithelial cell interactions.

1.4 Summary

The major role of neutrophils in lung inflammation is well recognised, however the presence of high levels of NMVs in the lungs of patients with both chronic and acute lung inflammation, along with their demonstrated immunomodulatory activity, highlight a novel neutrophil function which is as yet underexplored. Furthermore, very little is known about the interaction with or functional effects of NMVs on the delicate lung epithelium, or indeed about the fate of NMVs in the lung.

In this study, we characterised NMVs from both healthy individuals and in COPD patients, investigated the interaction of NMVs with bronchial epithelial cells *in vitro*, and finally determined their effects and localisation on the lung *in vivo*. The overall aim of this research was to determine whether NMVs contribute to lung inflammation, improving current understanding of the role of NMVs in health and disease.

Chapter 2: Materials and Methods

2.1 Materials and suppliers

Item	Supplier	Cat. no
0.2 µm Minisart NML Syringe Filter	Sartorious	16534
0.9% sterile sodium chloride solution	Baxter Healthcare Ltd.	UKF7124
30% Acrylamide/Bis Solution	Bio-Rad	1610154
348-well PCR plate	Thermo Fisher Scientific	AB1384
4-well Ibidi µ-slide	Thistle Scientific	80426
5-(N-Ethyl-N-isopropyl)amiloride	Sigma	A3085-25MG
AbC anti-mouse bead kit	Thermo Fisher Scientific	A10344
AccuCount Blank Particles	Spherotech	ACBP-20-10
Alexa Fluor 647-conjugated wheat germ agglutinin	Thermo Fisher Scientific	11510826
Anhydrous DMSO	Sigma	276855
BEAS-2B cells	American Type Culture Collection	ATCC® CRL-9609
Benzyl dimethylamine accelerator	Agar Scientific Ltd.	AGR1061
Bovine Serum Albumin	Sigma	A7906
CD14 Microbeads anti-human	Miltenyi Biotec	130-050-201
Cell dissociation solution	Sigma	C5914-100ML
CellEvent caspase 3/7 detection reagent	Thermo Fisher Scientific	C10723
Collagen I (rat-tail)	Corning Inc.	354294
Collagenase type IV, powder	Thermo Fisher Scientific	17104019
Colour Prestained Protein Standard, Broad Range (11–245 kDa)	New England Biolabs	P7712
Corning 96-well EIA/RIA plates	Sigma	CLS3590
CY212 araldite resin	Agar Scientific Ltd.	AGR1040
Cytochalasin D	Sigma	C8273-1MG
Dextran (molecular weight 450,000–65,0000,	Sigma-Aldrich	31392-50G
Direct-zol RNA MicroPrep kit	Zymo Research	R2061
DMEM, high glucose	Thermo Fisher Scientific	11965092
Dodecenyl succinic anhydride hardener	Agar Scientific Ltd.	AGR1052
DQ collagen IV	Thermo Fisher Scientific	D12052
Dulbecco's phosphate-buffered saline (with Ca^{2+} and Mg^{2+})	Thermo Fisher	14080055
ECL Select™ Western Blotting Detection Reagent	Fisher Scientific	12644055
ELISA substrate reagent pack	R&D systems	DY999
Ficoll-paque Plus	GE-Healthcare	17-1440-03
FITC-conjugated phalloidin	Sigma	P5282-.1MG
FITC-dextran (10 kDa)	Sigma	FD10S-100MG
FITC-dextran (70 kDa)	Sigma	46945
Foetal Bovine Serum	Life Technologies	10500
Foetal Bovine Serum (ultralow endotoxin)	VWR	S1860-500
Formalin (10%)	Sigma	252549
Glass microscope slides (76 × 260)	VWR international	1508031/1
Hanging cell culture insert, PET 0.4 µm, 24-well	Merck Millipore	CHT24H48
Histopaque-1077	Sigma-Aldrich	10771-500ML
Hoechst 33342	Thermo Fisher Scientific	62249

Human CCL2/MCP1 DuoSet ELISA	R&D systems	DY279
Human CXCL8/IL8 DuoSet ELISA	R&D systems	DY208
Human MMP-9 DuoSet ELISA	R&D systems	DY911-05
Human TIMP-1 Mini ABTS ELISA	Peprotech	900-M438
Immobilon-P PVDF membrane	Merck Millipore	IPVH00010
iScript cDNA synthesis kit	Bio-Rad	170-8891
Kentucky Reference Cigarettes	University of Kentucky	3R4F
L-glutamine	Lonza	BE17-605E
Lipopolysaccharide	Sigma	L7018-100MG
LS-columns	Miltenyi Biotec	130-042-401
Mega mix calibration beads	BioCytex	7801
Micro BCA™ Protein Assay Kit	Thermo Scientific	23235
Mouse JE/CCL2 DuoSet ELISA	R&D systems	DY479-05
Mouse KC/CXCL1 DuoSet ELISA	R&D systems	DY453-05
N-formyl-met-leu-phe	Sigma	F3056-10MG
Normal goat serum	R&D systems	DY005
NucView® 530 Caspase-3 Substrate	Biotium	10406
Nunc™ MicroWell™ 96-Well Optical-Bottom Plate	Fisher Scientific	10281092
Penicillin/Streptomycin	Life Technologies	15140-122
PKH26 Red Fluorescent Cell Linker Kit	Sigma	PKH26GLsig
PKH67 Green Fluorescent Cell Linker Kit	Sigma	PKH67GLsig
ProLong Gold antifade reagent	Life Technologies	P36930
Recombinant human TIMP-1	Biolegend	592402
Recombinant human TNF-α	eBioscience	DMS301
RIPA lysis buffer (10x)	Merck Millipore	20-188
RPMI-1640 (without L-glutamine)	Life Technologies	31870-025
Shandon Kwik-Diff™ Kit	Thermo Fisher Scientific	9990700
Sodium Citrate	Martindale Pharma	MP543
Sodium Dodecyl Sulphate	Sigma	L3771
Ssoadvanced universal SYBR green supermix	Bio-Rad	1725271
Sterile saline (0.9%)	Baxter	PMC2104
Tetramethyl ethylenediamine (TEMED)	Bio-Rad	1610801
TO-PRO-3-iodide	Life Technologies	T3605
Triton-X-100	Sigma	T8787
TRIzol Reagent	Thermo Fisher Scientific	15596018
Trypsin-EDTA	Life Technologies	25200056
Tunicamycin	Sigma	T7765
Tween20	Sigma	P1379
β-mercaptoethanol	Sigma	M3701

Antibodies

Item	Supplier	Cat. no
Alexa Fluor® 647 anti-mouse CD11c Antibody	Biolegend	123110
APC mouse IgG1 κ (MOPC-21)	Biolegend	400120
APC rat anti-mouse anti-CD326 [Ep-CAM] (G8.8)	Biolegend	118213
BV421 mouse IgG2a κ (MOPC-173)	Biolegend	400260
FITC anti-mouse Ly-6G Antibody (1A8)	Biolegend	127606
FITC mouse IgM (MM-30)	Biolegend	401606
Goat Anti-Mouse Immunoglobulins/HRP	Dako Agilent	P044701-2
Goat Anti-Rabbit Immunoglobulins/HRP	Dako Agilent	P044801-2
GRP78, Anti-KDEL [10C3] Mouse Monoclonal Antibody	Abcam	ab12223
Mouse anti-human anti-MMP-9	R&D systems	MAB911
Mouse anti-human APC anti-CD41a (HIP8)	Biolegend	303710
Mouse anti-human APC anti-CD44 (C26)	BD Biosciences	560890
Mouse anti-human APC-Cy7 anti-CD14 (MφP9)	BD Bioscience	557831
Mouse anti-human BV421 anti-CD14 (M5E2)	Biolegend	301830
Mouse anti-human BV421 anti-CD66b (G10F5)	BD Bioscience	562940
Mouse anti-human FITC anti-CD66b (G10F5)	Biolegend	305104
Mouse anti-human FITC anti-ICAM-1 (HCD54)	Biolegend	322719
Mouse anti-human FITC anti-MMP9	R&D	IC9111F
Mouse anti-human PE anti-CD18 (6.7)	BD Biosciences	555749
Mouse anti-human PE anti-CD41a (HIP8)	eBioscience	303709
Mouse anti-human PE anti-CD62L (DREG-56)	Biolegend	304840
Mouse anti-human PE-Cy7 anti-CD144 (16B1)	Invitrogen	25-1449-42
Mouse anti-human PerCP-Cy5.5 anti-CD144 (557H1)	BD Bioscience	561566
PE anti-mouse F4/80 Antibody (BM8)	Biolegend	123110
PE-Cy7 mouse IgG1 κ (P3.6.2.8.1)	Invitrogen	25-4714-42
Rabbit anti-human anti-GAPDH (14C10)	Cell Signalling Technologies	2118S
Rabbit anti-human anti-ZO-1 (ZMD.437)	ThermoFisher Scientific	40-2300

2.2 Experimental methods

2.2.1 Human peripheral blood neutrophil and neutrophil-derived microvesicle isolation

2.2.1.1 Participant information and statement of ethics

In order to isolate primary human peripheral blood neutrophils, up to 80 ml of venous blood was taken from healthy volunteers aged 21–55 years. Ethical approval for this study was obtained from the University of Sheffield Ethics Committee (ref: SMBRER310), and written informed consent was obtained from all volunteers.

2.2.1.2 Neutrophil isolation and microvesicle generation

Neutrophils and NMVs were isolated as previously described in our group, see Nolan et al. (2008) and Gomez et al. (2020) with some modifications (summarised in fig 2.1). All isolation steps were carried out at room temperature (RT) unless otherwise stated. Into a 50-mL Corning Falcon conical centrifuge tube, 40 mL of fresh whole blood was added along with 4 mL of 3.8% (w/v) sodium citrate to prevent coagulation. The mixture was then centrifuged at 260 g for 20 min. The resulting platelet-rich plasma layer was removed and discarded, and to the remaining layer, 6 ml of 6% (w/v) dextran was added to promote erythrocyte aggregation and hence sedimentation. Sterile saline (0.9% sodium chloride) was added to a final volume of 50 mL and the tube was gently inverted to ensure thorough mixing. Any air bubbles were removed with a plastic Pasteur pipette and the solution was allowed to sediment for up to 30 min. The top leukocyte-rich layer was removed, placed in a fresh 50 mL tube, and sterile saline was added to a final volume of 35 ml. This mixture was then gently layered onto 16 mL of Histopaque-1077, followed by density-gradient centrifugation (25 min, 400 g). The pellet containing granulocytes and red blood cells was subjected to hypotonic lysis by resuspension in 25 mL sterile-filtered (0.2 µM) 0.2% NaCl and gently inverted ten times to lyse any remaining erythrocytes. The solution was then restored to isotonicity by the addition of 25 mL of 1.6% sterile-filtered NaCl. The cell solution was centrifuged again (7 min, 250 g) to obtain a neutrophil-rich pellet, which was subsequently resuspended in 10 mL of RPMI-1640. Of this cell suspension, 10 µL was removed and added to 90 µL of fresh RPMI to manually determine the cell concentration using a haemocytometer. The 10 mL cell suspension was then centrifuged at 250 g, 7 min, as a washing step and the pellet was resuspended to a concentration of 1×10^6 neutrophils per 1 mL Dulbecco's phosphate buffered saline (DPBS) containing calcium and magnesium, providing an extracellular source of Ca^{2+} to the cells necessary for normal cell activation and NMV generation. fMLP (10^{-5} M), 10% CSE, or PBS (control) was added to stimulate NMV production.
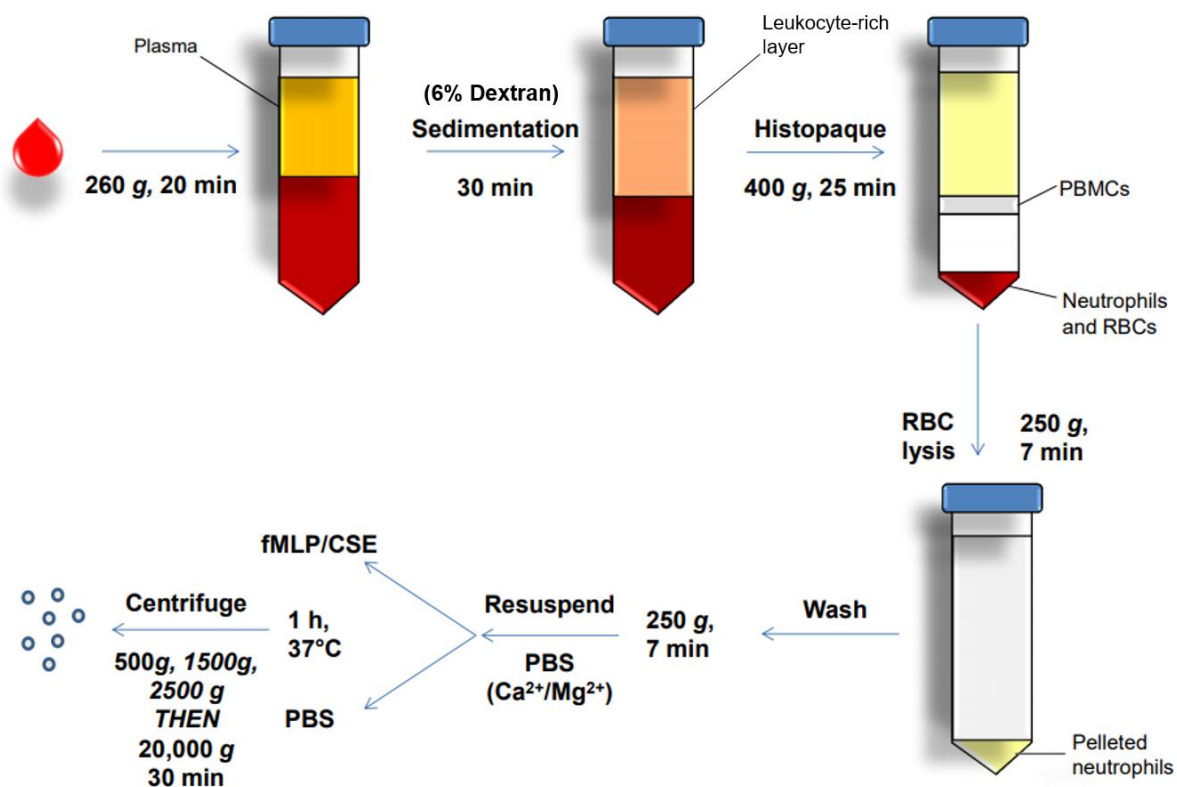
Figure 2.1 Neutrophil isolation and microvesicle generation

Schematic summarising isolation of neutrophils from peripheral blood taken from healthy participants and subsequent generation and isolation of neutrophil-derived microvesicles (NMVs), represented by blue spheres. Anticoagulated blood was centrifuged and plasma removed. Red blood cells (RBCs) were aggregated and sedimented, then the resulting leukocyte-rich layer was further separated by density-gradient centrifugation using Histopaque. Remaining RBCs were removed by hypotonic lysis. Neutrophils were washed and then incubated in various conditions to promote NMV formation. After 1h incubation, cells and cell debris were removed by three centrifugation steps, then NMVs were pelleted at 20,000 g and used for subsequent applications. fMLP: N-formyl-met-leu-phe, CSE: cigarette smoke extract.

The cell suspensions were then each divided into 15–50 ml falcon tubes depending on resuspension volume and incubated for 1 h at 37°C, 5% CO2, with gentle inversion every 10–15 min. To measure effect of these stimuli on cell viability, 10 µl of this solution was removed and added to 10 µl of 0.4% trypan blue. This cell suspension was analysed using a haemocytometer and light microscope. After neutrophil stimulation as mentioned above, the cell suspensions were centrifuged once at 500 g, 4°C, for 5 min to remove the cells, then a further two spins for 5 min each at 1500 and 2000 g were performed to pellet remaining cells and cell debris, transferring the supernatant to a fresh tube after each centrifugation step. To pellet microvesicles, the suspension was centrifuged at 20,000 g, 4°C, for 30 min, in 1.5 ml Eppendorf tubes. Typically, a very small NMV pellet could be seen after this step. The supernatant was then removed carefully with a pipette and replaced with ~100–200 µL of sterile-filtered (0.2 µm) PBS per tube. Samples from the same donor were combined into a single tube for microvesicle counting using flow cytometry, for which a 20 µl counting sample was removed. The remaining NMV suspension was centrifuged again at 20,000 g to wash the NMVs and remove any free protein which may have pelleted during this initial step. NMVs were then resuspended in the desired media at the appropriate concentration, to be used as soon as possible after isolation.

2.2.1.3 Cigarette smoke extract preparation

To generate CSE, the filter was cut from a Kentucky reference cigarette (3R4F), inserted into an appropriately cut p1000 pipette tip to ensure a tight fit so that smoke did not escape from the mechanism later, and the small end of the tip was inserted into a clamp and tubing connected to a Masterflex pump. The cigarette was lit inside a fume hood, and once it started to burn the pump was switched to "reverse" mode. Smoke was bubbled through 10 ml DPBS (Ca^{2+}/ Mg^{2+}) for 5 min. The resulting CSE was considered as 100% stock as per Bourgeois et al. (2016). This was then sterile filtered using a 0.2-µm filter to remove any particles. CSE was used fresh, ≤30 min after generation, and was never stored.

2.2.1.4 Neutrophil activation status by flow cytometry

To confirm the ability of neutrophils to respond to fMLP after isolation and determine the effects of neutrophil isolation on cell activation status, flow cytometry was used to detect CD18 and CD62L surface expression (as activation markers upregulated or shed on the membrane upon activation, respectively) of these cells in whole blood, after isolation, and after stimulation. For whole blood labelling, 100 µl blood was added to 15 ml tubes, in single and double stained conditions only (20 µl FITC anti-CD66b and 5 µl PE anti-CD18 or 10 µl PE-CD62L). Tubes were incubated for 30 min on ice. 2 ml of cold 1% BSA/PBS was added and samples were centrifuged at 300 g for 6 min, 4°C to pellet cells. Erythrocytes were lysed using 2 ml homemade 1X lysis buffer (20X stock: 16.6 g NH4Cl, 2 g

KHCO3, 400 µL 0.5 M EDTA, 200 mL distilled, dH2O; 0.2 µm sterile-filtered). The suspension was incubated for 10 min, then 2 ml PBS was added and cells were pelleted again. Cells were resuspended in 0.5 ml 1% BSA/PBS and kept on ice until analysis to halt any further cell activation. Isolated neutrophils were labelled using the same procedure, without RBC lysis as no RBSs should be present at this stage. Samples were analysed on an LSRII flow cytometer. Figure 2.2 shows the results of this analysis, confirming cell activation by this stimulus in isolated cells as shown by increased CD18 expression on stimulated cells and loss of CD62L expression, whilst cells in whole blood, freshly isolated, and stimulated cells had lower CD18 and higher CD62L expression. Although, some cell activation did occur as a consequence of the isolation process, incubation period and potentially via the labelling process itself.
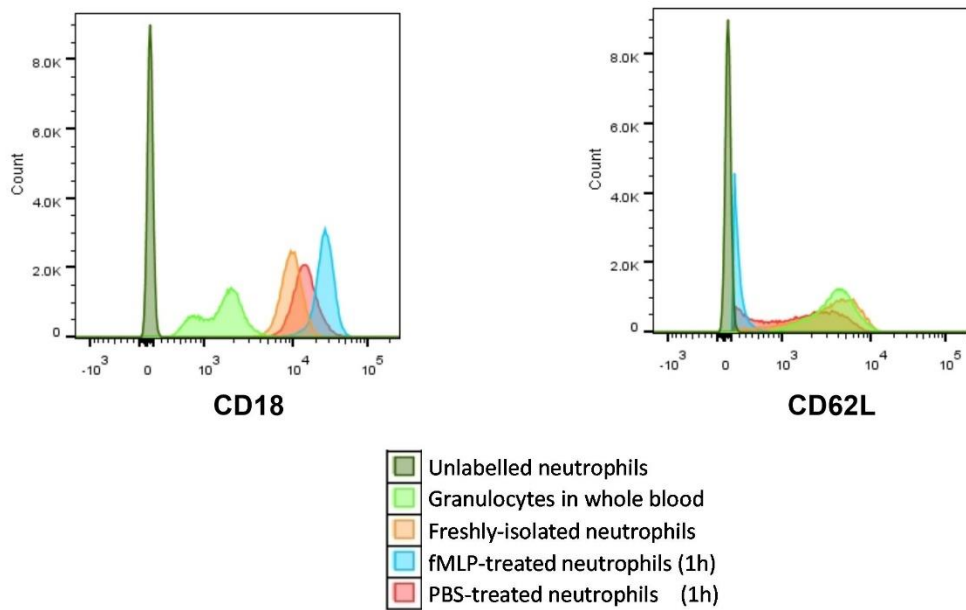
Figure 2.2 Peripheral blood neutrophil activation status after isolation and stimulation

Neutrophils were labelled with anti-CD18 and CD62L antibody according to the key provided and analysed by flow cytometry to determine neutrophil activation status at various stages of the isolation and stimulation process utilised here. Unlabelled cells (dark green histograms) indicated baseline cellular fluorescence without antibody labelling. Fluorescence intensity is shown on the x-axis and cell count on the y-axis. A shift to the right indicates upregulated expression and to the left, downregulated. Throughout the isolation process, neutrophils shed and lost CD62L and showed increased expression of CD18, for which maximal effects were seen in the fMLP-stimulated cells (blue histograms), therefore indicating increasing cellular activation. fMLP: N-formyl-met-leu-phe, PBS: phosphate-buffered saline.

2.2.2 Neutrophil-derived microvesicle quantification by flow cytometry

The NMV number in isolated samples was determined using the BD LSRII flow cytometer, based on the method proposed by Lacroix et al. (2010) and Poncelet et al. (2016). As the size range of NMVs resides at the lower limit of detection for the LSRII and most other flow cytometers (Lacroix, 2010), the use of Megamix beads facilitated the calibration of the flow cytometer for this purpose and allowed gating on a region of interest indicating a relevant size range. Thus, the NMV sample could be discriminated from debris and background noise.

Calibration with Megamix beads was done according to the manufacturer's protocol. Briefly, fluorescent beads of sizes 0.5 µM, 0.9 µM, and 3 µM were run through the flow cytometer. To distinguish between the bead populations, a dot plot for the fluorescence intensity in the blue channel with a 530/30 filter (Blue 530/30-A) against SSC-A was created (fig 2.3 (A)), using a combination of this graphs and a plot of FSC-A vs. SSC-A to visualise the beads, events below the 0.9 µM-sized beads were identified as a region of interest (ROI) (fig 2.3 (B), i.e. containing the NMV size range (~100-1000 nm).

Once the ROI had been identified, a known volume of sample could be processed by the flow cytometer using Sphero AccuCount Blank Particles (2.0–2.4 µM; ACBP-20-10; Spherotech). For this, 10 µL of AccuCount particles (10,000 beads) were added to 290 µL filtered PBS containing 20 µL of resuspended NMV sample to measure the number of vesicles. The stopping gate was set to 1,000 beads, corresponding to a sample volume of ~30 µL. Using a dot plot of SSC-A vs. FSC-A (log-scale), the counting beads and the NMVs were gated upon for quantification (fig 2.3 (C) and (D)). Representative flow cytometry plots containing calibration beads and subsequent NMV populations are demonstrated in figure 2.3.

The following equation was then used to calculate the total NMV number in a sample:

$$\frac{no.\,of\,NMVs\,(events)}{no.\,of\,beads\,counted} \times \frac{total\,no.\,of\,beads\,in\,sample}{final\,volume\,of\,undiluted\,sample}$$
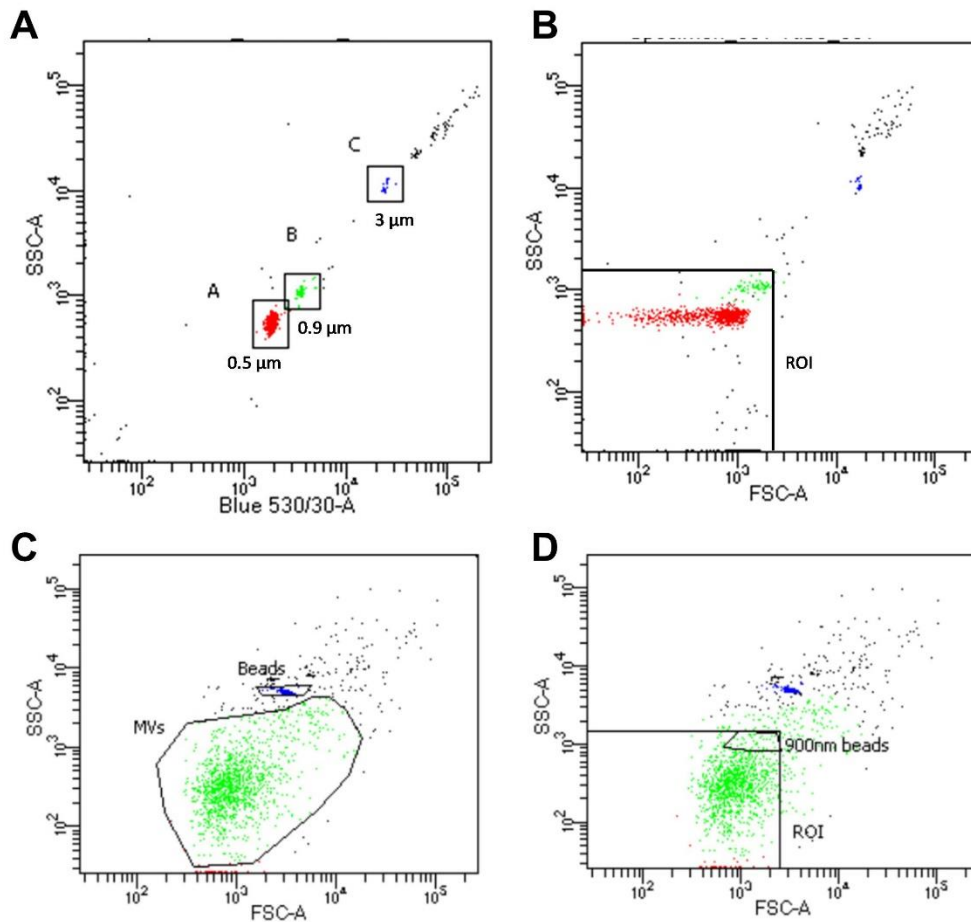
Figure 2.3 Flow cytometry set up for microvesicle analysis

Megamix calibration beads of size 0.5, 0.9 and 3 μm were identified by their size and fluorescent properties (A) and then used according to manufacturer's instructions to calibrate flow cytometry set up including setting of voltages, then finally were used to identify an appropriate region of interest (ROI; B) based on the 0.9 μm sized beads for subsequent analysis of microvesicles (C+D). (C) shows an isolated neutrophil-derived microvesicle population (MVs) and identification of counting beads for determination of absolute MV numbers. (D) shows were this population lies within the identified ROI.

2.2.3 Fluorescent Labelling of Neutrophil-Derived Microvesicles

NMVs were labelled using the membrane intercalating dyes, PKH26 (imaging) or PKH67 (flow cytometry), using a commercially available kit. For this, pelleted NMVs were resuspended in 200 µL of diluent C (kit component), a solution that helps to maintain cell viability. To a fresh tube, 200 µL diluent C was added plus 1.5 µL of PKH stain. This solution was immediately added to the NMV suspension and the mixture was slowly resuspended for ~2 min. The suspension was then centrifuged at 20,000 g for 30 min, the supernatant was removed and discarded, and the labelled vesicles were resuspended in ~300 µL of PBS ready for counting by flow cytometry.

2.2.4 Cytospin Preparation and Kwik-Diff Staining for Isolated Neutrophils (and Murine Bronchoalveolar Lavage Fluid)

Isolated neutrophil cell pellets were resuspended in DPBS at a concentration of 1×10^6 cells/ml, 10 µL of the suspension was added to 90 µL of 1% bovine serum albumin (BSA)/PBS to obtain approximately 1×10^5 cells. For murine BALF, cell pellet was resuspended in 400 µL of 1% BSA. The cytocentrifuge equipment was assembled, including a glass microscope slide, filter card, and chamber. 100 µL of the cell solution was then added into the chamber funnel and centrifuged at ~400 rpm for 5 min to adhere the cells to the slide. After air-drying overnight, the slides were stained using Kwik-Diff stain, incubating in each stain for 5 min to achieve a strong and clear stain, and then rinsing with distilled water (dH$_2$O). By this method, neutrophils could be morphologically distinguished from other cell types by the presence of a strongly stained blue/lilac multi-lobed nucleus, and light blue cytoplasm due to methylene blue uptake, quantified in figure 2.4. The granules of eosinophils became stained with eosin and could be distinguished by their pink-stained cytoplasm. Five images from random areas of the stained sample were then taken at ×20 magnification using a Nikon brightfield microscope. Cells were counted using the manual particle counting feature in ImageJ software, and the following formula was used to determine the proportion of each cell type:

$$\frac{average\ no.\ of\ cell\ type\ per\ image}{average\ total\ cell\ no.\ per\ image} \times 100$$
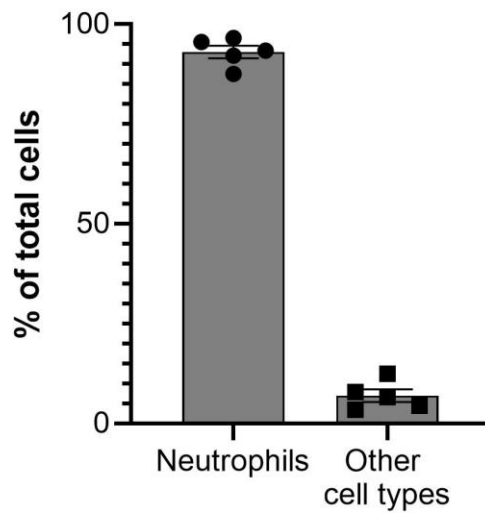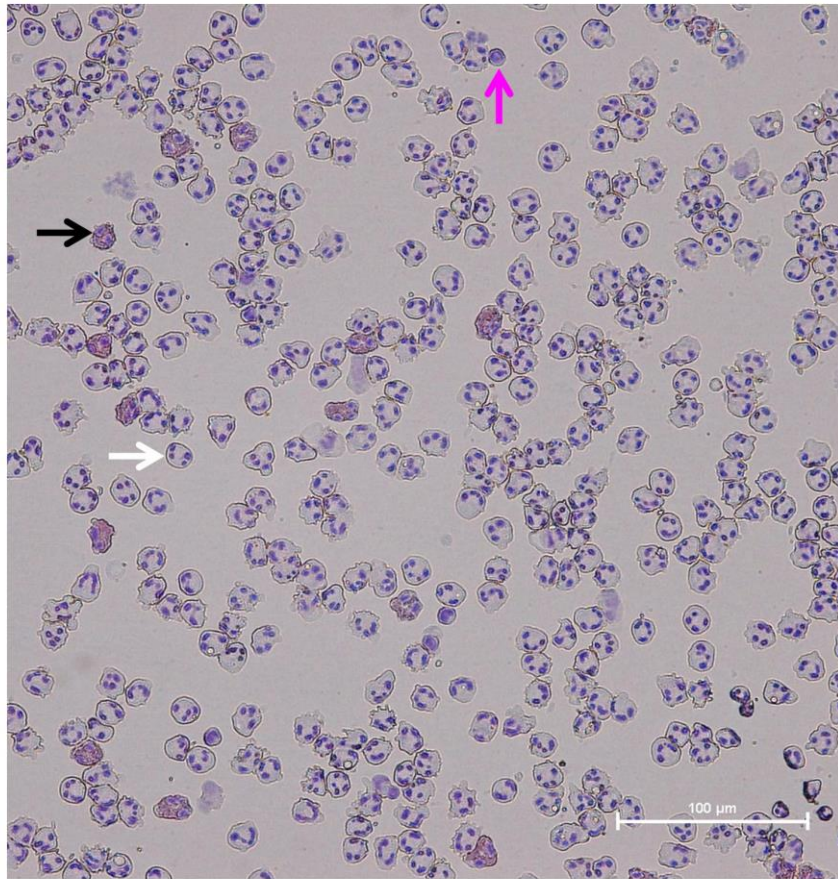
Figure 2.4 Isolated neutrophil sample cytospins and purity quantification

Representative cytospins of a neutrophil sample after isolation from peripheral blood stained with Kwik-Diff (A). White arrow indicates a neutrophil, black arrow identifies an eosinophil, and magenta arrow indicated a mononuclear cells, the latter define the two most common contaminating cell types in the neutrophil samples. Cytospins from five different isolations and different healthy participants were analysed to determine the purity of the neutrophil samples (B). Graph shows mean±SEM. Mean neutrophil purity was 93%.

2.2.5 Transmission Electron Microscopy

2.2.5.1 Resin embedding

To image the NMV population and check sample purity, transmission electron microscopy (TEM) was utilised. For this, NMVs pelleted at 20,000 g (30 min) in a 1.5 ml Eppendorf tube were fixed with ~200 μL of 2.5% glutaraldehyde for 2 hours. The pellet was then washed with 0.1 M sodium cacodylate buffer (prepared with distilled, deionised water) to maintain neutral pH without introduction of phosphates as in PBS and kept in this solution at 4°C overnight. NMVs were post-fixed in 2% osmium tetraoxide (OSO_4) for 30 min and washed with dH_2O three times by inserting and removing this solution, then replacing with fresh water, repeatedly. After that, the sample was washed with sodium cacodylate buffer again (washing procedure as for dH_2O), which was then discarded after ~5 secs, replaced with fresh buffer and incubated for ~3 min. The sample underwent ethanol dehydration using a graded ethanol series, with concentrations of 70%, 85%, 95%, 100%, and again 100% ethanol dried over anhydrous copper sulphate, for 15 min each. Following this, the NMV pellet was immersed in epoxy propane for 20 min to remove any residual ethanol. This solution was discarded and replaced with a 1:1 mixture of epoxy propane and resin (1:1 mix of CY212 araldite resin and dodecenyl succinic anhydride hardener, with 1 drop/ml of benzyl dimethylamine accelerator) and incubated in the fume hood on a circular rotator overnight. The resin mixture was removed and replaced with araldite resin without epoxy propane and incubated on the rotator for a further 4 h. Fresh resin was then added to the NMV pellet, at which point further processing was carried out by Christopher Hill from the Electron Microscopy Unit at Sheffield University. The NMV pellet was removed and placed into a mould for baking in a bench-top oven at 60°C for 24–48 h for solidification. The resin-embedded sample was then cut into 0.4 um-thick sections using a Lecia UC6 Ultramicrotome (Lecia Microsystems, Milton Keynes, UK) and block stained with 1% uranyl acetate in 50% ethanol for 30 min. Imaging was done on a Technai G2 Biotwin transmission electron microscope (FERI, Cambridge, UK).

2.2.5.2 Negative staining

NMV samples were pelleted using the isolation protocol described above in section 2.2.1.2 and then resuspended in ~20 μL of PBS and kept on ice until use. Using the Cressington 208carbon High Vacuum Carbon Coater (Cressington Scientific Instruments Ltd), copper grids were glow-discharged for ~25 secs in order to make the grids hydrophilic and enable subsequent sample absorption. After that, 5 μL of the resuspended NMV sample was absorbed onto the carbon-coated copper grid for 1 min. The grid was quickly blotted with filter paper and washed with ~50 μL of distilled water for a few seconds, blotted and washed again. After blotting for a third time, 50 μL of uranyl formate was added to stain the background and incubated for 20 secs. The grid was blotted again and any

remaining moisture was removed using a vacuum pump. A Philips CM100 transmission electron microscope was then used to image the grid. Final imaging steps were performed by Dr Svetomir Tzokov from the Electron Microscopy Core Facility at Sheffield University.

2.2.6 Zeta-View Nanoparticle Tracking Analysis

Nanoparticle tracking analysis (NTA) using the Zeta View (Particle Metrix, Meerbusch, Germany) was performed to determine NMV diameter in order to better characterise the NMV population isolated here. The machine was first calibrated with 110 nm polystyrene beads diluted 1:250,000 before each use to ensure accurate detection of particles. NMVs kept in a small amount of filtered PBS were then diluted to an appropriate concentration, established by testing a series of dilutions at the time of measurement, in 2-ml milliQ water and loaded into the cell. For the measurements, the frame rate was 3.75 frames per second and shutter speed 70, to detect larger particles. For post-acquisition analysis, parameters were: minimum brightness 25 and minimum area 5 and maximum area 999 pixels as per the established settings previously utilised in the department and recommended by the manufacturer. At 11 positions in the cell, measurements were captured, cycling twice at each position. Data analysis was performed using Particle Metrix software (ZetaView 8.03.08.03) and Microsoft Excel 2010 (Microsoft Corp., Seattle, WA, USA). Outlier positions were automatically removed by the Particle Metrix software. When compared to total NMV counts measured by flow cytometry, NTA measured over 300-fold more NMVs in the same sample (e.g. 0.663×10^6 vs. 266×10^6, respectively, in a sample utilised with both techniques), highlighting an important difference between technologies used for EV quantification.

2.2.7 Analysis of Neutrophil-Derived Microvesicle Surface Protein Expression by Flow Cytometry

2.2.7.1 Human plasma microvesicle quantification and characterisation

Plasma samples were obtained from COPD patients from two separate studies and analysed for circulating MV content. Blood samples from COPD patients and age-matched controls for the first study were collected by Dr Katharine Lodge (Study no.: 06/Q0108/281 and 08/H0308/281) from Cambridge University, Department of Medicine, as part of her PhD work, and the MV analyses performed here were part of a collaboration. These patients were admitted to hospital due to COPD exacerbation, and blood was taken within 48h from admission. Samples from 6 patients and 5 controls were analysed. The second study utilised samples collected in STH-Obs (study no. 15222) which included patients with co-morbid COPD and pulmonary hypertension (PH). Samples from 12 patients and 13 healthy, age-matched controls from this study were analysed. This study was in

collaboration with Prof. Allan Lawrie, the principal investigator for STH-Obs, at the Department of Infection, Immunity and Cardiovascular Disease, University of Sheffield.

MVs were labelled with fluorescently-conjugated antibodies and analysed by flow cytometry. For a batch of samples run together, one unlabelled sample plus four fluorescence minus one (FMO) controls, and four single-stained isotype controls (added at equal concentrations to target antibodies) were included, along with fully stained samples for all individuals. Platelet-poor plasma (PPP) was used, and 50 µl sample was added to 1.5 ml Eppendorf tubes in the formation mentioned above. To this, 50 µl of filtered PBS was added. Antibodies and volumes utilised for these two studies are described in table 2.1 below.

MV TYPE	EXACERBATING COPD		COPD WITH PH	
GRANULOCYTE	BV421 anti-CD66b [G10F5]	5 µL	FITC anti-CD66b [G10F5; 200 µg/ml]	2.5 µL
MONOCYTE	APC-Cy7 anti-CD14 [MφP9]	5 µL	BV421 anti-CD14 [M5E2; 70 µg/ml]	2.5 µL
ENDOTHELIAL	PerCP-Cy5.5 anti-CD144 [557H1]	5 µL	PE-Cy7 anti-CD144 [16B1; 100 µg/ml]	5 µL
PLATELET	PE anti-CD41a [HIP8]	5 µL	APC anti-CD41a [HIP8; 25 µg/ml]	2.5 µL

Table 2.1 Antibodies for plasma microvesicle labelling and identification in two studies of COPD patients.
Volumes and concentrations as well as clones of stock antibody formulations utilised are shown.

Optimum antibody volumes as well as flow cytometer voltages for each of these had been determined previously by carrying out titration experiments (performed by MRes student Darcy Sidebotham under my day-to-day supervision and supervision of Dr Victoria Ridger) and analysed in FlowJo software to calculate the separation index (SI) for each condition/setting. Examples of the output from these experiments are shown below in figure 2.5 and 2.6. The larger the SI value, the better the separation between negative and positively-stained MV populations. The equation used

to calculate SI was as follows, where each value refers to use of the appropriate fluorescence intensity:

$$\frac{MedianPositive - MedianNegative}{(84\%Negative - MedianNegative)/0.995}$$

In addition to these panels, MMP-9 was labelled on CD66b$^+$ MVs using 5 µl mouse anti-human FITC anti-MMP-9 in the same protocol described here in both isolated NMV samples from healthy donors and plasma MVs from the two patient studies.

Samples were incubated in the dark, on ice, for 45 min with gentle shaking. After the incubation, the samples with topped up with 200 µl of filtered PBS to permit MV washing, and then centrifuged at 4°C for 30 min, 20,000 g. The supernatant was removed and discarded, and the MV pellet was resuspend in 290 µL of 0.2 µm-filtered PBS. 10 µl of vortexed counting beads were added to each tube to allow calculation of absolute MV numbers. Samples were pipetted vigorously before loading into flow tubes and analysing on the LSRII flow cytometer.

Compensation experiments were performed for these antibodies using AbC anti-mouse bead kit according to the manufacturers protocol, using the optimised volumes of antibody. These data were then analysed and compensation was applied to the samples in FlowJo software post-analysis.
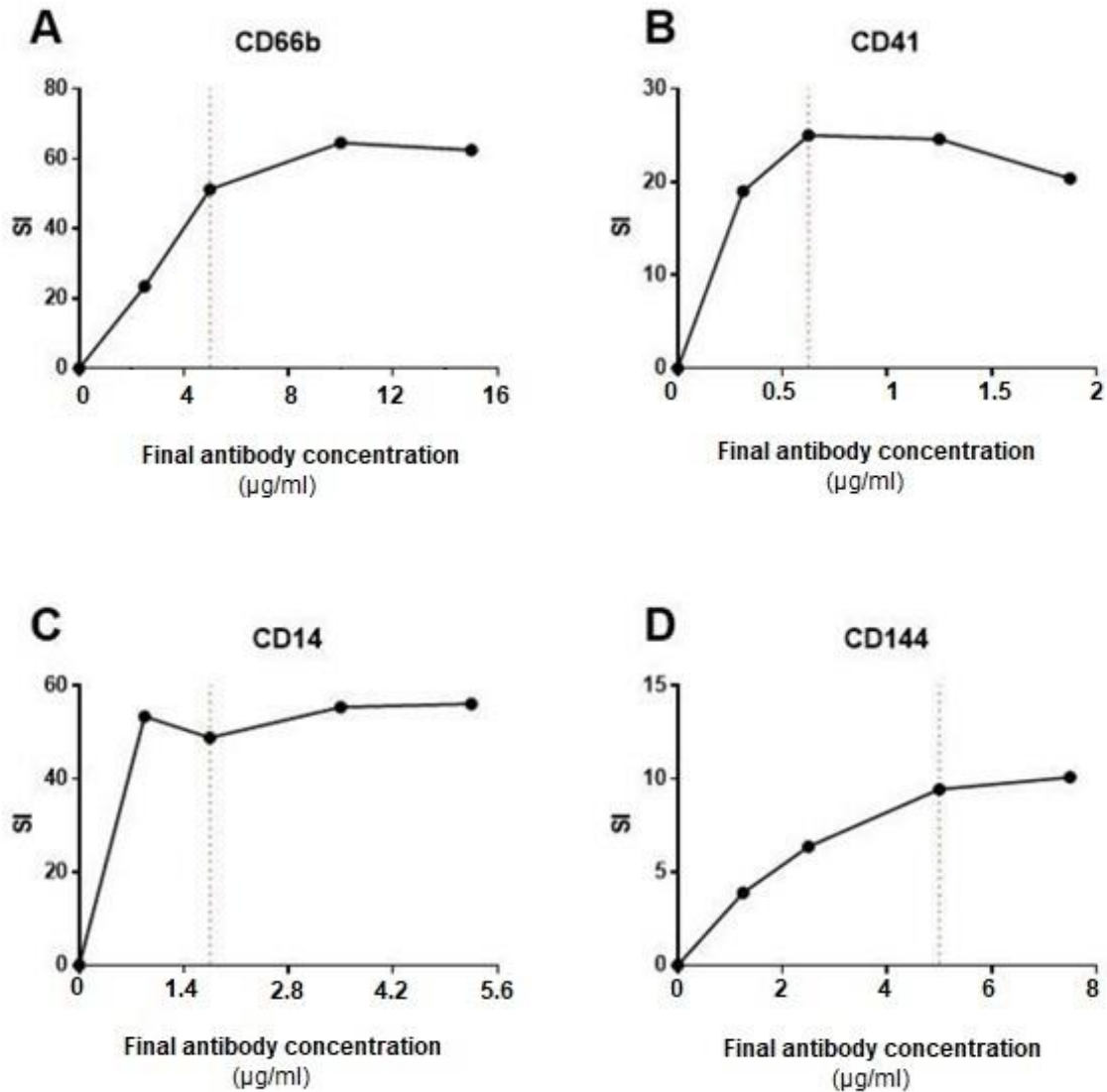
Figure 2.5 Optimisation of antibody concentration for plasma microvesicle labelling and flow cytometry analysis

Antibodies against human (A) CD66b, (B) CD41a, (C) CD14 and (D) CD144 were tested at a range of concentrations (volumes of 1.5, 2.5, 5, 7.5 µl tested; final concentrations of each antibody used at these volumes is shown) for labelling human plasma microvesicles (MVs). MVs were analysed for surface labelling by flow cytometry. Separation index (SI) was calculated using the formula function in FlowJo software to determine the concentration providing maximal separation of negative and positively-labelled MV populations. Experiments performed by Darcy Sidebotham (MRes student) under my day-to-day supervision. Representative examples of 1 experimental run shown. Dotted line shows optimal concentration chosen for further experiments.
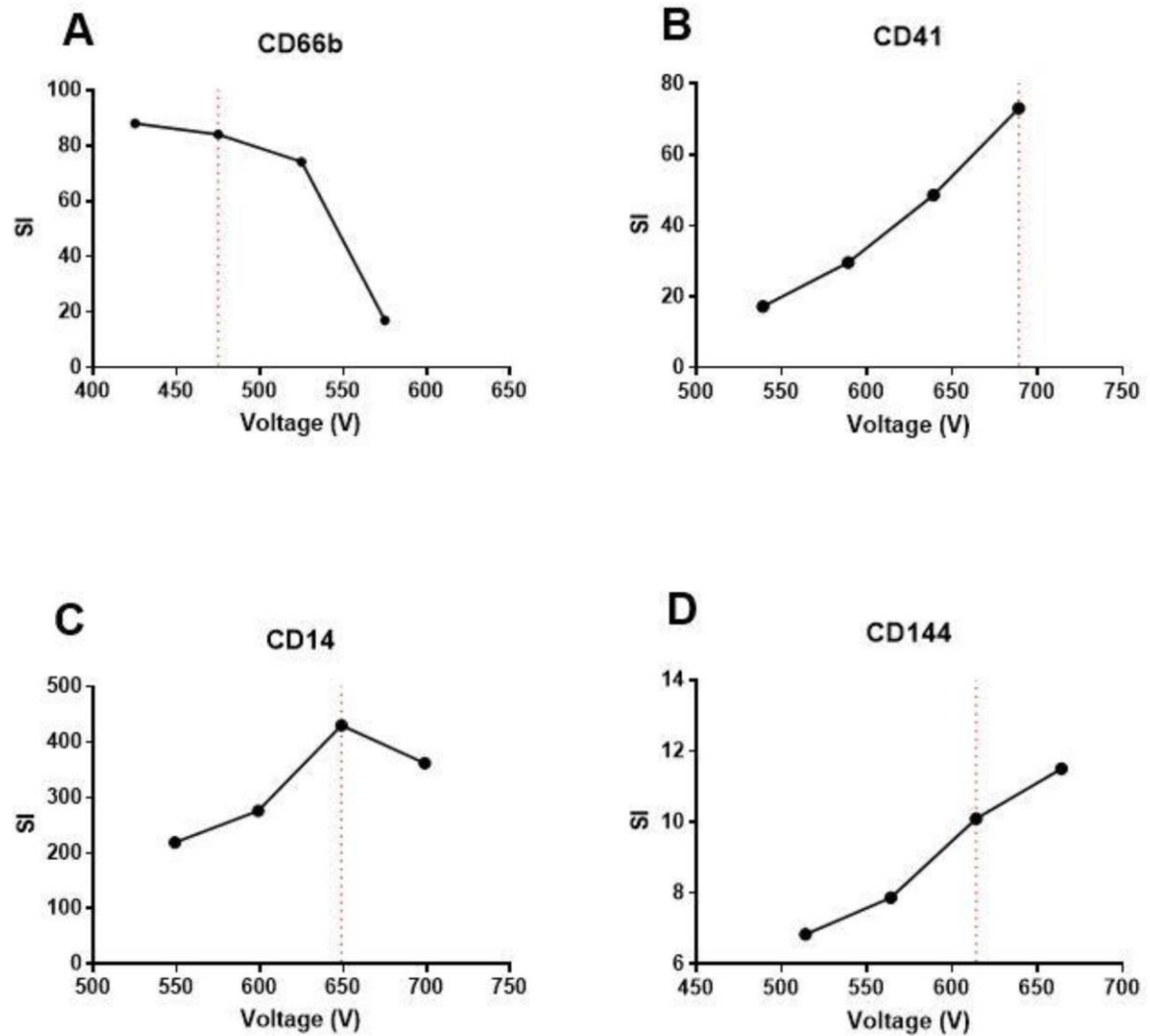
Figure 2.6 Optimisation of laser voltages flow cytometric analysis of labelled plasma microvesicles

Antibodies against human (A) CD66b, (B) CD41a, (C) CD14 and (D) CD144 were tested at the concentration determined in figure 2.5, at a range of laser voltages. Plasma microvesicles (MVs) were analysed for surface labelling by flow cytometry. Separation index (SI) was calculated using the formula function in FlowJo software to determine concentration providing maximal separation of negative and positively-labelled MV populations. Experiments performed by Darcy Sidebotham (MRes student) under my day-to-day supervision. Representative examples of 1 experimental run shown. Dotted line shows optimal voltage for each antibody chosen for further experiments.

2.2.7.2 Healthy participant NMV antibody labelling for MMP-9 and CD44 and analysis

In order to further elucidate potential mechanisms by which NMVs exert protease activity, NMVs isolated from peripheral blood neutrophils were analysed for surface expression of MMP-9 and the adhesion molecule CD44.

For this, 1×10^5 NMVs resuspended in 100 µl of 1% BSA/PBS, which has been twice filtered (0.2-µm filter), were incubated with either mouse anti-human FITC anti MMP-9 (5 µl) and APC anti-CD44 (5 µl), or equal concentrations of the respective isotype controls. An unlabelled control was also included to determine baseline fluorescence. NMVs were incubated, protected from light, for 45 min on ice with gentle shaking. Following this, 200 µl of filtered PBS was added and NMVs were washed and pelleted by centrifugation at 30 min, 20,000 *g*. The supernatant was discarded and 200 µl of filtered PBS was added. Resuspended NMVs were analysed by flow cytometry. Data was analysed in FlowJo software.

2.2.7.3 Murine microvesicle analysis: bronchoalveolar lavage fluid

Neutrophil (Ly6g+), macrophage (f4/80+) and epithelial (EpCAM+) -derived MVs were detected and quantified in murine BALF samples by flow cytometry. For this, after pelleting and removing cells at 500 *g*, 5 min, BALF was stored at -20°C until analysis, which was less than 1 week later for all samples. 50 µL of cell-free BALF thawed on ice was added to 50 µl of 0.2µm-double-filtered 1% BSA to facilitate blocking of non-specific antibody binding. For MV labelling, the same method as described here in section 2.2.7.1 was utilised. After antibody incubation, BALF was centrifuged at 20,000g to pellet MVs and these were resuspended in filtered PBS for analysis. Spherotech counting beads were used to determine absolute MV counts as described in section 2.2.2.

2.2.8 BEAS-2B Subculture

The transformed BEAS-2B human bronchial epithelial cell line was used to model pulmonary epithelial function in this study. Cells were purchased from ATCC (LGC Standards, Teddington, UK).

Cells were counted using a manual haemocytometer and seeded at ~2×10^6 cells/flask in 12 mL of culture medium. Cells were cultured in T75 cell culture flasks in RPMI 1640 medium supplemented with 1% L-glutamine, 1% penicillin-streptomycin and 10% foetal calf serum (FCS). When ~80% confluent, cells were detached from the flask using 2 mL of cell dissociation solution in which was subsequently neutralised with 8 mL of media. However, in 2018, when supplier recommendations changed, 0.4% Trypsin diluted 1:2 in PBS was performed for cell detachment instead, neutralised in

the same amount of culture media. Cells passaged twice per week and were used for experiments at passages 4–15 after defrosting from storage at −80°C.

2.2.9 Epithelial Intracellular Adhesion Molecule-1 Labelling and Analysis by Flow Cytometry

Epithelial ICAM-1 (CD54) expression was measured using flow cytometry to determine effects of NMVs on the expression of this adhesion molecule and activation marker. BEAS-2B cells were seeded at a density of 2×10^4 cells/well in 100 µl culture media in a 96-well plate and grown to confluency (approx. 24h). NMVs (3000 NMV/µl; i.e. 240,000 NMV/well), 10 µg/ml LPS (positive control), or media only (control) were added and cells were incubated for the indicated time points. The approximate ratio of epithelial cells to NMVs at the start of the experiment was 1:6. Cells were then washed three times by addition and removal of fresh PBS to remove serum and stimuli and detached by gentle trypsinisation (0.4% trypsin diluted 1:6 in PBS; 5 min, 37°C) to avoid cleavage of surface ICAM-1. Culture media containing serum was added to neutralise trypsin and cell suspensions were added to 1.5 ml Eppendorf tubes and centrifuged at 300 g, for 5 min, 4°C. Cells were washed twice with cold PBS by resuspension of the cell pellet and then centrifugation to pellet once more, and then resuspended in 100 µl 1% BSA/PBS. 1 µl mouse anti-human FITC-conjugated ICAM-1 antibody was added. Samples were incubated on ice, protected from light, for 30 min with gently shaking. Following this, cells were washed twice with cold PBS and then finally resuspended in 400 µl of 1% BSA/PBS for analysis on the LSRII flow cytometer. The cell population was identified using an FSC-A vs. SSC-A dot plot, and single cells were subsequently identified using a plot of FSC-A vs. FSC-H. These cells were then analysed for fluorescence in the blue channel with 530/30 filter. Unlabelled cells were used to determine baseline fluorescence in each experiment.

2.2.10 Confocal Imaging of Neutrophil-Derived Microvesicle Internalisation in BEAS-2B Cells

2.2.10.1 Collagen-I Coating of Glass Coverslips

To allow imaging of BEAS-2B cells, glass coverslips were coated with rat-tail collagen-I to facilitate cell adhesion and spreading. For this, collagen-I stock (8.2 mg/ml) was diluted to 0.5 mg/ml in 0.02 M sterile-filtered acetic acid. To each coverslip-containing well, 400 µL of collagen-I solution was added and incubated for 1 h at RT. The solution was removed and the coverslips were left to air-dry to allow evaporation of any remaining acetic acid. The wells were then washed three times by repeated addition and then removal of fresh PBS and air dried again. When completely dry, BEAS-2B cells were seeded onto coverslips at a concentration of ~6×10^5 cells/well and grown in supplemented RPMI as above for 2–3 days (37°C, 5% CO_2) until a confluent monolayer had formed.

2.2.10.2 Staining and Imaging of Neutrophil-Derived Microvesicle Internalisation in BEAS-2B Cells

When BEAS-2B cells were confluent on the coated glass coverslips, 200 μL of PKH-26-labelled NMVs resuspended in growth media at a concentration of 400 NMVs/μL were added to the cells. To the control sample, an equal amount of media was added. The co-cultures were then incubated at 37°C, 5% CO_2 for 2 h. To remove any unbound NMVs, incubation media was removed, then cells were washed twice by gently pipetting pre-warmed PBS into the well then removing and discarding this and replacing once more with PBS. All washing steps in this section were done following this procedure. Cells were then fixed using 4% paraformaldehyde (PFA, 15 min, RT). This was followed by three 5 min washes with PBS to remove the PFA, and cells were then permeabilised by incubation with 0.1% Triton X-100/PBS for 5 min. Cells were washed three times again with PBS (5 min each, as above) and then non-specific binding was blocked by incubation with 1% BSA/PBS for 30 min. FITC-phalloidin (1:50 in PBS, 40 min) was used to stain cellular F-actin. The coverslips were washed twice with PBS and then incubated with the nuclear stain TOPRO-3-iodide (1:500 in PBS) for 3 min. Following a final washing step with PBS, coverslips were removed from the wells and blotted to eliminate excess moisture. For sample and stain preservation, 10 μL of Prolong Gold mounting media was added and coverslips were then mounted onto glass microscope slides. The slides were shielded from light to avoid photo-bleaching and the mountant was left to set overnight. After this, the slides were stored in aluminium foil at 4°C until imaging with a Zeiss confocal microscope using a 64x oil-immersion lens. Images were then processed using LSM image software (Zeiss).

2.2.11 Fluorescence Microscopy Imaging of Neutrophil-Derived Microvesicle Uptake in BEAS-2B Cells

For faster imaging, to compare uptake of NMVs from different stimuli (CSE and fMLP), BEAS-2B cells grown in a 96-well plate were incubated with 3000 NMV/μl of NMVs from these stimuli or media alone was added to the wells for 2h at 37°C, 5% CO_2. Cells were then washed three times with PBS by addition and removal of this solution, and fixed using 4% PFA for 15 min at RT. Wells were washed again, nuclei were stained with Hoechst 33342 (1:2000) and cell membranes were stained using Alexa Fluor 647-conjugated wheat germ agglutinin (AF657-WGA; 1:200) in 1% BSA/PBS and providing an advantage over phalloidin labelling of F-actin and To-Pro-3-idiode in being cell permeant and removing a permeabilization step. After 15 min staining, cells were washed again and then kept in PBS. Cells were imaged within 24h of fixation using a Leica AF6000 widefield microscope. Three individual fields of view (f.o.v) per well were imaged.

2.2.12 Flow Cytometry Analysis of Neutrophil-Derived Microvesicle Internalisation in BEAS-2B Cells

2.2.12.1 Detection of internalisation

In order to quantify the proportion of BEAS-2B cells that internalised NMVs, flow cytometry of quenched samples was employed. The principle behind the experiment is that unlabelled BEAS-2B cells that internalised PKH-67-labelled NMVs acquire a fluorescent signal, and external fluorescence (representing NMVs adherent to the cell surface) was quenched using trypan blue (Patino, Soriano et al., 2015). More commonly used to quench extracellular fluorescence in assays of immune cell phagocytosis of fluorescent bacteria, trypan blue is able to quench fluorescence excited by the 488 nm laser, including cellular autofluorescence. The baseline fluorescence was set using unlabelled BEAS-2B cells without NMVs which had been incubated with media alone for 2 h. Confluent BEAS-2B cells in 96-well plates were incubated with PKH-67-labelled NMVs, derived from either fMLP or CSE stimulation, at a concentration of 3000 NMVs/µL for 2 h (37°C, 5% CO2). Cells were then washed twice with PBS to remove unbound NMVs and detached using 50 µL of pre-warmed trypsin/EDTA. Trypsin was neutralised with 200 µL of cell media and cells were transferred into 1.5 mL Eppendorf tubes and pelleted by centrifugation at ~500 g for 5 min. The supernatant was removed and replaced with 500 µL PBS. Trypan blue (100 µL) was added to quench extracellular fluorescence and the population of single cells was gated upon using SSC-A and FSC-A on the LSRII flow cytometer. This method was previously optimised and performed in the Ridger lab, and trypan blue quenching was confirmed in later MDM NMV internalisation experiments, shown in figure 2.7. PKH-67-positive cells were identified using the Blue (488 nm) channel with 530/30-A filter. Analysis of flow cytometry data was then conducted using FlowJo software (FlOWJO LLC., Ashland, OR, USA).

2.2.12.2 Inhibitors of internalisation

To investigate the mechanism if NMV internalisation by BEAS-2B cells, the experiments above were repeated with the addition of the inhibitors. To inhibit actin polymerisation, and therefore several endocytic processes, cytochalasin D (1 µM) or vehicle control (DMSO) was added to cells 30 min before NMV addition, as this was shown to be an optimal concentration for NMV uptake inhibition in several cell types in our lab previously (Ben Ward, PhD thesis, 2018)(Ajikumar *et al.*, 2019). This inhibitor was kept in the cell media for the duration of the experiment. Cells were analysed as above. To examine whether NMV uptake in general was energy dependent, cells were incubated at 4°C for the duration of the experiment.

	Sample Name	Subset Name	Median : Blue 530_30-A
	MDM_MV 1 w,2f,o trypan_003.fc	Single Cells	165
	MDM_MV 1 with trypan_004.fcs	Single Cells	105
	MDM_unlabelled 1_001_002.fcs	Single Cells	66.2
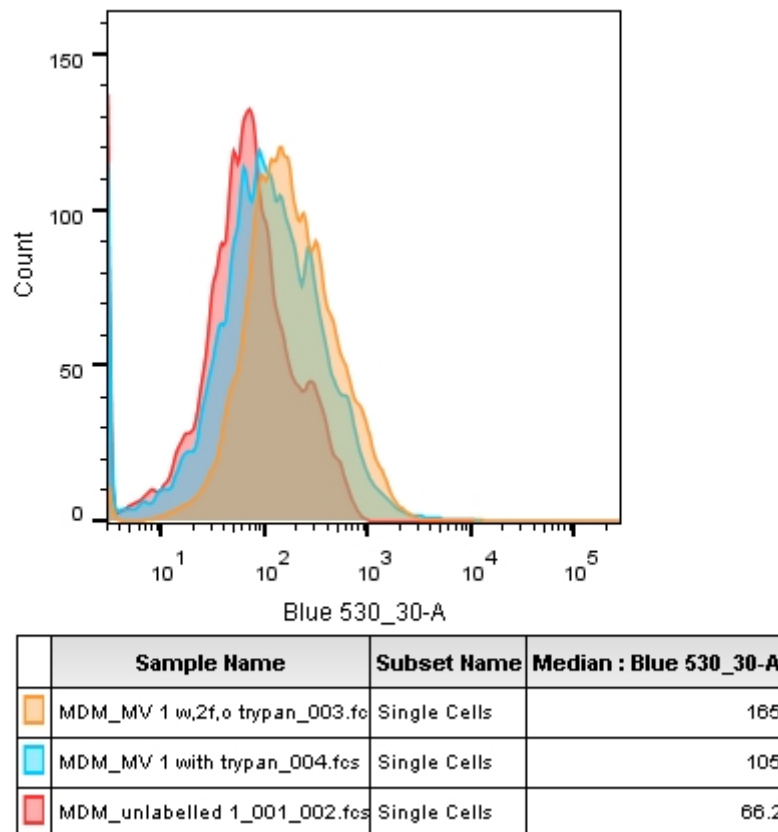
Figure 2.7 Trypan blue quenching of extracellular fluorescence in monocyte-derived macrophage NMV internalisation experiments

Human monocyte-derived macrophages (MDM) were incubated with PKH67-labelled neutrophil-derived microvesicles (NMVs) for 2h. Cells were then detached using gentle trypsinisation and fluorescence intensity measured by flow cytometry. MDM incubated with NMV were initially analysed (orange), then 100 µl of Trypan blue was added and the sample was reanalysed (blue). Red = control condition i.e. cells without NMV addition. Median fluorescence intensity (MFI) is shown in the third table column, reduced MFI was observed after trypan blue addition compared with no trypan addition. 1 experimental run is shown.

2.2.13 Enzyme-Linked Immunosorbent Assay

Human MMP-9 DuoSet ELISA from R&D was used to measure the concentration of this protein in isolated NMVs, neutrophils, plasma MVs, and MV-depleted plasma. TIMP-1 ELISA from PeproTech was performed in human plasma MV and MV supernatant. In addition, IL-8 and MCP-1 ELISAs were carried out in BEAS-2B conditioned media/supernatant, and murine KC/CXCL-1 and JE/CCL-2 ELISAs (all from R&D) were performed using mouse BALF or plasma. These assays were performed according to the manufacturer's instructions, with one modification for MMP-9 and MCP-1. Briefly, a 96-well flat-bottom high-binding plate (EIA/RIA Clear Flat Bottom Polystyrene High Bind Microplate, Corning Inc.) was coated with capture antibody diluted in PBS and incubated overnight (approx. 16h) at RT, with a plastic covering. All washing steps were carried out three times using wash buffer and an automated plate washer (ELx50 auto washer; BioTek), unless otherwise stated. Wells were washed and then blocked with 300 µL blocking buffer (1% BSA (w/v) in PBS) for 1 h. The plate was washed again and then 100 µL of sample or standard was added. 1% BSA was used as the reagent diluent. Samples were incubated for 2h at RT, apart from MMP-9 and MCP-1 ELISAs, which were incubated for 3h due to weak signal using the standard protocol, including for standard curves. The plate was washed, 100 µL of detection antibody (diluted in BSA/PBS or in diluent plus 20% normal goat serum for the MMP-9 ELISA) was added, and the plate was incubated at RT for 2 h. This was followed by washing and then incubation with 100 µL of streptavidin-horseradish peroxidase (HRP) at RT for 20 min. The plate was washed again and 100 µL of substrate solution was added to activate the HRP. After incubation for max. 20 min, or when strong but differential signal was observed in the top two standards, 50 µL stop solution (1N H_2SO_4) was added to the wells to terminate the reaction. The optical density was determined using a microplate reader at 450 nm. A blank subtraction was performed for all the values and then the standard absorbances were log transformed and plotted using a four-parameter logistic curve, allowing interpolation of unknowns using GraphPad Prism version 7.00 for Windows (GraphPad Software, La Jolla, CA, USA).

2.2.14 Investigation into Neutrophil-Derived Microvesicle-Induced Changes in Cytokine Gene and Protein Expression

To determine the effects of NMVs on epithelial proinflammatory gene expression, quantitative polymerase chain reaction was used. BEAS-2B cells grown to confluency in 96-well plates were treated with NMVs (3000/µl) generated from either fMLP or CSE stimulation. Small well size was used to due to NMV numbers required to mimic physiological concentrations in the lung. Control wells were treated with media only, LPS (10 or 1 µg/ml, relevant concentration indicated in results sections) or TNF-α (10 ng/ml) for 2 h to measure gene expression by qPCR or 24h to measure protein secretion by ELISA.

Following treatment, cells were washed three times with PBS, and lysed using 100 µl TRIzol. Wells were scraped using a p200 pipette tip for 30 s to detach cells and added to a 1.5 ml Eppendorf. To this 100 µl of 100% ethanol was added, and the solution was transferred to a MicroPrep Zymo-Spin IC column, designed for optimal RNA isolation from smaller amounts of starting material. RNA extraction was performed according to manufacturer's protocol. Briefly, columns were centrifuged at 16000 *g* for 30 s. All proceeding centrifugation steps were performed with these settings unless otherwise stated. The flow-through was discarded and 400 µl of wash buffer (provided in Zymo kit) was added. Tubes were centrifuged again with the same settings to isolate the RNA. 5 µl DNase I plus 35 µl DNase digestion buffer was added to the columns and these were incubated at RT for 15 min. To remove digested DNA, 400 µl RNA prewash was added and tubes were centrifuged again. Flow-through was discarded and this step was repeated once more. 700 µl RNA wash buffer was added and tubes were centrifuged again but for 2 min to ensure all buffer was removed from the column filter. RNA was then eluted into an RNase-free tube by adding 15 µl nuclease-free water and centrifuging once more. The resulting RNA was then stored at -80°C until further processing or used directly for cDNA synthesis.

The RNA concentration obtained using this protocol was determined on the day of cDNA synthesis, using the Nanodrop 1000 Spectrophotometer. A blank sample of 1 µl nuclease-free water was used to determine background from this medium at 260 nm, then a 1 µl sample of RNA was taken from each tube and measured using the same method. Purity was determined by measuring the ratio of absorbances at 260/280 nm (indicating protein contaminants) and 260/230 nm (chemical contaminants).

2.2.14.2 cDNA synthesis

After extracting and quantifying RNA using the protocol above, complementary deoxyribonucleic acid (cDNA) synthesis was done using the iScript cDNA synthesis kit. Within a reasonable range, the lowest RNA concentration obtained above was used as the target concentration for all samples obtained in the experimental run. cDNA synthesis was performed according to the manufacturers protocol. Briefly, a volume of RNA sample was taken according to the desired concentration of cDNA and made up to a final volume of 15 µl with nuclease-free water in a PCR tube. To this, 4 µl of reaction mix and 1 µl of reverse transcriptase was added. Tubes were inserted into a Verti 96-well thermocycler and the iScript protocol was followed for temperatures and incubation time (5 mins at 25°C, 30 mins at 42°C, 5 mins at 85°C, then 4°C, 10 min- ∞)

After cDNA synthesis from NMV-treated BEAS-2B cells as detailed above, the mRNA expression levels of MCP-1 and IL-8 were measured. GAPDH was used as a housekeeping gene. Primers for these genes were as follows:

GENE TARGET	FORWARD	REVERSE
CXCL-8/IL-8	5´-GGCACAAACTTTCAGACACAG-3´	5´-ACACAGAGCTGCAGAAATCAGG-3´
CCL-2/MCP-1	5´-GCAGAAGTGGGTTCAGGATT-3´	5´-TGGGTTGTGGAGTGAGTGTT-3´
GAPDH	5´-CATCAATGGAAATCCCATCA-3´	5´-TGGGTTGTGGAGTGAGTGTT-3´

´

Reactions were carried out in triplicate for each sample and gene. Per reaction, i.e. one well in a 348-well plate, 4.4 µl cDNA (at a final concentration of 2 ng/µl), 0.3 µl each of forward and reverse primers and 5 µl of Ssoadvanced Universal SYBR green supermix was added. An adhesive plate sealer was applied to prevent contamination and the plate was centrifuged for 1 min at 1500 rpm to mix well content and ensure this was at the bottom of the well. A BioRadCFX384 Touch Real-Time PCR detection system was then used to analyse the samples. SYBR green allowed the quantification of gene expression though detection of the fluorescent signal emitted by the dye upon binding to DNA amplified during the PCR. The PCR cycles employed are detailed below.

Step	Temperature (°C)	Time (s)	Cycles
Denaturation and probe activation	95	30	1
Denaturation	95	10	40
Annealing/extension	64	30	
Melt curve	65–95 (0.5 increments)	5	1

Fold change of target genes was analysed using ΔΔCt analysis. CT values were averaged across the triplicates and then normalised to GAPDH expression (by subtracting the average GAPDH Ct value), providing the ΔCt. This was then subtracted from the ΔCt for the control condition, generating the ΔΔCt. The relative fold-change in gene expression was then calculated using $2^{-\Delta\Delta Ct}$. A change greater than or less than 1 indicated an up- or downregulation of these genes, respectively.

2.2.15 Micro Bicinchoninic Acid Assay

To ensure equal total protein loading for each sample for subsequent MMP-9 western blotting, a micro bicinchoninic assay was used. Its ability to quantify low protein concentrations was particularly advantageous due to the small size and protein yield of the NMV samples. The principle behind the

assay consists of the reduction of Cu^{2+} to Cu^{1+} by proteins in an alkaline solution, indicated by a colour change. The assay was carried out according to the manufacturer's instructions, with some modifications. Briefly, 30 µL of sample, which had been diluted with lysis buffer (between 1:40 and 1:320 for neutrophil samples and 1:10 to 1:20 for NMV samples), was added to a 96-well high binding plate in duplicate. A BSA standard curve was generated from 0–200 µg/mL, and 30 µL of each standard was added in triplicate. To each well was then added 150 µL of working reagent (in the ratio 25:24:1 for reagent A:B:C). The sample to working reagent ratio was 1:5 in order to preserve the small amount of NMV sample available. This dilution was checked against the recommended protocol and yielded similar results in preliminary investigations (data not shown). The plate was then incubated at 37°C for 2 h to promote the reduction reaction. The optical density was then determined at 562 nm using a microplate reader. The average absorbance of the blank standard was then subtracted from all other absorbance readings and a quadratic polynomial standard curve was plotted in GraphPad Prism. From this, the absorbances of the unknown samples were interpolated to calculate the protein concentrations present.

2.2.16 Western Blotting

In order to investigate MMP-9 protein expression in the neutrophil and NMV samples, and junctional protein (ZO-1) and ER-stress markers in NMV-treated BEAS-2B cells, western blotting was used. To fresh samples, 1x RIPA lysis buffer containing 0.1%SDS plus 1:100 protease inhibitor cocktail was added. Samples were thoroughly resuspended by scraping (where culture plates were used for BEAS-2C cells) and vigorous pipetting, then incubated for 30 min in ice. Samples were then sonicated three times in a small sonication bath containing ice-cold water, for 7 min, three times. In between sonication cycles, samples went through freeze-thawing three times in total, to ensure maximal cell break down. Subsequently, samples were centrifuged at 10,000 *g,* for 10 min, to pellet cellular debris, supernatant was removed to a fresh tube and stored at -20°C until use within 2 weeks. To promote protein denaturation and sorting of proteins by size using sodium dodecyl sulphate polyacrylamide gel electrophoresis, a 5× stock solution of lamellae buffer (5% SDS, 50% Glycerol, 0.1% Bromophenol Blue, 25% β-mercaptoethanol, 250 mM Tris-HCl, pH 6.8) was diluted to 1× with the diluted samples. To ensure protein denaturation the samples were boiled at 95°C for 5-10 min. They were then very briefly centrifuged (1 min) using a benchtop microcentrifuge to avoid sample loss due to condensation, and loaded onto a gel made up of a 4% stacking gel (3.57 mL dH$_2$O, 1.875 mL 0.5 M pH 6.8 Tris-HCl, 1 mL 30% acrylamide, 75 µL 10% SDS, 75 µL 10% ammonium persulphate (APS), 10 µL Tetramethyl ethylenediamine (TEMED)) and a 7.5% running gel (11.5 mL dH$_2$O, 6 mL 1.5 M pH 8.8 Tris-HCl, 6 ml 30% acrylamide, 240 µL 10% SDS, 240 µL 10% APS, 24 µL TEMED). For the neutrophil and NMV samples, 1.5 µg of total protein was loaded due to the high expression of MMP-

9 in these samples and low abundance of protein. For BEAS-2B cells, equal volume loading was employed (18 µL). 1x sample buffer was added to empty wells after sample loading. A broad-range protein ladder was added to determine the size of proteins detected in the sample. The gel tank (Bio-Rad) was filled with running buffer (1 L dH$_2$O, 14.4 glycine, 3 g Tris, 1 g SDS) and run at 150 V for ~80 min until the dye front had run to the bottom of the gel.

For protein transfer, am Immobilon-P polyvinylidene fluoride membrane was used. This was first activated by incubation with methanol for 2 min, followed by washing once with dH$_2$O. The gel was then removed from the glass mould and put into the transfer cassette sandwiched with filter paper, sponges, and topped with the membrane.

A roller was used to ensure the removal of any air bubbles between the gel and membrane and then the cassette was added to a gel tank filled with transfer buffer (800 mL dH$_2$O, 14.4 g glycine, 3 d Tris, 200 mL methanol) and transferred for 75 min at 35 V. To ensure that the temperature in the tank remained low, an ice block was added for the duration of the transfer. The membrane was when removed from the apparatus and non-specific binding was blocked with 5% milk/tris-buffered saline with Tween 20 (TBST) for 1 h. Following this, the membrane was cut according to the size of the target proteins and incubated overnight at 4°C with primary antibody (Mouse anti-human MMP-9, 1:200, rabbit anti-human glyceraldehyde 3-phosphate dehydrogenase (GAPDH), 1:3000, rabbit anti-human ZO-1 (1:2000) or mouse anti-human GRP78, 1:1000) diluted in 3% BSA/TBST. This was followed by three washes with TBST for 5 min each, or 30 min each for GRP78 using 5% Milk/TBST. Secondary HRP-conjugated antibody (for mouse antibodies: polyclonal goat-anti mouse HRP, 1:4000; for rabbit antibodies: polyclonal goat anti-rabbit HRP, 1:3000) was then added and the membrane sections were incubated separately on a plate shaker for 1 h. Three washes of 5 min (30 min for GRP78) each with TBST were done, and in order to detect the antibody-bound protein bands, chemiluminescence reagent (~1 ml per membrane section) was added to activate the HRP. After a 3 min incubation, the membrane was imaged using the C-DiGit blot scanner (LI-COR Biosciences, Lincoln, NE, USA) for MMP-9 or the Bio-Rad Chemidoc MP for all other antibodies.

2.2.17 Gelatin Zymography using Neutrophil-Derived Microvesicles and BEAS-2B Supernatant

To determine the activity of MMPs in NMVs and supernatant of NMV-treated BEAS-2B cells, gelatin zymography was performed. This technique allows separation and identification of MMPs based on size or protein length and also semi-quantitative measurement of enzyme activity based on substrate degradation. For analysis of NMVs only, vesicles were pelleted and lysed in 1x non-

reducing lamellae buffer according to the recipe described above. Samples were sonicated as described above to release NMV contents but were not boiled, to promote non-reducing conditions. To understand the effect of NMVs on epithelial MMP expression, BEAS-2B cells seeded in a 96-well plate and grown to confluency were treated with NMVs (3000/µl), TNF-α (10 ng/ml; positive control) or media only (control) for 24 or 48 h. Conditioned media was then collected and stored at -20°C until use within 1 week. Upon thawing, media was added to non-reducing lamellae buffer for loading, no other processing was performed, and equal volume loading was employed.

For zymography, the standard protocol available from Abcam was followed, with minor changes. A 7.5% acrylamide separating gel was prepared containing gelatin (stock constituents: 1.5 M Tris pH 8.8, 30% acrylamide, dH_2O, 4 mg/ml gelatin, 10% SDS, 10% APS) and also stacking gel (0.5 M Tris pH 6.8, 30% acrylamide, dH_2O, 10% SDS, 10% APS) containing 10 wells. Sample (~18 µl) was loaded to wells, along with pre-stained protein ladder as above, and 1x sample buffer was loaded into empty wells. The gel was then run at 150 V until the dye front had run to the bottom of the plates, to achieve good separation of the proteins. The gel was then carefully removed and washed twice in recommended wash buffer (2.5% Triton X-100, 50 mM Tris-HCl pH 7.5, 5 mM $CaCl_2$, 1 µM $ZnCl_2$) for 5 min each to remove SDS and facilitate protein re-folding. The gel was then washed once in incubation buffer (1% Triton X-100, 50 mM Tris-HCl pH 7.5, 5 mM $CaCl_2$, 1 µM $ZnCl_2$) for 10 min with gentle shaking. Finally, fresh incubation buffer was added, the gel container was covered with parafilm, and then this was incubated for 24 h at 37°C to provide optimal conditions for protease activity.

The following day, the incubation buffer was removed and replaced with staining solution (40% Methanol, 10% acetic acid, dH_2O, 0.5% Coomassie blue), covered again with parafilm and incubated with gently shaking for 1h at RT. The staining solution should strongly stain the gelatin within the separating gel. The used staining solution was then decanted for re-use, the gel was washed two to three times with dH_2O the remove excess stain, and then destaining solution (40% methanol, 10% acetic acid, dH_2O) was added. Gel was incubated, covered, for a further 30 min to 1 h at RT, until clear bands could be visualised, indicating areas of gelatinase activity. Destaining solution was then removed and replaced with dH_2O, and gel was imaged on a white light converter plate using a Bio-Rad gel imager as above with Coomassie blue setting. Images were then analysed by densitometry using Image J.

2.2.18 DQ Collagen IV Degradation Assay

As a major component of lung ECM, and produced by epithelial cells, the ability of NMVs to cleave collagen IV was measured. $2x10^5$ freshly isolated NMVs were resuspended in 200 µl of phenol-red-

free RPMI (i.e. 1x10^6 NMV/ml). Collagenase type IV was made up to a final concentration of 1 U/ml in RPMI as a positive control for collagen degradation. RPMI only was also used as a control. For some experiments, TIMP-1 was added, as an endogenous inhibitor of MMP-9, to investigate the contribution of this enzyme to collagenolytic activity. For this, the same number of NMVs were pre-incubated with TIMP-1 (1.4 µg/ml; approximately double the concentration of MMP-9 in NMVs [0.7µg/ml at 1x10^6 NMV/ml] measured previously by Reece Dow as part of MSc project, [MSc thesis, 2018]) for 1 h at 37°C, and a TIMP-1-only control was also included. 100 µl of DQ-Collagen IV diluted 1:100 in RPMI was added to the appropriate wells in a 96-well optical bottom black plate. This regent is fluorescently labelled but highly quenched when intact, when the protein is cleaved the fluorescent molecules are able to be excited by the appropriate laser and therefore cleavage can be measured by an increase in fluorescence intensity. The VarioSkan flash spectrophotometer was pre-warmed to 37°C, and immediately before reading, samples and controls were added to the plate, any bubbles were quickly burst using a needle, and the plate was inserted into the reader. Fluorescence (ex/em: 495/515 nm) was measured every 30 min for 6–24 h, dependant on the assay.

2.2.19 Fluorescein Isothiocyanate-Labelled Dextran Transwell Permeability Assay

To determine the effects of NMVs on epithelial cell monolayer permeability, flux of 10 kDa FITC-dextran, a fluorescent tracer molecule, from upper transwell insert into the lower well beneath was measured. BEAS-2B cells were seeded at 5x10^4 cells/well and cultured on 24-well 0.4 µm pore-size PET transwell inserts until confluent (typically ~2–3 days). Confluency was confirmed by performing rapid Kwik-Diff staining on an extra well before beginning any assays as visibility in the wells was poor. FITC-dextran was diluted in phenol red-free cell culture medium, and this was used to resuspend NMVs at 3000 MV/µl. The media was removed from the insert and replaced with FITC-dextran media alone (control) or plus NMVs. 100 µl samples of media were taken from the lower well at 4 and 24 h, and the same volume of media was added back into the well to ensure no loss in total volume. Samples were added to an optical bottom black plate and analysed using the VarioSkan spectrophotometer at ex/em 492/520 nm. The experimental set up is illustrated in figure 2.8.
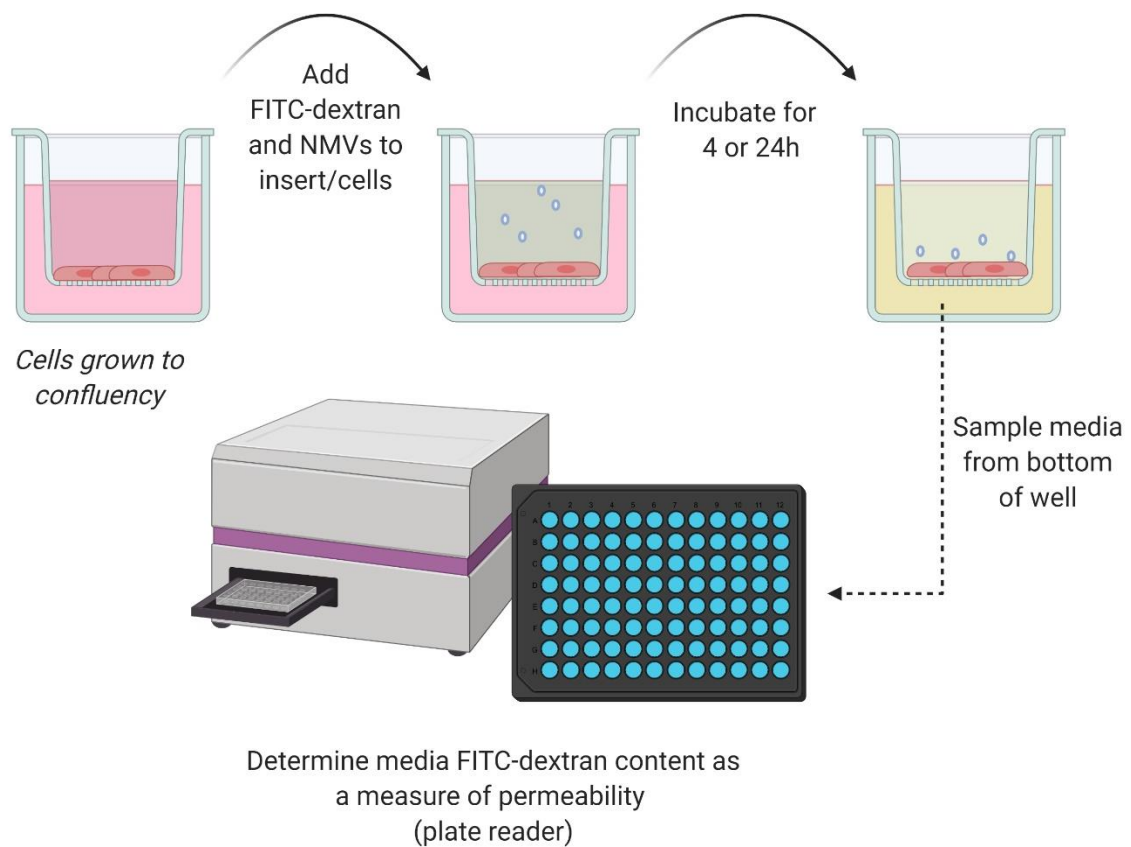
Figure 2.8 Schematic illustrating transwell epithelial monolayer permeability assay

Cells were grown to confluency in transwell inserts and then FITC-dextran with NMVs (or FITC-dextran in media only as a control) were added in phenol red-free cell media, only to the insert and not to the main wells. After either 4 or 24h, media was sampled from the well and added to an optical-bottom black plate. FITC-dextran fluorescence of the media was determined using a plate reader. Higher fluorescence intensity demonstrated greater monolayer permeability.

2.2.20 Epithelial Zonula Occuldens-1 Expression

To further investigate effects of NMV on epithelial monolayer permeability, expression of the key junctional protein ZO-1, previously shown to be affected by MMP activity, was measured. For this, BEAS-2B cells were cultured to confluency in 96-well plates as described previously here. Freshly isolated NMVs (3000/µl), 10 µg/ml LPS, or media only was added to cells, followed by incubation for 4 or 24 h. At those timepoints, cells were washed three times with pre-warmed PBS and lysed according to the protocol described for western blotting above in section 2.2.16.

2.2.21 Epithelial Cell Apoptosis

2.2.21.1 Fluorescence microscopy

Cells were grown to confluency in a 96-well tissue culture plate. Cells were then treated with either media only (phenol-red free RPMI, 10% FBS, 1% pen step, 1%L-glutamine), NMVs resuspended in media to 3000/µL, TIMP-1 or NMVs pre-incubated with TIMP-1. To determine the potential contribution of MMP, and particularly MMP-9 to any effects observed on cell death, as described in section 2.2.18 for the NMV collagen degradation assay, NMVs were pre-incubated for 1h with TIMP-1 at 4 µg/ml, at approximately double the concentration of MMP-9 estimated to be in 3000 NMV/ul utilised for this experiment (~2 µg/ml).

CellEvent (5 µM) caspase 3/7 detection reagent was added to cells immediately and then cells were imaged for 24h at 37°C, 5% CO_2. Detection of dead cells was validated by imaging with both fluorescence and brightfield to check whether cells which were apoptotic and visually blebbing from the monolayer were positive for caspase 3/7 activity.

For quantification of total cell number per f.o.v, cells were gently washed once with warm PBS, then fixed for 10 mins with pre-warmed 4% PFA. Cell nuclei were stained using 1µg/ml DAPI in PBS, incubated for 5 mins, then gently washed again with PBS twice to avoid cell loss. Wells were then imaged again using the same "mark and find" function settings to identify previous imaging positions.

2.2.21.2 Epithelial cell loss analysis by flow cytometry

After completion of the experiment described above in section 2.2.21.1, cell media was pipetted gently up and down twice then removed from the well and added to 300 µl PBS. Cells present in the media were analysed immediately by flow cytometry to detect CellEvent positive events (i.e. apoptotic cells detached into the cell media) using the Blue laser with 530/30-A filter. To normalise the amount of media analysed, the stopping gate was set to 60 seconds. All samples (n=3) were analysed at the same time.

2.2.22 Mouse Studies

2.2.22.1 Ethics

All studies involving mice were approved by the University of Sheffield ethics committee and performed in accordance with the UK Home Office Animals Act 1986 under Project Licence P4802B8AC. Female mice only were used in this study for ease of caging strategy. C57BL/6 mice were sourced from Jackson Laboratories.

2.2.22.2 Murine intranasal NMV instillation

In a pilot study, 6–8-week-old C57BL/6 mice (n=2 per timepoint) were intranasally administered 5×10^5 NMVs (pooled from three different healthy participants) in 50 µl PBS via p200 pipette under recovery inhalation anaesthesia (isoflurane) and subsequently sacrificed at 0, 4, 8, and 24 h by overdose of pentobarbital administered via intraperitoneal injection. The study protocol is summarised in figure 2.9, upper panel. Handling and treatment of animals was performed by individuals with Home Office-approved personal licenses: Carl Wright, Jessica Willis and Dr Helen Marriot at the University of Sheffield.

In a further, larger study, C57BL/6 mice were anaesthetised as above and initially administered either low-dose LPS (5 µg; n=12) or vehicle (50 µl PBS; n=4) intranasally. 16 h later, all vehicle-receiving mice and six mice from the LPS-treated group mice were intranasally administered 1×10^6 NMVs (pooled from multiple donors) in 50 µl PBS. The remaining six LPS-treated mice were administered NMV supernatant (PBS supernatant remaining from final NMV centrifugation step) in 50 µl PBS to control for effects of any remaining stimulus or neutrophil-derived proteins in the NMV pellet. Mice were sacrificed 6 h later, according to the protocol above, with the experiment running for a total of 22h in total after these two incubation times. The study is summarised in figure 2.9, lower panel.
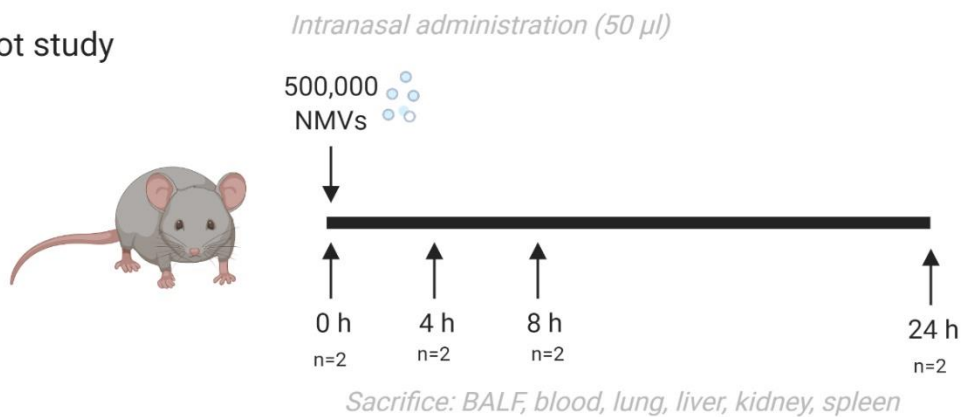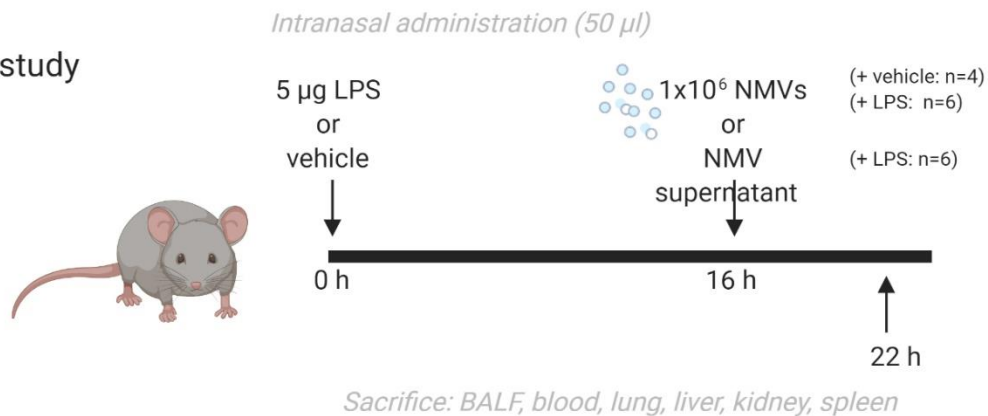
Figure 2.9 Schematic showing experimental procedures for pilot and full murine studies of the effects of intranasally administered neutrophil-derived microvesicles (NMVs) on lung inflammation

Pilot study: mice were administered 5×10^5 NMV intranasally in 50 µl PBS and culled at T=0, 4, 8, or 24h. Inflammation was measured by bronchoalveolar lavage fluid (BALF) protein analysis, other samples were taken for later analysis. N=2 mice used per timepoint. Full study: Mice were administered LPS or vehicle, then after 16h were administered 1×10^6 NMVs (vehicle and LPS groups) or NMV supernatant (LPS group only) intranasally. 6h later (T=22h) mice were culled and samples and tissues were harvested as per the pilot study, to determine effects on lung inflammation. NMV + vehicle: n=4, NMV + LPS: n=6, NMV supernatant + LPS: n=6.

2.2.22.3 Blood samples

For both of these studies, after sacrifice and performing two checks to lethal anesthetisation, blood was collected into a heparinised syringe via the femoral artery and then decanted into an Eppendorf tube. Plasma was centrifuged at 200 *g* for 20 min at RT to separate plasma. The top layer of plasma was then removed and added to a fresh tube and centrifuged at 2000 *g* for 15 min at RT to pellet platelets. PPP was then removed again to a fresh tube for later analysis, and all fractions and cell pellets were stored at -20°C. Plasma was used for ELISA analyses.

2.2.22.4 Bronchoalveolar lavage

After obtaining a blood sample, the trachea was exposed and bronchoalveolar lavage was performed by inserting a canula to the trachea, securing this with thread, and gently flushing and retrieving 1 ml of ice-cold 0.2-μm-filtered PBS in the lungs using a 1 ml syringe, a total of three times, each time with fresh PBS. This was pooled into a 15 ml falcon tube and kept on ice. The sample was then centrifuged at 500 *g* for 5 min at 4°C to pellet cells. The BALF supernatant was then stored in an Eppendorf tube at -20°C until analysis. The cell pellet was resuspended in 220 μl of 1% BSA/PBS. 10 μl was removed and added to 10 μl 0.4% trypan blue to perform total cell count using a haemocytometer. 100 μl samples were used to perform cytospins in duplicate, as detailed for human neutrophil sample processing above, and later stained with kwik-diff.

Murine BALF was used for ELISA, total protein, and MV analysis as described in sections 2.2.13, 2.2.15, and 2.2.7.3, respectively.

2.2.22.5 Organ/tissue processing and sample analysis

The spleen, liver and kidneys were then removed, added to cryovials and flash frozen in liquid N_2. Finally, the right main bronchus was tied off with thread, and the right lung was removed and snap frozen to enable later qPCR analysis. The left lung was then perfusion fixed using 10% formalin at 25 cm H_2O pressure for 7 min. The fixed lung was then removed and stored in formalin overnight at 4°C. The following day this was exchanged for emersion in PBS for subsequent histological processing.

2.2.23 Macrophage Uptake of Neutrophil-Derived Microvesicles

As alveolar macrophage uptake of NMVs was of interest in our *in vivo* studies, to choose an appropriate timepoint for these animal experiments, NMV uptake by monocyte-derived macrophages (MDM) was investigated.

2.2.23.1 Monocyte isolation and differentiation

To obtain peripheral blood monocytes, blood (~80 ml) was taken from healthy participants who provided written, informed consent. Ethical approval for this study was granted by the University of

Sheffield ethics committee and was under the same reference as neutrophil isolation (SMBRER310). Cells in these experiments were kindly prepared by Dr Kajus Baidzajevas, Department of Infection, Immunity and Cardiovascular disease, University of Sheffield. For this, blood was mixed with 3.8% sodium citrate as an anticoagulant, and then 30 ml of this was carefully layered onto 15 ml of Ficoll-paque plus, avoiding mixing of these layers. Density-gradient centrifugation was then performed by centrifuging the suspension for 20 min at 900 g (acceleration 1, brake 1). The following layers could then be observed: plasma, peripheral-blood mononuclear cells (PBMCs), Ficoll, granulocytes, and finally red blood cells. Plasma was removed and discarded into bleach and PBMCs were transferred into a 50 ml falcon tube containing PBS/EDTA (2 mM), taking care not to contaminate this layer with the granulocytes below. PBMCs were centrifuged at 1500 rpm for 5 min to pellet the cells, the supernatant was aspirated and cells were resuspended in 10 ml of red blood cell lysis buffer (20X stock: 16.6 g NH4Cl, 2 g KHCO3, 400 µL 0.5 M EDTA, 200 mL distilled, dH2O; 0.2 µm sterile-filtered), to remove any remaining erythrocytes. After incubation at RT for 5 min, cells were pelleted again , resuspended in PBS/EDTA and counted using a haemocytometer, then pelleted once more.

Monocytes were then isolated by positive immunomagnetic bead selection for CD14$^+$ cells. Miltenyi Biotech MACS magnetic separation system was used, following manufacturers protocol. Briefly, after quantification, cells were resuspended in 90 µl of chilled (4°C) MACS buffer (0.5% BSA + PBS/EDTA) and 10 µl human anti-CD14 microbeads were added for every 10×10^6 cells. The suspension was incubated for 15 min, at 4°C. To this, 2 ml of MACS buffer was then added and cells were pelleted at 1200 rpm, RT for 5 min. The pellet was resuspended in 500 µl of MACS buffer and the suspension was added to a pre-washed MACS column. The column containing cells was then washed three times with MACS buffer to remove CD14-negative cells. The column was then removed and washed again to release the remaining monocytes, this solution was collected into a falcon tube and the cell yield was determined using a haemocytometer. The purity of cell suspensions isolated by this method has been previously validated and confirmed using flow cytometry to measure CD14 positivity.

Isolated monocytes were then differentiated into macrophages. For this, cells were pelleted by centrifugation at ~280 g, RT, for 5 min, resuspended in culture media (RMPI-1640, 10% ultra-low endotoxin FBS, 1% L-glutamine, 1% penicillin/streptomycin), and added to 12-well plates. 100 ng/ml recombinant human M-CSF was added to promote differentiation. Cells were cultured for 7 days at 37°C, 5% CO_2. The protocol was previously validated by members of the Kiss-Toth and Wilson labs. In the present experiments, differentiation was checked visually using light microscopy; a mixture of adherent elongated and rounded cells should be observed after 1 week. These cells were then used for further studies of NMV internalisation.

2.2.23.2 NMV internalisation by human monocyte-derived macrophages

MDM from three separate donors were used for these experiments. To these macrophages, $1x10^5$ freshly isolated PKH67-labelled NMV were added. This number was chosen as $3x10^5$ NMV would be instilled in subsequent murine experiments. Control wells for each donor contained no NMVs.

Cells were imaged at 2, 4, 16, and 24 h using a Leica DMI4000B widefield microscope, and both brightfield images and fluorescence at 488 nm was captured for each f.o.v to enable cell quantification. Three images/f.o.v at were taken at random positions within each well at each time point. As macrophages exhibit some autofluorescence at 488 nm, settings at the first timepoint were as such that in the control condition, negligible signal could be detected in this channel. NMV uptake was then quantified using by performing image analysis in Image J/Fiji software.

2.2.24 Ex vivo and in vivo NMV administration in mice and generation of precision-cut lung slices

2.2.24.1 Preparation of PCLS

Animal studies were carried out with approval from the University of Sheffield Animal Care and Welfare Committee as per the ethics statement in section 2.2.22. Handling and treatment of animals was carried out by individuals with a Home Office-approved Personal License. NMV administration was performed by Dr Helen Marriott and Jacob Rudman. Sacrifice, sample collection and processing of tissue to generate precision cut lung slices (PCLS) was done by Jacob Rudman (according to the protocol published in Rudman et al. (2019).

Mice were sacrificed by overdose of pentobarbital, injected i.p., and exsanguination. The trachea was subsequently exposed and a cannula inserted. Pre-warmed 2% low melting point agarose was then injected into the lung via syringe and the whole animal was placed onto ice to set the agarose. After setting (approx. 2 min), lungs were dissected out and immersed in RT PBS in a 50 ml falcon tube. The left, single lobed lung was used for PCLS generation. Tissue adhesive was used to attach the lung to the cutting block. Care was taken to ensure the tissue did not dry out during this time by adding PBS. The block was then inserted into a Vibratome and the tissue was immersed in pre-warmed (37°C) DMEM containing 10% FBS, 1% penicillin-streptomycin, for the duration of the slicing process. Slices of 300-µm thickness were then generated. The first ~2 smaller slices were discarded, and intact slices of similar size for each lung were chosen. Slices were added to a 4-well polymer-bottom Ibidi slide in 1ml DMEM (described above). Home-made weights were utilised to sink and secure tissue to the bottom of the well for optimal imaging.

In an initial pilot study, a single mouse was sacrificed and PCLS were generated as described above. 20 µl of PE-conjugated anti-CD11c was added to label myeloid cells, mainly alveolar macrophages, in the tissue. 5×10^4 PKH67-labelled NMVs were then added to a single well. After approx. 0.5-1h, confocal imaging was performed using an Airyscan microscope to determine NMV localisation. A schematic of this initial pilot study protocol is illustrated in figure 2.10, upper panel.

In a final pilot study to determine the optimal method of NMV administration *in vivo*, mice were administered 3×10^5 labelled NMV in 50 µl PBS either via intratracheal instillation (i.t.; n=1; sedation by i.p. ketamine injection) or oropharyngeal aspiration (o.p.; n=1; sedation by inhalation anaesthesia using isoflurane). After 4 h, mice were sacrificed as described above for the initial pilot experiment and PCLS were created. PCLS were stained with AF647-WGA (1:200), a lectin that binds sialic acid and N-acetylglucosaminyl residues (found in the cell membrane), and Hoechst 33342 (1:2000) to stain cell nuclei. The combination of fluorophores was chosen after careful consideration of emission and excitation spectra of these fluorescent molecules. PCLS were then imaged using a Nikon Eclipse Ti widefield microscope with a climate control stage set to 37°C in 5% CO_2/95% air. A summary of this experiment is shown in figure 2.10, lower panel.

2.2.24.3 NMV oropharyngeal aspiration and imaging of NMV localisation

Approval for this study, treatment of animals, and individuals performing live animal work was as describe above for PCLS. C57BL/6 mice aged 13-18 weeks were used. Mice were randomised into treatment groups using a random number generator. Mice were administered 3×10^5 PKH-67-labelled (4 h timepoint; n=3) or unlabelled (7-day timepoint; n=4) NMVs, from an individual donor, in 50 µl of PBS via o.p. as described above for the pilot studies. NMVs were freshly isolated on the same day that the murine experiments were performed and were administered ≤2h after PHK labelling. As a control treatment, three mice in the 4 h group and 4 mice in the 7-day group were administered NMV-supernatant remaining after the final NMV wash, in a final volume of 50 µl PBS, via the same method. This controlled not only for remaining neutrophil or stimulus contaminants remaining in the NMV pellet, but also any remaining dye. A schematic summarising the full study protocol is shown in figure 2.11.
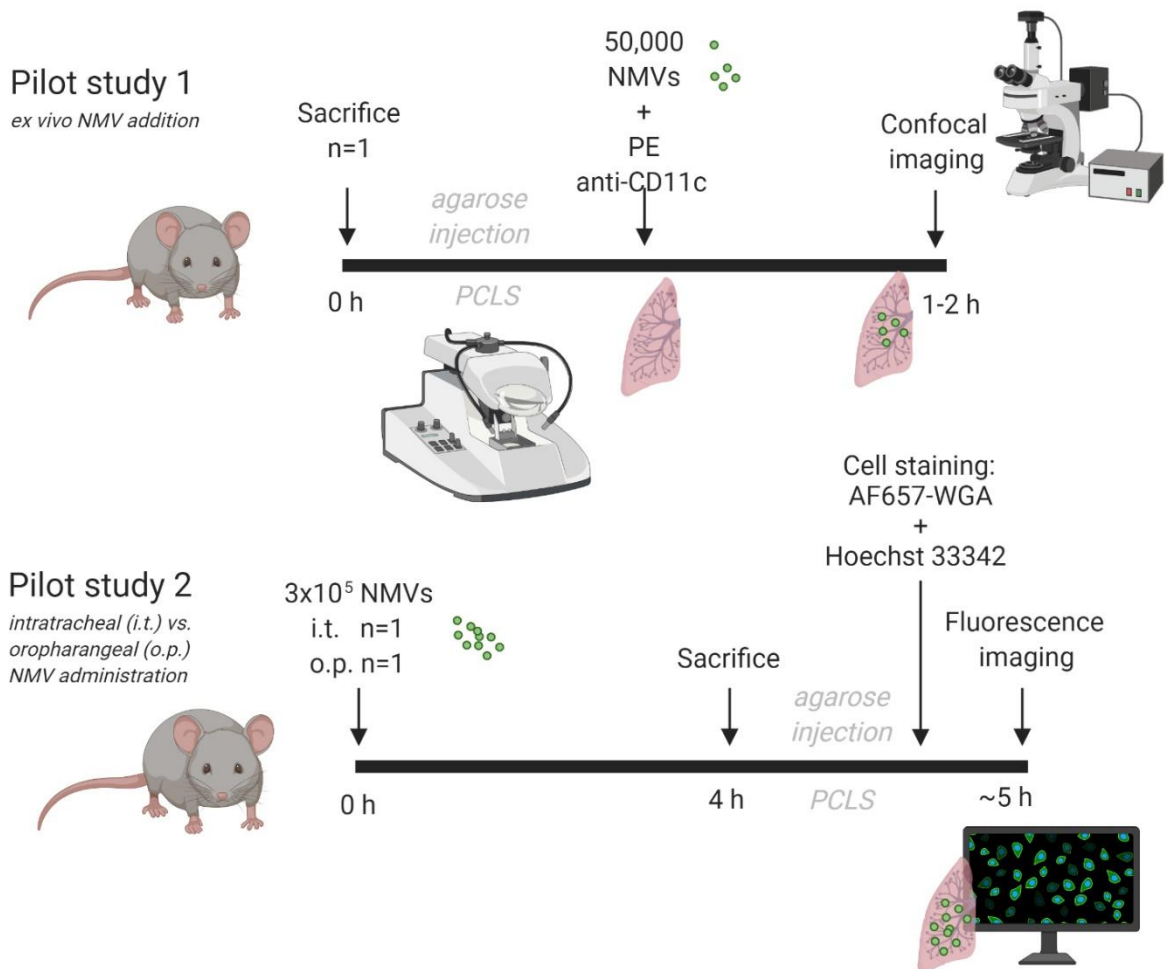
Figure 2.10 Schematic showing experimental procedures for two sequential murine studies into the use of precision-cut lung slides to determine the effects and localisation of neutrophil-derived microvesicles (NMVs) in the lungs

Pilot study1: a single mouse was sacrificed, lungs were injected with agarose and then sectioned into precision cut lung slices (PCLS). To a slice, 5x10^4 PKH67-labelled NMVs were added ex vivo in tissue culture wells. Anti-CD11c antibody was used to label alveolar macrophages. After approximately 1-2h PCLS were imaged using an Airyscan confocal microscope to visualise NMV location.

Pilot study2: Mice were administered 3x10^5 of PKH67-labelled NMVs intratracheally or via oropharyngeal aspiration (n=1 per technique) to determine the optimal mechanism of administration. After 4h, mice were sacrificed and processed to prepare PCLS. Lung slices were labelled using fluorescent wheat germ agglutinin (WGA) to stain cell membraned and with Hoechst to label nuclei for better visualisation of lung structures. After preparation and staining, PCLS were imaged using a Nikon fluorescence microscope.
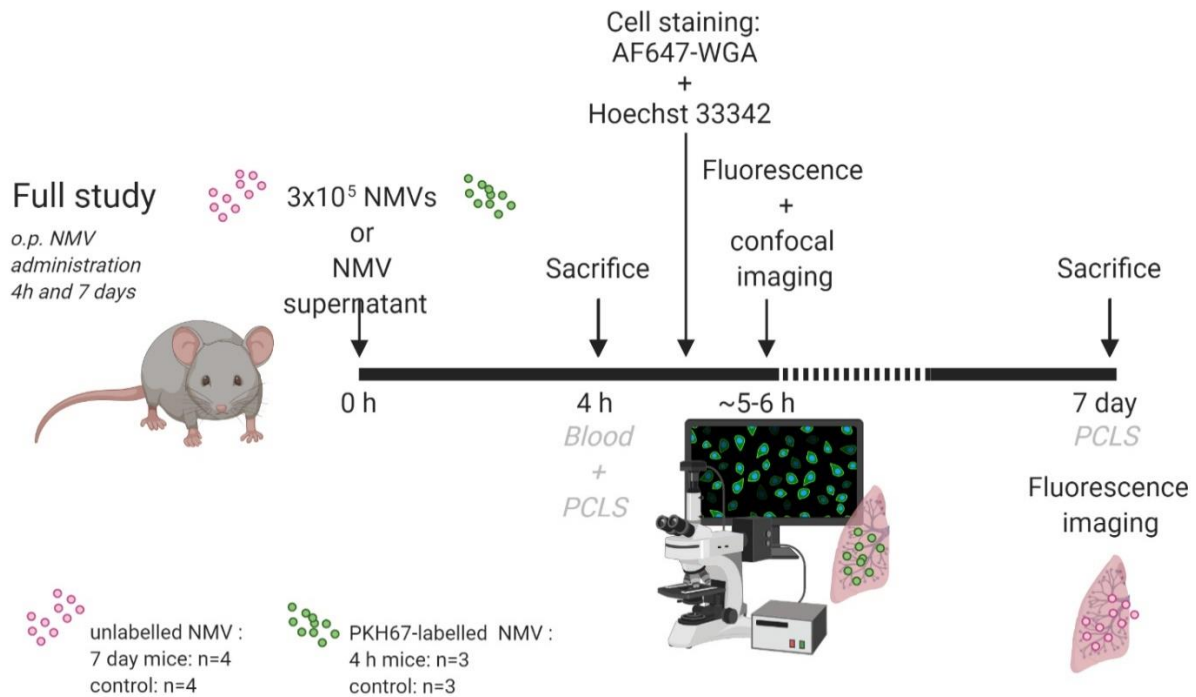
Figure 2.11 Schematic of murine study to determine neutrophil-derived microvesicle function and localisation in the lungs, utilising precision cut lung slices (PCLS)

Mice were administered $3x10^5$ PKH67-labelled (4h; n=3) or unlabelled (7 day; n=4) NMVs via oropharyngeal aspiration. A control group of NMV supernatant was used at each timepoint. After 4h, mice that received labelled NMVs (or supernatant) were sacrificed and processed to prepare PCLS. Blood samples were obtained from these mice, and one lung was fixed in formalin for further histological analysis. PCLS were labelled using fluorescent wheat germ agglutinin (WGA) to stain cell membranes and with Hoechst to label nuclei to visualise lung structures. After preparation and staining, PCLS were imaged using a Nikon fluorescence microscope and using an Airyscan confocal microscope. Mice receiving unlabelled NMV (or supernatant) were sacrificed after 7 days. The same samples were obtained as for the 4h group, with the omission of fluorescence imaging for NMV localisation.

After 4 h or 7 days, depending on the treatment group, mice were sacrificed by overdose of pentobarbital and processed as described in the PCLS section above, with one modification: after removing the lungs into PBS, the right, multi-lobed lung was separated off, one lobe was snap frozen in liquid N2 to permit subsequent gene expression analysis, and the rest of the right lung was placed into 10% formalin for tissue fixation and subsequent histological processing. After 24h at 4°C the right lung was transferred to PBS and kept refrigerated until further use. The spleen, liver, and kidneys were also frozen in liquid N2 to allow later analyses.

Processing of the left lung for PCLS was performed as described above, and the lung was stained as in the final pilot study, with AF647-WGA and Hoechst 33342 (4h timepoint only), and then imaged using a Nikon Ti widefield microscope to determine NMV localisation in tissues. Additional slices were washed three times with PBS and then fixed using 4% PFA after staining. Slices were incubated in fixative overnight at 4°C and were then washed again with PBS and the stored in PBS, refrigerated, until imaging on an Airyscan confocal microscope to further investigate NMV localisation in the tissue. Fixation was performed due to the timing of these experiments and allowed confocal imaging to be delayed to the following day.

Further to NMV imaging, to determine whether NMV treatment had an effect on cell apoptosis in the lung at both 4h and 7 days, extra slices were stained with Hoechst 33342 and NucView 530 caspase 3/7 probe (1 µM) for 30 min. After this time, slices were washed three times with PBS, and fixed using 4% PFA for overnight at 4°C. Following this, slices were washed with PBS again and then kept in PBS at 4°C until imaging ~1-2 days later. Imaging was performed on a Leica AF6000LX widefield microscope.

2.2.25 Statistical Analyses

Data shown in this thesis are provided as mean ± standard error of the mean (SEM) where indicated in the results sections. GraphPad Prism (GraphPad Software, San Diego, USA) version 8 was utilised for statistical analysis of all data, where appropriate statistical test was applied upon assessment of data normality (gaussian distribution), if this was not assumed. Where two or more conditions were present and data was parametric, one-way ANOVA was used with a post-hoc test of Tukey's multiple comparisons where significant results was identified. Unpaired t-tests were used in the cases of two conditions or less, no matched data was present. A p-value of ≤0.05 was considered statistically significant.

Chapter 3: Neutrophil-derived microvesicle characterisation in healthy participants and COPD patients

3.1 Introduction

Chronic obstructive pulmonary disease (COPD) is associated with neutrophilic inflammation, and neutrophils are drivers of damage during COPD pathogenesis and exacerbations, with a protease–anti-protease imbalance hypothesised to play a major role in this damage (Laurell and Eriksson, 2013; Stanescu *et al.*, 1996). Cigarette smoking (Vestbo *et al.*, 2013) and/or burning of biomass fuels in poorly ventilated areas (Liu *et al.*, 2007; Zhou *et al.*, 2014) are thought to be the two major risk factors for COPD pathogenesis. Several studies have reported increased circulating leukocyte numbers in COPD patients and in smokers compared with non-smoking controls (Dentener *et al.*, 2001; Mannino *et al.*, 2003; Gan *et al.*, 2004; Friedman *et al.*, 1973). Gunay et al. (2014) found that stable COPD patients also had a higher neutrophil-to-lymphocyte ratio than age-matched controls. Circulating and airway neutrophil numbers have been inversely correlated with lung function in smokers (Sparrow *et al.*, 1984; Stanescu *et al.*, 1996) and circulating neutrophils have also been shown to predict risk of pneumonia (Pascoe *et al.*, 2019). COPD exacerbations, which can cause rapid disease worsening and impact mortality (Anzueto, 2010), are frequently due to bacterial and/or viral infection (Bafadhel *et al.*, 2011). Further increases in circulating neutrophil counts may be observed during COPD disease exacerbations (Noguera *et al.*, 1998), and in fact, the largest increases in these levels have been seen in response to bacterial pathogens (Hurst *et al.*, 2006). Although there have been difficulties in establishing consistent systemic biomarkers in COPD, neutrophil counts as well as other neutrophil-related parameters including protease activity (Thulborn *et al.*, 2019) and extracellular matrix degradation (Lindberg *et al.*, 2012) may be indicative of the cause of exacerbation and important indicators of patient condition.

In addition to immune cell parameters, various comorbidities are associated with COPD and have been linked to worse clinical outcomes for these patients; amongst the most frequent of these is cardiovascular disease (de Lucas-Ramos *et al.*, 2012). Consequently, cardiovascular events such as heart failure and stroke are common causes of hospitalisation and death in COPD patients (Sidney *et al.*, 2005; Curkendall *et al.*, 2006). These cardiovascular comorbidities include pulmonary hypertension (PH), a relatively rare condition with an estimated prevalence of all-cause PH of 1% worldwide, which reaches 10% in individuals over 65 years of age (Hoeper *et al.*, 2016). This disorder is characterised by narrowing of the arteries and is typically defined by a resting mean pulmonary

arterial pressure (mPAP) of ≥25 mmHg (Badesch *et al.*, 2009). Secondary PH occurring in COPD is lesser studied, but represents one of the six PH groups proposed by the World Health Organisation; PH resulting from lung disease and/or hypoxia defines group 3 (Galie *et al.*, 2015) and prevalence estimates vary between 10–70% in COPD patients (Naeije, 2005; Thabut *et al.*, 2005; Doi *et al.*, 2003; Elwing and Panos, 2008). Although PH is most often mild-to-moderate in COPD rather than severe (Kessler *et al.*, 2001), pulmonary vascular remodelling in COPD is the main cause of increase in pulmonary artery pressure and is thought to result from the combined effects of hypoxia, inflammation and loss of capillaries in severe emphysema (Hoeper *et al.*, 2013). Increased mPAP is associated with increased exacerbation and hospitalisation rates (Kessler *et al.*, 1999) and reduced survival rates in COPD (Oswald-Mammosser *et al.*, 1995). Whilst studies are lacking in secondary PH, as in COPD, increased neutrophil-to-lymphocyte ratio has been observed and the PH subgroup of pulmonary arterial hypertension (PAH) (Yıldız *et al.*, 2013), and a role of neutrophils including via the protease neutrophil elastase (NE) (Rose *et al.*, 2003) and also myeloperoxidase (MPO) (Klinke *et al.*, 2018) activity has been demonstrated in PAH in vascular damage and remodelling. Furthermore, neutrophils isolated from PAH patients have been shown to more readily release proteases such as NE amongst other inflammatory mediators (Rose *et al.*, 2003).

In COPD, functional changes in circulating neutrophils have been demonstrated, as discussed in Chapter 1, section 1.1.3., including being more readily primed for activation (Lokwani *et al.*, 2019), increased expression of adhesion molecules such as Mac-1 (Noguera *et al.*, 1998), and increased reactive oxygen species (ROS) release in response to proinflammatory stimuli (Noguera *et al.*, 2001). Both exacerbating and stable state COPD patients also have increased levels of matrix metalloproteinase-9 (MMP-9) and neutrophil elastase (NE) (Paone *et al.*, 2011; Thulborn *et al.*, 2019). Importantly, neutrophil protease release and activity has been shown to be resistant to effects of glucocorticosteroids, a mainstay therapy in COPD (Vlahos *et al.*, 2012). Neutrophils are the major source of MMP-9 both systemically and at local sites of inflammation (Culpitt *et al.*, 2005); MMP-9 is stored in the gelatinase/tertiary granules of neutrophils, and is readily released in response to pro-inflammatory stimuli including N-formyl-met-leu-phe (fMLP) (Takafuji *et al.*, 2003), tumour necrosis factor-α (TNF-α) (Chakrabarti *et al.*, 2006) and both tobacco smoke (Friedrichs *et al.*, 2014) and electronic cigarette vapour (Higham *et al.*, 2016; Ghosh *et al.*, 2019). This protease is secreted from cells in the pro-form and is converted to an active gelatinase extracellularly by other proteases including mmp-2, -3 and -13 (Ramos-DeSimone *et al.*, 1999; Knauper *et al.*, 1997)—which themselves require activation by other proteases (Fridman *et al.*, 1995)—and NE (Jackson *et al.*, 2010). The most well-known endogenous inhibitor of MMP-9, along with several other MMPs, is tissue inhibitor of metalloproteinase-1 (TIMP-1). Whilst most cell types release MMP-9–TIMP-1

complexes (Roderfeld *et al.*, 2007), neutrophils have been shown to release inhibitor-free MMP-9, indicating that it may have rapid action upon leaving the cell (Ardi *et al.*, 2007). Also known as type IV collagenase or gelatinase B, MMP-9 is capable of degrading collagen IV, V, VII, X and elastin and fibronectin (Araki and Mimura, 2017); intracellular substrates including actin, tubulin and gelsolin are also increasingly recognised (Cauwe *et al.*, 2009). Both elastin and collagen degradation are common in COPD lungs and circulating levels of their cleavage products have been shown to correlate with lung function (Stolz *et al.*, 2017).

Despite its demonstrated activities and upregulation in COPD, surprisingly, MMP-9-knockout mice exposed to cigarette smoke did not show differences in emphysema development or airspace enlargement (Atkinson *et al.*, 2011). However, the contribution of MMP-9 to COPD development may relate to less well-known mechanisms; MMP-9 application to differentiated lung epithelial cells *in vitro* increased apoptosis and permeability of these cells to viral infection via dysregulation of junctional proteins (Vermeer *et al.*, 2009), indeed, MMP-9 has been shown to increase susceptibility to infection *in vivo* (Malik *et al.*, 2007). These effects are further discussed in chapter 4. MMP-9 may also be responsible for creating chemotactic peptides via cleavage of extracellular matrix (ECM) components which subsequently recruit neutrophils to the tissue (Weathington *et al.*, 2006; van Houwelingen *et al.*, 2008; Houghton, 2015). Along with other metalloproteases, MMP-9 is thought to play a role in cigarette smoke-induced vascular remodelling, with transiently increased levels in the intrapulmonary arteries, contributing to the development PH (Wright *et al.*, 2007).

As discussed in chapter 1, section 1.3.2, protease packaging into neutrophil-derived microvesicles (NMVs), and particularly MMP-9, from fMLP-stimulated neutrophils has been described by several studies, including by proteomics (Dalli *et al.*, 2013), western blotting and gelatine zymography (Butin-Israeli *et al.*, 2016a). Furthermore, differences in MMP-9 content depending on the method of neutrophil stimulation were suggested by Dalli et al. (2013). NMV biogenesis and characterisation is also discussed in chapter 1, section 1.3.1. Increased numbers of NMVs have been shown in acute respiratory distress syndrome (ARDS) (Guervilly *et al.*, 2011) and COPD (Lacedonia *et al.*, 2016). Additionally, differential levels of circulating extracellular vesicles (EVs) have been demonstrated in individuals with hypertension (Preston *et al.*, 2003), although to our knowledge, NMV levels have not yet been studied. The functional effects of NMV MMP-9 are not completely understood, especially in the lung, but evidence from interactions with intestinal epithelium suggest a role in cleavage of epithelial cell junctions to increase neutrophil transepithelial migration (Butin-Israeli *et al.*, 2016a).

3.2 Hypothesis and Aims

As degranulation and protease release are triggered by inflammatory cues, we hypothesised that NMVs generated in response to proinflammatory stimuli would have differential content, with higher levels of proteases packaged into these vesicles, and greater capacity for protein degradation. Furthermore, we hypothesised that—as is the case for their parent neutrophils—COPD patients and particularly those undergoing disease exacerbation would have higher level of WBC-derived MVs that contain differential levels of MMPs.

Aim 1: To analyse the number, origin and MMP content of circulating microvesicles in COPD patients compared to healthy controls.

Aim 2: To characterise isolated NMV physical properties including size and morphology and confirm successful isolation.

Aim 3: To determine whether these NMVs contain potentially damaging proteases, with specific focus on MMP-9, and investigate whether NMV numbers and content change depending on the stimuli parent neutrophils are exposed to.

3.3 Results

Both circulating and airway neutrophils have shown important differences in their numbers and activity in COPD compared with those in matched controls in the literature, particularly during disease exacerbations; patient sputum contains NMVs (Lacedonia *et al.*, 2016) and isolated NMV express a variety of neutrophil proteases (Dalli *et al.*, 2013), however, very little is known about these vesicles in COPD. In order to determine whether NMVs may play a role in the disease and identify further relevant avenues of investigation *in vitro* and *in vivo*, we first performed a patient study to analyse circulating MVs as both easily accessible potential disease biomarkers and contributors to disease progression.

3.3.1 Quantification and Characterisation of Circulating Microvesicle Types in Exacerbating Chronic Obstructive Pulmonary Disease Patients

Study participant demographics

In order to determine whether there may be disease-related changes in the circulating MV profile of exacerbating COPD patients compared to age-matched healthy controls, flow cytometry analysis of platelet-poor plasma (PPP) was performed. PPP was obtained from blood samples from a small sample of (n = 6) within 24-48 h of hospital admission by Respiratory Specialist Dr Katharine Lodge, University of Cambridge. PPP was also obtained from 5 healthy age-matched control subjects.

	Controls	Patients
number	5	6
Age (yrs)	66.4±6.1	71.5±8.9
Sex (F:M)	4:1	3:3
COPD	0	6
Current smokers	0	1
Ex-smokers	3	5
Pack years	1.4±2.1	53.8±24.4
estimated GOLD stage*	n/a	I = 0 II = 0 III = 3 IV = 2
FEV1 (%)	n/a	35.8±11.7
* lung function data unavailable for 1 patient		

Table 3.1 Study participant demographics of exacerbating COPD patients (n=6) and age-matched controls (n=5)

Participant demographics are shown in table 3.1. The age range of study participants with COPD was 59–79 years and of age-matched controls was 58–74 years.

Of the COPD patients, two had confirmed infective, two had likely infective and two had non-infective exacerbations. Additionally, only two patients had blood neutrophil counts above the normal range, at 9.93 and 12.89 × 10^9 cells/L. The latter patient was the only one of the group to have an elevated total leukocyte count, of 15.2 × 10^9 cells/L, and was one of the two patients with a non-infective exacerbation. The same patient had high C-reactive protein (CRP) levels (above 10 mg/L), along with two other patients who did not have elevated total leukocyte or neutrophil counts. All of the COPD patients had comorbidities, which included amongst others, bronchiectasis, previous pulmonary emboli, hypertension, osteoporosis and chronic kidney disease. These patients were all taking prescribed respiratory medications including combinations of mucolytics and long-acting beta agonists and corticosteroids. Of the age matched controls, two had no known health conditions, whilst the remaining three had conditions including hypertension, osteoporosis and hypercholesterolemia. Other than supplements, only one of these participants was recorded as taking prescribed medications (a statin).

Microvesicle phenotype

MV phenotype was determined by labelling plasma MVs with fluorescently-conjugated antibodies for granulocyte/neutrophil (CD66b), monocyte (CD14), platelet (CD41a) and endothelial (CD144) markers. MVs were then pelleted at 20,000 *g* and analysed by flow cytometry as descried in chapter 2 section 2.2.7.1 using calibration beads to identify a region of interest in which MVs should appear and using appropriate compensation and fluorescence minus one (FMO) controls. The relative proportion of each circulating MV type for both of these groups is shown in figure 3.1 (A–D). The most abundant MV type identified was platelet-derived (CD41a+), followed by neutrophil (CD66b+), monocyte (CD14+) and endothelial (CD144+) MVs. Endothelial MVs represented a very small proportion of the total MV population, making up approximately 6%, in both COPD patients and in age-matched subjects. There were no statistically significant differences between the two groups for any of these MV types by unpaired t-test.

Whilst the mean percentage of immune cell-derived (neutrophil and monocyte) MVs was higher in COPD patients than in age-matched controls, this is mostly due to one patient who had a notably higher levels of these MVs (highest data point in fig 3.1 (A+B)). Upon application of a robust regression and outlier removal (ROUT) outlier test with Q=0.2% and Grubbs test with α = 0.05, no outliers were identified in this data set.
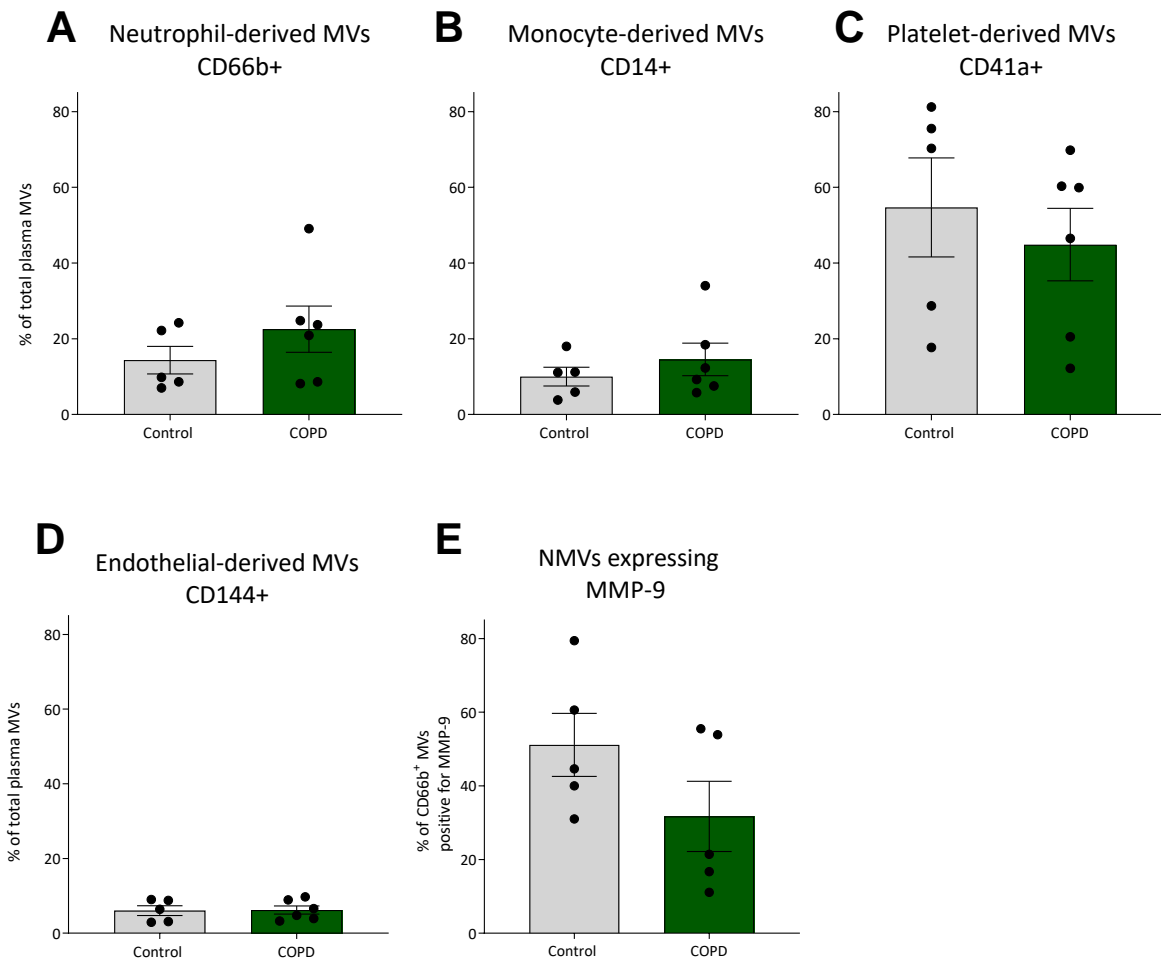
Figure 3.1 Circulating microvesicle (MV) phenotypes from exacerbating COPD patients and age-matched control plasma samples

Surface expression of the cellular markers (A) CD66b, (B) CD14, (C) CD41a and (D) CD144 on MVs from platelet-poor plasma samples from exacerbating COPD patients (n=6) and age-matched controls n=5) was probed using fluorescently-conjugated antibodies. After labelling, MVs were pelleted by high-speed centrifugation and then analysed by multi-colour flow cytometry using the BD LSRII. Due to the small size of MVs, a region of interest was initially identified for MV analysis using Megamix calibration beads. AbC compensation beads were utilised to perform compensation in the antibody panel, and this was applied to sample data in FlowJo analysis software. (E) MMP-9 surface expression was measured on CD66b+ MVs using the same method. The percentage of CD66b+ MVs which were also MMP-9+ is shown. For graphs without y-axis titles, the nearest label on the left side applies. Data shows mean±SEM. No significant differences were detected using unpaired t-test.

The rest of the sample population showed a similar distribution to that of the control group. CD66b+ MVs made up, on average, 14.37 and 22.54% of the total MV population in age-matched controls and COPD patients, respectively. Whilst some variation was evidenced for all of the MV types, the greatest variability was seen for platelet-derived (CD41a+) MVs, which ranged 17.7–81.2% of the total MV population in the control group and 12–69.8% in the COPD group.

Correlation analyses were not carried out in this study due to small sample sizes. A post-hoc power calculation was performed on this data; $CD66b^+$ MVs = 20.9%, $CD14^+$ MV = 14.8%, $CD41a^+$ = 8.8%, $CD144^+$ MV = 3.1% power to detect a biological effect, when α = 0.05 with the current group sizes, using the mean±SD of the data. A further calculation was performed to determine the sample size required to detect a 20% difference between the two independent groups, based on the mean±SD for the NMV analysis in COPD patients. For 80% power, the adequate sample size was calculated as n=172 per group, and demonstrating that the statistical power of the present analyses was low.

Matrix metalloproteinase-9 expression

In addition to identifying the origin of plasma MVs using flow cytometry, CD66b+ MVs were analysed for surface expression of MMP-9. For this, it was only possible to analyse five of the six COPD patient samples, due to limited sample volume for one of the patients. MMP-9 could be detected on 52.78 and 35.31% of CD66b+ MVs in the control and patient groups, respectively (fig 3.1 (E)). There was no statistically significant difference between these groups by unpaired t-test.

3.3.2 Quantification and Characterisation of Circulating Microvesicle Types in Patients with Chronic Obstructive Pulmonary Disease and Co-morbid Pulmonary Hypertension

No differences were found in MV types during COPD exacerbation compared with the control group in the small cohort analysed. However, due to the low sample size we were unable to determine whether numbers of MVs may be linked to clinical parameters in these patients. We therefore sought to characterise the MV profile of a larger group of well characterised stable COPD patients with the systemic co-morbidity pulmonary hypertension (n=13) available as stored samples in a pulmonary hypertension biobank, to determine if circulating MV profile may be informative in these cases. The STH-Obs biobank for which Prof. Allan Lawrie, University of Sheffield, is lead investigator was utilised. Whilst rare, PH is a relatively underdiagnosed condition, and as discussed earlier in this chapter, incidence in older people and in COPD patients is increased, therefore identification of a biomarker of the condition would be of value. PPP was analysed for both MV types by flow cytometry and also MV content (MMP-9 and TIMP-1) by ELISA. An age-matched control group (n=12) from the same biobank was also analysed.

Patient and age-matched control participant demographics are shown in table 3.2. The age range of the COPD patients was 50 to 81 years and of age-matched healthy volunteers was 51 to 82 years. Most of the participants in the patient group had moderate to severe disease, with GOLD stage II–IV.

Only two of the COPD patients had a neutrophil count above 7.5×10^9 cells/L, i.e. above the normal upper range, and the same participants also had a total leukocyte count above 11×10^9 cells/L. In addition, one of these participants also had high CRP levels (28.8 mg/L), along with one other participant without an elevated neutrophil count.

Patient platelet counts did not appear elevated and were within the normal range. The CRP levels were not available for all patients, and cell counts or other blood analyses were not performed for healthy volunteers so could not be compared here.

Microvesicle phenotype

The mean numbers of neutrophil (CD66b+), monocyte (CD14+), endothelial (CD144+), and platelet-derived MVs (CD41a+) are individually plotted for each participant in figure 3.2 (A–D). Additionally, antibody concentrations and laser voltages were further optimised using isotype controls and by calculating the separation index in a variety of settings (detailed in materials and methods section 2.2.7). One key difference which should be noted for these samples is the use of stored platelet-rich plasma, from which platelets were subsequently removed to create PPP after initial thawing. Due to this process, some debris remained in the pelleted MV population which was evident upon flow cytometric analysis. Therefore, to avoid inclusion of debris in any subsequent calculations, MV frequencies were plotted as MV/µL plasma rather than as a percentage of the total MV population used for the exacerbating group.

Although comparisons are difficult due to use of different outputs in the two groups (% vs. MV/µl), in contrast to the previous study using exacerbating patients and matched controls, in this cohort, for both patients and controls, endothelial MVs were the most abundant circulating MV type detected (fig 3.2. (C)), followed by platelets (D). This finding may have been influenced by the method of sample storage and also the antibody used to detect these MV types, which were both different between the two studies. As the matched controls in this study showed the same trend, it is unlikely that this represents an effect of exacerbation vs. stable disease or presence of PH.

The mean concentration of monocyte MVs and NMVs were highly similar in the patient group, with 211 MV/µL for both populations, although there was no correlation between individuals' values for these two MV types (spearman's rank correlation coefficient = 0.014).

	Healthy volunteers	Patients
Number	12	13
Age (yrs)	65±9	66±10
Sex (F:M)	6:6	6:7
COPD	0	13
Asthma	0	1
PH	0	13
VTE	0	3
estimated GOLD stage	-	I = 0 II = 5 III = 6 IV = 2
FEV1	-	1.3±0.6
FEV1 (%)	-	49±15.1
FVC (%)	-	89.9±22
FEV1/FVC	-	44.9±13
mPAP	-	39.3±10.5
WBC	-	8.3±1.8
Neutrophil	-	5.7±1.5
Platelets	-	211.8±73.4
Hct	-	0.4±0.07
Hb	-	32.9±44.5
GFR	-	50.5±33.2
Alt	-	21.6±9.9

Table 3.2 Study participant demographics for COPD patients with pulmonary hypertension (PH; n=13) and age-matched controls (n=12).

Abbreviations: VTE: venous thromboembolism. FEV1, forced expiratory volume in 1 minute. FVC: forced vital capacity (L). mPAP: mean pulmonary arterial pressure (mmHg). WBC: white blood cell count (x10^9/L; units for WBC, neutrophils and platelets). Hct: haematocrit (L/L). Hb: haemoglobin (g/dL). Gfr: glomerular filtration rate (ml/min/1.73m^2). Alt: alanine aminotransferase (IU/L).
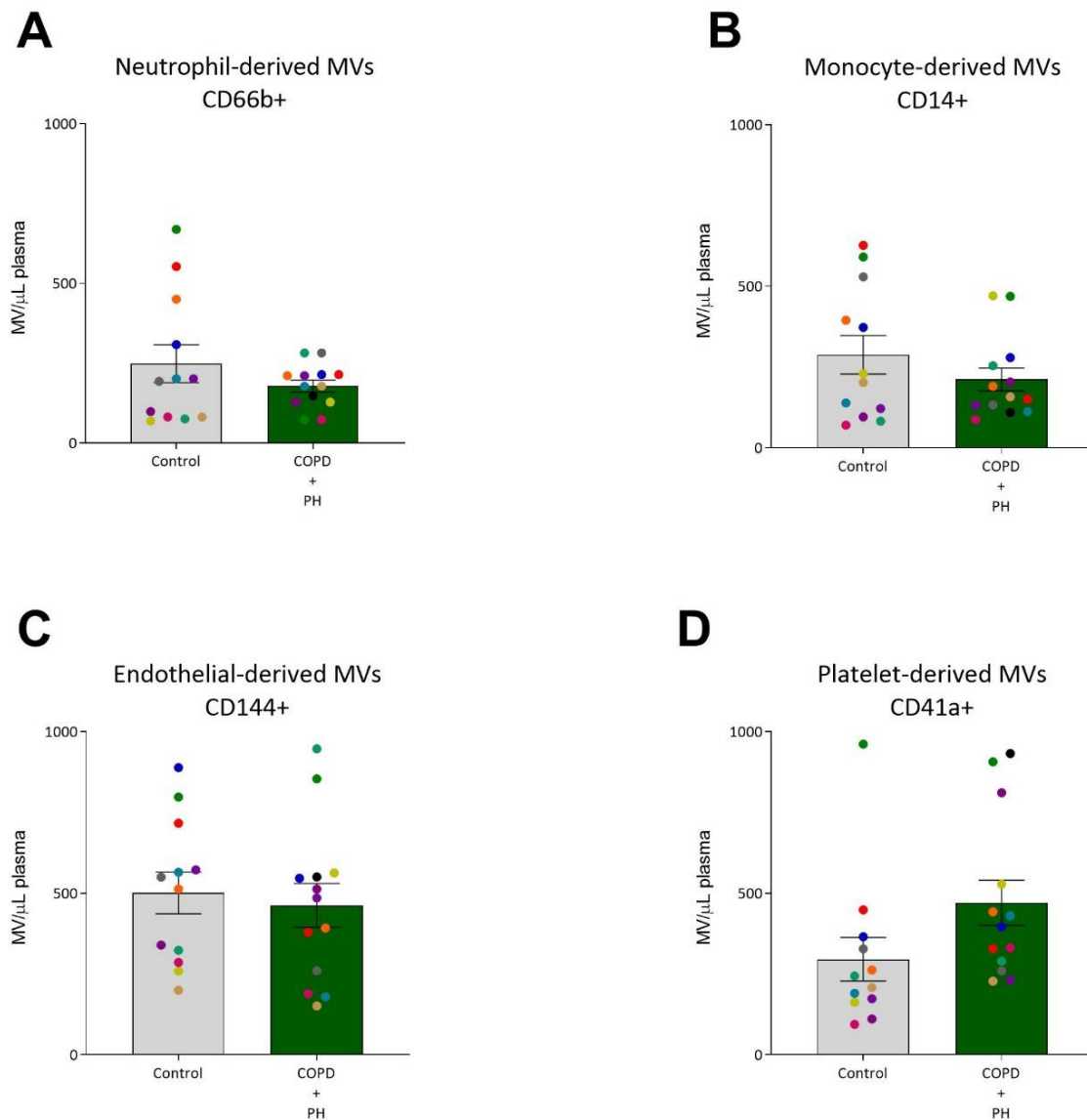
Figure 3.2. Circulating microvesicle (MV) phenotypes from COPD patients with pulmonary hypertension (PH) and age-matched control plasma samples

Surface expression of the cellular markers (A) CD66b, (B) CD14, (C) CD144 and (D) CD41a on MVs from platelet-poor plasma samples from COPD patients with PH (n=13) and age-matched controls (n=12) were probed using fluorescently-conjugated antibodies. After labelling, MVs were pelleted by high-speed centrifugation and then analysed by multi-colour flow cytometry using the BD LSRII. Due to the small size of MVs, a region of interest was initially identified for MV analysis using Megamix calibration beads. AbC compensation beads were utilised to perform compensation in the antibody panel, and this was applied to sample data in FlowJo analysis software. Data shows mean±SEM. Unpaired t-test was used for statistical analyses. Individual participants identified throughout the graphs by colours.

Patient platelet counts did not appear elevated and were within the normal range. The CRP levels were not available for all patients, and cell counts or other blood analyses were not performed for healthy volunteers so could not be compared here.

Microvesicle phenotype

The mean numbers of neutrophil (CD66b+), monocyte (CD14+), endothelial (CD144+), and platelet-derived MVs (CD41a+) are individually plotted for each participant in figure 3.2 (A–D). Additionally, antibody concentrations and laser voltages were further optimised using isotype controls and by calculating the separation index in a variety of settings (detailed in materials and methods section 2.2.7). One key difference which should be noted for these samples is the use of stored platelet-rich plasma, from which platelets were subsequently removed to create PPP after initial thawing. Due to this process, some debris remained in the pelleted MV population which was evident upon flow cytometric analysis. Therefore, to avoid inclusion of debris in any subsequent calculations, MV frequencies were plotted as MV/µL plasma rather than as a percentage of the total MV population used for the exacerbating group.

Although comparisons are difficult due to use of different outputs in the two groups (% vs. MV/µl), in contrast to the previous study using exacerbating patients and matched controls, in this cohort, for both patients and controls, endothelial MVs were the most abundant circulating MV type detected (fig 3.2. (C)), followed by platelets (D). This finding may have been influenced by the method of sample storage and also the antibody used to detect these MV types, which were both different between the two studies. As the matched controls in this study showed the same trend, it is unlikely that this represents an effect of exacerbation vs. stable disease or presence of PH.

The mean concentration of monocyte MVs and NMVs were highly similar in the patient group, with 211 MV/µL for both populations, although there was no correlation between individuals' values for these two MV types (spearman's rank correlation coefficient = 0.014). Interestingly, the three highest concentrations of immune-cell-derived MVs (CD66b+ and CD14+) were found in the control group (fig 3.2. (A+B)). However, there were no statistically significant differences in the concentrations of these MV types between the two groups.

The patient and control groups did tend to diverge for platelet-derived (CD41a+; fig 3.2 (D)) MVs, where six of the 12 healthy volunteers had an MV concentration lower than any of the COPD patients. However, this difference did not reach statistical significance (p = 0.087). A post-hoc power calculation was performed on this data; CD66b+ MVs = 20.3%, CD14+ MV = 19.5%, CD41a+ = 6.1%, CD144+ MV = 43.5% power to detect a biological effect, when α = 0.05 with the current group sizes, using the mean±SD of the data. A further calculation was performed to determine the sample size

required to detect a 20% difference between the two independent groups, based on the mean±SD for the NMV analysis in COPD patients. For 80% power, the adequate sample size was calculated as n=56 per group. This was repeated based on the COPD patient CD41+ MV data and sample size was calculated at n=113 per group. As a potentially biologically meaningful effect, a 20% change in NMV numbers was chosen, as high-fat diet in mice induced a 20% increase in circulating NMVs, with demonstrated functional consequences on atherogenesis and inflammation(Gomez *et al.*, 2020).

Upon performing a ROUT outlier test on both the patient and control populations with a strict Q = 0.2% and also Grubbs test with α = 0.05, one healthy participant was identified as a highly likely outlier, with a high CD41a+ MV concentration. When this participant was removed from the analysis and a t-test was performed on the cleaned data, the two populations were statistically significantly different (p = 0.009), where healthy volunteers tended to have less CD41a+ MVs (mean MV concentration/µL: 235.29 vs 470.51). No other outliers were identified for any of the other MV types upon applying these tests. It is unclear whether this individual result occurred due to chance or whether this is genuinely an outlier which should be removed; use of the circulating platelet count in this participant would have been useful in helping to assess this and whether these levels were also elevated, but this information was unfortunately unavailable. However, this individual did have the highest NMV concentration of the control group, and second highest monocyte-derived and endothelial-derived MV concentrations, therefore was likely an accurate result. Three patients also had platelet-derived MV concentrations which were much higher than that in the rest of the population. The patient with the highest platelet MV concentration did have the highest number of monocyte-derived MVs of the patient group, and second highest endothelial-derived MVs, although their NMV concentration was surprisingly the lowest of the group. The platelet count for this participant was also the highest of the patient group (356×10^9/L) and they had the second highest neutrophil count (7.96×10^9/L). The other two patients did not seem to demonstrate any trends across MV types and had mid-range platelet counts within the group. When the three higher patient values for CD41a+ MVs and highest control were removed, these results were also statistically significantly different (p = 0.025). Understanding the reasoning behind these high platelet MV levels would be of interest, particularly in the cardiovascular condition PH.

Correlation analysis was performed to determine whether numbers of each vesicle type, or marker expression (median fluorescence intensity [MFI]) was linked with that of the other MV types. Table 3.3 shows the outcomes of this analysis, with statistically significant correlations included. The strongest correlation in the control group was a positive correlation between numbers of neutrophil and platelet-derived MVs (r=0.838, r^2=0.702, p=0.0007).

A

	CD66b MV/µl	CD66b MFI	CD14 MV/µl	CD14 MFI	CD41a MV/µl	CD41a MFI	CD144 MV/µl	CD144 MFI
CD66b MV/µl			0.824 0.679 ***		0.838 0.702 ***		0.777 0.604 **	
CD66b MFI								
CD14 MV/µl	0.824 0.679 ***				0.76 0.578 **		0.672 0.451 *	0.713 0.509 **
CD14 MFI								
CD41a MV/µl	0.838 0.702 ***		0.76 0.578 **				0.668 0.446 *	
CD41a MFI								
CD144 MV/µl	0.777 0.604 **		0.672 0.451 *		0.668 0.446 *			
CD144 MFI			0.713 0.509 **					

B

	CD66b MV/µl	CD66b MFI	CD14 MV/µl	CD14 MFI	CD41a MV/µl	CD41a MFI	CD144 MV/µl	CD144 MFI
CD66b MV/µl					-0.63 0.402 *	-0.58 0.335 *		
CD66b MFI								0.66 0.436 *
CD14 MV/µl					0.623 0.388 *		0.649 0.421 *	
CD14 MFI								
CD41a MV/µl	-0.63 0.402 *		0.623 0.388 *					
CD41a MFI	-0.58 0.335 *							
CD144 MV/µl			0.649 0.421 *					
CD144 MFI		0.66 0.436 *						

Table 3.3. **Correlation between circulating microvesicle (MV) types and expression of other MV surface markers in COPD.**

*(A) Statistically significant correlations are shown for age-matched healthy participants (n=12) and (B) COPD patients with pulmonary hypertension (n=13, 1 value removed for CD41a analysis due to ROUT outlier test). Numbers indicate R-value, R^2, and level of significance. * p≤0.05, **p≤0.0099, ***p≤0.001*
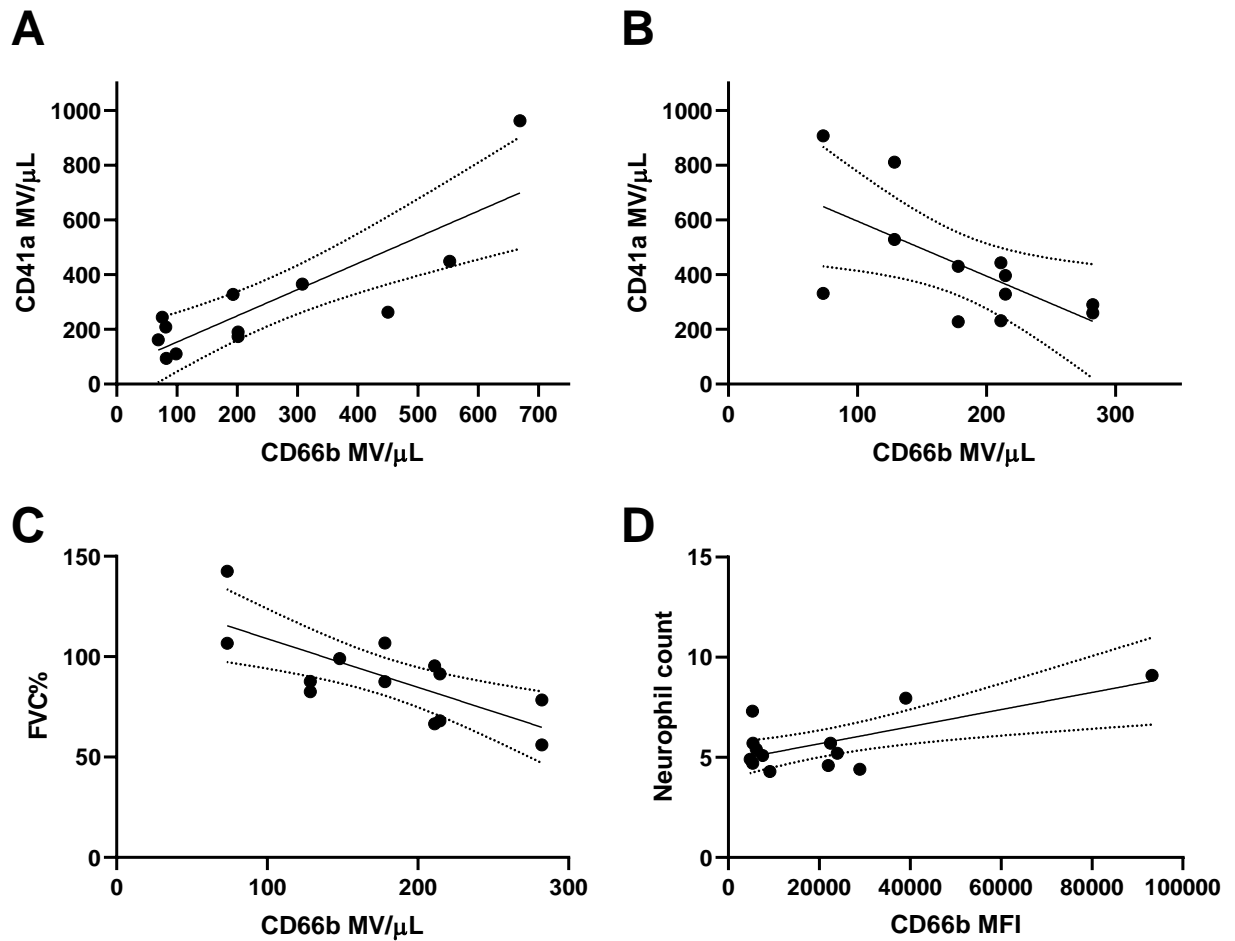
Figure 3.3. Correlation analysis of circulating microvesicle (MV) numbers in COPD

Correlation between circulating CD66b+ (neutrophil-derived) and CD41a+ (platelet-derived) MV are shown in (A) age-matched control subjects (n=12; r=0.0824, p≤0.001) and (B) COPD patients with pulmonary hypertension (n=12; r=-0.63, p≤0.05). ROUT outlier test was used and one outlying data point was removed from CD41a dataset in the COPD cohort.

(C) The strongest correlation between circulating MVs and clinical parameters in the COPD cohort analysed is shown: CD66b+ MV/μL significantly, negatively correlated with FVC% predicted (FVC%; r=0.7392, p≤0.0099; n=13).(D) The second strongest correlation in this group is shown here between CD66b median fluorescence intensity (MFI) and blood neutrophil count (r=0.7038, p≤0.01; n=13). 95% confidence intervals are shown in all groups but the dotted lines.

	Parameter	Age	WBC	neut.	platelets	Hct	Hb	Gfr	Alt	mPAP	FEV1	FEV1%	FVC%
CD66b	MV/µL	ns	ns	ns	ns	ns	ns	ns	ns	ns	ns	ns	-0.7392 (0.5464) p=0.0039
	MFI	ns	0.6877 (0.4729) p=0.0094	0.7038 (0.4953) p=0.0073	ns	0.5791 (0.3353) p=0.0381	ns	ns	ns	ns	ns	ns	ns
CD14	MV/µL	ns	ns	ns	ns	ns	ns	ns	ns	ns	ns	ns	ns
	MFI	ns	ns	ns	ns	ns	ns	ns	ns	ns	ns	ns	ns
CD41a	MV/µL	ns	ns	ns	ns	ns	0.6622 (0.4386) p=0.0190	ns	ns	ns	ns	ns	0.5805 (0.3370) p=0.0478
	MFI	ns	ns	ns	ns	ns	ns	ns	ns	ns	ns	ns	0.5977 (0.3573) p=0.031
CD144	MV/µL	ns	ns	ns	ns	ns	ns	ns	ns	ns	ns	ns	ns
	MFI	ns	0.6846 (0.4686) p=0.0098	ns	ns	ns	ns	ns	ns	ns	ns	ns	ns

*T*able 3.4. Correlation between circulating microvesicle (MV) types in COPD and clinical parameters.

Statistically significant correlations are shown for COPD patients with pulmonary hypertension (n=13, 1 value removed for CD41a analysis due to ROUT outlier test). Numbers indicate R-value, R^2, and level of significance (p-value). Orange square highlights the strongest correlation of the parameters analysed.

Abbreviations: VTE: venous thromboembolism. FEV1, forced expiratory volume in 1 minute. FVC: forced vital capacity (L). mPAP: mean pulmonary arterial pressure (mmHg). WBC: white blood cell count ($x10^9$/L; units for WBC, neutrophils and platelets). Hct: haematocrit (L/L). Hb: haemoglobin (g/dL). Gfr: glomerular filtration rate (ml/min/1.73m^2). Alt: alanine aminotransferase (IU/L).

Interestingly, an inverse, but weaker correlation between these parameters was found in the patient group (r=-0.63, r^2=0.402, p=0.0268), these trends are illustrated in figure 3.3 (A) and (B), respectively. In the control group NMV (CD66b+) numbers were also significantly and positively correlated with monocyte and endothelial MV numbers, but these relationships were no longer observed in the COPD patient group. Table 3.4 shows the correlation of circulating MV numbers (MV/µl) and marker expression (MFI) with clinical parameters in these patients.

The strongest correlation here was between CD66b^{+} MV/µl and FVC% (i.e. ratio to reference values), demonstrating a statistically significant negative relationship. This is shown in figure 3.3 (C). However, this MV type did not correlate with other lung function parameters such as FEV1 which is more relevant to the disease stage in COPD. A weaker but statistically significant positive correlation was also observed between both CD41a MV/µl and MFI and FVC%. CD66b MFI, but not concentration, significantly and positively correlated with white blood cell count (WBC) and also neutrophil count, although for the latter this trend may be driven by the few higher values in the group (fig 3.3 (D), it would be interesting to determine if this was linked to neutrophil activation status, where CD66b expression is upregulated and may reflect NMV MFI. In COPD with PH, platelet-derived MVs may have a role systemically, however the number of NMVs did not appear to be an important factor, although neutrophil activation status may be changed. We therefore sought to understand next whether content of these MVs is different rather than the MV concentration.

Microvesicle-associated matrix metalloproteinase-9 and tissue-inhibitor of metalloproteinase-1 content
Previous studies have shown that MMP-9 is a key protease in the interaction and effects of NMVs in epithelial cells (Butin-Israeli et al., 2016). To determine whether these vesicles may have differential internal cargo and therefore different effects, ELISA was performed for MMP-9 and its endogenous inhibitor, TIMP-1. Both pelleted plasma MVs (20,000 *g*) resuspended in buffer to the same original plasma sample volume and MV-depleted plasma were analysed. No significant differences were found in MV-depleted plasma between the two study groups (fig 3.4 (A); mean concentrations 8278 and 7907 pg/ml); however, the plasma MVs from stable COPD patients with PH contained significantly more total MMP-9 than that in the control group (3100 vs. 1605 pg/ml, respectively, p = 0.0277) (fig 3.4 (B)), with nearly double the concentration in patient MVs compared with controls. Whilst one subject in the patient group had substantially higher levels of MMP-9 than the rest of this group, removing this data point still indicated a statistically significant difference from the control group (data not shown; p = 0.0314). Moreover, this patient was not found to be an outlier by statistical testing.
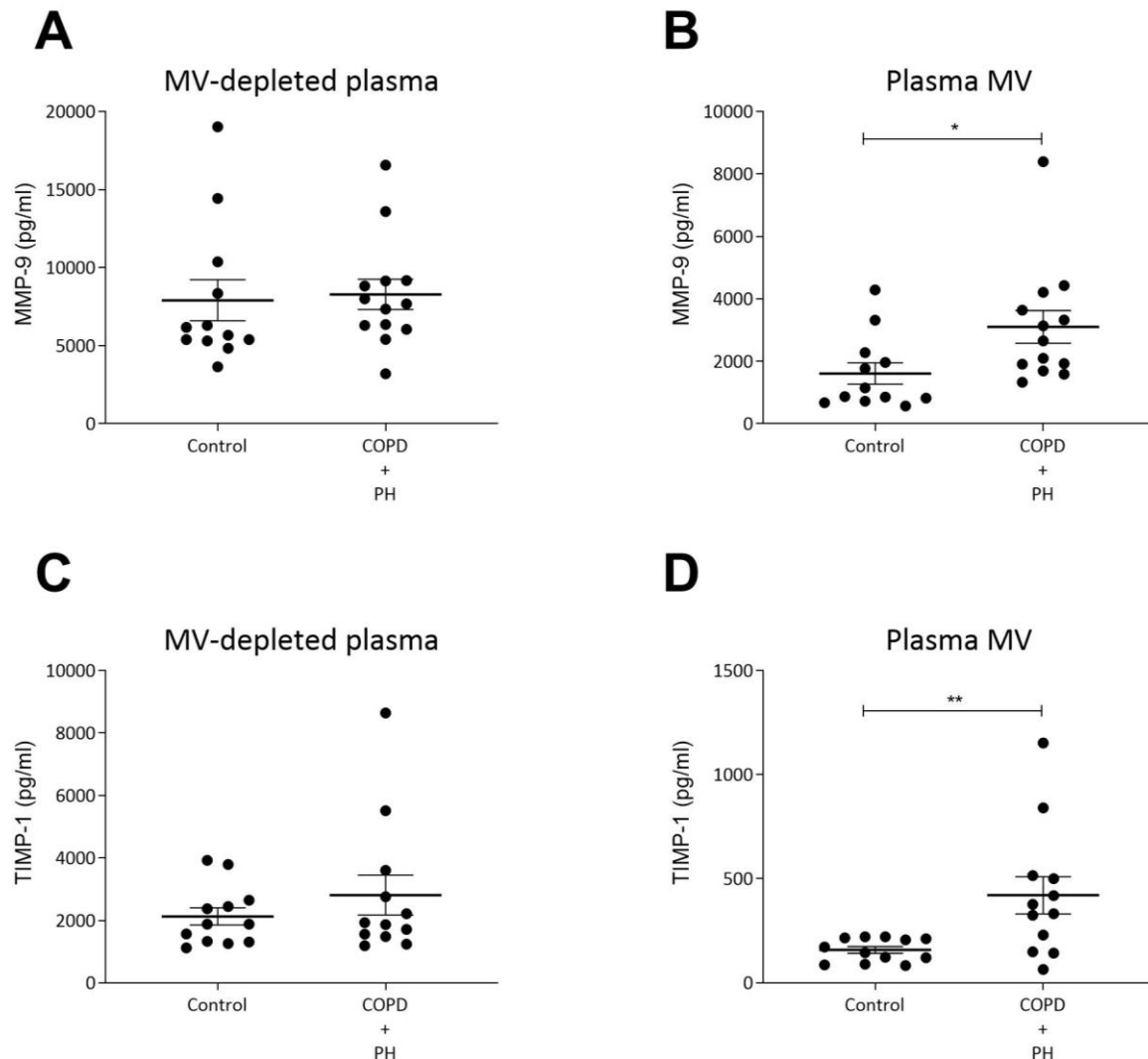
Figure 3.4 Matrix Metalloproteinase-9 (MMP-9) and tissue inhibitor of metalloproteinase-1 (TIMP-1) content of plasma microvesicles (MVs) and MV-depleted plasma in COPD patients with pulmonary hypertension (PH) and age-matched controls

(A+B) Total MMP-9 and (C+D) TIMP-1 in plasma MVs pelleted by high-speed centrifugation (B+D) and in the remaining MV-depleted plasma (A+C) from COPD patients with PH (n=13 for MMP-9 and n=12 for TIMP-1; not enough sample remaining for one participant) and age-matched controls (n=12) was quantified by ELISA. Data shows mean±SEM. Unpaired t-test was used. * p ≤ 0.05 , ** p ≤ 0.0099.

Plasma MVs contained less than half the levels of MMP-9 detected in the MV-depleted plasma, and this differential concentration was further exaggerated for TIMP-1 (fig 3.4 (C) and (D)). TIMP-1 was found at much lower levels in the plasma MVs (421 and 158 pg/ml in the COPD and control groups, respectively), but significantly more of this protein was still found in the patient group compared with the age-matched controls (p=0.0086). There were no statistically significant differences in TIMP-1 levels in the MV-depleted plasma. It was therefore not possible to conclude whether the activity of MMP-9 in these vesicles was increased since TIMP-1 was also at higher levels and due to limited amount of patient sample, this investigation was then continued using neutrophils from healthy participants, exposed to pro-inflammatory stimuli to generate NMVs.

3.3.3 Transmission electron micrographs of microvesicles from N-formyl-methionyl-leucyl-phenylalanine stimulated peripheral blood neutrophils from healthy participants

To characterise the NMVs generated from fMLP-stimulated peripheral-blood neutrophils and to check sample purity, NMVs were first isolated by differential centrifugation and eventual pelleting at 20,000 g (chapter 2, section 2.2.1), then negative staining of unfixed NMVs was carried out and imaging using transmission electron microscopy (TEM) as per section 2.2.5 in the materials and methods section (chapter 2). For this, I performed sample processing and staining, and TEM imaging was done by Dr Svetomir Tzokov, University of Sheffield Electron Microscopy facility. With this technique, NMVs could be imaged from a suspension, avoiding potential artefacts arising from sample processing when embedding in resin. In the resulting images (fig 3.5 (A+B)) rounded vesicles of around 200 nm diameter were seen, however the NMV membrane was partially collapsed, likely due to a lack of fixation using this protocol. Existence of a plasma membrane was strongly supported by the lack of uranyl formate dye uptake, indicating presence of a tight network of lipids. An individual NMV is shown at high magnification in figure 3.5 (B), allowing further detail to be studied, with possible protein bound to the surface of the vesicle on the top left side of the membrane.

An NMV sample was also embedded in araldite resin to permit sectioning and staining and then imaged using TEM . Here, I performed sample fixation and staining, and Dr Chris Hill performed sectioning and TEM imaging. Upon imaging, an NMV population that pelleted at 20,000 g could be observed (fig 3.5 (C)). NMVs were typically spherical in shape and had a diameter ranging ~100–300 nm in agreement with the negative staining in (A) and (B), and their density, as shown by similar stain intensities of the NMVs, was similar for all imaged vesicles.
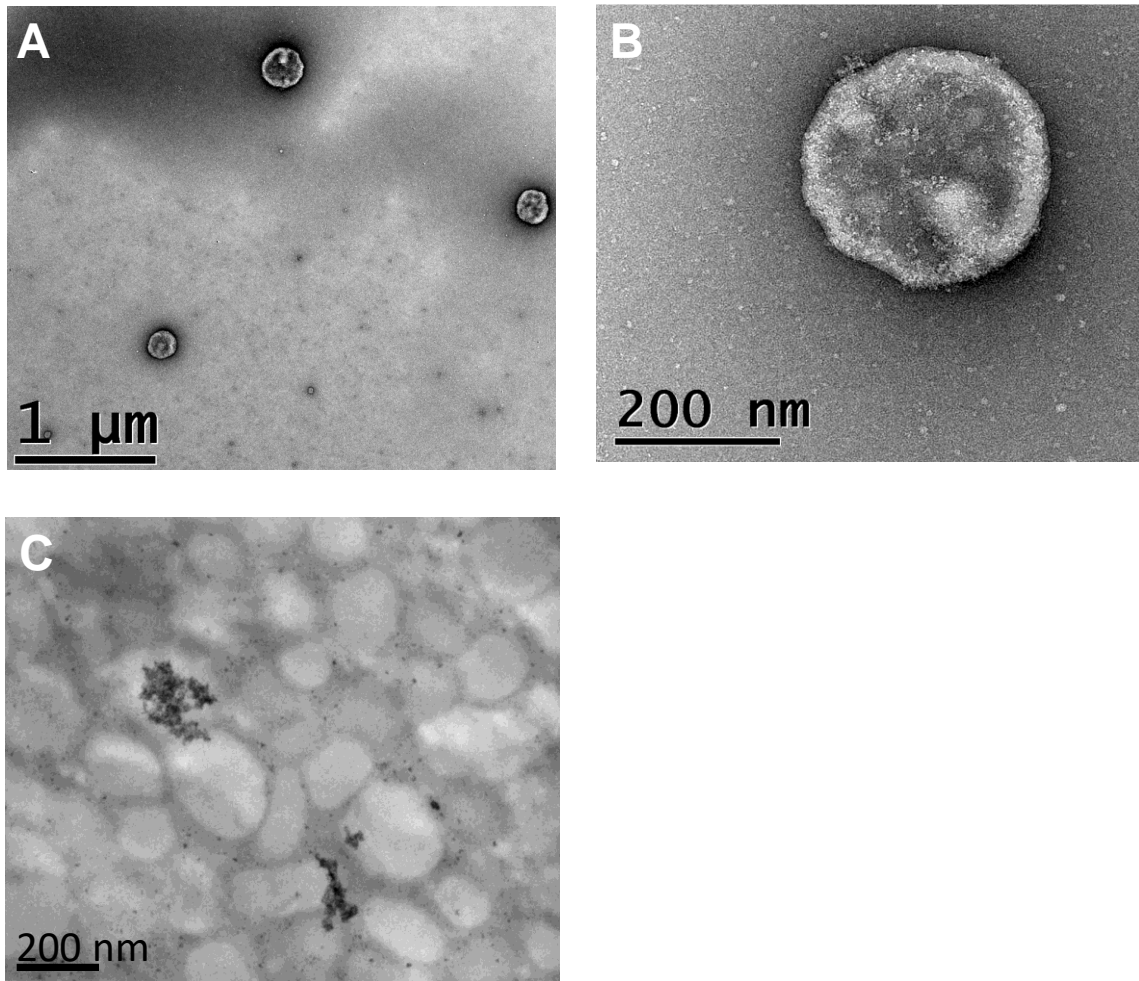
Figure 3.5 Transmission electron micrograph of resin-embedded and negatively-stained neutrophil-derived microvesicles (NMVs)

Transmission electron microscopy was used to image negatively stained (A, B) or resin-embedded (C) NMV sample generated from fMLP-stimulated neutrophils by ultracentrifugation.

(A) Nominal magnification approx. 5,700x. (B) Nominal magnification: 28,500×. Micrographs were produced using a Philips CM100 transmission electron microscope. (C) Nominal magnification: 6.800×. Micrographs were obtained using a Technai G2 Biotwin transmission electron microscope.

However, other structural features of these NMVs could not be clearly distinguished using this technique, and no organelles or other internal architecture were evidenced inside the vesicles. No contamination with intact cells, cell fragments, or granules was found in the sample, as shown by lack of other structures and uniform staining intensity of most NMVs.

3.3.4 Zeta-view nanoparticle tracking analysis of neutrophil-derived microvesicles

NTA (a technique that relates the rate of Brownian motion to particle size) was used to determine the size distribution of the isolated population of NMVs, and to assess the purity of the sample in terms of EV types present. To optimise the settings for this experiment and ensure NMVs were accurately detected, submicron calibration beads of 200, 500, and 800 nm were used. Three frame rates of 30—the recommended settings for exosome detection—7.5 and 3.75 frames/sec were tested. The size distribution histograms for each of these runs are shown in figure 3.6 (A–C). The settings which gave the best separation of the different bead populations in this size range was the slowest frame rate, 3.75 frames/sec (fig. 3.2 (C)), which allowed detection of more if the larger sized particles than any of the other frame rates, whilst 30 frames/sec (fig 3.6 (A)) provided a normally-distributed population with a smooth curve containing a single peak at ~135 nm with less separation. The lowest frame rate was subsequently used for NMV analyses. Interestingly, despite the change in size distribution, the absolute concentration of particles detected was similar for all three frame rates (30: 8.9E+8 Particles/mL, 7.5: 1.5E+9 Particles/mL, 3.75: 8.5E+8 Particles/mL).

The size distribution histogram for NMVs generated from fMLP-stimulated neutrophils is shown in figure 3.6 (D). Negligible numbers of EVs of less than 50 or greater than 1000 nm were detected in the sample, indicating absence of smaller EVs such as exosomes and larger apoptotic bodies, and the population was normally distributed indicating a single population. In combination with the TEM data this signified a relatively pure NMV sample. The modal diameter calculated by median peak analysis was 194.7 nm, in agreement with the size range (100–300 nm) indicated by the electron micrographs in figure 3.5. Having confirmed that NMVs could be successfully isolated here from healthy participant neutrophils, we then began to characterise NMV content and activity to identify the potential for a role in inflammation.
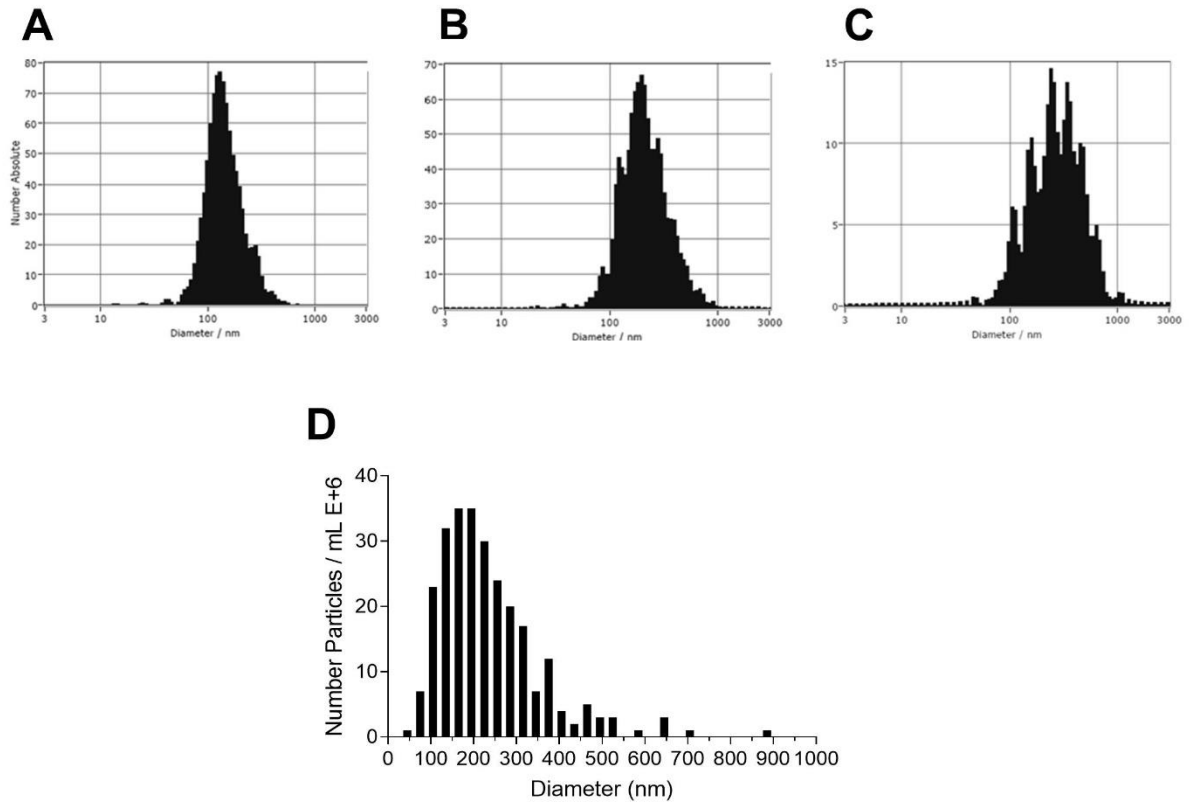
Figure 3.6 ZetaView nanoparticle tracking analysis of synthetic calibration beads and neutrophil-derived microvesicles (NMVs)

After initially calibration with 110 nm polystyrene beads, further optimisation of ZetaView settings for NMV detection was done using submicron 200, 500, and 800 nm beads (A-C). Frame rates of (A) 30, (B) 7.5, and (C) 3.75 frames/sec were tested to achieve optimal separation of the bead populations.

(D) Representative histogram showing size distribution of NMVs isolated from fMLP-stimulated neutrophils.

3.3.5 Detection and quantification of matrix-metalloproteinase-9 in neutrophil-derived microvesicles from healthy participants

Matrix metalloproteinase-9 western blotting of phosphate-buffered saline and f-met-leu-phe neutrophil-derived microvesicles

Higher levels of the protease MMP-9 and its endogenous inhibitor TIMP-1 were found to associate with COPD patient plasma MVs compared with matched-controls. However, we were unable to confirm if this translated to greater protease activity and also whether MMP-9 was associated with NMVs specifically or with other MV types due to limited amounts of patient samples and inability to isolate NMVs alone from the plasma. Further, plasma was tested for use in protease activity assays in both gelatin zymography and a kinetic enzyme activity assay and results were variable and unreliable, potentially due to long-term storage or high levels of antiproteases and many other circulating proteins (data not shown). Therefore, we aimed to confirm the presence of MMP-9 in NMV samples generated from healthy participant peripheral blood neutrophils, providing a pure sample of NMVs rather than a mixed population, and model conditions during lung inflammation by the addition of the pro-inflammatory stimulus fMLP, for further functional studies of this enzyme. Use of freshly generated NMVs from healthy participant cells allowed investigation of activity and protein expression unimpeded by storage conditions.

This was initially done by western blotting using whole NMV and neutrophil lysates. To compare the MMP-9 content in unstimulated, quiescent, and activated neutrophils and the resulting NMVs, cells were lysed either immediately after isolation (unstimulated) or after 1 h incubation with PBS or fMLP. NMVs from PBS and fMLP-stimulated neutrophils were then lysed, and an equal amount of total protein was loaded for SDS-PAGE.

As shown in figure 3.7 (A) in an example blot, the parent neutrophils evidenced a strong band corresponding to pro-MMP-9 (92 kDa) but contained negligible amounts of active MMP-9 (82 kDa). although not all blots in the series showed as strong staining, this trend was consistent, as shown in the quantification using densitometry in (C). NMVs from PBS and fMLP stimulation both contained pro-MMP-9, however, only fMLP NMVs also strongly expressed the active form of this protease. Equal protein loading was employed after quantification with microBCA assay.

Levels of pro-MMP-9 (92 kDa) were quantified and normalised to GAPDH expression (fig 3.7 (B)). GAPDH has previously been shown to be secreted by cells and associate with NMVs (Dalli *et al.*, 2013) and was identified to be stably expressed and as a good candidate housekeeping gene in some EV types (Gouin *et al.*, 2017).
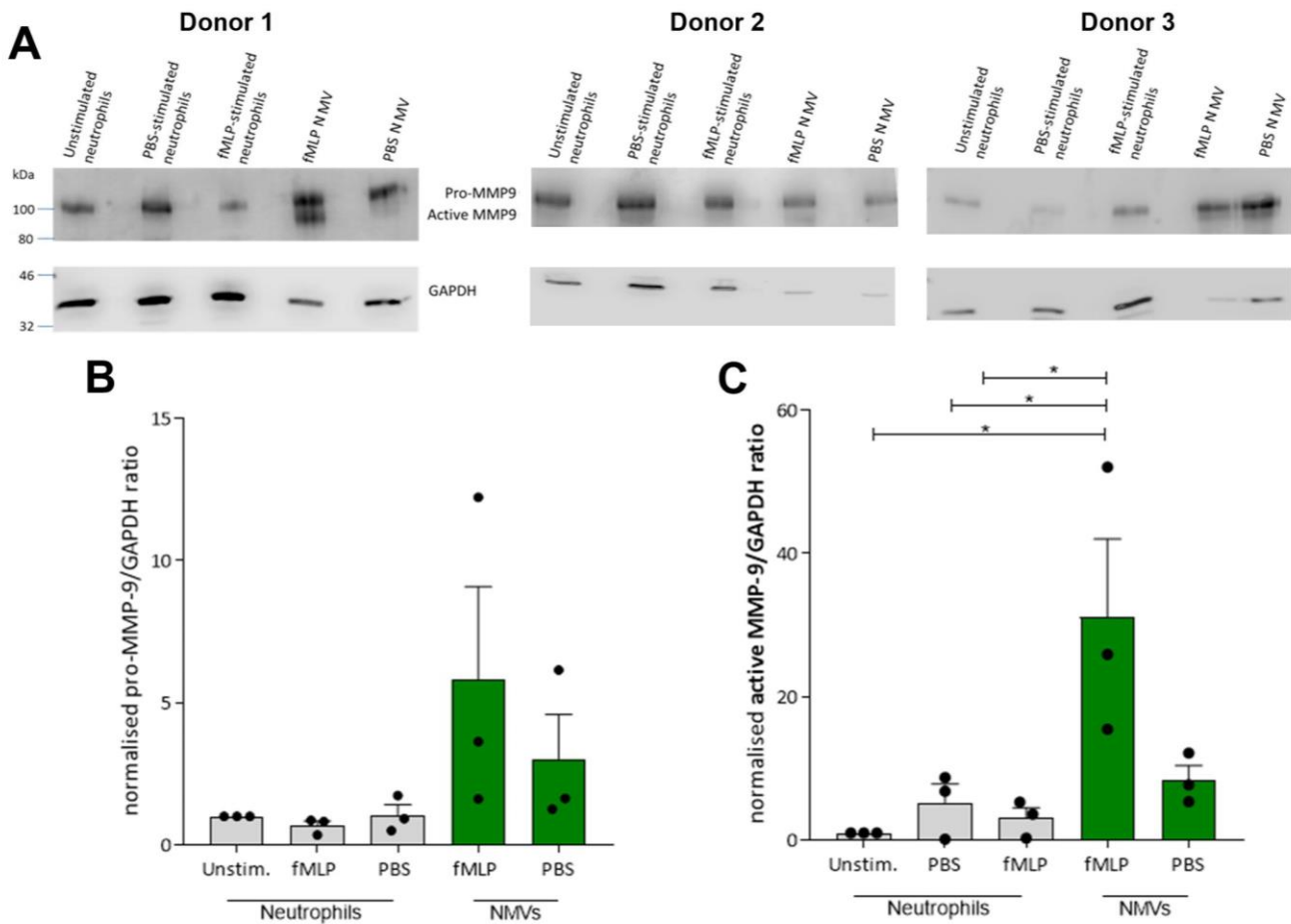
Figure 3.7 Western blotting for matrix metalloproteinase-9 (MMP-9) in parent neutrophil and generated microvesicle lysates

(A) NMVs were generated from neutrophils stimulated with PBS (control) or 10 µM fMLP. Neutrophils were either lysed after 1h stimulation or immediately after isolation (unstimulated). Approx. 1.5 µg of total protein, quantified using micro bicinchoninic acid assay, per sample was loaded for SDS-PAGE. Blots from three different neutrophil donors are shown. Pro- and active MMP-9 expression was determined by western blotting. (B) Pro-MMP-9 and (C) active MMP-9 densitometry normalised to GAPDH. MMP-9:GAPDH ratio was then normalised to the corresponding value for unstimulated cells (unstim.) for each donor. N = 3. Data shows mean+SEM, one-way ANOVA with multiple comparisons to analyse data. * p ≤ 0.05

However, as a limitation here it is unknown whether the expression levels of GAPDH are the same between parent neutrophils and NMVs. On the other hand, this was highly useful here to compare the differentially stimulated neutrophils, and also to compare the NMVs from different stimuli.

Pro-MMP-9 was detected in all of the samples. Whilst MVs tended to contain more pro-MMP-9 than their parent neutrophils, there were no statistically significant differences between any of these sample types. Additionally, levels of pro-MMP-9 in the NMV samples were similar regardless of stimulus.

Active MMP-9 expression (82 kDa band) was also quantified from three individual donors, as shown in figure 3.7 (C). This confirmed that active MMP-9 was highly expressed in fMLP NMVs, with over 31-fold greater expression than the barely detectable level seen in MVs from unstimulated cells. Whilst fMLP MVs from the same donor always contained more active MMP-9 than PBS MVs, this difference was not statistically significant overall ($\underline{p = 0.06}$) by one-way ANOVA with multiple comparisons, and likely low N-numbers and variation in active MMP levels in the fMLP MVs impacted this result. When using GAPDH to normalise expression, fMLP MVs did contain significantly more active MMP-9 than unstimulated, PBS (control) and fMLP-stimulated neutrophils ($p = 0.013$, 0.032 and 0.02, respectively) from the same donor.

Quantification of NMV numbers and total matrix metalloproteinase-9 in neutrophil microvesicles from different stimuli

Previous results described above showed no differences in circulating granulocyte-derived MV concentrations between matched controls and COPD patients with PH or in surface MMP-9 expression in exacerbating COPD patients and controls; however, MMP-9 content of the circulating MVs did diverge significantly. Therefore, we aimed to investigate these effects further using healthy participant isolated neutrophils. These cells were stimulated with PBS (control) and fMLP, as above, and also with a further COPD-relevant inflammatory stimulus, 10% cigarette smoke extract (CSE), freshly generated by bubbling a Kentucky reference cigarette (3R4F) through PBS, utilising a Masterflex pump. This CSE concentration was chosen due to limited effect on neutrophil viability in a 1h exposure period (data not shown). The resulting NMVs were then quantified by flow cytometry. This analysis revealed no significant differences in the numbers of NMV produced in response to any of the stimuli used, including a combination of fMLP and CSE (fig 3.8 (A)). Experimental work here using CSE was performed by MSc student Magdalena Grudzien under my day-to-day supervision.
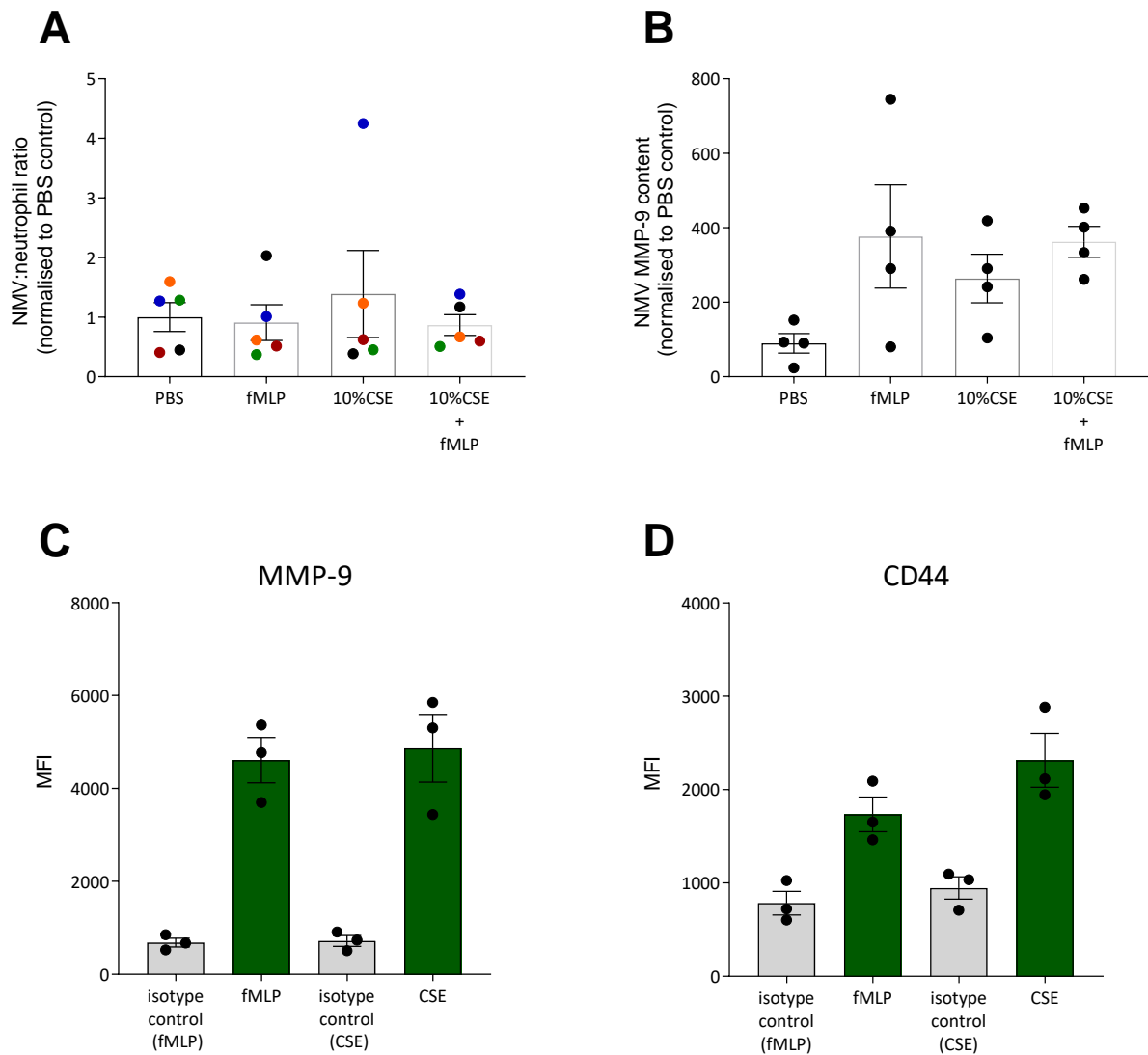
Figure 3.8 Neutrophil-derived microvesicle (NMV) quantification and matrix-metalloproteinase-9 (MMP-9) content and surface expression

(A) Neutrophils were exposed to stimuli for 1 h to induce NMV generation, the number of NMVs produced was then quantified by flow cytometry. NMV absolute number was divided by the number of neutrophils obtained to calculate the NMV:neutrophil ratio. This ratio was normalised to the PBS (control) condition to compare between stimuli and between donors. Colours represent individual donors. (B) Total MMP-9 content of lysed NMVs, generated as above, was quantified by ELISA. This concentration was then normalised to that in the PBS condition. Data shows mean±SEM. N=5 individual donors. (C) MMP-9 and (D) CD44 surface expression on NMVs from either fMLP or CSE stimulated neutrophils was analysed by flow cytometry. Isotype controls were used to determine non-specific binding capacity of the antibodies. N=3 individual donors. fMLP: N-formylated met-leu-phe (10 µM), CSE: cigarette smoke extract (10%). MFI: median fluorescence intensity. Experiments carried out by MSc student Magdalena Grudzien under supervision of Merete Long and Dr Victoria Ridger.

The effects of these differing stimuli upon total MMP-9 content, and therefore protease packaging, of these vesicles were then measured using ELISA. PBS, fMLP, and CSE NMVs generated from the same donor were analysed in this experiment. Use of ELISA facilitated more rapid and quantitative measurement of MMP-9 levels, however, was limited in that active and pro-MMP-9 could not be discerned here, and only total levels were therefore reported. The highest MMP-9 concentrations were observed after stimulation with fMLP, and combined addition of CSE did not augment this effect (Fig 3.8 (B)). PBS NMVs contained consistently lower total MMP-9 concentrations than fMLP NMVs; however, CSE stimulation alone only produced NMVs with higher total MMP-9 than control levels in two out of five experiments. High levels of variation were observed within each stimulation group, and none of the trends found here were statistically significant by one-way ANOVA.

Surface expression of matrix metalloproteinase-9 and CD44 on f-met-leu-phe and cigarette smoke extract neutrophil-derived microvesicles

Since we showed that active MMP-9 associated with MVs, we looked further into the potential for interactions in the lungs by initially examining the location of MMP-9 in these vesicles; intravesicular MMP-9 for example would require either degradation of MVs or fusion with cells to have an effect, whilst surface MMP-9 would permit interaction with cell-surface and extracellular proteins. By labelling these NMVs with FITC-conjugated MMP-9 antibody without permeabilisation, MMP-9 expression above the levels of isotype binding was confirmed on the surface of NMVs by flow cytometry (figure 3.8 (C). Flow cytometry was used to detect surface expression of MMP-9 on both CSE and fMLP NMVs generated from the same neutrophil donor; whilst MMP-9 expression was detected on both NMV types, there was no significant difference in surface expression levels. As a limitation, it was unfortunately unfeasible to measure this protein on PBS NMVs from the same donor due to the numbers needed for two stimuli and two labelling protocols here, and it would have been interesting to determine if PBS NMV had differential surface MMP-9 expression.

In other cell types, the adhesion molecule CD44 has been shown to anchor MMP-9 on the cell surface, protecting this enzyme from inhibition and degradation, and enhancing its proteolytic activity (Yu and Stamenkovic, 1999). Therefore, NMVs from these two stimuli were also probed for CD44, to determine whether they express this molecule on their surface. Figure 3.8 (D) shows that this protein was indeed detectable on NMVs, although there was a high level of non-specific binding shown by the isotype control which made it difficult to perform dual staining with MMP-9, however, CD44 labelling did show approximately two-fold more fluorescence than the isotype control. There were no significant differences in CD44 expression between the two vesicle types.

Matrix metalloproteinase-9 activity of cigarette smoke extract and f-met-leu-phe neutrophil-derived microvesicles

Although NMV-associated active MMP-9 was detected in fMLP NMVs by western blotting, this technique was limited in that it requires NMV lysis, therefore, does not provide information on the location of this active enzyme or on the capability of intact NMVs to degrade substrates. We found MMP-9 on the NMV surface, however could not confirm whether this was active by flow cytometry. The proteolytic activity of whole/non-lysed NMVs was therefore tested by measuring the capacity of these vesicles to degrade the MMP-9 substrate, Collagen IV, to investigate physiologically relevant mechanisms of ECM degradation.

DQ Collagen IV—a protein highly labelled with fluorescein isocyanate molecules, which is thereby quenched when intact but emits fluorescence upon cleavage and excitation by a 488-nm laser—was used for this assay. Initially, this method was tested using the positive control collagenase type IV, an enzyme highly capable of cleaving collagen IV, amongst other ECM components. Collagenase induced a rapid increase in the fluorescent signal in these wells, shown in figure 3.9 (A), which was proportional to the amount of proteolytic cleavage. This activity increased rapidly over the first 30 min and subsequently continued to increase more steadily. In parallel, 1×10^5 NMVs from fMLP or CSE stimulated neutrophils were added to wells in duplicate. The chosen NMV concentration permitted investigation of multiple conditions in a single donor (approximate total NMV yields from a single donor: $6–10\times10^5$ as quantified by flow cytometry; data not shown) and was approximately half that utilised for later investigations of NMV–epithelial cell interactions (2.4×10^5). NMVs also received washing by resuspension and then pelleting in filtered PBS before use in this assay to aid in removal of free proteins. Incubation with both of these NMV types induced collagen cleavage (fig 3.9 (B)). Collagen IV degradation by NMVs began at 0–1 h and peaked at approximately 7-8 h. Comparatively, collagen degradation in the control well, incubated with phenol-red-free media alone, remained at a low level. For two out of three donors used in this experiment, CSE NMVs had greater proteolytic activity than fMLP NMVs from the same donor. The area under the curve (AUC)±standard error (SE) for these was 5.573±0.258, 31.57±2.743, and 36.03±1.306 for media alone, fMLP and CSE NMVs, respectively, and represented statistically significant differences between these two NMV types and the control condition ($p = 0.029$ and 0.0127, respectively); however, significant differences were not found between the two MV types themselves.
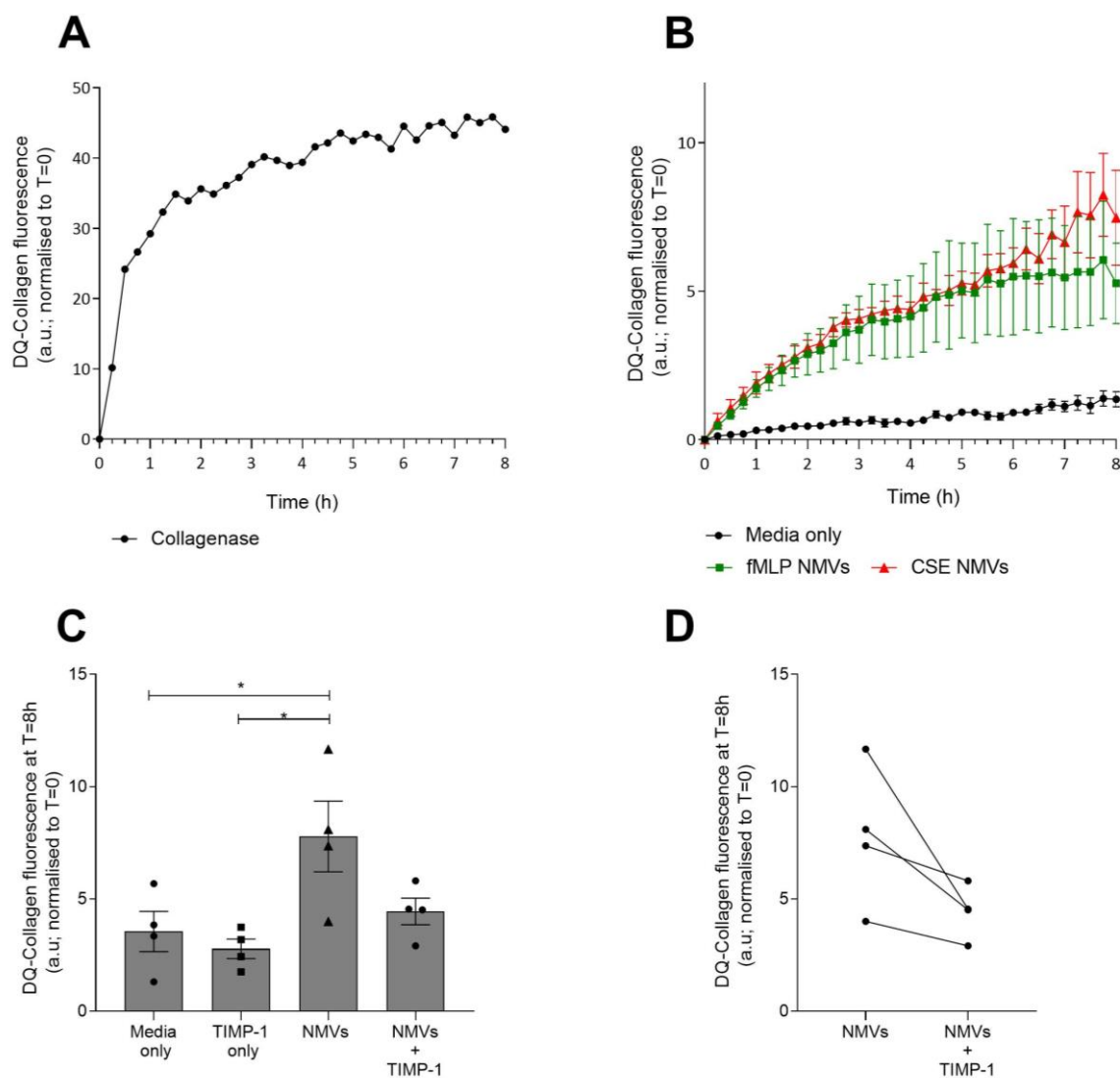
Figure 3.9 DQ Collagen IV degradation by NMVs from f-met-leu-phe and cigarette smoke extract stimulated neutrophils

(A) Collagenase was used as a positive control for substrate degradation. An individual run is shown here. (B) Collagen IV degradation by CSE and fMLP NMVs was compared. Data shows mean±SEM, n = 4 individual donors. 100,000 NMVs were added to a well in duplicate with DQ collagen IV. Substrate plus media only was used as a control. Fluorescence measurements were taken every 15 min for 8h. Fluorescence (arbitrary units; a.u.) was normalised to respective values at T=0h for all analyses. (C) fMLP NMVs were pre-incubated with the inhibitor TIMP-1, and this experiment was repeated (n=4). Data at 8h are shown here. (D) Data in (C) is displayed here as normalised fluorescence for the NMV and NMV+TIMP-1 conditions only at 8 h, the time at which Collagen IV cleavage began to level off. Linked data points indicate NMVs from the same donor. fMLP: N-formylated met-leu-phe (10 μM), CSE: cigarette smoke extract (10%). Experiments for (A) and (B) carried out by MSc student Magdalena Grudzien under supervision of Merete Long and Dr Victoria Ridger. * p ≤ 0.05. One-way ANOVA with multiple comparisons (Tukey's test) utilised.

To determine whether this degradation was due to MMP-9 or other proteases, NMVs were preincubated with the endogenous inhibitor of MMP-9, TIMP-1, for 1 h before the start of the assay. The assay was then repeated using only NMVs from fMLP-stimulated neutrophils (Fig 3.9 (C)), as this vesicle type was used for later functional assays with bronchial epithelial cells, and it was not possible to obtain sufficient quantities of NMVs to undertake this study with additional stimuli in the presence and absence of the inhibitor.

Results are shown at the 8h timepoint, where maximal activity was found in the previous experiment within the time course investigated. This assay showed that again, NMVs induced significant cleavage of the substrate compared with the control (p =0.042; 3.55±0.90) and TIMP-1 only (p = 0.016; 2.78±0.44) conditions. Use of TIMP-1 pre-incubation in the NMV sample resulted in a 43% reduction in mean collagen IV degradation (NMVs: 7.79±1.57, NMVs+TIMP-1: 4.45±0.60). However, this difference did not reach statistical significance (NMVs v. NMVs+TIMP-1: p=0.1262, one-way ANOVA with Tukey's multiple comparisons test), and large variation was seen in the NMV sample activity. Nevertheless, reductions in NMV collagen IV cleavage were seen in every experimental run, as shown in figure 3.9 (D), however there was variation in the magnitude of this effect for each donor.

3.4 Discussion

3.4.1 Exacerbating COPD patients and age-matched controls showed no differences in circulating MV phenotypes or surface protease expression

The first aim of this work was to determine whether circulating NMVs are different in COPD and whether these differences may be used to gain further insight into this disease and a potential role for these vesicles. To investigate the use of MV phenotype identification as a biomarker of disease in COPD, and to further understand the role of circulating MVs, flow cytometry was used to detect cell surface markers and determine the origin and relative proportions of these vesicles from stored plasma samples. As discussed above, flow cytometry has previously been validated for use in MV analyses after careful calibration of the relevant size parameters, which was done here using Megamix calibration beads (detailed in materials and methods section 2.2.2). PPP samples from exacerbating COPD patients were available through a collaboration with Dr Katharine Lodge from the University of Cambridge, a respiratory specialist who collected these samples as well as performing neutrophil isolation and functional studies in these patients. N=6 samples had been stored at -20°C as well at N=5 matched control samples. In her PhD work, Dr Lodge demonstrated

that neutrophils from exacerbating COPD patients showed increased release of a subset of granule and cytoplasmic proteins from these cells (Lodge, 2018) (manuscript in progress, "Hypoxia potentiates neutrophil-mediated endothelial damage in chronic obstructive pulmonary disease. Katharine M Lodge, Arlette Vassallo, Merete Long […] Alison Condliffe).

In these samples, the proportions of each MV type corresponded with the expected proportion of their respective parent cell types; i.e. the proportion of granulocyte-derived (CD66b+) MVs was higher than that for monocyte-derived (CD14+) MVs in both the control and COPD groups—since neutrophils are the most common circulating immune cell (Rosales, 2018), and platelet (CD41a+) MVs were the most common MV type overall (platelets are the second most abundant circulating cell type after erythrocytes (Maduskuie *et al.*, 1998)). Surprisingly, there were no statistically significant differences between the two groups for any of these MV types. In particular, we had hypothesised that the levels of immune cell-derived MVs, and particularly NMVs, would be higher in exacerbating COPD patients, as increased levels of platelet- and monocyte-derived MVs have recently been shown in exacerbating COPD patients (Tokes-Fuzesi *et al.*, 2018). It has previously been shown that higher levels of circulating and BALF leukocyte-derived MVs in ARDS patients correlated with better survival (Guervilly *et al.*, 2011). Additionally, elevated levels of NMVs have been detected in several inflammatory conditions, including in pneumonia in BALF (Hess *et al.*, 1999). Furthermore, 4 h after LPS instillation in mice, there was a significant increase in NMVs in the BALF (Soni *et al.*, 2016). Whilst many of these studies looked in the lungs and not the blood, obtaining BALF from exacerbating COPD patients is practically and ethically challenging as the procedure is not clinically indicated and could cause deterioration and even death in this setting; therefore, circulating biomarkers in these patients would be of value.

In support of the present findings, only two of the COPD patients had elevated blood neutrophil counts. Blood was drawn from these exacerbating patients within 48h of hospital admission and post-intervention, and it is also possible that these participants may have been experiencing a worsening of symptoms for some time before admission. One explanation for the observed effect may be that these patients had already received treatments and medicines which reduced systemic inflammation including systemic corticosteroids (Barnes, 2017). Whilst circulating neutrophil levels have been shown to increase during disease exacerbation, neutrophil influx to the lungs provides a more dramatic increase in this cell type. Although, one report suggested neutrophil turn over may be increased without increases in total neutrophil counts, and there is more sequestration of these cells in tissues, particularly the lungs in COPD patients, which may be one reason for discrepancies in the literature (Tregay *et al.*, 2019). An important limitation of the present study was the limited

patient sample size, however, based on our observations it was speculated that local production, rather than systemic production of CD66b+ MVs may be key during COPD exacerbation. Furthermore, this permits the supposition that neutrophils may not produce more NMVs under inflammatory conditions, but NMVs may reflect neutrophil number, although further investigation is needed to validate this hypothesis. Additionally, contrasting evidence exists showing that CD66b+ MV numbers in stable COPD patient induced-sputum samples did not correlate with neutrophil numbers (Lacedonia *et al.*, 2016), and reasons for this are unclear.

Despite observing no differences between study groups, of note, the patient with the highest CD66b+ and CD14+ MV levels also had COPD GOLD stage IV and had the highest number of pack years (100) of the patient cohort, where pack years represents number of cigarettes smoked per day multiplied by the years the individual has smoked. This observation may warrant further investigation of circulating MV levels in a larger patient group incorporating additional stage IV patients, to understand whether these MVs correlate with severity, or with other factors which may be diagnostically or prognostically useful.

In addition to further characterise plasma MVs using flow cytometry, CD66b+ MVs were analysed for surface expression of MMP-9. For this, it was only possible to analyse five of the six COPD patient samples, due to limited available sample volume for one of the patients. MMP-9 could be detected on 52.78 and 35.31% of CD66b+ MVs in the control and patient groups, respectively (fig 3.3 (E)). Although there was no statistically significant difference in NMV surface MMP-9 expression between these groups by unpaired t-test; nevertheless, this raised the possibility that whole NMVs may be capable of proteolytic activity in certain settings.

3.4.2 Platelet-derived and neutrophil-derived MVs may be important in COPD with comorbid pulmonary hypertension

A larger patient cohort with stable COPD and co-morbid PH was investigated for circulating MV profile and also plasma MV content. Most of the participants in the patient group had moderate to severe disease, with GOLD stage II–IV. In the patient population, higher levels of CD41a+ (platelet) MVs tended to be observed. However, no differences were found in CD144+ (endothelial), CD66b+ (granulocyte), or CD14+ (monocyte) MVs, although the levels of CD144+ MVs were surprisingly high in both the patient and control groups, as mentioned in the results section, this may be due to changes in the antibody used between the patient populations. Increased circulating leukocyte, endothelial and platelet-derived MVs have previously been noted in COPD (Tokes-Fuzesi *et al.*, 2018). It is unclear why we did not observe these differences for all MV types in our cohort. As discussed here below, the influence of surface marker choice to define MV types may play a role in

this, as the authors in the above study used a combination of two to four surface markers for each MV type.

In the control group the concentration of NMVs positively correlated with that of platelet-derived MVs, whereas in the COPD patient group this correlation was the inverse (table 3.3 and fig 3.3 (A) and (B)). As mentioned in the results section in the control group the individual with the highest platelet-MV concentration also had high levels of all the other MV types. Interestingly, the COPD patient with the highest concentration of platelet-MVs also had high levels of the other MV types except NMVs, for which they had the lowest concentration of the patient group. Whilst clinical data for platelet and neutrophil counts was not available for the control group, the patient with the highest platelet-MVs also has the highest platelet count and second highest neutrophil count, although no significant correlations were observed between these parameters. Therefore, the lower NMV concentration that they exhibited did not seem to be linked to neutrophil count here.

Although these correlations of platelet and neutrophil MVs were statistically significant, when these individual points were plotted it may be possible that these trends are driven by individuals at the extremes of the population (i.e. highest or lowest concentrations of these vesicle types). Nonetheless, this further highlights the potential importance of platelet-derived MVs in these patients and indicates a potential relationship with NMVs; indeed platelet–neutrophil MV doublets have been noted in our lab. These cells have complementary surface proteins which promote their interaction (P-selectin and platelet glycoprotein Ibα on platelets and P-selectin glycoprotein ligand-1 and MAC-1 on neutrophils (Moore *et al.*, 1995; Simon *et al.*, 2000a)) and circulating platelet–neutrophil complexes have been noted and investigated in both cardiovascular (Ott *et al.*, 1996) and pulmonary disease (Gresele *et al.*, 1993; Caudrillier *et al.*, 2012). In the setting of acute lung injury, platelet binding to neutrophils was found to induce NETosis and many contribute to lung damage (Jenne *et al.*, 2013; Carestia *et al.*, 2016). Importantly, this cell–cell adhesion has been shown to induce neutrophil EV release, which are in turn internalised by platelets, and stimulates platelet production and aggregation (Rossaint *et al.*, 2016), increased platelet numbers have indeed ben observed during COPD exacerbations. Platelet-derived EVs have also been shown to adhere to and be internalised by neutrophils, increasing neutrophil adhesion to endothelial cells (Kuravi *et al.*, 2019), and therefore the higher levels of platelet MVs in the COPD patient group in the present study may contribute to increased neutrophil adhesion and by extension facilitate migration to the lung tissue. Although the role of platelet–neutrophil MV complexes is currently unclear, and the negative correlation in COPD between these two vesicle types is interesting but unexplained.

Patients with PH have previously been shown to have increased numbers of circulating MVs (Bacha *et al.*, 2019), where increased levels of platelet and endothelial MVs was correlated with blood pressure. It was hypothesised that this reflects the activation of these two cell types in this condition, and of note, levels could be reduced by treatment with Treprostinil, a synthetic prostaglandin analogue. High levels of platelet vesicles have also been reported for other cardiovascular conditions including coronary artery disease (Bulut *et al.*, 2011). Although, it should be noted that the markers used to identify each MV type vary significantly between publications. For example, many authors use Annexin V as a criterion for MV identification (Fink *et al.*, 2011; Wisgrill *et al.*, 2016; Hosseinzadeh *et al.*, 2018). CD31, CD51/61 and CD105 have also been used to identify endothelial MVs (Jimenez *et al.*, 2003), and CD61 (Skeppholm *et al.*, 2012), CD62P and CD42 (Chyrchel *et al.*, 2019) to define platelet MVs. In the present study Annexin V binding was not used as a defining criterion of MVs, since it has previously been observed that not all MVs may be phosphatidylserine positive (Jimenez *et al.*, 2003; Connor *et al.*, 2010), therefore this may bias an analysis towards looking only at a particular MV subset, and some authors have used this as a marker of MVs produced by apoptotic cells (Werner *et al.*, 2006; Dieker *et al.*, 2016).

Additionally, from pure cell culture populations, it has previously been evidenced that for some markers, only a small proportion of the MVs from a cell type may stain positively for the protein by flow cytometry. For example, one report showed that only 6% of endothelial cell-derived MVs generated from human umbilical cord venous cells were CD144+, whilst 90% of platelet MVs were CD41A+. Additionally, only 8.5% of monocyte MVs were CD14+ and 10% of granulocyte MVs were CD66b+ (Ayers *et al.*, 2011; Dragovic *et al.*, 2013). Therefore, differences in marker use, and in antibody formulations or clones, may significantly impact the results of such studies. This may go some way towards explaining the differences in CD144+ MVs found in the present study between the first study cohort and the second, where different antibodies and fluorophores were employed. This highlights an important point that the proportions of MVs identified should be interpreted with caution, it also cannot be ruled out that using different surface markers may generate different results.

3.4.3 Circulating NMV numbers correlated with FVC% in COPD patients with pulmonary hypertension

Despite finding no differences in NMV concentration between the COPD patient group and age-matched controls, a statistically significant negative correlation was identified between NMV (CD66b$^+$) concentration and FVC% in the patient group; there was no correlation with FEV1% or FEV1/FVC ratio (Table 3.4 And fig 3.5 (C)). Circulating leukocyte-derived MVs have previously been

shown to negatively correlate with FEV1/FVC ratio in COPD patients (Tokes-Fuzesi *et al.*, 2018), although in their study it should be noted that only annexin V$^+$ MVs were analysed. In contrast, neutrophil EVs (i.e. mixture of exosomes and MVs) detected in COPD sputum samples did not correlate with any lung function parameters, although endothelial-derived (CD31$^+$) EVs did negatively correlate with FEV1% (Lacedonia *et al.*, 2016), a finding echoed by Tokes-Fuzesi et al. (2018). The only clinical parameter that correlated with endothelial MV number was white blood cell count (WBC; table 3.4), and this may therefore reflect systemic inflammation in these patients.

Interestingly, no correlation was found between NMV concentration and neutrophil or white blood cell (WBC) count. Although there was a significant correlation between CD66b MFI and WBC, this relationship was weak and likely driven by a few individuals with high expression levels (Table 3.4 and fig 3.3 (D)). A lack of correlation between neutrophil numbers of NMVs was also shown in COPD sputum samples (Lacedonia *et al.*, 2016), and it is possible that the number of NMVs produced by neutrophils is dependent on other factors. A limitation of the present study is the small sample size, however in two different studies and patient populations, we found that leukocyte-derived MV numbers were not differential between these patients and matched controls and conclude that measuring circulating numbers of these MVs is not clinically useful.

3.4.4 Plasma MV-associated MMP-9 and TIMP-1 content are significantly increased in COPD patients with pulmonary hypertension

Whilst MV numbers were not differential, protease content was further investigated in plasma MV lysates by ELISA, and MMP-9 was found to be present at significantly higher levels in the COPD/PH patient group compared with matched controls. This difference was only observed for the MV fraction and not in MV-depleted plasma. Whilst it was not possible to distinguish whether MV MMP-9 in this group was in the pro- or active form as western blotting, and gelatine zymography failed using plasma samples (data not shown), likely due to the presence of serum proteins in abundance and relatively lower levels of MMPs and TIMP, the content of TIMP-1, the endogenous inhibitor of several MMPs including MMP-9, was measured. MVs from stable COPD/PH patients contained higher levels of TIMP-1 than those from age-matched controls; overall levels of MV-associated TIMP-1 measured by ELISA were more than five times lower than those in the MV-depleted plasma for the patient group, although the proportion of TIMP-1 to MMP-9 in plasma MVs was similar between patients and controls. This result would suggest that at least part of the MMP-9 in plasma MVs is inhibited by TIMP, however, neutrophils have previously been shown to release TIMP-free MMP, an action that few cell types have been reported to do (Ardi *et al.*, 2007); the lesser TIMP-1 levels in these MVs compared with the MV-depleted plasma is of interest.

There is conflicting evidence regarding trends in MMP-9 and TIMP-1 levels in COPD. In their study D'Armiento et al. (2013) showed significantly reduced plasma levels of MMP-9 and TIMP-1 in emphysema compared with a healthy control group, whilst levels of these proteins in the BAL of these patients was significantly higher. However, several studies in COPD have shown increased plasma MMP-9 as well as TIMP-1 concentrations (Uysal and Uzun, 2019). Wells et al. (2018) showed that in two large COPD patient cohorts (from the SPIROMICS and COPDgene studies), elevated MMP-9 levels were also associated with increased risk of acute exacerbations. In serum, Linder et al. (2015) showed increased MMP-9 concentrations in COPD significantly correlated with decline in FEV1%, but there were no associated differences in TIMP-1 levels. The patient cohort chosen may be one reason for these differences, for example Ilumets et al. (2007) showed that plasma MMP-9 was not significantly elevated in those with early-stage COPD. In the present study, the patient group contained no GOLD stage I patients, and in addition choosing those with comorbid pulmonary hypertension may bias our analysis towards more severe disease with systemic inflammation. It would be interesting to determine whether MV-associated MMP-9 was increased in a wider range of COPD patients.

These results demonstrated the content of circulating MVs is altered in COPD and whilst there may not be differences in numbers of immune cell-derived MVs, alterations in protein content and potentially activity (which have rarely been studied due to the inherent challenges of these assays) may be highly relevant, both as a potential biomarker and maybe as an injurious agent. The potential for differential action of NMVs in inflammation was further investigated in more readily available peripheral blood neutrophils from healthy participants.

3.4.5 NMVs could be clearly identified and characterised by TEM

The second aim of the work presented in this chapter was to characterise the physical properties of NMVs and determine the purity of vesicles generated from peripheral blood neutrophils of healthy participants to inform later functional investigations. When studying MVs, contamination with other types of extracellular vesicles (EVs) and proteins has been identified as an important issue which should be addressed in such investigations; recently published "Minimal Information for Studies of Extracellular Vesicles" guidelines from the International Society for Extracellular Vesicles (ISEV) on working with EVs recommend the use of at least two independent methods to confirm successful EV isolation (Thery *et al.*, 2018). Therefore, to validate the NMV isolation method used here, EM—previously proposed as a reliable method for MV analysis and characterisation (Ridger *et al.*, 2017)—was initially employed.

For TEM, two techniques were used in this study: resin-embedding and sectioning of a pelleted NMV sample, and negative staining of a sample from suspension. Both methods showed that a highly pure population of NMVs were successfully isolated. These NMVs were spherical, approximately 100–300 nm in diameter, and had a clearly visualised plasma membrane (fig 3.5). Additionally, the sample did not appear to be contaminated with other EV types (i.e. exosomes of <100 nm or apoptotic bodies of ≥1000 nm), and in particular no characteristically cup-shaped exosomes were found. However, the potential presence of extracellular protein aggregates was noted using resin-embedding (fig 3.5 C; shown by dark staining surrounding NMVs). These aggregates may include proteins released from the neutrophils upon activation with fMLP. To address this issue, a further washing step (PBS) was added in the final stages of NMV isolations.

The morphology of these NMVs agrees with previously published data from both our group (Gomez *et al.*, 2018) and from other authors using similar isolation methods (Gasser *et al.*, 2003; Hess *et al.*, 1999). However, some groups have evidenced the presence of larger NMVs (≥500 nm in diameter); in their study Timar et al. (2013) showed that NDMVs generated after neutrophil stimulation with *Staphylococcus aureus* had a 200–800 nm size range; almost no NMVs in this upper range were observed in the TEM images presented here. This difference may be due to differences in isolation protocols. These authors used different density-gradient separation media to isolate neutrophils(Ficoll-Paque vs. Histopaque used in the present study) and two-stage centrifugation at 400 and 3000 *g* to separate the MVs, whilst I employed a three-stage centrifugation at 500, 1500, and then 2500 *g*, which may in part account for the lack of larger sized vesicles. Additionally, NMVs used for TEM in the present study were freshly isolated, and whilst storage conditions have not been shown to change neutrophil EV appearance in TEM using resin-embedded samples (Lorincz *et al.*, 2014), changes in negatively stained samples which require less sample processing have not yet been evaluated. Furthermore, these authors showed that storage temperature, particularly at -20°C, induced increases in EV size as measured by dynamic light scattering, and to avoid storage-related changed in this study, NMVs isolated from healthy participants were always used freshly. Additionally, the NMVs in the present study were not fixed before negative staining was carried out, making them more susceptible to changes induced by dehydration which would make these vesicles smaller and promote deformation of the plasma membrane. Slater et al. (2017) fixed their samples with 2% PFA before staining, and subsequently demonstrated neutrophil microparticles of ≥500 nm in size; although, these authors did not confirm this sizing with a technique such as DLS or NTA, which provides a better overview of the size distribution of the whole EV population.

It should also be noted that MVs cannot be definitively identified based on their size alone, and there is some overlap between the proposed size range for MVs and that of other EVs such as exosomes (Kanada *et al.*, 2015). Nevertheless, whilst a method to determine the origin of these EVs (i.e. from ecto- or exo-cytosis) is currently lacking, size discrimination remains one of the best methods available for the distinction of MVs from other EV types.

3.4.6 Pure populations of NMVs were isolated

After optimisation for detection of EVs within the established MV size range using calibration beads (fig 3.6 (A-C)), a slower frame rate than that typically used for exosome analysis (3.75 vs. 30 fps) was employed for NTA. Using these settings, the isolated NMV population was found to have a modal diameter of ~200 nm, in agreement with the TEM discussed above. A similar size distribution has been previously evidenced in our group using tuneable pulse resistive sensing with the qNano device (Gomez *et al.*, 2020).

The concordant results of these two very different techniques (NTA and TEM) strongly support their use as gold-standard techniques in EV analysis. However, the variability in ZetaView NTA EV size distribution depending on device settings also highlights an important issue for the interpretation of these results, and more standardised protocols may be needed for the accurate detection of EV diameter between institutions. Of note, the present analysis of NMVs by both of these techniques showed the isolation of some MVs that are below the current detection range of the LSRII flow cytometer (~200 nm–400 nm; (Chandler *et al.*, 2011)). This cytometer is commonly used for MV sample quantification and analysis and was used here in the current study for this purpose. At present, most flow cytometers are limited by their inability to accurately detect EVs in lower size ranges. Therefore the NMV numbers presented here may be an underestimation of the true number (Chandler, 2016). However, until more sensitive methods are developed, there remains no superior method for the rapid quantification and analysis of NMV numbers and surface protein expression, which is the only way to infer cellular origin.

3.4.7 Healthy participant NMVs from fMLP-stimulated neutrophils contain active MMP-9

Following an initial proteomics study by Dalli et al. (2013), Butin-Israeli et al. (2016a) showed that neutrophil-derived microparticles (i.e. EVs pelleted at 100,000 *g*) contain active MMP-9 and can exert effects on the monolayer integrity and junctional protein expression in target cells via this protease. Due to the crucial role of MMP-9 in ECM degradation and tissue remodelling during lung inflammation, and particularly in COPD exacerbations (Papakonstantinou *et al.*, 2015), and after evidencing differential expression of this protease in COPD MVs, we postulated that the NMV-mediated mechanism demonstrated by Butin-Israeli et al. may also be applicable to lung epithelium.

To begin to investigate this hypothesis, we first sought to establish whether the NMVs generated *ex vivo* express MMP-9. Whilst inhibitor-free MMP-9 was suggested to be present in MVs in our patient cohort by the lesser levels of MV-associated TIMP-1 than those found in MV-depleted plasma, it was not possible to use these limited and precious samples to identify active MMP-9, and we therefore utilised heathy volunteer neutrophils to generate a more abundant and pure sample of NMVs for further testing. Cells were stimulated with either the bacterial peptide fMLP or PBS (control), and then these parent cells and resulting NMVs were analysed for MMP-9 content.

Western blot analysis of NMV lysates verified the presence of pro-MMP-9 (92 kDa, fig 3.7 (A) and (B)) in both PBS and fMLP NMV as well as all of the parent neutrophil samples. In addition, when equal protein loading was employed and expression levels were adjusted to GAPDH expression (limitations of GAPDH use were previously mentioned in the results section here), levels of the active form of MMP-9 (~82 kDa) were much higher in fMLP NMVs than in their parent neutrophils (fig 3.7 (C)). Unstimulated neutrophils (i.e. neutrophils lysed directly after isolation from peripheral blood) contained no detectable active MMP-9, whilst this was abundant in NMVs derived from fMLP-stimulated cells. PBS-treated neutrophils and their released NMVs contained negligible active MMP-9, indicating that the cleavage of pro-MMP-9 to the active form is not a consequence of the neutrophil isolation process but rather a consequence of fMLP-induced cell activation. Additionally, these unstimulated neutrophils underwent two washing steps directly before lysis as part of the normal neutrophil isolation procedure; due to the limited wash steps for the stimulated cells, (which were lysed directly after 1h incubation and pelleting to avoid further cell activation) it is possible that some NMVs were present in the neutrophil lysates of the stimulated cells and may have contributed to the active MMP9 detected in the cell lysates of these stimulated cells. However, of note fMLP has previously been shown as a strong inducer of MMP-9 release from cells, eliciting larger responses than C5a, and PAF, amongst other stimuli (Takafuji *et al.*; Doerner *et al.*, 2011), hence it seems plausible that at least some of the active MMP-9 was cell-associated.

This difference between fMLP- and PBS-NMVs provides support for the theory that NMVs generated by different stimuli have different protein expression and activation profiles; resting NMVs may contribute to homeostasis (Ridger *et al.*, 2017) whilst it is plausible that NMVs triggered by an inflammatory or infective stimulus have a pro-inflammatory effect that is stimulus-specific. This is supported by the work of Timar et al. (2013) who showed that a range of stimuli including opsonised bacteria resulted in NMVs with differential antibacterial capacities; the amount of antibacterial proteins was almost doubled in bacterial-elicited MVs relative to control MVs, incorporating abundant granule proteins such as lactoferrin, myeloperoxidase and elastase. However, MMP-9 was

not listed as one of the most abundant proteins upregulated by exposure to bacteria (*Staphylococcus aureus*).

The presence of MMP-9 in some of the control samples in my study is in contrast to the findings of Butin-Israeli et al. (2016a) who found that control NMVs (from unstimulated neutrophils) contained only a very small amount of MMP-9, and no active MMP-9. However, their control sample consisted of unstimulated neutrophils kept on ice at ~4°C for the same time period as the fMLP stimulation (20 min) and the difference between the results may simply indicate differences in NMV content at different temperatures. We believe that the results presented herein with samples kept at body temperature more closely recapitulate the biological situation.

The most well-defined mechanism of MMP-9 activation is by proteolytic cleavage into the 82 kDa active form. MMP-9 is thought to be secreted as the pro-form into the extracellular space and then undergo subsequent activation. The MMPs capable of this action are MMP-2 (Fridman *et al.*, 1995) and MMP-3 (Ogata *et al.*, 1992). The MMP-9 antibody used for the western blotting experiments performed in the present work is documented by the supplier to have 20% cross-reactivity with MMP-2, and bands corresponding to the observed size of this enzyme (72 kDa) were observed on the western blots, particularly in the neutrophil samples (data not shown). In the future, research into potential activators and inhibitors of MMP-9 should be carried out to understand the mechanism of processing and packaging of MMP-9, and particularly the active form, in NMVs, which may potentially include packaging of MMP-2 into MVs and subsequent activation after MV release.

By flow cytometry, MMP-9 was detected on the surface of NMVs. This agrees with previously published results from Butin-Israeli et al. (2016a) who showed MMP-9 expression on the surface of microparticles derived from fMLP-stimulated neutrophils, although their sample contained all extracellular vesicles pelleted at 100,000 *g* which should also include exosomes. Whilst they showed that the majority of these MPs presented MMP-9, they did not compare with an isotype control; whilst we found some non-specific binding with an isotype control, we were able to show that specific binding exceeded non-specific levels strongly indicating expression of MMP-9 on the NMV membrane. There was no difference observed in the surface expression of MMP-9 between fMLP and CSE NMVs, whilst ELISA results showed that total expression did seem to diverge somewhat for MVs produced in response to these two stimuli; although these differences were not statistically significant this may reflect large variation between individual donors. This indicates that any differences in total MMP-9 levels likely comes from the interior of these NMVs, however differences in surface expression of active or pro-MMP-9 cannot be ruled out, as the conjugated antibody used

for flow cytometry experiments detected both forms of this protease, therefore does not provide information about activation status.

Whilst MMP-9 is not typically a membrane-associated MMP, it has been reported to bind to the surface of cells in the pro-from via binding to cell-surface expressed CD44, also known as homing cell adhesion molecule (HCAM), a cell-surface hyaluronan receptor (Yu and Stamenkovic, 1999), which also protects MMP-9 from TIMP-1 binding and inhibition. This interaction is typically associated with tumour cells and facilitates cell invasion; CD44 serves a wider variety of functions including as a phagocytic receptor in macrophages (Vachon *et al.*, 2006). It is expressed on the surface of neutrophils and although neutrophil CD44 has been little studied, it was found to engage with E-selectin to facilitate slow rolling (Yago *et al.*, 2010) and to be important for the inflammation resolution in inflammatory conditions including pneumonia in murine models (Wang *et al.*, 2002a). Here, we demonstrated by flow cytometry that CD44 is expressed on the surface of NMVs, and therefore identified one potential mechanism by which MMP-9 may be anchored to the surface of these vesicles. However, no direct link was demonstrated with this receptor and protease here and further investigation is needed.

3.4.8 NMVs generated from pro-inflammatory stimuli degrade Collagen IV

MMP-9 is critically involved in the breakdown of ECM in the lungs to facilitate neutrophil transmigration and influx to the sites of inflammation (Bradley *et al.*, 2012; Keck *et al.*, 2002), and although results in animal models have varied vastly (Brass *et al.*, 2008; Foronjy *et al.*, 2008; Churg *et al.*, 2007), when activity is prolonged or increased during disease exacerbations (Finlay *et al.*, 1997), neutrophil production of this protease is thought to contribute to the airway changes and damage occurring in COPD (Betsuyaku *et al.*, 1999). To demonstrate that the NMV MMP-9 we detected had such functional relevance, and to further investigate any potential differences in MMP-9 activity between fMLP and CSE NMVs, a DQ Collagen IV degradation assay was used. Collagen IV is a major component of the ECM in many tissues including the lung, and typically forms part of the basement membrane (Khoshnoodi *et al.*, 2008). As far as I can ascertain, this is the first instance of use of this specific assay to analyse samples other than isolated enzymes, however, in support of the technique, a DQ Collagen I degradation assay was recently used to determine neutrophil-derived exosome NE activity by Genschmer et al. (2019). Whilst Collagen IV is a major substrate for MMP-9, it should be noted that other metalloproteases are capable of degrading this protein, including MMP-2 (Monaco *et al.*, 2006), -3, -10, -11, -12 (Chandler *et al.*, 1996), and -25, as well as elastase (Pipoly and Crouch, 1987) and cathepsin G (Starkey, 1977). We performed preliminary experiments to detect NE in these samples by western blotting but were unable to detect this protein using the antibody and protocol

utilised (data not shown), likely due to technical issues. However, two previous proteomics studies indicated only the presence of MMP-9 and MMP-25 in fMLP NMVs and also elastase and cathepsin G (Dalli *et al.*, 2013; Timar *et al.*, 2013), we found by western blotting and gelatin zymography (data shown in methods section 2.2.17) that NMVs strongly expressed MMP-2, and therefore the presence of other MMPs cannot be ruled out.

Collagen IV degradation by NMVs was reduced by addition of TIMP-1 (fig 3.9 (B) and (D)) almost to the baseline values in most cases, however this difference was not statistically significant. TIMP-1 binds and inhibits MMP-9 in a 1:1 ratio. In this experiment, based on the average MMP-9 concentration determined by ELISA results, TIMP-1 was added at double the concentration of MMP-9 to permit application in excess. This worked out to an approximately 1:6 molar ratio of MMP:TIMP. However, previous authors have shown that for membrane-bound MMP-9, the IC50 for inhibition of this protease by TIMP-1 is around 21-fold greater than that for soluble MMP-9, and still did not completely inhibit membrane MMP-9 at 150-fold greater concentrations (Owen *et al.*, 2003). Whilst the exact reasoning for this is unknown, Owen et al. (2003) proposed that potential mechanisms include steric hindrance or binding of MMP-9 to the cell surface at a site which subsequently blocks TIMP-1 binding. Therefore, the enzyme-inhibitor relationship assumed in the present study may not be true, since we have evidenced by flow cytometry that at least some NMV-associated MMP-9 is located on the plasma membrane of both healthy participant and COPD patient NMVs (fig 3.1 (E) and 3.8 (C)). Levels of TIMP-1 needed to reliably inhibit NMV MMP-9 may therefore be higher than those used here. Additionally, TIMP-1 is not a specific inhibitor of MMP-9, but also binds other MMPs including ADAM10/MMP-10, which has previously been shown to be present on the surface of NMVs from cigarette smoke-exposed neutrophils (Folkesson *et al.*, 2015). This protease is also capable of collagen IV cleavage (Millichip *et al.*, 1998). Insufficient concentration of TIMP-1 to effectively inhibit MMP-9, either due to membrane localisation of MMP-9 or TIMP binding to other proteases, reducing its availability, is therefore one potential explanation for inconsistent effects. On the other hand, TIMP-1 has not been demonstrated to inhibit the activity of other types of protease including elastase or cathepsin G, in fact elastase is capable of inactivation of this protein (Nunes *et al.*, 2011). Therefore, at least part of this cleavage activity is due to NMV-associated MMPs. Future work using specific chemical inhibitors for MMP-9 and carrying out a concentration-response experiment should be done to decipher whether this protease is responsible for the collagen IV cleavage found here.

Nevertheless, we demonstrated that NMVs are capable of degrading ECM components. Collagen degradation products have been investigated as a potential biomarker in COPD, and in particular the

collagen IV degradation product called C6M was found to be a predictor of mortality (Sand *et al.*, 2016). Our findings are also in agreement with a recently published study showing that neutrophil-derived exosomes produced from fMLP-stimulated cells caused alveolar destruction when administered intratracheally in mice, although this was shown to be via an NE-mediated effect (Genschmer *et al.*, 2019). Furthermore, the effect shown by those authors was resistant to both endogenous (alpha-1 antitrypsin) and specific chemical inhibitors of NE. NMVs may therefore represent a mechanism of enhancing protease activity and life span.

3.5 Conclusion

In contrast to the findings of some previously published data, studying two different COPD patient cohorts, we found no significant differences in immune cell-derived MV numbers between patients and age-matched controls. COPD circulating MVs did diverge in their total MMP-9 and TIMP-1 content, both significantly increased in these patients, suggesting that protein content rather than MV numbers may relevant to disease pathogenesis and/or progression, an effect which needs to be further explored in COPD and in other inflammatory lung diseases. Further investigation of this and other differences in NMV protein expression may contribute to our understanding of the role of these vesicles in disease pathologies, and particularly their ability to deliver proteins to specific target cells, such as the pulmonary endothelium and alveolar epithelial cells.

Furthermore, NMVs from stimulated neutrophils contained active MMP-9, amongst other proteases reported in the literature (Dalli *et al.*, 2013), which could not be totally inhibited by conventional concentrations of TIMP-1 (see figure 3.9 for a summary of these results). NMVs may therefore represent a method of protease activity preservation and further investigation into the effects of NMV-associated proteases is warranted. We hypothesised that MMP-9 may be, at least in part, anchored on the surface of NMVs by adhesion molecules, including CD44 which was detected on NMV membrane. This would allow for direct delivery and activity of proteases on target cells without the need for internalisation or breakdown. However, we were unable to thus far demonstrate colocalization of these two surface proteins. The role of this protease in lung inflammation and potential functional effects will be further explored using a human bronchial epithelial cell line.
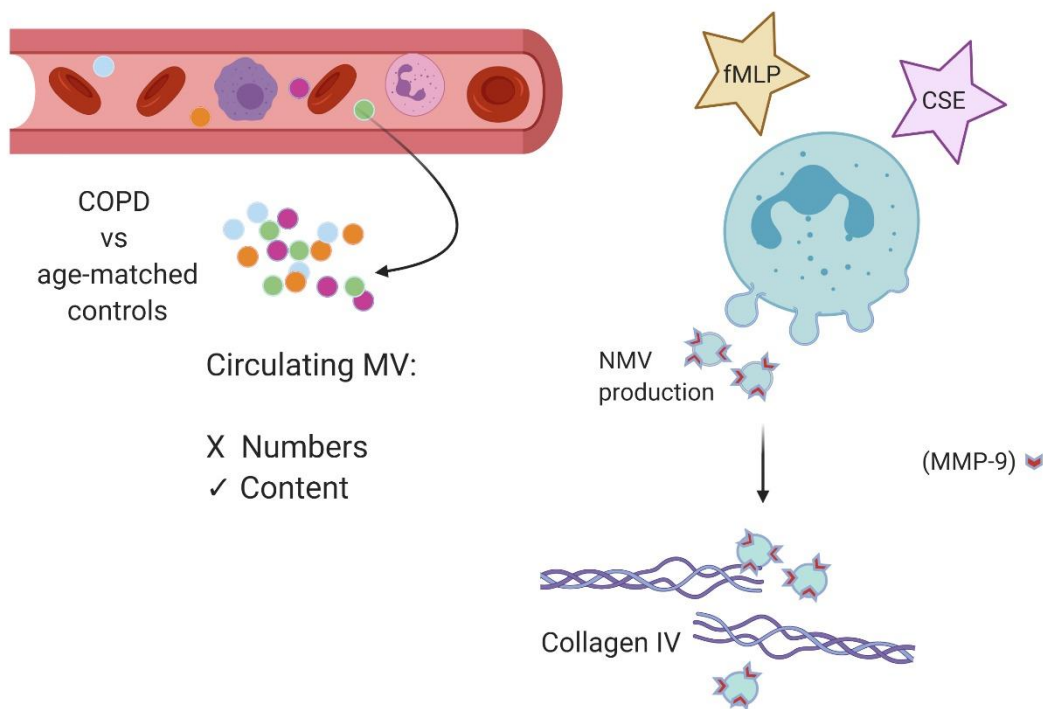
Figure 3.9 Summary of findings in chapter 3

Numbers of leukocyte-derived plasma microvesicles (MVs) from COPD patients and age-matched controls do not differ, but plasma MV-associated MMP-9 and TIMP-1 levels were significantly increased in these patients. Healthy participant neutrophils stimulated with fMLP or CSE express surface-associated MMP-9, and both of these vesicle types were capable of degrading the extracellular matrix component Collagen IV. fMLP: N-formyl-met-leu-phe; CSE: cigarette smoke extract.

Chapter 4: Microvesicle-induced epithelial cell dysfunction

4.1 Introduction

Epithelial cell activation, dysfunction, and damage are hallmarks of inflammatory lung diseases like chronic obstructive pulmonary disease (COPD) and acute respiratory distress syndrome (ARDS). Neutrophil-mediated cell damage has been implicated in disease pathogenesis and progression in these conditions. Neutrophils are recruited to the lungs via chemotactic gradients, either by pathogen-derived chemoattractants such as N-formyl-met-leu-phe (fMLP) or by endogenous cues like interleukin-8 (CXCL-8) released from the lung endo- and epithelium as well as alveolar macrophages (Barnes, 2008). The damaging effects of neutrophils begin with degradation of host tissue by neutrophil proteases, which is necessary to facilitate neutrophil transmigration to the area. COPD patient neutrophils have been shown to more rapidly migrate in response to chemotactic stimuli, but with lower accuracy, and therefore have elongated and more destructive migratory paths, compared with those of healthy individuals (Sapey *et al.*, 2011). Although this activity is targeted to the host tissue, the majority of neutrophil activity is directed towards pathogen clearance, and much of the host injury is considered as "bystander" tissue damage as a result of this antimicrobial action (Parkos, 2016). A further example of this effect is damage to host cells induced by reactive oxygen species (ROS) and myeloperoxidase (MPO) released by neutrophils as part of their antimicrobial response in the airway reviewed by Jasper et al. (2019). Whilst airway cells are equipped to repair themselves and their surrounding environment, e.g. via replenishing extracellular matrix (ECM) components and via wound healing mechanisms after these events, the chronic nature of COPD means that the burden of repeated tissue damage outweighs the reparative and resistive capabilities of these cells.

Neutrophil proteases have been shown to have a role in several dysfunctional behaviours in the lung epithelium in COPD. Whilst epithelial cells possess antiprotease defences such as secretory leukoprotease inhibitor (SLPI), as well as other endogenous inhibitors like alpha-1 antiprotease (AAT), these are often ineffective and overwhelmed by the high protease concentrations released by neutrophils, particularly in disease states (Vogelmeier *et al.*, 1991; Jasper *et al.*, 2019; Liou and Campbell, 1996). Neutrophil proteases, including matrix metalloproteinases (MMPs), stimulate mucus hypersecretion from submucosal and goblet cells, partially by upregulating MUC-family gene transcription and promoting goblet cell hyperplasia (Song *et al.*, 2005; Nadel *et al.*, 1999; Arai *et al.*, 2010; Deshmukh *et al.*, 2005), alongside inducing impaired mucociliary clearance, this provides an ideal environment for bacterial colonisation (Henke *et al.*, 2011). Furthermore, after neutrophil

cigarette smoke exposure, neutrophil-derived supernatants have been shown to induce the release of human bronchial epithelial cell pro-inflammatory mediators including the chemoattractant CXCL-8 (Heijink *et al.*, 2012). There are various neutrophil components that may mediate this effect, amongst which is neutrophil elastase (NE), a serine protease found to be consistently increased in several chronic inflammatory lung diseases, which has been shown to induce epithelial cell activation and CXCL-8 release, perpetuating the cycle of neutrophil recruitment and epithelial damage (Nakamura *et al.*, 1992). Subsequently, MMP-9 is also capable of cleaving CXCL-8, resulting in a greater chemotactic potential of this neopeptide (Zariffard *et al.*, 2015; Van den Steen *et al.*, 2000).

Whilst degranulation and neutrophil extracellular trap (NET) release describe major mechanisms of protease release from these cells, neutrophil-derived microvesicles (NMV) represent a potential method of neutrophil protease delivery which facilitates prolonged activity of these enzymes as well as transport of neutrophil proteins to target cells without the need for neutrophil adhesion or migration (Gomez *et al.*, 2020). The presence of NMVs has been demonstrated in COPD patient sputum samples by Lacedonia et al. (2016), and in Chapter 3 of this thesis, I showed that plasma MVs from COPD patients contain significantly higher levels of MMP-9 than those in age-matched controls, that NMVs express cell-surface MMP-9 and contain active proteases which tend to be at higher levels after parent cell stimulation and that NMVs are capable of ECM degradation. In addition, cell-surface NE has been evidenced in neutrophils (Owen *et al.*, 1995), and recently published data from Genschmer et al. (2019) showed that active, inhibitor-resistant NE exists on the surface of neutrophil exosomes. As NE is bound to the exosome—and indeed the neutrophil—surface via an electrostatic interaction with the plasma membrane, it is highly likely that this also occurs on NMVs which are encompassed by a part of the parent cell membrane. Detrimental effects of NMV-proteases on the epithelium have been demonstrated previously; Butin-Israeli et al. (2016b) showed that intestinal epithelial cell permeability was increased both *in vivo* and *in vitro* via an NMV-derived MMP-9 dependent mechanism which resulted in decreased junctional protein expression.

In addition to their protease content, effects of other NMV-derived neutrophil granule content have been shown; MPO contained within NMVs has been shown to increase the permeability of endothelial cell monolayers by reducing membrane integrity and inducing morphological changes in these cells (Pitanga *et al.*, 2014b), although specific inhibitors were not used to confirm this mechanism. Our laboratory has also demonstrated NMV-induced permeability in human brain microvascular endothelial cell (HBMEC) monolayers. Though the mechanism of this effect remains to be determined, NMVs induced significant changes in the transcriptional profile of these cells after 24h; in particular, inflammatory pathways and those associated with junctional protein expression

were identified by microarray analysis (Ajikumar *et al.*, 2019). Whilst the majority of these effects were demonstrated in endothelial cells, NMV-derived MPO has also been shown to affect epithelial wound healing by impairing cell migration and proliferation responses (Slater *et al.*, 2017). These authors expanded on previously published work from Pitanga et al. (2014b) by showing that these effects could be abrogated using an MPO-inhibitor.

Airway epithelial cell apoptosis, a potential mechanism of increased epithelial permeability, is significantly increased in emphysema (Yokohori *et al.*, 2004; Segura-Valdez *et al.*, 2000) (further discussed in Chapter 1, section 1.1.4). This change is suggested to be at least partially responsible for the irregular alveolar wall structure characteristic of COPD (Kasahara *et al.*, 2001). Furthermore, although tobacco smoking has been shown to induce epithelial apoptosis majorly via its chemical constituents and free radical delivery, ongoing apoptosis after smoking cessation has indicated that innate mechanisms also contribute to this cell death (Hodge *et al.*, 2005). Whilst the contribution of neutrophils to these effects remains to be fully determined, and some contrasting evidence exists regarding the role of neutrophil infiltration to the lungs (Vernooy *et al.*, 2001), oxidative stress and protease activity of immune cells including neutrophils and T-cells have been implicated in increasing epithelial cell apoptosis (Majo *et al.*, 2001; Vermeer *et al.*, 2009). Defective clearance of apoptotic cells by COPD macrophages further exacerbates these effects (Vandivier *et al.*, 2002; Hodge *et al.*, 2003). NMVs have been implicated in intestinal epithelial cell apoptosis via induction of the DNA damage response via microRNA activity, for which NMVs have been shown to be a rich source (Butin-Israeli *et al.*, 2019), although the potential role of proteases in these processes remains to be determined.

Finally, rapid uptake of NMVs by target cells, particularly by macropinocytosis and dynamin-dependent endocytosis, and subsequent effects on cell activation and inflammation—specifically increasing proinflammatory cytokine production and activating inflammatory pathways including nuclear-factor κB (NFκB) signalling—has been demonstrated in both our lab *in vitro* and *in vivo* in endothelial cells (Gomez *et al.*, 2020; Ajikumar *et al.*, 2019), and by other authors in various cell types (Mesri and Altieri, 1999; Butin-Israeli *et al.*, 2019). Interestingly, exposure of airway epithelial cells to cigarette smoke extract (CSE), widely investigated for its effects on these cells and application to chronic lung inflammation, has been shown to reduce macrophage-derived MV uptake (Schneider *et al.*, 2017); although NMVs generated from CSE exposure and their effects have not yet been investigated, I noted in this thesis in chapter 3 that CSE and fMLP NMVs did not have differential protease activity, several authors have shown key differences in content and activity of NMV derived from different stimuli (Dalli *et al.*, 2013; Gomez *et al.*, 2020). Uptake of NMVs in airway epithelial cells remains to be investigated and is the subject of experimental work in this chapter but

has been suggested as highly likely given the broad range of NMV target cells, and the non-specialised mechanisms of internalisation employed by these vesicles. The contribution of epithelial activation to COPD pathogenesis and progression is important, with increases in epithelial proinflammatory and immunomodulatory proteins found in COPD patient bronchoalveolar lavage fluid and systemically, in the circulation (Mori *et al.*, 2002; Cromwell *et al.*, 1992; Obeidat *et al.*, 2017). Neutrophil effects on the lung epithelium and their contribution to the development of inflammatory lung disease are thought to be highly significant in a context-dependent fashion, but much remains to be uncovered about these mechanisms. NMV release and activity is a much lesser studied function of neutrophils, and evidence of their ability to induce epithelial and endothelial dysfunction makes the study of these vesicles in the context of lung inflammation highly relevant.

4.2 Hypothesis and aims

We hypothesised that NMVs are taken up by lung epithelial cells and induce inflammatory activation, leading to increased permeability and airway barrier integrity.

Aim 1: To determine whether NMVs interact with, and are internalised by, BEAS-2B bronchial epithelial cells, investigate whether this is dependent on the NMV-generating stimulus and elucidate the pathway(s) by which these interactions occur.

Aim 2: To determine the functional effects of NMV–epithelial cell interaction in terms of inflammation, barrier function, and apoptosis by measuring cytokine production, permeability and junctional protein expression, and caspase activation and cell loss, respectively.

4.3 Results

4.3.1 Neutrophil-derived microvesicle internalisation by bronchial epithelial cells

Differences in COPD patient MVs compared with matched controls were shown in the previous chapter here (chapter 3), along with findings from other authors that NMVs are present in the lungs of both stable COPD patients (Lacedonia *et al.*, 2016) and also in animal models of acute lung inflammation (Soni *et al.*, 2016). We therefore sought to determine whether there may be an interaction between NMVs and the delicate airway epithelium, and whether investigation of subsequent functional consequences may therefore be pertinent. For this, the widely utilised normal bronchial epithelial cell line BEAS-2B was employed, which although a substitute for primary epithelium, has advantages over several other common airway cell lines including A549 cells originating from adenocarcinoma, and allowed rapid preparation and use of epithelial cell cultures to align with neutrophil isolation from human peripheral blood. To investigate whether BEAS-2B cells

interacted with and internalised NMVs, a combination of microscopy and flow cytometry was used. NMVs were fluorescently labelled with either PKH-26 or -67. Uptake of these vesicles by confluent BEAS-2B cells was investigated after 2h, an optimal timepoint previously determined in our lab for both uptake and function effects in endothelial cells *in vitro* (Gomez *et al.*, 2020). Additionally, in order to determine whether the stimulus used to generate NMVs may influence uptake, internalisation of NMVs from fMLP and CSE stimulated neutrophils was compared (fig 4.1).

For fluorescence microscopy, experiments were performed in a 96-well plate, facilitating the use of a physiologically-relevant concentration of NMVs (3000/µl) in the range of that measured in COPD patient sputum by Lacedonia et al. (2016) (mean of approx. 7000 NMV/µl; range of approx. 1800–13000 NMV/µl). Although, induced sputum samples by process of collection using saline are diluted, and therefore the true number in the airways may be even higher. This experiment was performed with the assistance of Magdalena Grudzien, MSc student under my day-to-day supervision. Cells incubated for 2h with labelled NMV were thoroughly washed, fixed and stained using wheat-germ agglutinin (WGA) to label cell membrane glycoproteins, and the DNA stain Hoechst-33342 (fig 4.1 (A)). Fluorescence imaging showed that there was large-scale uptake and/or binding of NMVs to BEAS-2B cells at this time point, with most cells appearing to be associated with several labelled NMVs. No fluorescence was demonstrated in samples without NMV upon excitation at 488 nm (excites PKH67 dye used for NMVs here). No obvious differences in cell morphology were observed between any of these conditions, and no differences in uptake of the two NMV types (elicited by fMLP or CSE) were seen.

To further confirm NMV internalisation by these cells, confocal microscopy was used. Figure 4.1 (B) shows an orthogonal view of BEAS-2B cells incubated with fMLP-elicited NMV for 2h. Although a lower concentration of NMVs was used here due to the larger cell growth area (collagen-I glass coverslips inside a 24-well plate) and media volume, with limited number of NMVs obtained from each isolation, intracellular NMVs (PKH26-labelled; red) associated with cellular F-actin staining (grey) were observed. BEAS-2B cells grew less uniformly on glass compared with plastic of the 96-well plates used for fluorescence imaging, and cells appeared to be more elongated.

To definitively quantify NMV internalisation, PKH67-labelled CSE or fMLP NMVs (3000/µl) were again incubated with BEAS-2B cells in a 96-well plate, after 2h these cells were detached, extracellular fluorescence quenched using trypan blue as per (Nuutila and Lilius, 2005), and then immediately analysed by flow cytometry. As shown in figure 4.2 (A) and in confirmation of uptake shown in figure 4.1 (A), almost 100% of cells had internalised NMVs after 2h, demonstrated by a large shift in fluorescence (blue histogram) from that of control cells incubated without NMV (red histogram).
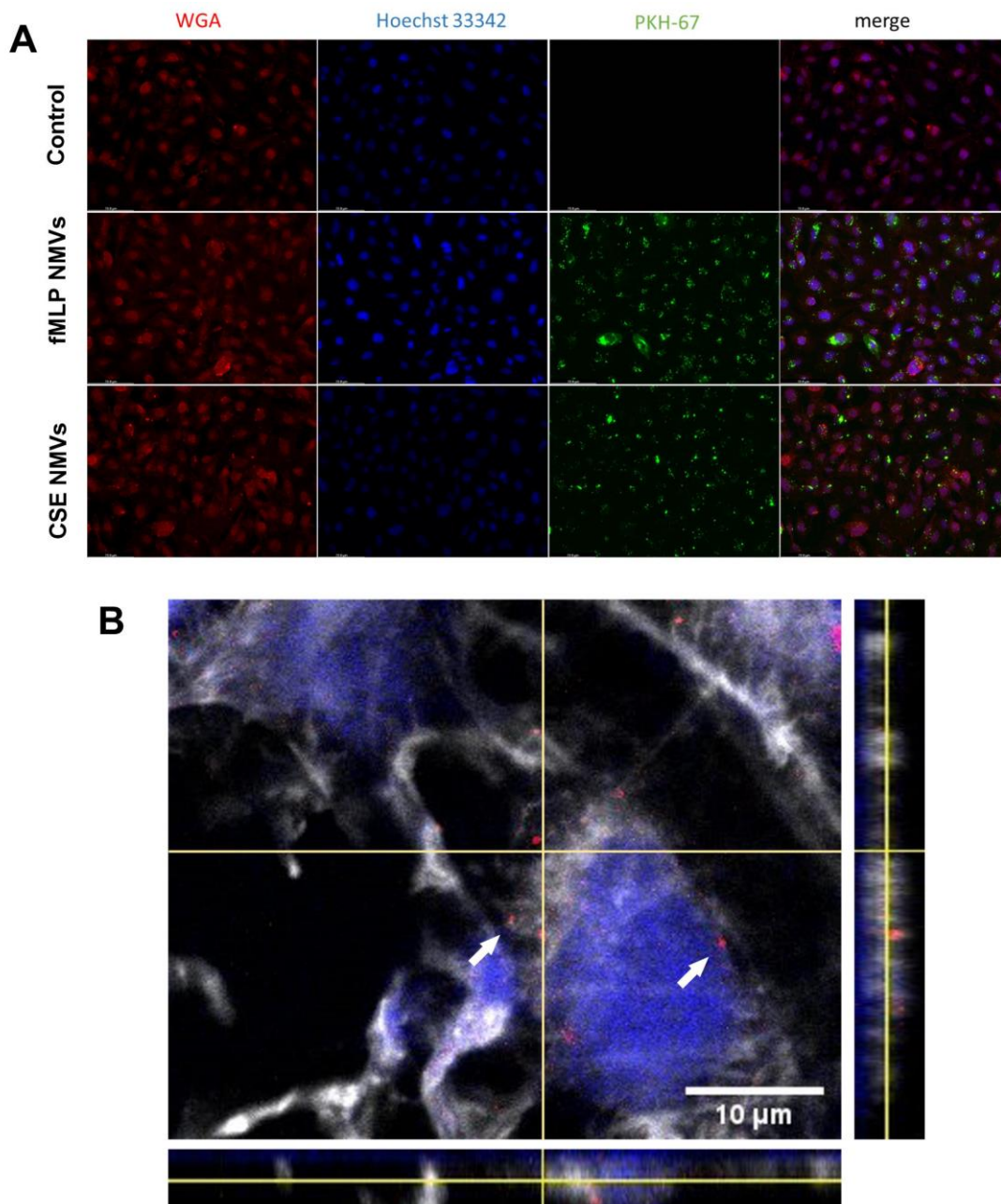
Figure 4.1 Internalisation of neutrophil-derived microvesicles (NMVs) by BEAS-2B bronchial epithelial cells visualised by microscopy

(A) BEAS-2B cells were incubated for 2h with PKH67-labelled NMVs (3000/µl) derived from either fMLP or CSE-stimulated neutrophils in a 96-well plate. Cells were thoroughly washed with PBS at the end of the incubation, fixed using 4% PFA, and then stained with alexafluor647-conjugated wheat-germ agglutinin (WGA; red, cell membrane) and counterstained with Hoechst (Blue; nuclei). Wells were imaged by fluorescence microscopy. Scale bar = 100 µm. (B) Confocal microscopy was used to further investigate this interaction. PKH26 (red) labelled fMLP NMVs (400/µl) were incubated with BEAS-2B cells cultured on glass collagen-I-coated coverslips. Washing and fixation procedure above was repeated, then cells were permeabilised using 0.1% Triton and labelled with FITC-phalloidin to visualise F-actin (grey) and To-pro-3-iodide (blue; nuclei). Orthogonal view demonstrating colocalization of NMVs (red) and F-actin (grey) is shown. White arrows indicate examples of NMVs. Experiments for (A) were performed by MSc student Magdalena Grudzien under supervision of Merete Long and Dr Victoria Ridger. CSE: 10% cigarette smoke extract, fMLP: N-formyl-met-leu-phe.
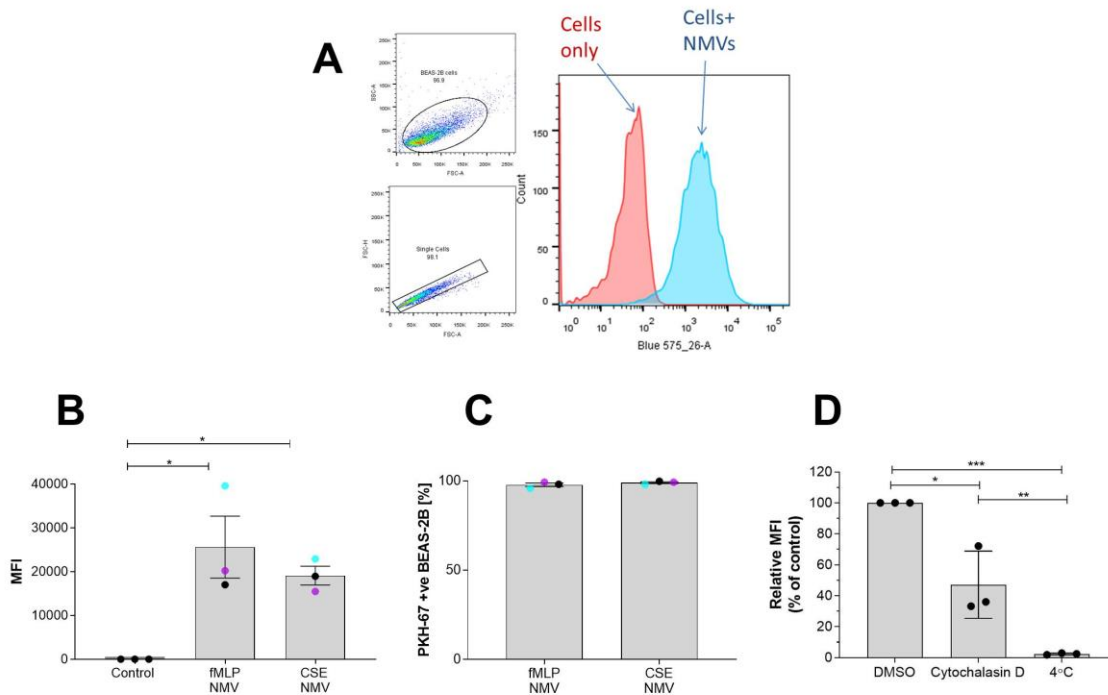
Figure 4.2 Internalisation of neutrophil-derived microvesicles (NMVs) by BEAS-2B bronchial epithelial cells measured by flow cytometry

BEAS-2B cells were incubated for 2h with PKH67-labelled NMVs (3000/µl) derived from either fMLP or CSE-stimulated neutrophils. Cells were thoroughly washed with PBS at the end of the incubation and then detached by gentle trypsinisation, before quenching extracellular fluorescence using trypan blue and analysing on the BD LSRII. (A) shows a representative histogram of control vs. fMLP-treated cells. (B+C) Internalisation of both CSE and fMLP NMVs was investigated, (B) median fluorescence intensity (MFI) and (C) the percentage of NMV-positive cells for each vesicle type is shown. Colours of data points indicate NMVs derived from the same participant. (D) To delineate the mechanism of NMV internalisation, BEAS-2B cells were pre-treated with cytochalasin D (inhibitor of pathways including macropinocytosis) or incubated at 4°C (inhibitor of energy-dependent uptake), then NMV internalisation was investigated by the same method as above, for fMLP NMVs only. DMSO (0.01%) vehicle control was used to determine maximal NMV uptake. (D+E) analysed using t-test, (F) using one-way ANOVA with multiple comparisons (Tukey's test). * p < 0.05, ** p < 0.01 *** p = 0.001. For each experiment, NMVs from n = 3 healthy participants were utilised. Data shows mean±SEM. Experiments for (B) and (C) were performed by MSc student Magdalena Grudzien under supervision of Merete Long and Dr Victoria Ridger. CSE: 10% cigarette smoke extract, fMLP: N-formyl-met-leu-phe.

There were no significant differences in NMV uptake between the two vesicle types investigated, in terms of either numbers of vesicles internalised—represented by median fluorescence intensity (MFI; fig 4.2 (B); fMLP-NMV: 25642±7062, CSE-NMV: 19143±2147 [mean±SEM])—or in the percentage of NMV-positive cells (fig 4.2 (C); fMLP-NMV: 97.77±1%, CSE-NMV: 99.07±0.88%), although the MFI for fMLP NMVs in one experimental repeat was much higher for fMLP than for CSE NMV.

Finally, the mechanism of the apparent NMV internalisation demonstrated here was investigated. Due to limited NMV numbers and requirement for quantification of at least two NMV-treated conditions (i.e. control and internalisation inhibitor), a limited inhibitor strategy was utilised, demonstrated to have effects on NMV uptake in our lab and by others previously. Cytochalasin D (1 µM), an inhibitor of actin polymerisation which hence curtails endocytic processes including macropinocytosis, was utilised, as well as treatment at 4°C to inhibit energy-dependent uptake in general. Cytochalasin treatment significantly reduced NMV uptake by almost 65% compared with vehicle control (p = 0.005), demonstrating a role for endocytosis and supporting the conclusion that NMVs are indeed internalised by BEAS-2B cells. Although, Cytochalasin D disrupts several processes in the cell and therefore inhibition of surface binding rather than active uptake may also be represented here, and further investigation would be warranted. Cooling to 4°C had an even greater effect, almost totally abolishing internalisation and reducing uptake by 82% (p=0.0002 vs. control), showing that NMV internalisation is an energy-dependent process. These results in summation indicate active uptake of NMVs by these cells, irrespective of the type generating stimulus for the NMVs, and we next sought to understand the implications of NMV internalisation.

4.3.2 Neutrophil-derived microvesicle effects on epithelial inflammation and cytokine production

After confirming rapid and large-scale uptake of NMVs by bronchial epithelial cells, the functional consequences of this interaction were investigated. NMVs have been shown to elicit a proinflammatory response from endothelial and epithelial cells both by our lab and others. However, this interaction has not yet been examined in the lung epithelium. In particular, it was shown previously in our lab that NMV addition significantly upregulated intracellular adhesion molecule-1 (ICAM-1) expression in arterial endothelial cells as part of their pro-inflammatory action (Gomez *et al.*, 2020). In fact, NMV uptake in these cells was at least partially dependent in NMV interaction with this adhesion molecule. ICAM-1 is an important adhesion molecule involved in epithelial–neutrophil interaction in the lungs and is increased in COPD, hence initial experiments into this effect in BEAS-2B cells were performed to determine potential for increased neutrophil binding. NMVs (unlabelled) were incubated with epithelial cells for either 4h or 24h to determine the kinetics

of any response. As a positive control, LPS was utilised (10 μg/ml). After this time, cells were washed by addition and removal of PBS and detached by gentle trypsination, then stained with FITC anti-ICAM-1 antibody for 30 min or isotype control. ICAM-1 surface expression was analysed by flow cytometry. As shown in figure 4.3 (A) and (B), no change in the expression of this protein was found at either of the time points investigated after NMV incubation (4h:100% [control] vs. 104.8±6.48% [NMV]; 24h: 100 vs. 101.4±3.39%), and whilst ICAM-1 expression was not significantly increased after 4h of LPS treatment (110.4±3.93%; p = 0.2182 vs. control), at 24h a statistically significant increase was observed (140.5±4.24%; p < 0.0001). Although there was no significant difference between LPS alone and the combined treatment with both LPS and NMVs, this combined stimulus was the only one to elicit a statistically significant change in ICAM-1 expression at 4h compared with control levels (120.4±9.68%; p = 0.0074 vs. control, p = 0.2418 vs. LPS only.

We therefore investigated the effect of these vesicles on the protein secretion and gene expression of CXCL-8 (IL-8)—a key signalling molecule involved in neutrophil-mediated inflammation and chemotaxis—to determine whether NMVs had an effect on epithelial activation in a feed-forward loop. Either 24h (protein; fig 4.4 (A) and (B)) or 2h (mRNA; fig 4.4 (C)) after co-incubation with NMVs derived from either (A, B, C) fMLP or (B) 10% CSE stimulation, expression levels of the cytokine and neutrophil chemoattractant CXCL-8 were determined. Epithelial CXCL-8 secretion into the cell media was measured by ELISA. LPS was used as a positive control for all experiments. fMLP NMVs (3000/μl) elicited a statistically significant increase in CXCL-8 of approximately three-fold after 24h, compared with control levels (NMVs: 2105±483.5, Control: 681.7±52.13 pg/ml; p = 0.0266; fig 4.2 (C)). LPS induced an almost six-fold increase from control levels (3936±246.2 pg/ml, p = 0.0001).

To elucidate whether NMVs derived from different stimuli may have differential effects, this experiment was repeated with both fMLP- and CSE-NMVs. These experiments were performed by MSc Student Carolina Silva, under my day-to-day supervision. A lower LPS concentration of 1 μg/ml was utilised to align more closely to the NMV response. As shown in figure 4.4 (B), there were no significant differences in the activity of these two vesicle types in terms of CXCL-8 secretion after 24h. However, in these experiments only NMVs from two of the three participants elicited an increase in CXCL-8 (control: 186.4±14.45, fMLP NMV: 5361±4648, CSE NMV: 6966±3596 pg/ml), and no differences in the effects of these two vesicle types were observed. As expected, this lower LPS concentration also generated a lower but consistent response (507.1±67.55 pg/ml). Despite changes in CXCL-8 secretion, there were no statistically significant differences between any of the conditions utilised in this experiment, including for the positive control, LPS.
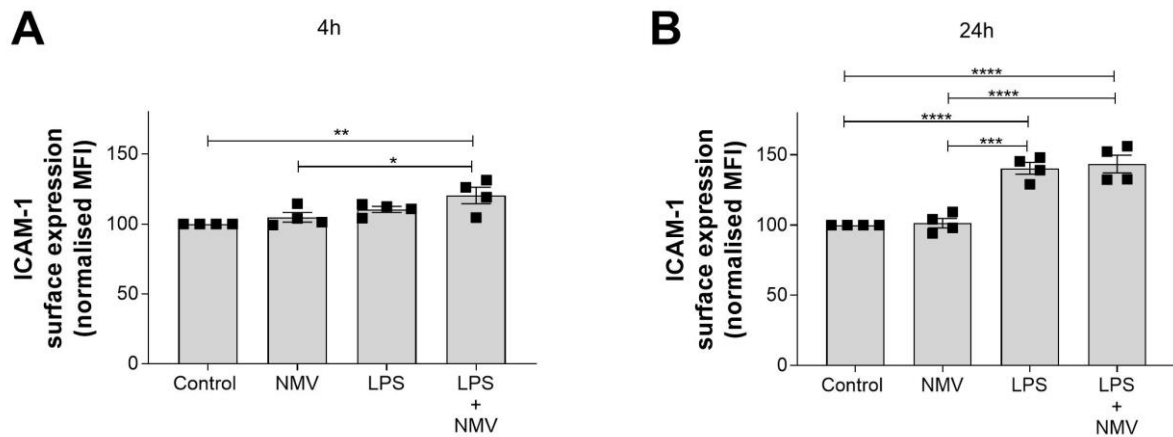
Figure 4.3 Neutrophil-derived microvesicle effects on bronchial epithelial cell adhesion molecule expression

BEAS-2B bronchial epithelial cells were incubated with NMVs (3000/µl) from fMLP-stimulated neutrophils, LPS (10 µg/ml) or LPS plus NMVs, for either 4h (A) or 24h (B). Cells were detached, labelled with FITC anti-ICAM-1 antibody and analysed by flow cytometry to determine ICAM-1 surface expression. Graph shows MFI normalised to timepoint control. ICAM-1: intracellular adhesion molecule-1. * p < 0.05, ** p < 0.01, ***p < 0.001, **** p < 0.0001. Data shows mean±SEM. All data in this figure were analysed by one-way ANOVA with multiple comparisons (Tukey's test). Note: when the same statistical test was performed on pre-normalised data at 4h: no significant differences. 24h Control v LPS *, Control vs. LPS+NMV **, NMV vs. LPS *, NMV vs. LPS+NMV *, comparisons between remaining groups not significant.
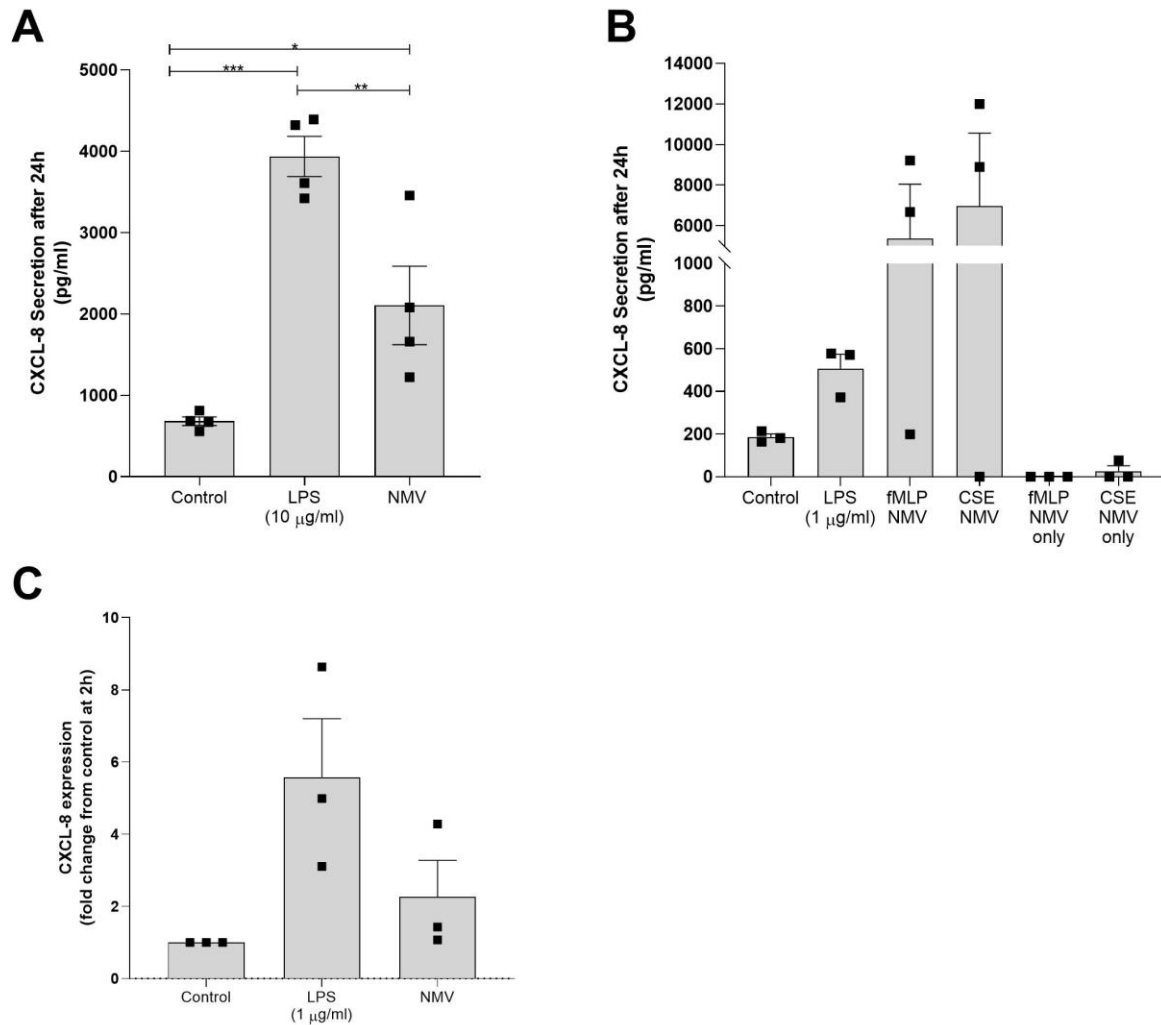
Figure 4.4 Neutrophil-derived microvesicle effects on bronchial epithelial cytokine production

(A) BEAS-2B bronchial epithelial cells were incubated with NMVs (3000/µl) from fMLP-stimulated neutrophils or LPS (10 µg/ml). After 24h, epithelial CXCL-8 secretion into the cell media was then measured by ELISA. (B) The experiment in A was repeated with either fMLP- or CSE-NMVs and a lower concentration of LPS (1 µg/ml) and CXCL-8 secretion measured. Y-axis split to allow visualisation of data at lower concentrations. (C) BEAS-2B cells were incubated with either fMLP NMV or LPS for 2h, then cells were washed, lysed with TRIzol, and processed for RNA extraction and subsequent cDNA synthesis. Samples were analysed for CXCL-8 mRNA expression levels using qPCR. To determine fold-change in gene expression, data was normalised to the respective experimental control (untreated cells). All experiments represent n=3-4 different healthy participants. Data shows mean±SEM. Experiments for (B+C) performed by MSc student Carolina Roque Silva under supervision of Merete Long and Dr Victoria Ridger. CSE: 10 % cigarette smoke extract. LPS: lipopolysaccharide. fMLP: N-formyl met leu phe. * p < 0.05, ** p < 0.01, ***p < 0.001. All data in this figure were analysed by one-way ANOVA with multiple comparisons (Tukey's test).

This may in part be due to variation between experimental repeats and NMV donors. Finally, when NMVs alone were measured for CXCL-8 content, at the same concentration as that used for cell treatments (3000/µl), negligible levels of this cytokine were detected (fMLP NMV only: 0 pg/ml, CSE NMV only: 25.61±25.62 pg/ml), and therefore the source of CXCL-8 in this experiment was concluded to be BEAS-2B cells.

Finally, since an (albeit variable) effect of NMVs on airway epithelial CXCL-8 secretion was observed, effects on this chemokine at the mRNA level after 2h of fMLP NMV treatment were investigated using qPCR. As illustrated in figure 4.4 (C), there was a trend to increased CXCL-8 mRNA in LPS treated cells which did not reach significance (5.58±1.62-fold increase vs. control, p = 0.0596), with substantial variation demonstrated between repeats. Although one of the three NMV donors elicited a 4.3-fold increase in gene expression, overall, no significant differences were found between control and NMV treatment (2.26±1.01-fold change vs. control, p = 0.713). Taken together, these experiments suggest a modest but variable effect of NMVs on airway epithelial activation and pro-inflammatory response.

4.3.3 Epithelial cell monolayer permeability after neutrophil-derived microvesicle co-incubation

BEAS-2B take up large numbers of NMVs, with rather variable impact on the release of the archetypal neutrophil pro-inflammatory mediator CXCL-8, hence we sought other potential impacts of NMVs on the target cells. As protease activity was definitively demonstrated by NMVs in the previous chapter (chapter 3), potential protease-mediated effects on the epithelium were investigated.

Epithelial monolayer permeability was investigated by culturing BEAS-2B cells in transwells (submerged culture) and treating confluent cell monolayers with 3000 NMV/µl media containing 1 mg/ml of 10 kDa FITC-dextran to determine permeability to small molecules (measured by passage through to the lower transwell chamber), as a surrogate marker for permeability to, for example, chemokines and cytokines. The experimental set-up for this assay is illustrated in the materials and methods, section 2.2.19. Only NMVs generated from fMLP stimulation was used in these experiments due the large numbers required for functional studies with multiple timepoints and since we have found no differences to date in the properties of the 2 types of NMV. A sample of media from the basal compartment was taken at 4 or 24h after NMV addition and fluorescence was measured using a spectrophotometer, noted here as arbitrary units (AU) in figure 4.5 (A) and (B), respectively.
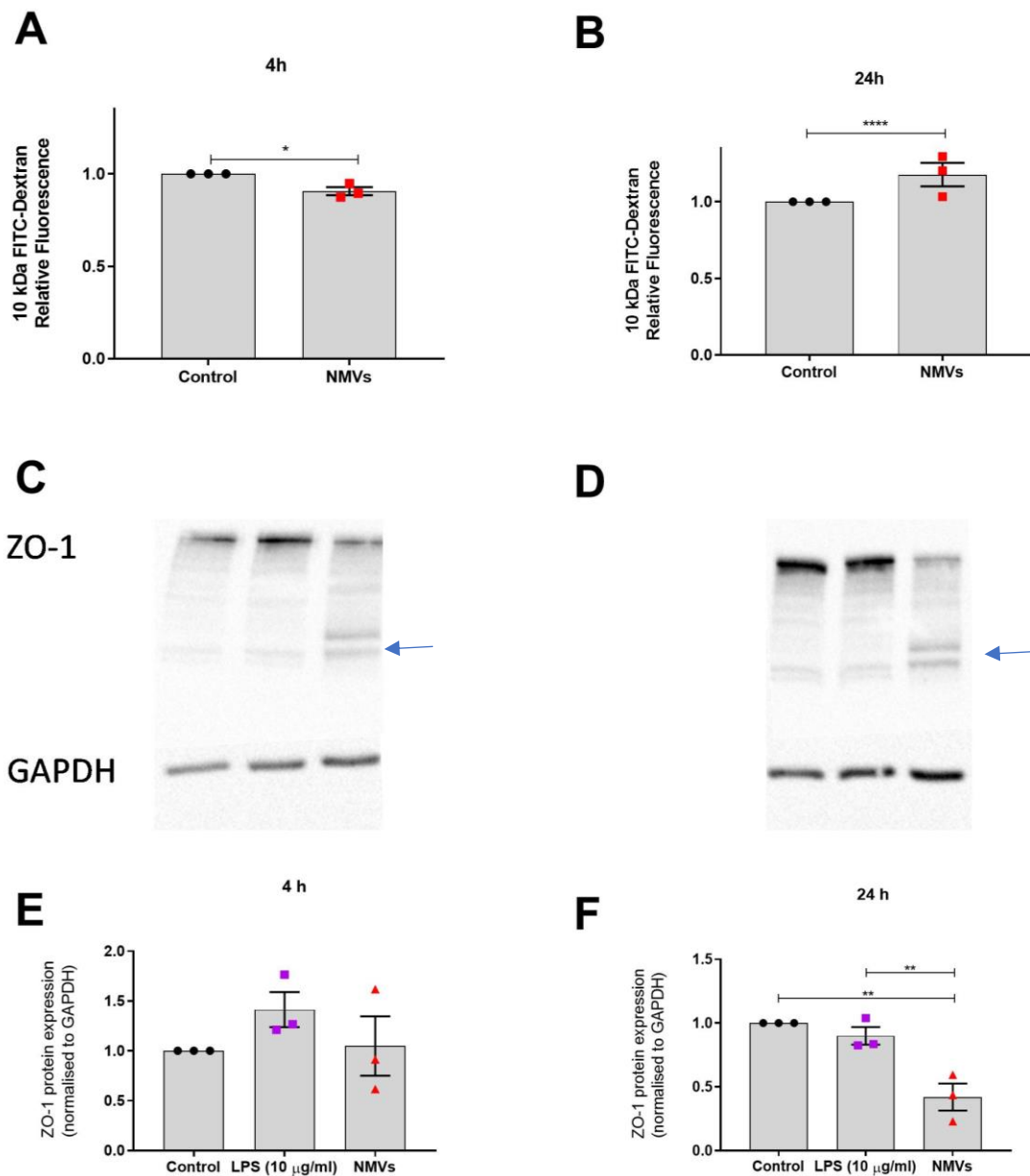
Figure 4.5 Neutrophil-derived microvesicle (NMV)-induced epithelial cell permeability

*(A+B) BEAS-2B bronchial epithelial cells were grown on transwell inserts and incubated with NMVs from fMLP-stimulated neutrophils or with media only, and with the tracer molecular FITC-dextran to measure monolayer permeability for (A) 4h or (B) 24h. At these timepoints the basal media was sampled and fluorescence was quantified using a spectrophotomer. Relative fluorescence indicated sample fluorescence relative to the time-point control condition, unpaired t-test was used to analyse data. (C-F) Cells were incubated in submerged culture with either media only (control) LPS, or fMLP NMVs for (C+E) 4h or (D+F) 24h and then lysed for SDS-PAGE and western blotting to quantify expression of the junctional protein ZO-1. Expression of this protein was normalised to that of GAPDH. C+D show representative western blots (blue arrows indicate potential cleavage products) which were quantified by densitometry (E+F). Sample loading order in C+D corresponds to x-axis labels in E+F. A+B analysed by t-test. E+F analysed using one-way ANOVA with multiple comparisons (Tukey's test). * p < 0.05, ** p < 0.01, **** P < 0001. Data show mean±SEM. All experiments represent n=3, utilising three different neutrophil donors. Blue arrows indicate potential cleavage products. Note: when the same statistical analyses in A and B were performed on pre-normalised data at 4 and 24h, differences were not statistically significant.*

After 4h (fig 4. (A)), rather unexpectedly, less FITC-dextran was detected in the lower chamber of the NMV-treated samples than that in the control wells (i.e. vehicle/PBS-treated) for all experimental repeats (mean±SEM: 0.9±0.021 of control as 1), with a decrease of approximately 10%, indicating a reduction in permeability or tightening of the cell layer. Although small, this difference was consistent and statistically significant (p = 0.012). However, after 24h the reverse was observed, with a net increase in permeability to FITC-dextran (1.17±0.078; p < 0.0001; approx. 20% increase) and a higher fluorescence intensity of the NMV treated basal well samples.

To further investigate potential mechanisms of increased permeability, expression levels of the key tight junction (TJ) protein zonula occludens-1 (ZO-1) were determined. Whilst initially immunofluorescence staining was attempted to measure ZO-1 expression, this staining was very variable across a single sample depending on the precise area imaged, and this technique was deemed to be unreliable with potential for imaging bias (data not shown). Western blotting was therefore employed to quantify total ZO-1 levels at the same time points as those used above (fig 4.5 (A) and (B)). In this experiment cells were not cultured in transwells due to the greater complexity of this culture method and the small number of cells within a well, but rather grown in normal submerged culture. LPS was used as a positive control previously reported to reduce ZO-1 protein expression levels in other epithelial cells (Yi *et al.*, 2000) and generally shown to disrupt TJs in the airway epithelium *in vivo* (Eutamene *et al.*, 2005).

After 4 h incubation (fig 4.5 (C+E)), there was a consistent trend for increased ZO-1 expression levels in LPS-treated cells (mean±SEM: 1.414±0.176 fold-change from control levels) although this was not statistically significant (p=0.369). In NMV-treated cells this response was variable with no clear trend (fold-change 1.049±0.297; p=0.984 vs. control). There were no significant differences between any of the treatment groups by one-way ANOVA. However, after 24 h (fig 4.3 (D+E)), NMV-treated cells showed significantly reduced ZO-1 expression (fold-change of 0.420±0.106 from control levels; p = 0.0033), which was also significantly different from the LPS-treated cell response (fold-change of 0.900±0.070; p = 0.0083 vs. NMV); the latter did not differ significantly from control expression at this timepoint.

Interestingly, NMV-treated samples also demonstrated stronger expression of two protein bands with lower molecular weight than intact ZO-1 (fig 4.3 (C) and (D), last lane, indicated by blue arrows at 4 and 24h) detected by the ZO-1 antibody; it is unclear whether they represent degradation products or even NMV proteins.

4.3.4 Epithelial apoptosis and endoplasmic reticulum stress

As effects of NMVs on epithelial permeability were demonstrated, associated with reduction in JP expression, we hypothesised that JP reduction may lead to epithelial cell detachment-induced death, a process known as anoikis, previously shown to be induced by MMP-9 in airway epithelium *in vitro* (Vermeer *et al.*, 2009), which ultimately results in the increased permeability we observed. In their work, Vermeer et al. (2009) also showed that application of MMP-9 resulted differential patterns of epithelial ZO-1 expression. To investigate this whilst minimising cell processing and loss of detaching cells, live cell time-lapse fluorescence microscopy was used. The CellEvent caspase-3/7 probe (to detect apoptosis) was added to confluent BEAS-2B cells in a culture plate, after which fMLP MVs were added and cells were imaged over 24h. To determine whether any observed effects may be dependent on metalloprotease activity, the endogenous MMP inhibitor, TIMP-1 (tissue inhibitor of metalloproteinase-1), was also added in combination with NMVs. A TIMP-1-only control was also utilised to determine effects of this protein on BEAS-2B cells. After the time course, cells were gently washed, fixed with warm 4% PFA, and stained with DAPI to determine number of cells per field of view (f.o.v) for data normalisation using the mark and find function of the microscope to obtain images of the same well areas.

Representative images from this experiment after 24h incubation are shown in figure 4.6 (A). Active caspase-3/7 positive cells, i.e. apoptosing cells, could be viewed as green events in the f.o.v. Images (3–5 f.o.v per condition, repeated for n=3 individual neutrophil donors) were quantified using image J by thresholding and automated analysis (fig 4.6 (B)). The basal rate of apoptosis in the control condition was relatively low at 1.93±0.36% (Mean±SEM). TIMP-1 treated cells showed similar levels of apoptosis to the media only control condition (1.72±0.31%) at 24h. NMV-treated cells exhibited a trend towards higher levels of caspase 3/7 positive cells at 6.12±1.75% but also greater variation than the control conditions. This difference was not statistically significant compared with the negative control (p = 0.0647), and it would be pertinent to increase the low n-numbers used here. When NMVs were added in combination with TIMP-1, levels of apoptosis were similar to NMV treatment alone (5.84±0.75%) and no reduction in caspase activation was observed using this MMP inhibitor. Loss of CellEvent positive cells into the cell supernatant after 24h incubation was measured by flow cytometry, media volume analysed by this method was normalised by setting the stopping gate to 60 seconds for each sample, and cell numbers were normalised to the average number in the control condition (fig 4.6 (C)). Cell detachment was found at similar levels in the control and TIMP-1 treated conditions (100±14.65% and 116±14.24%, respectively), whilst higher levels were seen in the NMV treated cells (219.9±56.26%), although this was not found to be statistically significant.
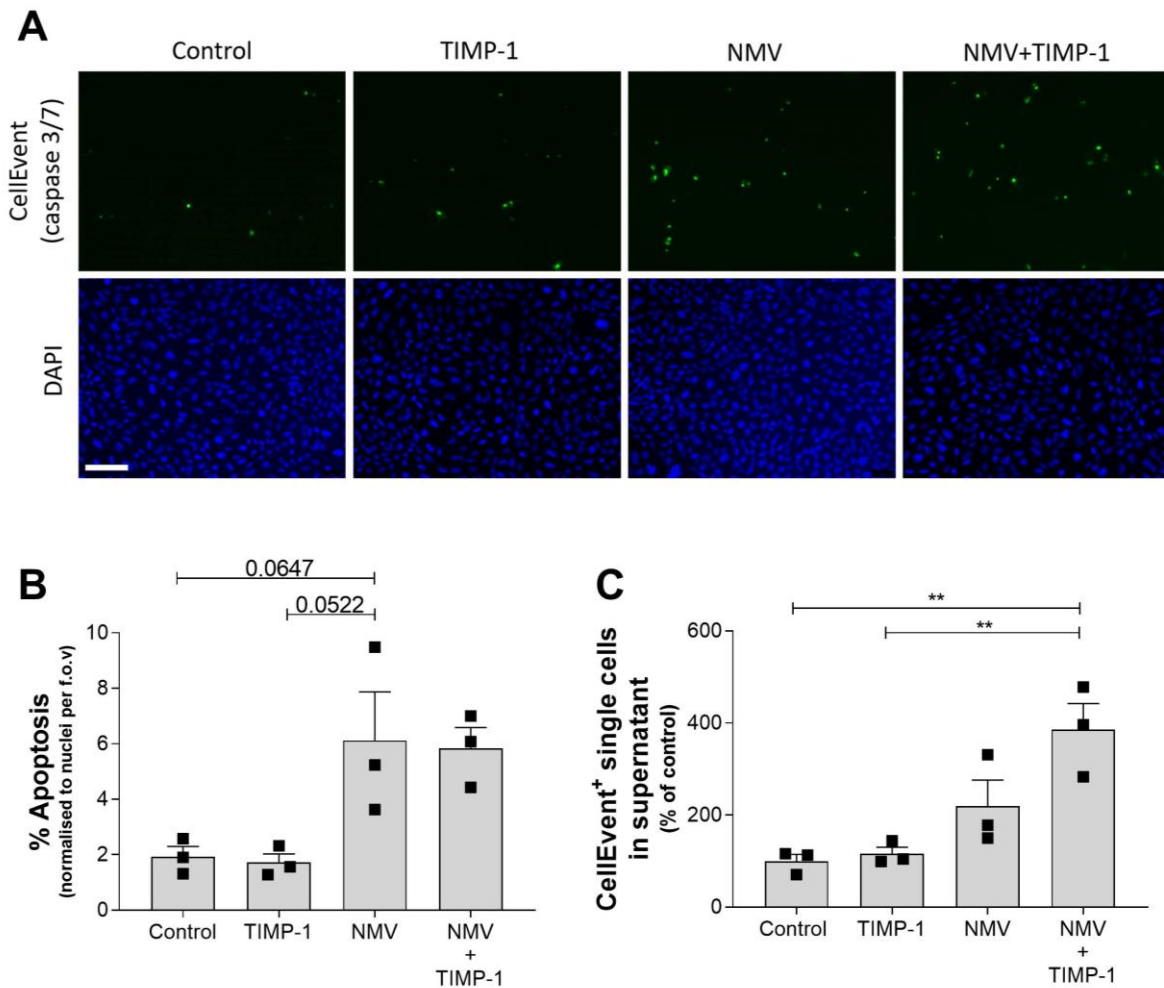
Figure 4.6 Effects of neutrophil-derived microvesicles on epithelial apoptosis

(A) BEAS-2B bronchial epithelial cells were incubated with CellEvent active Caspase-3/7 probe (green) and NMVs (3000/µl) with or without tissue inhibitor of metalloproteinase-1 (TIMP-1) for 24h. Representative images as shown in for each condition, apoptotic caspase-positive cells are indicated in green. Legend continued on next page. Lower panel shows DAPI-stained cell nuclei in the corresponding fields of view (f.o.v). 10X magnification, scale bar =100 µm. (B) Apoptotic cells per f.o.v were quantified in image j and normalised to nuclei per f.o.v to determine the percentage of apoptotic cells in each condition. 3-5 images quantified per condition. N=3 individual neutrophil donors utilised. (C) After 24h incubation, cell supernatants were analysed for cell detachment by quantification of number of CellEvent-positive single cells with a stopping gate of 60 seconds to normalise volume of sample analysed across all conditions. Cell number was normalised to the respective experimental control condition. Data show mean+SEM. ** p < 0.01. All data were analysed by one-way ANOVA with multiple comparisons (Tukey's test/post-hoc analysis).

Interestingly, there was significantly more cell detachment in the combined NMV and TIMP-1 treated cells (385.8±56.61%, p = 0.0052 vs. control, p = 0.0073 vs. TIMP-1 only). Increasing the number of biological replicates here may help to determine whether the trends observed are biologically relevant, and a limitation of these experiments is the low n-numbers used.

Although we found NMV-induced effects on permeability and pro-inflammatory activation, apoptosis was not significantly increased by NMVs. Subsequently we investigated whether NMVs may induce endoplasmic reticulum (ER) stress by determining the expression levels of a master regulator of ER stress, GRP78. ER stress has been evidenced in COPD (Min *et al.*, 2011), induced by oxidative stress and inflammatory cytokines (Kenche *et al.*, 2016), and has a role in epithelial dysfunction (Kim *et al.*, 2019; Eri *et al.*, 2011). After 24h incubation with NMVs or with the positive control Tunicamycin (3 µg/ml)—which induces cell cycle arrest and promotes the unfolded protein response—cells were lysed and GRP78 detected by western blotting (fig 4.7 (A)). In figure 4.7 (B) quantification of expression levels by densitometry showed that whilst Tunicamycin induced an increase in GRP78 levels of 9.6±1.87 fold from the control (p = 0.0058), there were no differences in GRP78 levels between the control condition and NMV treatment (1±0.59 vs. 1.460±0.6 respectively; p = 0.9615).

4.3.5 Effect of neutrophil-derived microvesicles on epithelial proliferation

Since effects on apoptosis were not significant here and no effect on ER stress was found, we investigated whether NMV-induced permeability and activation may be due to reduced cell proliferation, as shown in NMV-treated intestinal epithelial cells (Slater *et al.*, 2017), which may be an indicator of epithelial-to-mesenchymal transition or senescence, amongst other effects. For this, BEAS-2B cells were labelled with 5 µM Proliferation Dye eFluor700 and then seeded into 96-well plates. As shown in figure 4.8 (A), this allowed tracking of the cell proliferation rate by determining the difference in MFI, which decreases as the cell divides. Figure 4.8 (B) shows an example of this cell labelling, imaged by fluorescence microscopy. 24h after cell seeding, NMVs (3000/µl) were added to the wells and cell fluorescence was analysed 24 (fig 4.5 (C)) or 48h (D) later to determine the potential longer-term impact on epithelial cell barrier function. To account for differences in cell labelling between experiments, the MFI of NMV-treated cells was normalised to the control condition at the relative timepoint (i.e. untreated cells), and the control was designated as 100. Surprisingly, a statistically significant reduction in MFI of approximately 10% was seen after NMV treatment at 24h (90.75±1.56% of control [mean±SEM]; p = 0.0041) and reduction of approximately 15% at 48h (85.62±2.54% of control; p = 0.0048). Therefore, an increase in proliferation rather than a decrease was indicated after NMV incubation.
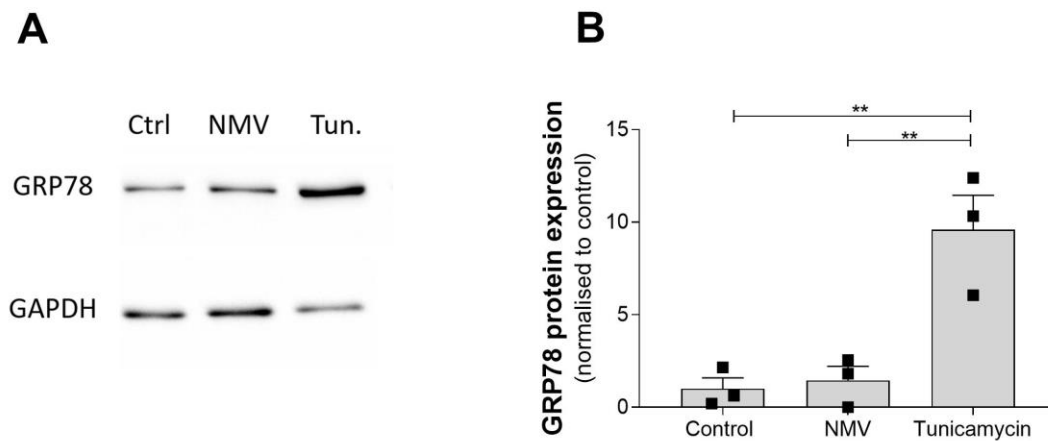
Figure 4.7 Effects of neutrophil-derived microvesicles on epithelial endoplasmic reticulum stress

*Induction of endoplasmic reticulum stress by NMVs was investigated in BEAS-2B bronchial epithelial cells by detection of GRP78 expression by western blotting. BEAS-2B cells were incubated with media only (control), NMVs, or 3 µg/ml tunicamycin (positive control; Tun.) for 24h, then lysed and processed for protein analysis. (A) Representative blot is shown. (B) GRP78 expression levels were quantified by densitometry, values were normalised to GAPDH expression and then to the average of the experimental control. Data show mean+SEM. ** p < 0.01. All data were analysed by one-way ANOVA with Tukey's post-hoc test. N=3.*
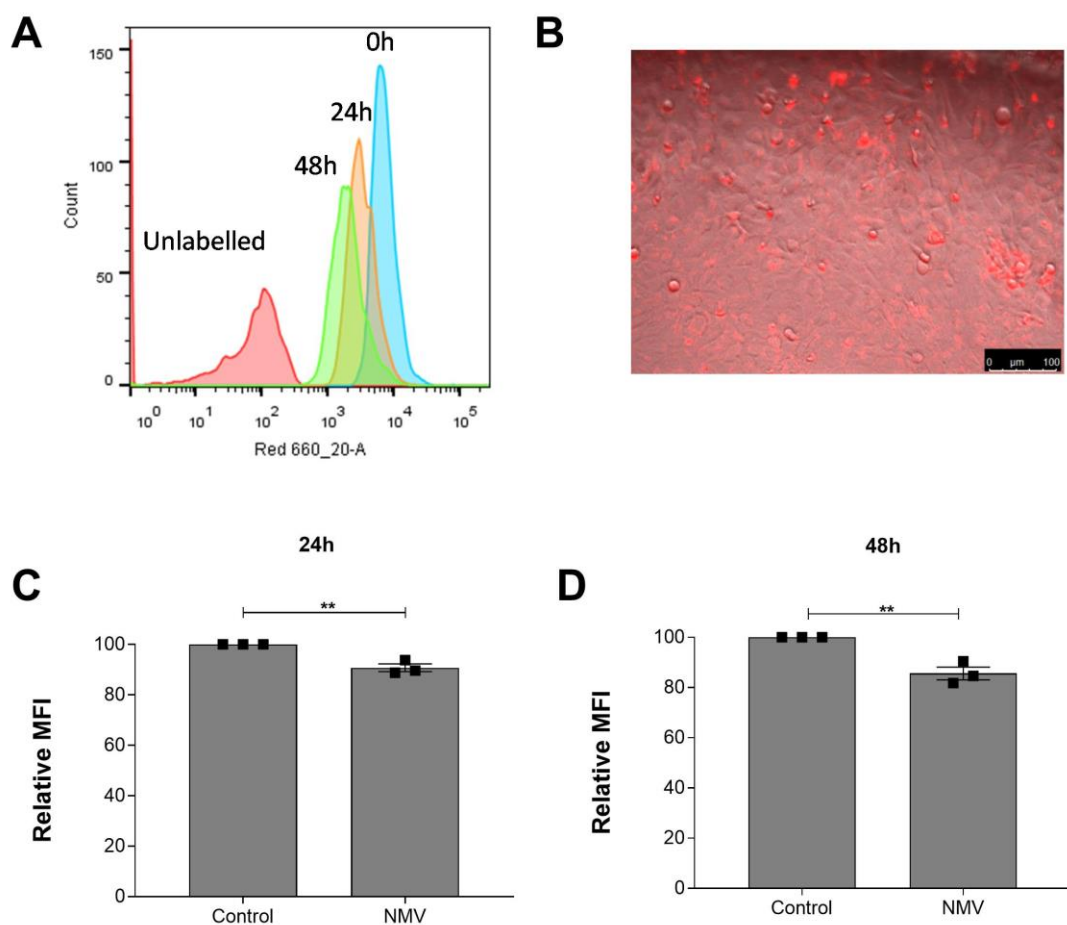
Figure 4.8 Neutrophil derived microvesicle effect on epithelial proliferation

BEAS-2B bronchial epithelial cell proliferation was tracked by staining cells with 5 µM eBioscience Cell Proliferation Dye eFluor 670. (A) Cells were immediately analysed by flow cytometry to determine fluorescence at 0h, unlabelled cells were used as a control. Remaining cells were seeded into 96-well plates. Histogram shows fluorescence of cells at each of the indicated time points after initial seeding. Labelling efficiency was 100% at 0h. (B) shows cell fluorescence 48h after seeding imaged by fluorescence microscopy and overlapped with brightfield image. 10X magnification, scale bar represents 100 µm. (C) NMVs (3000/µl) were added to labelled BEAS-2B cells and incubated for 24 or (D) 48h before cell detachment by gentle trypsinisation and analysis by flow cytometry. Data shows mean±SEM. Median fluorescence intensity (MFI) of NMV-treated cells was normalised to control cell fluorescence at the respective time point to control for differences in cell labelling between experimental repeats. N=3 individual neutrophil donors utilised. **p < 0.01. Data were analysed by unpaired t-test. Note: when pre-normalised data were used in the same test, at 24h p = 0.4744 and 48h p = 0.2033 (not significant).

4.4 Discussion

4.4.1 NMVs are rapidly and actively internalised by epithelial cells in vitro

We aimed to determine initially whether there was an interaction between NMVs and the airway epithelial cells. BEAS-2B cell uptake of fresh, fluorescently-labelled NMVs was investigated by confocal and fluorescence microscopy (fig 4.1 (A) and (B)) and quantified by flow cytometry (fig 4.2 (A-D)). All of these experiments together conclusively showed internalisation of NMVs by these cells after just 2h of co-incubation. Confocal microscopy experiments were carried out with a lower NMV concentration (~400 NMV/µl, approx. cell:NMV ratio of 1:0.7) to allow cell culture on glass coverslips in 24-well plates. The technique was useful in confirming the intracellular localisation of NMVs and indeed evidenced the presence of these vesicles in the cytosol (fig 4.1 (B)). Confocal microscopy has been used as one of the gold-standard techniques to confirm MV uptake in various cell types (Mondal *et al.*, 2019; Ajikumar *et al.*, 2019; Gomez *et al.*, 2018; Kuravi *et al.*, 2019; Faille *et al.*, 2012; Mohning *et al.*, 2018), however, cell morphology in the present images was notably stretched with cell-free gaps. Culture on glass was not favourable for BEAS-2B cells although the material was required to enable confocal imaging of the samples; using fluorescence microscopy (fig 4.1 (A)) permitted cell culture in 96-well plastic plates, where the cells appeared more confluent upon imaging and had a cobble-stone morphology. In the latter experiments and for flow cytometry, NMVs were used at an ideal concentration of 3000 NMVs/µl (approx. cell:NMV ratio of 1:6) due to smaller well sizes. At this concentration almost 100% of the cells had taken up NMVs at 2h (fig 4.2 (A) and (B)). Fluorescence microscopy revealed that each cell internalised multiple vesicles at this higher concentration. Furthermore, no neutrophil cell contamination was observed in these images, indicating a pure NMV sample in these experiments.

The rapid uptake of these vesicles is in agreement with previously published results, for example uptake of NMVs generated from fMLP stimulation was recently well characterised in brain endothelial cells in the Ridger lab (Ajikumar *et al.*, 2019) at 2h co-incubation, as well as in HCAECs (Gomez *et al.*, 2020). Additionally, bronchial epithelial cell uptake of macrophage-derived MVs has been described 1h after MV addition, and at sufficient concentrations ~100% MV-positive cells were shown (Schneider *et al.*, 2017). Surprisingly, EV uptake by macrophages is detectable in as little as 5 min after vesicle addition (Ofir-Birin *et al.*, 2018). Due to time restrictions and limited NMV numbers we were unable to further investigate the kinetics of NMV uptake here, but it would have been interesting to understand when maximal uptake of NMVs occurred in these cells, to aid further understanding of their potential effects.

NMV internalisation by target cells has been measured indirectly by some through quantifying levels of intracellular MPO or CD66b; whilst this is beneficial in that it required minimal processing of NMV samples (Hong *et al.*, 2012), the approach has a number of drawbacks. Firstly, NMVs generated from different stimuli have differential content, and MPO levels may reflect this rather than being proportional to NMV uptake. Secondly, this approach does not allow distinction between bound and internalised NMVs. For these reasons, the majority of NMV tracking and imaging has been done using lipophilic, membrane-intercalating dyes such as PKH used in the present study. Whilst this does require extra processing steps which could potentially change NMV activity, evidence for adverse effects is minimal, and these dyes allow specific tracking of labelled MVs using either confocal microscopy or flow cytometry. In addition, experimental controls both *in vitro* and *in vivo* have shown that free-dye is rarely seen in these analyses.

Interestingly, in the present study using flow cytometry analysis, fMLP and CSE NMVs did not differ in their uptake, either in the numbers of MVs taken up by the cells (i.e. MFI) or in the percentage of cells internalising NMVs (fig 4.2 (B) and (C)). When analysed by nanoparticle tracking analysis, the size of these two NMVs types was similar, and therefore it is plausible that they may share a common mechanism of internalisation. Schneider at al. (2017) previously showed that epithelial cell uptake of macrophage-derived MVs was majorly via dynamin-dependent endocytosis and dependent on actin polymerisation. Furthermore, these authors showed that CSE reduced MV uptake in these cells; a recent publication further characterised the effects of CSE on endocytic pathways by showing that CSE disrupted both clathrin-mediated endocytosis and macropinocytosis whilst promoting caveolin-mediated endocytosis (Duffney *et al.*, 2020); as a highly relevant stimulus in COPD, effects of cigarette smoke on this interaction with NMVs rather than macrophage MV would be very interesting future research. Further, actin-dependent pathways including macropinocytosis are also exploited in the lung epithelium by viruses to gain entry to the cell and CSE has been shown to promote epithelial viral uptake (Ketterer *et al.*, 1999; Sun and Whittaker, 2007; Duffney *et al.*, 2020).

The mechanism of uptake demonstrated by Schneider et al. (2017) has also been echoed in results from published work from our lab by Ajikumar et al. (2019) showing that internalisation of fMLP NMVs by brain microvascular endothelial cells was mostly via these two pathways. However, these authors also demonstrated an important role for protein–protein interaction in these cells, as shown by a large reduction in NMV uptake after proteinase K treatment, which was not investigated by Schneider et al. In our lab it was also shown that endothelial internalisation of NMVs could be reduced by 50% by pre-treatment with ICAM-1 blocking antibody, highlighting a role of surface protein interaction (Gomez *et al.*, 2020); this interaction seems to apply to a variety of extracellular

vesicles and cell types, including dendritic cells (Morelli *et al.*, 2004) . In the present study, we were restricted by the concentration of NMVs required for these experiments, which was much higher than those used by Ajikumar and also Gomez et al. in the above mentioned publication, due to the higher numbers evidenced in the airways in COPD (Lacedonia *et al.*, 2016), and therefore chose to look only at the two common mechanisms of endocytosis and actin polymerisation and investigated internalisation of fMLP NMVs. Using the inhibitor of actin polymerisation, cytochalasin D, an average decrease in NMV uptake of almost 65% was demonstrated. Further, incubation of cells at 4°C almost entirely inhibited internalisation. These results demonstrate a large role of actin rearrangement in uptake and energy-dependence of these processes, in agreement with the literature. Given these large effects, the lack of impact of NMVs on ICAM-1 expression (see below), and the constraints of the large number of NMVs required to undertake the experiments, the use of ICAM-1 blocking antibodies was not undertaken. Therefore, a limitation of the present study was that the precise mechanism utilised by NMVs cannot be pinpointed, however, these experiments in combination with current literature do demonstrate the modifiable nature of NMV uptake and indicated potential common mechanisms employed by immune cell MVs in epithelial cells and across several cell types.

4.4.2 NMVs have a modest but variable effect on epithelial cell activation

The primary aim of this study was to determine whether NMVs exert functional effects on the lung epithelium using an *in vitro* approach. We hypothesised that NMVs would induce a pro-inflammatory response in the bronchial epithelial cell line BEAS-2B based on published results in other cell types, evidence of neutrophil–epithelial cell interaction (Boots *et al.*, 2012), and knowledge of NMV contents known to have a damaging effect on the epithelium (i.e. proteases and miRs) (Butin-Israeli *et al.*, 2016a; Butin-Israeli *et al.*, 2019).

As we had shown large scale and rapid internalisation of NMVs, we next investigated a mechanism linked previously with NMV uptake and inflammation: ICAM-1 expression. Indicating further relevance of this investigation, ICAM-1—Mac-1 interaction represents a major mechanism of neutrophil adhesion to epithelial cells during lung inflammation which potentiates neutrophil-mediated cellular injury (Tosi *et al.*, 1992). Further, ICAM-1 is also a major receptor for rhinovirus, a common cause of COPD exacerbations (Papi *et al.*, 2006), where upregulation of this molecule increases the potential for viral entry and infection and is potentiated by rhinovirus-exposure itself (Staunton *et al.*, 1989). Despite upregulation of this adhesion molecule in NMV-treated endothelial cells shown in our lab previously (Gomez *et al.*, 2020), NMV incubation with BEAS-2B cells at either 4 or 24h had no effect on ICAM-1 expression. LPS upregulated ICAM surface expression at both of these timepoints, with the largest increase observed at 24h. Additionally, although combined LPS and NMV treatment was slightly higher at 4h, this combination did not seem to significantly

augment the response induced by LPS alone. Although not investigated here, it would be interesting to determine whether the LPS-induced increase in ICAM-1 expression had an effect on NMV internalisation levels. ICAM-1 has been shown to be increased in a variety of inflammatory conditions in the lung and upregulation can be mimicked in healthy cells by application of bronchial secretions from patients with chronic inflammatory lung disease (Chan *et al.*, 2008). Further, whilst LPS has been shown to upregulate ICAM expression, this is via a TNF-α-dependent mechanism, and direct application of this cytokine may be a better way to model and investigate changes in this adhesion molecule *in vitro* (Beck-Schimmer *et al.*, 1997).

Since ICAM-1 expression was not affected but there are many more markers of epithelial activation which make up a pro-inflammatory secretory profile, effects on release of the chemokine CXCL-8 was investigated. CXCL-8 has been shown to be increased in airway secretions in COPD including in induced sputum compared with both healthy controls and smokers, and has a key role in neutrophil recruitment (Osei *et al.*, 2016). In the present study, a modest but significant effect of NMV co-incubation on the secretion was observed (fig 4.4 (A)), approximately half that seen in these cells with a high concentration of LPS (10 µg/ml). A previous study from the Ridger lab using a three-fold lower NMV concentration (1000 NMV/µl) showed a statistically significant, two-fold increase in CXCL-8 secretion after 2h incubation of primary endothelial cells (HCAECs) with NMVs. However, due to variability in this response the change was not significantly different from control levels at 4 h (Gomez *et al.*, 2020). There was a low n-number in the present study (n=3) due to the high concentration of NMVs required for each experiment, therefore, increasing the number of NMV donors used may help to delineate whether this increase in cytokine secretion and expression is consistent and repeatable, and would aid in overcoming the limitations of donor variability. Of note, Schneider et al. (2017) showed that incubation of rat alveolar epithelial cells with alveolar macrophage MVs for 1h had no effect on epithelial CCL-2 gene expression, another inflammation-associated chemokine released by the airway epithelium. In fact, when cells were pre-incubated with these MVs and then treated with LPS, a significant reduction in CCL-2 expression from that of LPS alone was noted in the literature (Schneider *et al.*, 2017). These differences highlight the complexity of MV effects on different cell types and the mechanisms they employ to activate them.

Differences between airway epithelial cell lines, e.g. between BEAS-2B and the commonly used A549 type-II-like pneumocyte line, in LPS-response magnitude in terms of CXCL-8 secretion have been documented previously (Schulz *et al.*, 2002). However, in their study Schulz et al. found that BEAS-2B cells were more sensitive to LPS stimulation, and an LPS concentration at least 10 times lower than that employed in our study yielded a >20-fold increase in CXCL-8 secretion after 24h. However, culture conditions can vary dramatically for the cell line, and those authors used a BEAS-2B sub-

culturing routine in which cells were passaged at >95% confluency once per week, whereas in the present study we used <80% confluency as a cut-off point and passaged cells twice per week, since these cells may become senescent or differentiate into squamous cells upon reaching confluency(Zhao and Klimecki, 2015). On the other hand, CXCL-8 gene expression induced by LPS here was similar to that seen previously with a 10-fold lower concentration of LPS in the same cell line (Suzaki, Asano et al., 2011). Aside from passaging and cell confluency, other authors have reported significant effects of variables such as cell culture media and serum content on responses to inflammatory stimuli in BEAS-2B cells (Zhao and Klimecki, 2015; Veranth *et al.*). Furthermore, LPS from different bacterial species has been shown to differentially impact the resulting inflammatory response (Dehus *et al.*, 2006).

These experiments were repeated to compare the effects of fMLP and CSE NMVs in the present study, however no differences seemed to be present in the response to the two vesicle types; in one experiment, no increase in CXCL8 production was observed whilst the response to LPS was similar to the other biological replicates, illustrating the variability of this NMV response. Reasons for this may include innate differences in donors, presence of subclinical illness at the time of blood donation or variation or premature activation in the isolation process. fMLP and CSE stimulation are known to have differential effects on intact neutrophils, particularly on degranulation (Guzik *et al.*, 2011; Hoenderdos *et al.*, 2016), but CSE and fMLP stimulation did not alter the total MMP-9 content of NMVs (Chapter 3, fig 3.8), although there may be other key differences in the content of these NMVs that we did not investigate. The mechanisms of NMV pro-inflammatory activation of target cells are still being uncovered and there seem to be multiple pathways that may be employed. The serine protease NE has previously been detected in fMLP-MPs (Dalli *et al.*, 2013) and is capable of inducing CXCL-8 production from airway epithelial cells (Nakamura *et al.*, 1992) and NMV-derived miRs have been consistently implicated in target cell inflammatory mechanisms; in particular, miR-155 and miR-23a from NMVs have been shown to induce activation of endothelial cells (Gomez *et al.*, 2018) and intestinal epithelium (Butin-Israeli *et al.*, 2019) respectively. Classical NF-κB activation along with MAPK and JNK/ERK signalling have been recurrently shown to be activated in other cell types (Mesri and Altieri, 1998; Mesri and Altieri, 1999) as a result of NMV exposure, and NMV miR-155 was found to downregulate expression of the transcription factor, B-cell lymphoma 6 (BCL6), resulting in increased NF-κB expression and subsequent signalling (Gomez *et al.*, 2020). Differential content of neutrophil EVs from different stimuli has previously been evidenced, particularly between EVs from activated (i.e. fMLP-stimulated) and quiescent neutrophils (Genschmer *et al.*, 2019), and it would therefore be highly interesting to further investigate the content of these NMV types to further understand any other potential differential effects and provide insight into differential roles of the

neutrophil under different conditions (e.g. quiescent vs. infection vs. oxidative stress). However, as I found no difference in the effect of CSE- and fMLP-NMVs in the responses I was studying, I focussed on NMVs derived from fMLP-stimulated neutrophils for further study.

In the future, it would be interesting and pertinent to examine the effects of NMVs from a single individual upon the inflammatory activation of different epithelial cell lines and in primary cells to understand the significance of any activation indicated here and the influence of the cell type used in these experiments. The use of the BEAS2B cell line may not accurately recapitulate the complex architecture and environment of the respiratory epithelium *in vivo* and the use of air-liquid interface cultures using primary cells may be more representative of the gas-exchange surface, however I was studying the inflammatory airway not the alveolar interface. Due to the limited magnitude of effects observed here, induction of inflammatory cytokine expression in the airway epithelium may not be the most significant functional effect of NMVs in the lung environment. Furthermore, understanding the physiological relevance of these potential effects in the lung *in vivo* instead of in a monoculture here was our ultimate goal, and we later explored these effects using a murine model (chapter 5). Furthermore, anti-inflammatory effects of NMVs have also been demonstrated in other chronic inflammatory contexts such as arthritis (Dalli *et al.*, 2008; Headland *et al.*, 2015) via annexin A1 expression in NMVs. This protein has been found to resolve lung inflammation and is also a target for corticosteroids commonly used in the treatment of lung conditions (Perretti and D'Acquisto, 2009), particularly upregulated in alveolar macrophages (De Caterina *et al.*, 1993). The potential role of this NMV effect was not deliberately investigated here; although an anti-inflammatory response was not detected, future work on whether the inflammatory context may modulate these responses would be warranted and of interest.

4.4.3 NMVs affected airway epithelial monolayer permeability

NMVs were previously shown here and in the literature to contain active proteases, particularly MMP-9 (see Chapter 3, fig 3.7). MMP-9 activity has been linked to increases in epithelial permeability and expression of key junctional proteins (Vermeer *et al.*, 2009; Butin-Israeli *et al.*, 2016a). We therefore hypothesised that NMVs would increase bronchial epithelial permeability in a similar manner. As expected, after 24h incubation with NMVs, BEAS-2B monolayer permeability was increased (fig 4.5 (B)), as demonstrated by increased diffusion of the fluorescent molecule FITC-dextran, through the cell layer in a transwell system. This was associated with decreased expression of the junctional protein ZO-1 (fig 4.5 (F)). Butin-Israeli et al. (2016) previously showed that intestinal epithelial permeability could be regulated by NMV-associated MMP-9, an effect which was inhibited by a specific inhibitor (MMP-9 inhibitor II) and pan-MMP inhibitor (GM6001). These authors demonstrated that the junctional protein desmoglein-2 (Dsg-2) was affected, although this protein is

only weakly expressed by non-polarised epithelial cell lines (Wang *et al.*, 2011), and we therefore did not investigate this particular JP here. We did attempt to detect the key airway epithelial JP E-cadherin in these experiments, but we were unable to do so due to technical problems with the antibody used and detection method (immunofluorescence). Dysregulation of ZO-1 visualised as patchy loss of expression and redistribution by immunofluorescence staining has previously been shown following the addition of recombinant MMP-9 to air–liquid interface-cultured airway epithelia at concentrations approximately 10-fold higher than that determined in the present work in NMVs (Vermeer *et al.*, 2009). NMV co-incubation as described herein modulated total levels of ZO-1, with a comparable decrease detected at 24 h. Because of the patchy distribution of ZO-1 in monolayer culture I did not further assess the distribution of ZO-1 staining in response to NMVs due to the potential for error and bias in such measurements.

Interestingly, in the present study, cell monolayer permeability seemed to be reduced relative to control levels after the shorter incubation time of 4h in these experiments, whilst expression of ZO-1 was not affected at this time point, although in the image shown in fig 4.5 (E), there was already some indication of potential degradation products underneath the intact ZO-1 band. A cell tightening response has been shown previously in airway epithelial cell upon treatment with glucocorticoids via a mechanism dependent on claudin-8-mediated recruitment of occludin to TJs (Kielgast *et al.*, 2016). This treatment has therefore been suggested as beneficial in lung diseases associated with increased lung permeability; of note the corticosteroid dexamethasone has been reported to reduce lung injury and mortality in the setting of severe SARS CoV2 infection (Johnson and Vinetz, 2020). A short term increase in the gene expression of TJ proteins including ZO-1 has been noted in other epithelial cell types; for example induced by LPS from *Porphyromonas gingivalis* in oral epithelium after 2h treatment, whilst at 4h ZO-1 gene expression was significantly reduced from control levels (Guo *et al.*, 2018). Although these authors did not extend their time course beyond 4h, the subsequent longer-term decrease in ZO-1 protein seen in our cells may therefore reflect transcriptional changes. LPS in our experiments did not decrease ZO-1 expression. Although direct effects of LPS on airway epithelial junctional protein expression have not been well documented, in our cell line in particular LPS did not have large effects on any of the parameters measured, and potential reasons for these surprising results are discussed in this chapter in section 4.4.2.

Airway epithelial cell treatment with NETs has also been shown to strengthen the epithelial barrier and reduce permeability, increasing ZO-1, -2, and occludin protein and gene expression in these cells. Despite this tightening of this sinonasal epithelium, leukocyte transmigration was increased with NETs treatment due to upregulation of ICAM-1 expression (Hwang *et al.*, 2019). However, as

noted above we found that NMVs did not significantly change the expression of this adhesion molecule in our cells at either 4 or 24h (fig 4.3 (A) and (B)). Although there were limitations to this approach in requiring the use of gentle trypsination to detach cells for analysis, LPS-induced increases in ICAM-1 expression were identified, therefore any major changes in surface expression should be detectable. In contrast to Hwang et al., more transient effects of NETs on A549 alveolar epithelial cells were noted by another group, who showed that whilst permeability was reduced 6h after NET-treatment, this was significantly increased at longer timepoints (Saffarzadeh *et al.*, 2011). Whilst these authors both used Phorbol 12-myristate 13-acetate (PMA), a non-physiological but common stimulus for NET induction, one reason for the differences shown in these two publications may be the use of a cell line (A549) in submerged culture by Saffarzadeh et al. (2011) whilst Hwang et al. (2019) utilised primary sinus epithelial cells cultured at air–liquid interface, highlighting crucially how differences in *in vitro* models can potentially affect experimental results.

In contrast to findings in this thesis, published data from our lab by Ajikumar et al. (2019) showed that fMLP NMV incubation with endothelial cells began to increase permeability after just 1h, and that the TEER of these cells was significantly decreased at 3 h, whilst further work in our lab showed that ICAM-1 expression was indeed increased by NMVs (Gomez *et al.*, 2020), highlighting again the importance of cell type and potential specificity of NMV activity depending on the target cell.

Whilst protease content of NMVs, particularly MMP-9, NE and cathepsin G, as well as MPO, is attractive as an explanation for their effect on epithelial permeability, fMLP NMV proteomic analysis has previously shown that these vesicles contain other proteins potentially associated with increasing permeability. NMVs contain the antimicrobial proteins S100A8 and S100A9, and their complex Calprotectin, which are also known to act as Danger-Associated Molecular Patterns (DAMPs), are associated with ZO-1 disassembly and both epithelial and endothelial permeability. In fact, these proteins are recognised by TLR4 in airway epithelial cells, providing a potential link between the similar activating effects of LPS and NMVs in our previous experiments (Wang *et al.*, 2014; Dalli *et al.*, 2013; Chakraborty *et al.*, 2017). Furthermore, S100A8 was shown by Chakraborty et al. (2017) to be essential for neutrophil recruitment to the lungs using an *in vivo* model of ALI. Whilst Tardif et al. (2015) found that a relatively small proportion of these proteins was packaged into NMVs compared with that secreted freely by neutrophils (Tardif *et al.*, 2015), they only investigated NMVs generated from stimulation with monosodium urate crystals, and therefore it would be interesting to determine whether this remains the case for other inflammatory stimuli.

It would be highly interesting to carry out a time course with more time-points to understand the kinetics of this response. Physiologically, a short-term tightening of the epithelial barrier in response

to NMVs and inflammation may be beneficial to prevent infection with invading pathogens, whilst longer term exposure may result in impaired barrier integrity, and Vermeer et al. (2009) showed that MMP-9-induced permeability resulted in greater penetration of viruses into the basal layer of the airway epithelium. It may be hypothesised that excess NMVs not internalised by the epithelium should be eventually cleared by, for example, alveolar macrophages and migrated neutrophils, however in the absence of this response they may increase epithelial permeability and contribute to disease mechanisms. Alternatively, increased permeability at this later time-point may facilitate entry of neutrophils to neutralise any remaining pathogens.

Loss of ZO-1 and increased epithelial permeability is also associated with epithelial-to-mesenchymal transition (EMT). MMP-9 has been shown in some cell types to be required for TGF-β-induced EMT, and MMP-9 activation in airway epithelial cells is critical for CSE-induced EMT (Agraval and Yadav, 2019), furthermore, rhMMP-9 treatment alone can promote EMT (Bai *et al.*, 2017). MiR-155, highly expressed in NMVs, has also been shown to promote EMT via STAT3 signalling. We attempted to investigate this in these cells, however, we were unable to detect a change in EMT markers such as N-cadherin and Snail using the positive control TNF-α (data not shown) and did not continue this investigation due to time constraints. However, it would be highly relevant to determine whether NMV addition may augment CSE-induced EMT, to help further understand the role of NMVs in COPD pathogenesis.

4.4.4 The impact of NMVs on epithelial cell apoptosis and proliferation

Since a significant effect on permeability was found, the potential mechanism and functional consequences of this was further investigated. MMP-9 can induce a specific type of detachment-associated apoptosis called anoikis, which may contribute to compromised epithelial barrier function and is associated with dysregulated ZO-1 expression. Apoptosis was investigated by detection of active caspase-3 and -7 as early actors in programmed cell death, and although not statistically significant, a trend to increased apoptosis was identified (fig 4.6 (A), (B) and (C)). Surprisingly, addition of the endogenous MMP inhibitor TIMP-1 at similar concentrations to that shown in Chapter 3 to reduce the protease activity of fMLP NMVs, did not inhibit apoptosis/anoikis; in fact, the only condition to show a statistically significant increase in cell detachment was the combined TIMP-1 and NMV treatment. Whilst apoptosis might therefore be a minor contributor to NMV-induced increases in epithelial monolayer permeability requiring further characterisation, this is likely not via an MMP-dependent mechanism. The high levels of MMP-9 shown by Vermeer et al. (2009) to change epithelial barrier integrity and induce cell detachment may explain this difference, and it would be interesting to determine whether at higher NMV concentrations, as may be present in the airways in disease settings, these proteases may have a larger role. Interestingly, phagocytosis

of apoptotic epithelial cells by both alveolar macrophages and also by other airway epithelial cells has been shown to be pro-resolving, and it would be intriguing to determine firstly whether any effects on cell apoptosis are changed by the presence of proinflammatory stimuli and also whether this mechanism actually promotes the resolution of inflammation (Juncadella et al., 2013).

ER stress and the compensatory unfolded protein response (UPR) induced by stimuli such as TLR4 activation, increased protein production and oxidative stress, is also capable of causing airway epithelial cell apoptosis and inflammatory responses. These processes have been shown to be involved in COPD (Chung and Adcock, 2008) and can be induced by, for example, cigarette smoke exposure (Kenche et al., 2013; van Rijt et al., 2012). The highly-conserved ER chaperone GRP78, also called the immunoglobulin heavy chain-binding protein or BiP, has several roles including translocating peptides across the ER membrane, tagging misfolded proteins for degradation and sensing ER stress (Wang et al., 2009; Hendershot, 2004). GRP78 is increased in response to several UPR-associated response and is therefore used as a marker of this process (Lee, 2005). We found no effect of NMVs on GRP78 expression after 24h, whilst the positive control tunicamycin induced a significant increase in ER stress. Whilst GRP78 may be transiently induced, the ongoing functional effects of NMVs in association with the lack of increase make it unlikely that ER stress was contributing to the impact of NMVs on monolayer integrity or chemokine release.

Intriguingly, active caspases have also been shown to directly affect junctional protein expression, including the tight junction protein ZO-1 (Bojarski et al., 2004) and epithelial apoptosis is linked with impaired barrier integrity (Bojarski et al., 2001). Establishing whether caspase inhibition (e.g. using Z-DEVD-FMK) abrogated NMV effects on ZO-1 levels would be a simple experiment able to delineate any link between these two events demonstrated here. Furthermore, similar effects of caspase-dependent apoptosis and junctional protein degradation could be induced by TNF-α treatment (Bojarski et al., 2004), which would have been a highly relevant stimulus to include in the present study or further work, and this would allow distinction of the bands shown in figure 4.5 (E) (marker by arrows) underneath whole ZO-1 as either potential NMV proteins or as degradation products of ZO-1. These experiments were not undertaken due to time constraints but may be pursued by future members of the laboratory.

Finally, to determine whether epithelial permeability may be increased by inhibition of cell proliferation and potentially induction of cellular senescence, and as NMVs have been shown to affect intestinal epithelial cell wound healing, proliferation responses were investigated in BEAS-2B cells. Interestingly, proliferation was actually increased by 24h treatment with NMV, with an approximate increase in proliferation of 10%; this effect was further exaggerated at 48h, with

around 15% increase from control levels. Whilst this finding was unexpected in the context of increased permeability, similar effects of neutrophil-derived exosomes from LPS-stimulated cells have been documented in equine airway smooth muscle cells by Vargas et al. (2016); only exosomes from stimulated cells displayed this modulatory property, whilst those from unstimulated neutrophils did not. Although these authors did not examine the mechanism of this effect, they did identify several differentially expressed proteins in these exosomes compared with those from unstimulated cells which were associated with pathways including extrinsic apoptotic signalling (e.g. S100A9 and annexin A7) and ECM remodelling (e.g. Tenascin-X and Thrombospondin-1). It would be interesting to compare the effects of fMLP NMVs and those from unstimulated neutrophils, since published data has shown differential NMV and neutrophil exosome content (Dalli *et al.*, 2013; Genschmer *et al.*, 2019) depending on the generating stimulus. However, the numbers of NMVs that can be obtained from unstimulated neutrophils may limit the experimental repertoire that can be explored.

Effects on dysregulated proliferation in COPD have been associated with Wnt signalling, which also induces mitogen-activated protein kinase (MAPK) signalling (Guo *et al.*, 2016). A number of Wnt proteins are expressed on the surface of exosomes derived from several cells lines and may be transported between cells via this route (Gross *et al.*, 2012), and Wnt ligands have been demonstrated to have immunosuppressive effects (Ding *et al.*, 2008). Wnt/β-catenin signalling has been shown to have an important role in the repair response after lung injury (Cai *et al.*, 2015) and in particular can stimulate epithelial proliferation (Volckaert *et al.*, 2013). We speculate that the effect of NMVs on proliferation may be part of a repair response after NMV-induced injury, as shown by effects on permeability and cell loss. Murine models have demonstrated increased levels of airway epithelial cell proliferation after lung injury as part of a reparative response promoted by other immune cells including alveolar macrophages (Hung *et al.*, 2019) and T-cells (Mock *et al.*, 2014), it would be highly interesting to determine if similar mechanisms may be employed by NMVs and to explore the relevance of the complex Wnt pathway in this setting.

Butin-Israeli et al. (2019) showed that neutrophil extracellular vesicles (inclusive of both exosomes and MVs) induced intestinal epithelial apoptosis by delivering miR-23a and -155; these microRNAs induced double strand DNA breaks via both replication fork arrest and collapse and also by arresting homologous recombination. These effects led to genomic instability and prolonged cell injury. Accumulation of double-strand breaks eventually results in cell apoptosis. Moreover, these effects were observed at 24h of EV co-incubation. Since proliferation was increased in BEAS-2B cells at 24-48 h, this mechanism seems less likely in the current setting, and it is uncertain which vesicle type may be the main contributor to this effect observed by Butin-Israeli et al. since they did not separate

MVs from exosomes in their study. Nevertheless, work from our lab has previously demonstrated the expression and activity of miR-155 in fMLP NMVs in the context of atherosclerosis (Gomez *et al.*, 2020). It would therefore be highly relevant to further investigate these effects in airway epithelium, and indeed miR content may be as or even more important than protein content, and EVs are increasingly recognised as a mechanism to protect and deliver small RNAs. Furthermore, several studies have shown differential miR content in the lavage fluid of patients with inflammatory lung diseases including asthma (Levänen *et al.*, 2013), COPD (Conickx *et al.*, 2017) and idiopathic pulmonary fibrosis (Liu *et al.*, 2018). This work was beyond the scope of my PhD but would be interesting to pursue in future studies.

4.5 Conclusions

In our study, we found that NMVs conclusively interacted with bronchial epithelial cells, likely employing endocytic mechanisms of internalisation. Our hypothesis was that NMVs would induce epithelial activation and compromise epithelial barrier integrity, as shown in other cell types previously. Whilst effects on inflammation *in vitro* seemed to be moderate, significant effects on epithelial monolayer permeability were demonstrated, and epithelial apoptosis also seemed to be increased albeit significance was not reached for this particular effect. We subsequently postulated that these effects were dependent on NMV metalloprotease activity, however, this did not seem to be the case in our experiments, and apoptosis could not be reduced using an endogenous MMP inhibitor. Finally, we found unexpectedly that epithelial proliferation was increased by NMV co-incubation and propose that this effect may be part of a pro-resolving mechanism in response to cell injury by NMVs. See figure 4.9 for a summary of findings in this chapter.

Impaired epithelial barrier integrity and a trend to increased cell death found here after NMV treatment suggests that NMVs may facilitate neutrophil migration into the lung during inflammation, once initiated. This effect of NMV—epithelial cell interaction has been demonstrated in the gut *in vivo* in both animal models and in humans (Butin-Israeli *et al.*, 2016a; Butin-Israeli *et al.*, 2019) and will be further investigated *in vivo* in Chapter 5.
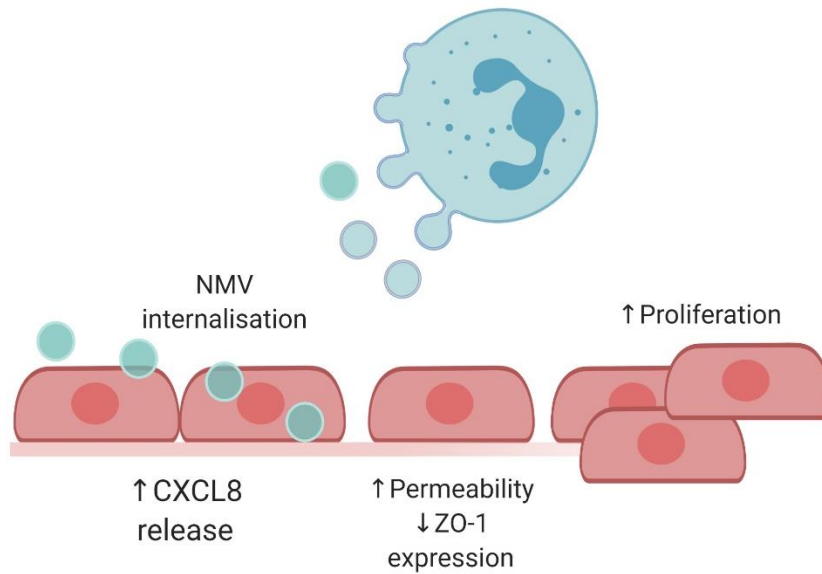
Figure 4.9 Summary of the findings presented in Chapter 4

Neutrophil-derived microvesicles (NMVs) generated by fMLP-stimulated peripheral blood neutrophils from healthy participants were internalised by BEAS-2B bronchial epithelial cells when investigated after 2h co-incubation. After 24 h significantly increased monolayer permeability and decreased expression of the junctional protein Zonula occludens-1 (ZO-1) was observed, as well as increased epithelial CXCL8 secretion, and increased proliferation at 24 and 48h post NMV addition. fMLP: N-formyl-met-leu-phe.

Chapter 5: Neutrophil-derived microvesicles in the lung *in vivo*

5.1 Introduction

In both acute and chronic lung inflammation, neutrophils have been shown to be profoundly important in host antimicrobial defence, but also act as drivers of host tissue damage, hence they are often referred to as a "double-edge sword". Murine models of lung inflammation have complemented research into human pathologies, enabling genetic manipulation to interrogate the function of specific proteins, allowing detailed tracking of neutrophils and their behaviour, and they have been particularly useful in understanding the kinetics of neutrophil responses in the lung (MacNee, 1990; Summers *et al.*, 2010a; Stackowicz *et al.*, 2019).

After an inflammatory insult such as lipopolysaccharide (LPS) administration, neutrophils are detectable in the lungs at timepoints as early as 4 h in some cases (Reutershan *et al.*, 2005; Rydell-Tormanen *et al.*, 2006). As well as their antimicrobial response, e.g. reactive oxygen species, degranulation, and extracellular trap release, both *in vitro* and *in vivo* studies have shown that the interactions between neutrophils and other immune cells and also the lung epithelium and endothelium involve complex and not yet fully uncovered signalling pathways and mechanisms of regulation. Neutrophil-depletion studies have shown conflicting results, with outcomes likely dependent on the precise inflammatory stimulus utilised; for example in the absence of neutrophils, LPS-induced inflammation and damage was reduced (Rittirsch *et al.*, 2008; Abraham *et al.*, 2000), whilst others have shown that neutrophil depletion enhances lung inflammation and damage and prolonged time to resolution in influenza infection (Tate *et al.*, 2009). Conversely, monocyte-depletion studies showed that neutrophil influx was reduced upon LPS exposure whilst compartmental oblation of lung macrophages did not significantly affect neutrophil numbers or lung inflammation (Dhaliwal *et al.*, 2012); other authors have shown depletion of alveolar macrophages (AMs) increased neutrophil recruitment (Beck-Schimmer *et al.*, 2005). These findings highlight an important interplay between immune cells in the lung as well as the key role for the micro-environment in which these interactions occur.

Extracellular vesicle (EV) release has been increasingly recognised as an important mechanism of cell–cell interaction and communication. *In vivo studies* by our lab recently demonstrated that NMVs in particular interact with murine vasculature and contribute to the complex process of atherosclerotic plaque formation by increasing monocyte recruitment and adhesion to the vessel wall (Gomez *et al.*, 2020). Presence of NMVs has also been demonstrated in various human

pathologies including COPD (Barnes *et al.*, 2019; Lacedonia *et al.*, 2016), ARDS (Guervilly *et al.*, 2011) and pneumonia (Lashin *et al.*, 2018), as well as in the murine lung after a single dose of LPS (Soni *et al.*, 2016). NMV interaction with the epithelium has also been demonstrated in comprehensive work by the Sumagin group in the intestine (Butin-Israeli *et al.*, 2016a; Slater *et al.*, 2017; Butin-Israeli *et al.*, 2019), where both protease activity and microRNA delivery were key effectors. Murine intratracheal administration of neutrophil exosomes from both healthy donor peripheral blood neutrophils and from COPD patient bronchoalveolar lavage fluid (BALF) has recently been shown to induce significant changes in lung pathophysiology, mostly via their protease activity (Genschmer *et al.*, 2019).

The *in vitro* work presented in this thesis has confirmed that NMVs contain active proteases, can be internalised by bronchial epithelial cells and could have a functional impact on cell permeability. However, these experiments were limited in their physiological implications since they were conducted using a cell monoculture and cell line, and the diverse cell–cell and cell matrix interactions possible in the lung might alter these outcomes. Therefore, to understand the relevance of these effects *in vivo* and further investigate the role of NMVs in lung inflammation, two animal studies were carried out to understand the functional impact of NMVs in the lung as well as the kinetics and localisation of their interactions.

5.2 Aims and Hypothesis

We hypothesised that, as in our *in vitro* study, NMVs would be internalised by the lung epithelium, and affect the permeability, viability, and integrity of the lung tissue. Furthermore, we hypothesised that via these pathways, NMV administration would augment LPS-induced inflammation, increasing neutrophil recruitment to the lung.

Aim 1: To determine whether NMVs administered intranasally have a functional impact on lung inflammation *in vivo* by measuring the secretion of key chemokines both systemically (in plasma) and locally (in lavage fluid) and by analysing immune cell influx to the lungs, with and without administration of a pro-inflammatory stimulus (LPS).

Aim 2: To further understand any functional effects of NMVs by investigating the interactions of NMV with lung cells, particularly the epithelium and AMs, using precision-cut lung slices (PCLS) to determine NMV localisation.

5.3 Results

5.3.1 Pilot study: intranasal neutrophil-derived microvesicle administration did not elicit an inflammatory response over 24h

In previous *in vitro* investigations (as described in chapter 4), as well as in the literature *in vivo*, NMVs have been shown to have a damaging effect on intestinal epithelial cells and to be increased in numbers by inflammatory stimuli in the lung (Butin-Israeli *et al.*, 2016a; Soni *et al.*, 2016). We therefore investigated the potential effect of NMVs instilled in the lung on the pulmonary and systemic inflammatory response *in vivo*. In a pilot study we first investigated whether NMV presence alone was capable of eliciting an immune response. For this, mice were administered 5×10^5 NMVs intranasally in 50 µl of phosphate-buffered saline (PBS), and a time course was carried out to determine a relevant timepoint for further investigations (chapter 2: section 2.2.22). Two mice per timepoint were used initially and mice were culled at T=0, and at 4, 8 and 24h post-NMV administration. Subsequently, as indicators of inflammation, one of the major chemoattractants involved in neutrophil recruitment during inflammation, CXCL-1 (i.e. KC, murine CXCL8 homologue), as well as a key chemokine in monocyte and macrophage recruitment, JE (i.e. murine CCL2/MCP-1), were measured in BALF and plasma at the protein level by ELISA, and total protein and cell counts were also quantified in BALF using bicinchoninic acid (BCA) assay and haemocytometer analysis, respectively.

JE (fig 5.1 (A) and (B)) and CXCL-1 (fig 5.1 (C) and (D)) levels in both the BALF and plasma were not consistently altered by NMV administration at any of the timepoints. Although there was variability between samples for each timepoint, including at T=0, levels of these proteins were overall low, particularly in the BALF, where the CXCL-1 concentration ranged 0–108 pg/ml across the samples and JE ranged 0–11 pg/ml. As a comparator, intratracheal LPS administration can induce BALF CXCL-1 levels of 1500 pg/ml after 24h in C57BL/6 mice (Verjans *et al.*, 2018), whilst 4 weeks of cigarette smoke exposure in this mouse strain induced increases up to just 40 pg/ml for BALF CXCL-1 and ~15 pg/ml for JE/CCL2 (Vernooy *et al.*, 2010). Since baseline levels here were slightly higher than those found in the smoke-exposure model, it was considered that no subsequent effects were observed here and these higher levels may be due to, for example, differences in mice or BALF technique.

Although BALF levels of CXCL-1 did not seem to change (fig 5.1 (C)), some of the mice did have higher plasma levels of this chemokine (fig 5.1 (D)) after NMV administration. In general, plasma levels of both chemokines were higher in the circulation (fig 5.1 (B) and (D)) than in the lung ((A) and (C)) at most timepoints, likely due to dilution of airway secretions by the process of lavage with PBS compared with undiluted plasma analysed for systemic levels.
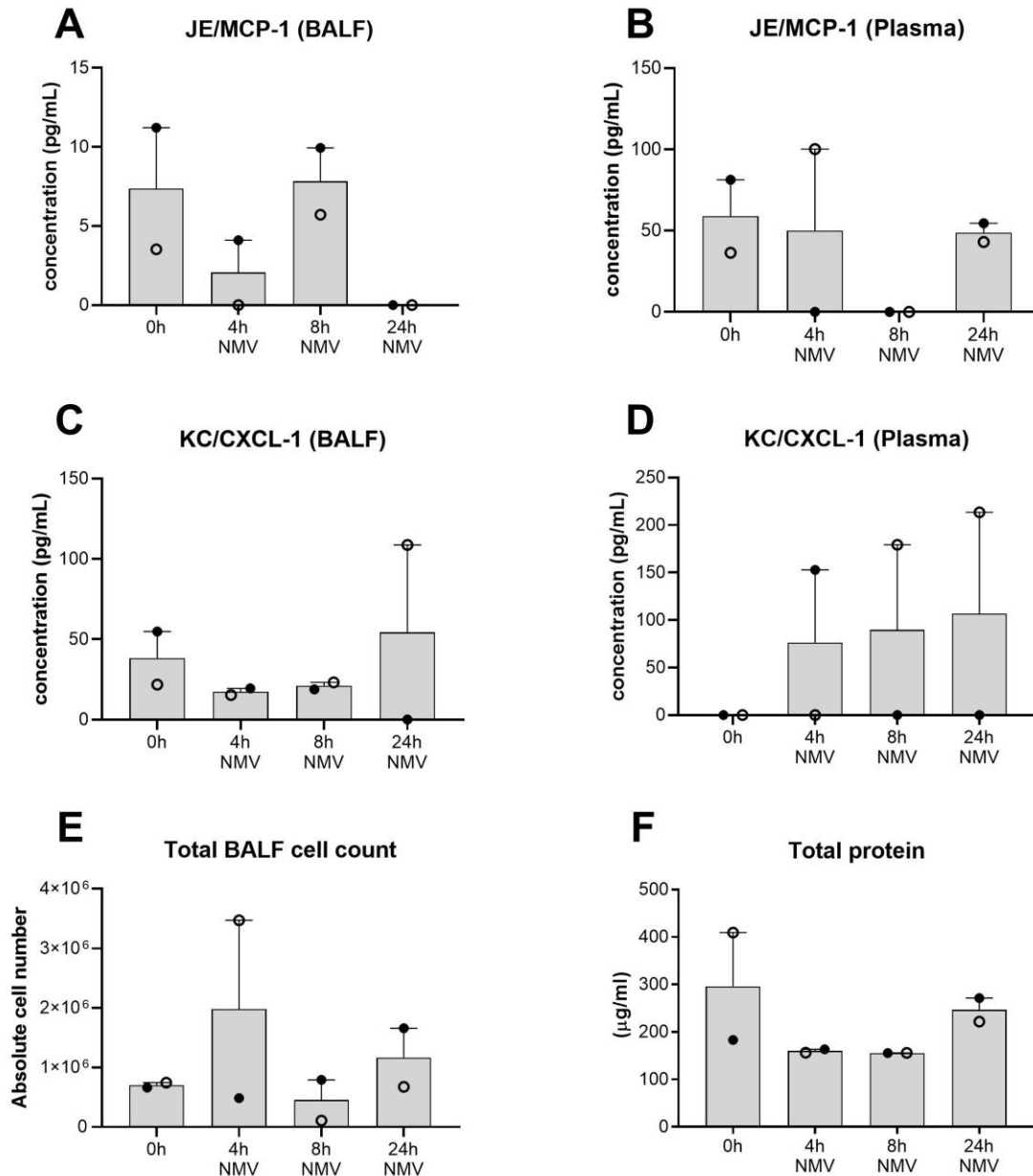
Figure 5.1 Pilot study: Effect of intranasal neutrophil-derived microvesicle (NMV) administration in C57BL/6 mice over 24h

Mice (n=2 per timepoint, 8 mice in total) were intranasally administered 5×10^5 human NMVs pooled from multiple donors (in an attempt to reduce variability between mice and human participants) in 50 µl of PBS. After 0, 4, 8, and 24 h mice were euthanised and bronchoalveolar lavage fluid (BALF) and blood samples were collected. JE/MCP-1 and CXCL-1/KC were measured in BALF (A and C) and plasma (B and D) using ELISA. BALF cell count was performed using a haemocytometer, and total protein in BALF was determined by bicinchoninic acid (BCA) assay. Data shows mean±SEM

No statistical analyses were performed due to small group size. Data represents mean+SEM. Open or closed symbols represent individual mice at each time point.

The concentration of BALF JE was also variable at each timepoint and between different mice (fig 5.1 (A)), but this is likely due to very small differences which seem to be amplified here due to the generally low levels of this protein. Corresponding data for individual mice across the graphs for each measurement in figure 5.1 are shown by open are closed circles, to allow visualisation of each of these levels in the same mice. Although some mice tended to have higher levels of both cytokines, e.g. at T=0 for both BALF CXCL-1 and JE, in general no trend was observed, indicating that there was no effect of NMV treatment consistently observed and differences were not due to different efficiencies of NMV administration.

Total cell count was similar across the time course, with the exception of one sample at T=4h (fig 5.1 (E)). Contrastingly, this particular mouse had low levels of JE and CXCL1 in the BALF (open circle at 4h, fig 5.1 (A) and (C)). Statistical analyses were not performed on this data due to the low sample size per group (n=2). Additionally, total protein measured in the BALF was unchanged by NMV administration (Fig 5.1 (F)), and although again there was some variation between timepoints.

5.3.2 Intranasal neutrophil-derived microvesicle administration did not augment LPS-induced lung inflammation

In our pilot study, although the numbers of mice used were limited, NMVs alone at the concentration administered (5×10^5) did not consistently affect any of the inflammatory markers we measured. We therefore hypothesised that NMVs alone may not elicit an inflammatory response in the lung, but these vesicles may instead play a role in augmenting existing inflammation once initiated. To investigate this, we intranasally administered LPS (5 µg) in 50 µL PBS, or vehicle, to mice and after 16h (overnight), we administered a higher NMV concentration

 (1×10^6) using the same methodology. At the same time point, as an additional control, the NMV supernatant which remained after washing NMVs was administered to some mice instead of NMVs to determine any effects of residual neutrophil proteins. Three treatment groups were therefore studied (vehicle + NMVs, LPS + NMV supernatant (s/n), and LPS + NMV), with 4–6 mice per group. 4h after NMV instillation (20h total after start of the experiment), mice were culled and the same inflammatory markers as those in the pilot study were examined in BALF and plasma samples.

Whilst higher JE concentrations were detected in BALF after LPS administration (fig 5.2 (A)), both with (646.8±74.46 pg/ml) and without (572.2±146.3 pg/ml) NMV addition, compared with mice treated with vehicle + NMVs (27.9±3.3 pg/ml), NMV treatment had no additive effect on these elevated levels induced by LPS administration (LPS + NMV vs. LPS + s/n: p = 0.94).
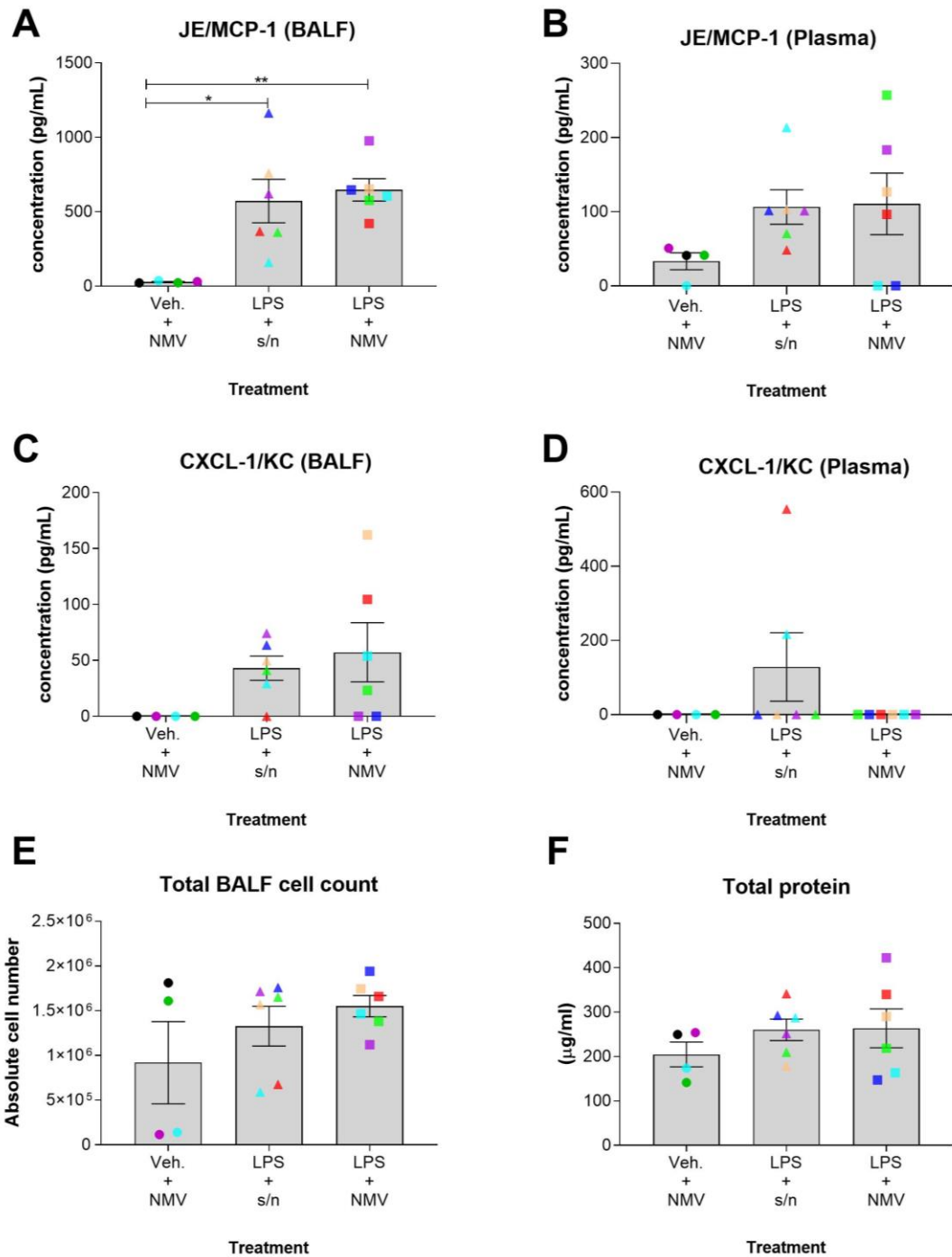
Figure 5.2 Inflammatory markers measured in BALF and plasma samples from mice after intranasal LPS and/or NMV instillation

Mice were initially administered LPS (lipopolysaccharide; 5 µg) or vehicle (veh.; 50 µL PBS), and after 16 h, were additionally given 1x10⁶ pooled, human neutrophil-derived microvesicles (NMVs) or NMV supernatant (s/n) which remained after the NMV washing step. 4h later, mice were euthanised, and bronchoalveolar lavage fluid (BALF) and blood samples were collected. JE/MCP-1 and CXCL-1/KC were measured in BALF (A and C) and plasma (B and D) using ELISA. BALF cell count was performed using a haemocytometer and trypan blue exclusion by microscopy, and total protein in BALF was determined by bicinchoninic acid (BCA) assay. Data shows mean±SEM. n = 4-6 mice per group. One-way ANOVA was used with multiple comparisons (Tukey's test). * p < 0.05 ** p < 0.01. Colours indicate individual mice. The same colour is used for the same mouse in each group across all measurements/graphs in this figure.

JE protein levels in the plasma (fig 5.2 (B)) tended to be higher in LPS-treated mice both with and without NMV addition (110.6±41.5 and 106.4±23.23 vs. 33.3±11.3 pg/ml), although no differences were observed between the LPS-treated groups, and no statistically significant differences were detected between any of these groups (p = 0.26 control v. LPS + NMVs; p = 0.30 control v. LPS + s/n; p = 0.99 LPS + NMV v. LPS + s/n). LPS-treated mice showed greater variability within their treatment groups than the control mice for these parameters.

CXCL-1 was undetectable in the BALF of mice treated with vehicle + NMVs; although still at low levels, this protein was detectable in four and five of the six mice in the LPS + NMV and LPS + s/n groups, with mean levels of 57.3±26.5 and 43.0±10.8 pg/ml, respectively (fig 5.2 (C)). However, these differences were not statistically significant by one-way ANOVA with multiple comparisons. With the exception of two mice in the LPS + s/n group, this cytokine was not detectible in plasma samples (fig 5.2 (D)).

BALF total cell counts tended to be increased with LPS treatment (fig 5.2 (E)), however control levels in the vehicle + NMV group were highly variable, and two of the four mice in this group demonstrated high cell numbers (vehicle + NMV: $9.2±4.6×10^5$, LPS + NMV: $15.5±1.2×10^5$, LPS + s/n: $13.3±2.2×10^5$ cells; mean±SEM), potentially due to sampling issues. There were no statistically significant differences between the groups, although the mice with LPS + NMV combined treatment demonstrated the highest cell counts and least variation (control vs. LPS + NMV group: p = 0.069).

Similarly, there were no statistically significant differences between any of the groups in total protein in the BALF (fig 5.2 (F)), although the highest values were found in the LPS-treated groups, the mean protein concentrations were similar (204.9±289.0, 260.2±24.3, and 263.6±43.7 µg/ml for the vehicle + NMV, LPS + s/n and LPS + NMV groups, respectively). In contrast to the total cell count, in this analysis the greatest variation was seen in the combined LPS+NMV-treated group.

5.3.3 LPS exposure induced changes in the lung microvesicle profile in vivo

Soni et al. (2016) showed that intratracheal LPS administration induced changes in the murine lung MV profile, particularly in immune cell-derived MV numbers. To determine if NMV administration contributed to this effect, in the same experiment described above, neutrophil (Ly6g+), macrophage (f4/80+) and epithelial (EpCAM+) -derived MVs were detected and quantified in BALF samples by flow cytometry. After removing cells by standard centrifugation, BALF was centrifuged at 20,000*g* to pellet MVs which were then labelled using fluorescently-conjugated antibodies. Counting beads were used to determine absolute MV counts. See materials and methods sections 2.2.7.3 and 2.2.22.2.

LPS instillation significantly increased levels of murine NMVs detected in the BALF (fig 5.3 (A)). Whilst some murine Ly6g+ NMVs were detected in the group receiving vehicle + NMV (157.7±9.2 MV/µl; mean±SEM), these numbers for both of the LPS groups were approximately two-fold higher (310.4±18.33, p = 0.0016 and 271.8±26.1 MV/µL, p = 0.010, with and without NMVs, respectively). However, there was no difference between the two LPS-treated groups (p = 0.513).

The numbers of macrophage-derived MVs (MMVs) were also significantly reduced in the LPS treatment group (control v. LPS + NMV p < 0.0001, control v. LPS + s/n p < 0.0001), and surprisingly demonstrated an approximately three-fold reduction in numbers compared with those in mice receiving NMVs alone (LPS + NMV: 185.0±26.45, LPS + s/n: 151.4±27.5 MV/µL; vehicle + NMV: 483.8±31.54 MV/µL; mean±SEM) (fig 5.3 (B)).

In contrast, the numbers of epithelial-derived MVs (EMVs) were unchanged by any of the treatments (fig 5.3 (C)), however, this MV type made up the largest proportion of the overall MVs measured, with mean concentrations of 1428±302.7, 1205±84.6 and 1126±179.7 MV/µl in the vehicle + NMV, LPS + NMV and LPS + s/n groups, respectively. The mean total MV concentration per µL of fluid was also similar across these groups; 3349±739.4, 3390±239.8, and 3371±347.6 MV/µL. Hence, on average EMVs accounted for approximately 37% of the total MV population, whilst murine NMVs in the LPS-treated groups constituted only 8.6% of total MVs overall, and MMVs represented 5% of total MVs on average in the LPS-treated groups and 14.4% of total MVs in the control group.

When examined in each treatment group, these percentages looked different. As shown in figure 5.4 (A), in the vehicle + NMV group, NMVs represented the smallest MV group, MMVs the second, with EMVs representing the majority. However, upon LPS treatment the proportion of NMVs increases (fig 5.4 (B) and (C)), and the proportion of MMVs is reduced. Interestingly, there were a proportion of BALF MVs which were not labelled in every group, whilst this could be due to a number of factors including labelling efficiency of each population, contamination with debris or small particles or indeed an MV type which was not labelled for here, this faction is lower in the vehicle + NMV group and consistently increased in the groups receiving LPS (fig 5.4 (B+C)). Further, since there was no differences in EMV concentrations in figure 5.4 (C), this unclassified MV population seems to be driving the reduction in the proportion of EMVs from 50.6% in the vehicle + NMV group (fig 5.4 (A)) to ~35% in both LPS-treated groups (fig 5.4 (B+C)). Although, two of the four mice in the vehicle group did have higher EMV concentrations (fig 5.3 (C)), and interestingly, the mouse with the highest number of EMVs did have the highest concentration of total MVs found in the BALF (green data points, fig 5.3 (C) and (D)).
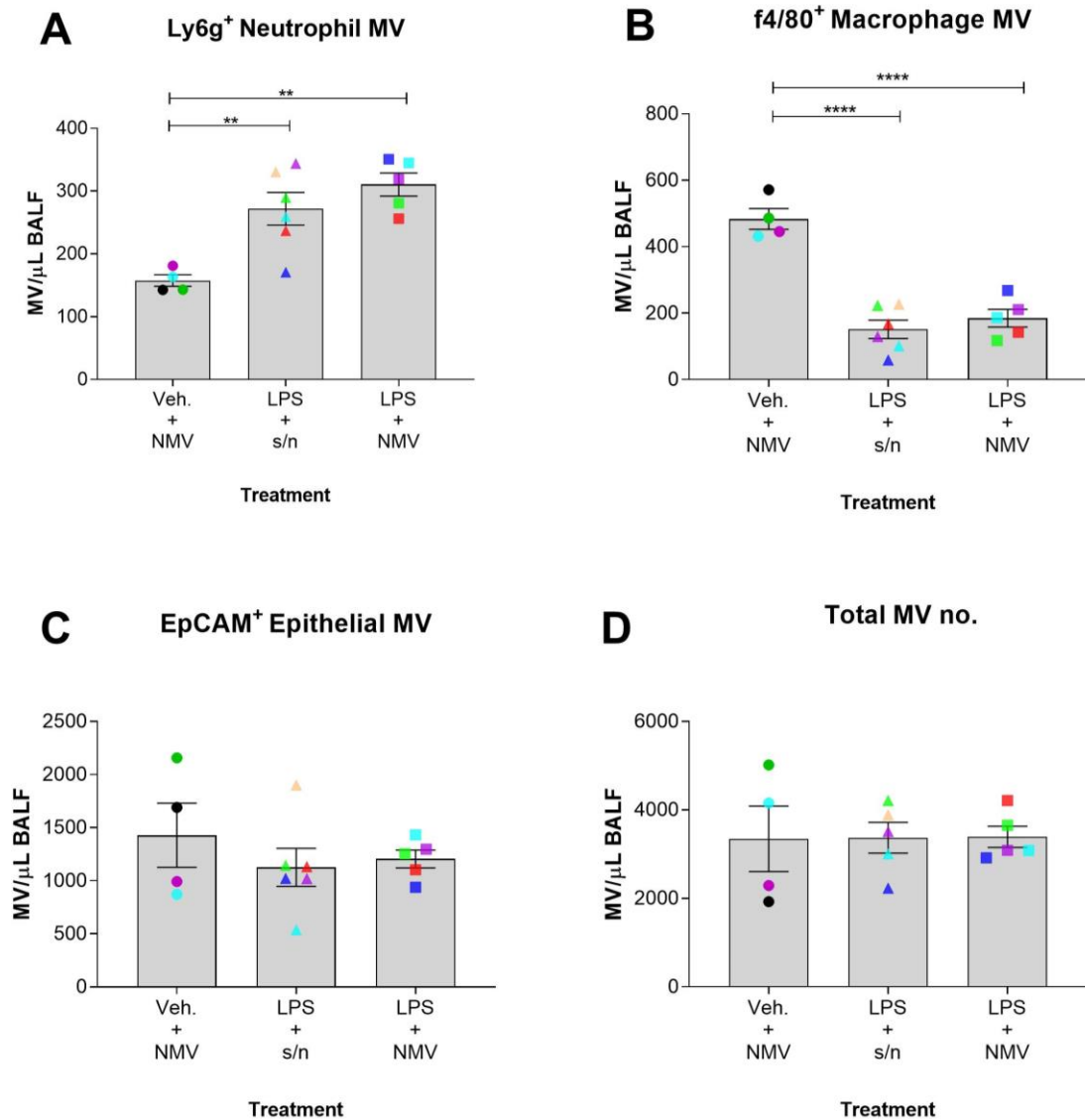
Figure 5.3 Characterisation and quantification of murine lung microvesicle (MV) content using bronchoalveolar lavage fluid (BALF)

*Mice were initially administered LPS (lipopolysaccharide; 5 μg) or vehicle (veh.; 50 μL PBS), and after 16 h, were additionally given 1x10⁶ pooled, human neutrophil-derived microvesicles (NMVs) or NMV supernatant (s/n) which remained after the NMV washing step. 4h later, mice were euthanised, and bronchoalveolar lavage fluid (BALF) samples were collected. Neutrophil (Ly6g+; A), macrophage (f4/80+; B) and epithelial (EpCAM+; C) derived MVs were labelled in the BALF using fluorescently-conjugated antibodies, pelleted by high-speed centrifugation, and analysed by flow cytometry. (D) Total MV number obtained from these analyses is shown. Megamix calibration beads were used to set flow cytometer parameters and find a region of interest within the MV size range. MVs were gated upon using a plot of FSC v SSC, and fluorescence of the MV population was then analysed using the appropriate lasers and filters. Quantification of MV concentrations was facilitated using counting beads of ~2 μm diameter, visible alongside, but distinguishable from, the MV population. One data point was removed from the LPS+s/n group here. The same colour is used for the same mouse in each group across all measurements/graphs in this figure. Data shows mean±SEM. n = 4-6 mice per group. One-way ANOVA was used with multiple comparisons (Tukey's test). ** p < 0.01 ****p < 0.0001. Colours indicate individual mice. The same colour is used for the same mouse in each group across all measurements/graphs in this figure.*
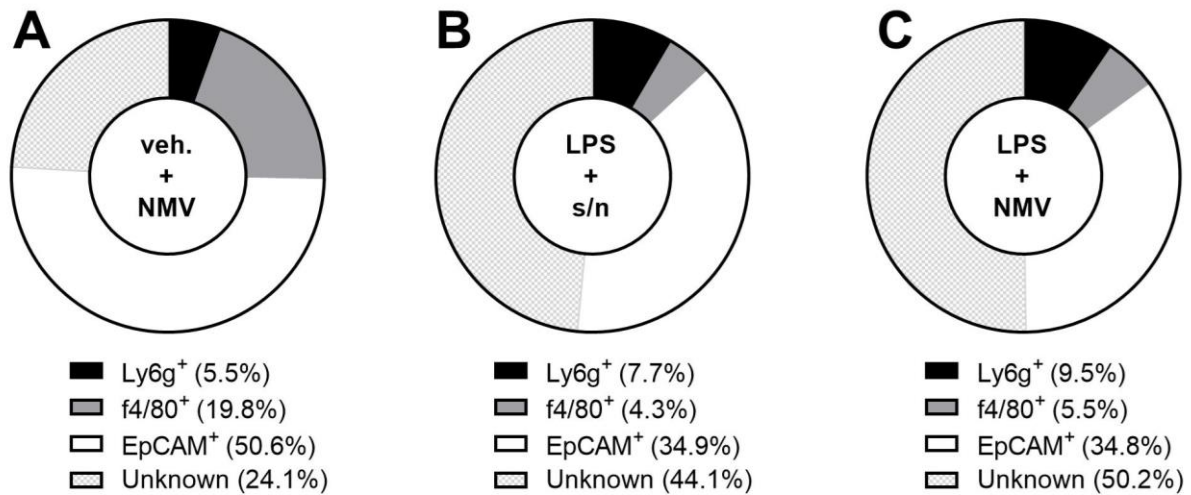
Figure 5.4 Relative proportions of murine lung microvesicle (MV) types in bronchoalveolar lavage fluid (BALF)

Mice were initially administered LPS (lipopolysaccharide; 5 µg) or vehicle (veh.; 50 µL PBS), and after 16 h, were additionally given 1x10^6 pooled, human neutrophil-derived microvesicles (NMVs) or NMV supernatant (s/n) which remained after the NMV washing step. 4h later, mice were euthanised, and bronchoalveolar lavage fluid (BALF) samples were collected. Neutrophil (Ly6g+), macrophage (f4/80+) and epithelial (EpCAM) derived MVs were labelled in the BALF using fluorescently-conjugated antibodies, pelleted by high-speed centrifugation, and analysed by flow cytometry. Total MV numbers were determined as well as numbers of positively-labelled MVs. Megamix calibration beads were used to set flow cytometer parameters and find a region of interest within the MV size range. MVs were gated upon using a plot of FSC v SSC, and fluorescence of the MV population was then analysed using the appropriate lasers and filters. Quantification of MV concentrations was facilitated using counting beads of ~2 µm diameter, visible alongside, but distinguishable from, the MV population. The number of MVs is shown here for all three treatment groups as a percentage of the total MV count. (A) veh. NMV = vehicle treatment + NMVs, (B) LPS+s/n: LPS treatment and NMV supernatant administration, (C) LPS treatment + NMV administration. n = 4-5 mice per group.

However, the average proportions of each immune cell-derived MV type did mirror changes in respective MV concentrations shown in figure 5.3, with NMVs increasing from 5.5% in the NMV control group to 7.7% and 9.5% in the LPS + s/n and LPS + NMV groups, respectively. Conversely, MMVs went from 19.8% in the first group to 4.3 and 5.5% in the latter two.

5.3.4 Neutrophil-derived microvesicles are time-dependently taken up by macrophages in the lung and in vitro

NMVs did not initiate or augment the inflammatory response *in vivo* as described above, although the present work and that of others demonstrated a significant increase in NMV presence during acute lung inflammation (Soni *et al.*, 2016). *In vitro* we showed in chapter 4 that NMVs interacted with the epithelium (4.3.1), induced CXCL-8 release (4.3.2) and impacted epithelial barrier integrity(4.3.3), which we had hypothesised would lead to enhanced neutrophil recruitment and transmigration, and an enhanced inflammatory response. Therefore, to understand the seemingly conflicting evidence from the *in vitro* and *in vivo* studies performed in the present work, we aimed to determine the fate and longer-term consequences of NMVs in the lung. For this, precision-cut lung slices (PCLS) were used to enable immediate live cell imaging of lung sections after MV addition. This previously established method was set-up here by Jacob Rudman, Department of Infection, Immunity, and Cardiovascular Disease, University of Sheffield who also validated the use of CD11c in PCLS for alveolar macrophage identification (Rudman *et al.*, 2019) and who was a collaborator for the following experiments.

In a pilot study, we initially aimed to add NMVs to PCLS *ex vivo,* limiting the numbers of NMVs and animals required for each condition. A single wild-type mouse was culled, the trachea was exposed and 2% low-gelling point agarose (pre-warmed to 37°C) was injected into the lungs (Materials and Methods, section 2.2.24). After dissecting out the lung, less than 1h later, PCLS of 300-μm thickness were cut using a vibratome and 5×10^4 PKH67-labelled NMVs were then added to a slice, in pre-warmed DMEM. Macrophages were labelled with AF647-conjugated anti-CD11c antibody and the slice was imaged using confocal microscopy after approximately 1h. Upon imaging, NMVs had not penetrated the agarose-infused tissue and could be seen suspended and moving in the media, therefore interaction with epithelial cells did not appear to have occurred (data not shown). However, as shown in figure 5.5 (A), multiple NMVs (green) were found inside a single macrophage (red) which existed at an outward-facing edge of one of the slices. This therefore strongly indicated further investigation of NMV interaction with airway cells should be further pursued.
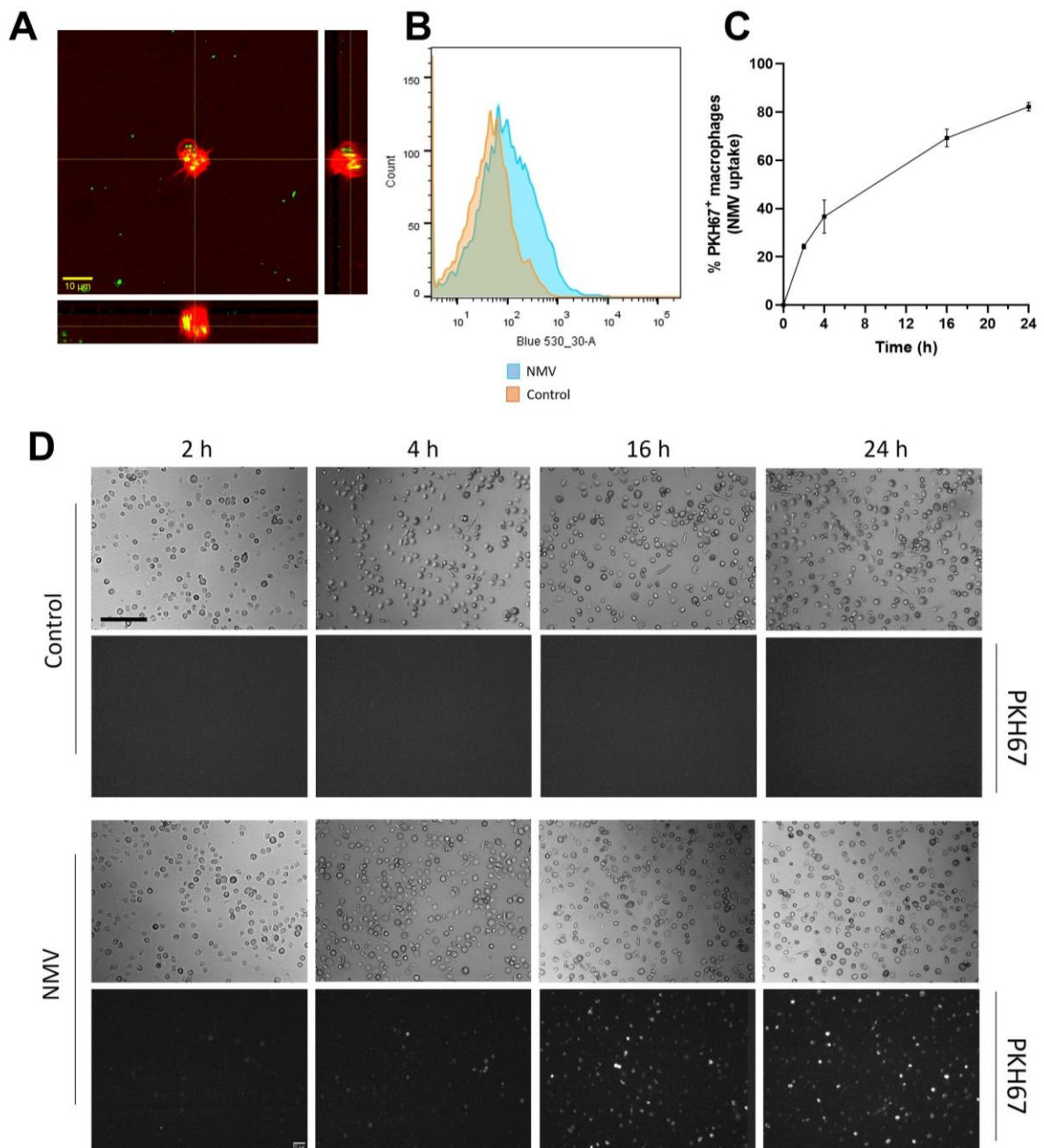
Figure 5.5 Macrophage uptake of neutrophil-derived microvesicles (NMVs) ex vivo and in vitro

(A) PKH67-labelled NMVs (green) were added to freshly prepared precision-cut murine lung slices in a pilot study, and macrophages were labelled with anti-CD11c (red). Samples were imaged by confocal microscopy, and orthogonal views are shown. (B) Monocyte-derived macrophages (MDMs) isolated from human peripheral blood were treated with PKH67-labelled NMVs for 2h and internalisation was measured using flow cytometry (blue). Untreated cells (orange) were used to determine baseline fluorescence. Extracellular fluorescence was quenched with trypan blue. Representative plot from n = 2 individual MDM donors. (C) For longer term analysis, PKH67-NMVs were added to MDMs and subsequently imaged by fluorescence microscopy after 2, 4, 16, and 24 h. Numbers of NMV-positive cells were quantified in Image J. Data shows mean±SEM. MDMs were repeatedly imaged over the time course. (D) Representative images from the same donor are shown. Scale bar represents 200 μm. Brightfield images were used to determine total cell number. N = 3 MDM donors were treated with labelled NMVs obtained from one neutrophil donor.

Results here and in Chapter 4 (fig 4.1) demonstrated in principle that lung cells (such as alveolar macrophages) can interact with NMVs. However, as the focus of the studies performed here so far was on the epithelium, further study into the potential effects of the NMV–macrophage interaction was warranted. To establish the fate of NMVs, these vesicles should remain intact to permit detection and therefore shorter time points are favourable before any potential degradation may occur, particularly in macrophages which are capable of neutrophil efferocytosis and breakdown. In order to determine the optimal short-term time point to investigate *in vivo*, labelled NMVs were added to human monocyte-derived macrophages (MDM) *in vitro* to observe the kinetics of NMV uptake in these cells. Initially, flow cytometry was used to determine NMV internalisation. MDMs (n = 2 individual donors) were treated with 1 x 10^5 PKH67-labelled NMVs from a single donor for 2h. NMV numbers here were lower than those used in previous BEAS-2B epithelial cell experiments to better model numbers that would later be used in murine experiments. Numbers chosen for PCLS experiments were roughly based on those used by Genschmer et al. (2019). The cells were detached, trypan blue was added to the suspension to quench extracellular fluorescence, and cells were immediately analysed. NMV uptake was clearly observed at this time point (fig 5.5 (B)), however, this was at a low level. To facilitate a longer time-course, fluorescence microscopy was then used to image uptake which allowed repeated imaging of live cells in a standard tissue culture plate, which could not be achieved with confocal imaging requiring much thinner material. MDMs from three individual donors were treated with 1 x 10^5 PKH67-labelled NMVs from a single donor and imaged at 2, 4, 16, and 24h (fig 5.5 (C)). A time-dependent increase in NMV uptake was observed which, by 24 h reached an average of 82% of total MDMs staining positive for NMV uptake. Representative images from this experiment are shown in figure 5.4 (D). Untreated MDMs from the same donors (D; upper panels) were used as controls and to determine any autofluorescence generated from these cells. The 4 h timepoint was chosen for further *in vivo* experiments to investigate early NMV uptake in airway and alveolar cells at a time which should allow for epithelial uptake to be investigated, previously demonstrated at 2h *in vitro* (Chapter 4, section 4.3.1) and at which internalisation in MDM could also be clearly observed, without a high risk of NMV loss due to intracellular degradation as rapid uptake in alveolar macrophages was indicated in the PCLS pilot study here (fig 5.5 (A)).

5.3.5 Rapid uptake of NMV by macrophages, but not other airway cells, was observed in the murine lung after 4 h

C57BL/6 mice (n = 3–4 per group) were administered either 3 x 10^5 NMVs or NMV supernatant (control) in a final volume of 50 µL PBS by oropharyngeal aspiration. It was suspected based on previous experiments that intranasal administration may result in loss of NMVs in the upper airways,

and in a final pilot study alternative methods of administration of oropharyngeal aspiration vs. intratracheal instillation were compared. NMVs, observed as green staining, were subsequently seen at similar levels in PCLS from each method (data not shown), and oropharyngeal aspiration was therefore chosen as the least traumatic method of administration for these animals. Mice were culled after 4 h (to track NMV location) or 7 d (to determine longer-term impact of NMVs). Mice at the shorter timepoint received PKH67-labelled NMVs whilst at the longer timepoint NMVs were unlabelled (chapter 2, section 2.2.24.3). Unlabelled NMVs were administered as it is highly likely that these vesicles would have been cleared after one week and labelling would not be useful at this timepoint. To visualise all airway cells at 4h, after obtaining PCLS as mentioned above, AF647-labelled wheat-germ agglutinin (WGA) was added to label cell membranes of all lung cells and Hoechst-33342 dye was added to stain cell nuclei.

Imaging was performed using a widefield Nikon Ti microscope and Z-stacks were taken, with 20x magnification. Whilst a small amount of background staining was observed by fluorescence microscopy in PCLS of in control samples (fig 5.6 (A); upper panel), this was diffuse and could clearly be discerned from the bright and punctate signal seen in NMV-treated mice (fig 5.6 (A); lower panel). Lung architecture could be discerned by both the nuclear and membrane stains used here, which aligned clearly in the merged 3-channel image in figure 5.6 (B). The orthogonal view shown here of the z-stack created indicated the presence labelled NMVs within the membrane stain, indicating internalisation. Clusters of labelled NMVs could be observed dispersed throughout the lung tissue (indicated by white arrows in figure 5.6A).

Confocal microscopy confirmed the presence of NMVs within cells (fig 5.6 (C)). Large numbers of NMVs were taken up by individual airway cells with rounded morphology (white arrow), whilst cells with flatter and more elongated morphology evidenced no detectable NMV uptake. Furthermore, NMVs were not found in the nucleus of positive cells.

Finally, to determine whether NMVs in the lungs entered the circulation, MVs in platelet-poor plasma from these mice were analysed by flow cytometry (fig 5.6 (E)). No fluorescent MVs were detected amongst the plasma MV population. Baseline fluorescence in this analysis was set using plasma from control (NMV supernatant-administered) mice.

Lungs from mice culled 7 days after NMV administration (and at 4 h) will be analysed by histological processing and staining at a future date via Sheffield University Medical School Histology Service, to investigate morphological changes and changes in TGF-β expression. This work is ongoing and has been delayed due to restrictions during the COVID-19 pandemic.
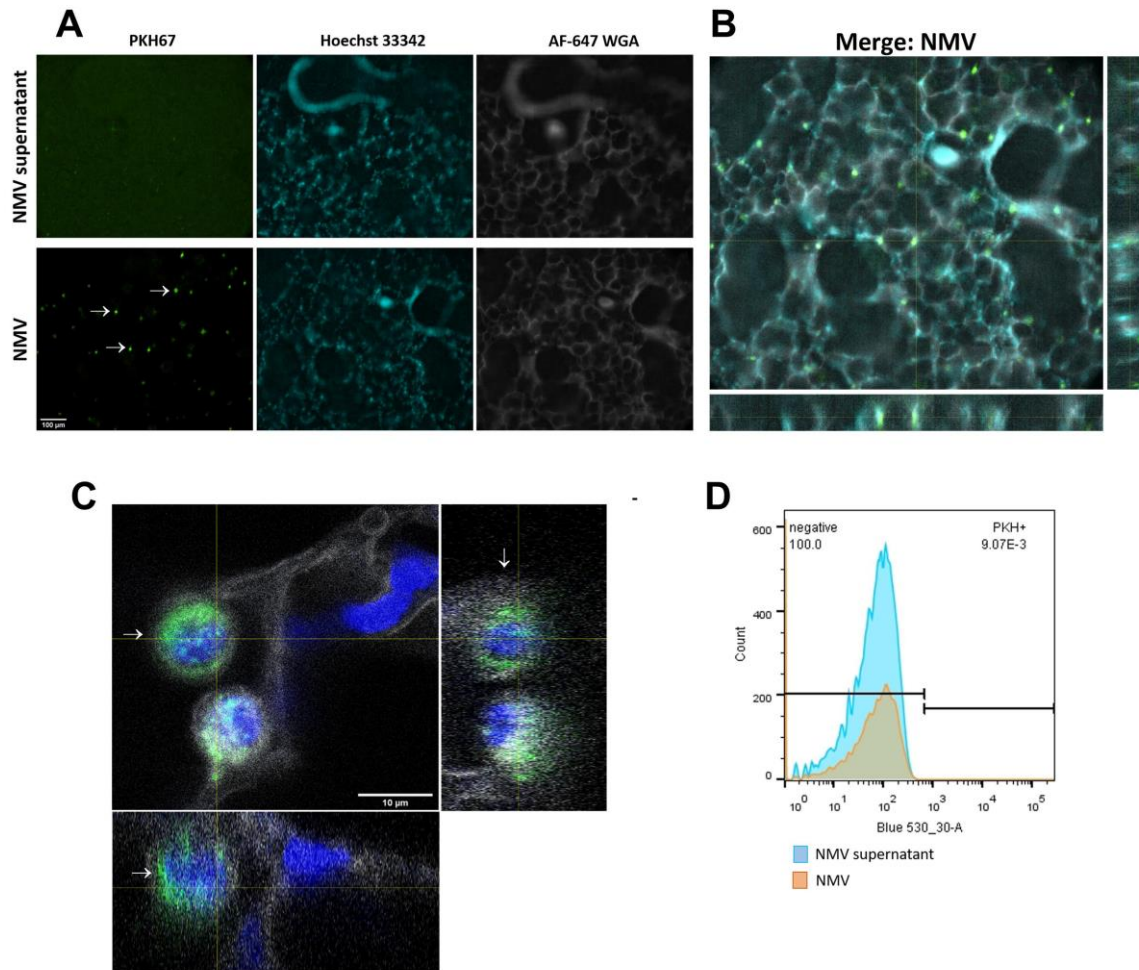
Figure 5.6 Tracking of labelled neutrophil-derived microvesicles (NMVs) in vivo

Mice were administered PKH67-labelled NMVs (green; n=3) or NMV supernatant (control; n=3) via oropharyngeal aspiration and sacrificed 4h later. Lungs were removed and filled with agarose to create precision-cut lung slices (PCLS) for live cell imaging. PCLS were stained with AF647-labelled wheat germ agglutinin (WGA; grey) and Hoechst 33342 (cyan) to visualise cell membranes and nuclei, respectively. (A) Z-stack images were taken using a Nikon widefield microscope. PCLS from control (upper panel) and NMV-treated (lower panel) mice are shown. White arrows indicate NMV clusters. Scale bar = 100 μm. Confirming NMV internalisation, an orthogonal and enlarged view of a PCLS from the NMV-treated mouse from images in (A) is shown in (B). Intersecting lines identify an NMV positive cell in each plane of view. (C) Confocal microscopy permitted visualisation of NMV uptake in further detail. NMVs are shown in green, nuclei in blue and WGA in grey. Staining was performed as described above, and an orthogonal view is shown. White arrows indicate a cell that has taken up labelled NMVs, and the same cell identified in each panel. (D) NMV presence in the circulation upon sacrifice at 4h was investigated using flow cytometry in plasma samples from NMV-treated mice. MVs were detected as described here previously, using a combination of flow cytometer calibration with Megamix beads and 2-μm counting beads to determine MV numbers. No PKH67-labelled MVs (using the 488 nm laser with 530/30 filter) were detected in these samples. All images and plots are representative of n = 3 mice per group.

5.4 Discussion

We previously showed that NMVs contain active proteases, interact with bronchial epithelial cells *in vitro* and induce functional changes in these cells including increased monolayer permeability. Furthermore, previously published data from our lab (Gomez *et al.*, 2020) and the work of others (Butin-Israeli *et al.*, 2019) has shown that NMVs have proinflammatory effects *in vivo*. In the present study, we aimed to determine the physiological impact of our *in vitro* findings by investigating the interaction between NMVs and cells in the lung and the functional consequences of this, using mice as a model organism.

5.4.1 The role of neutrophil-derived microvesicles in lung inflammation

In a pilot study in which NMVs were instilled intranasally in C57BL/6 mice (fig 5.1), no inflammatory response was detected, either locally in the lung or systemically, at any of the time points investigated, up to a maximum of 24h. Protein levels of key cytokines KC/CXCL-1 and CCL-2/MCP-1 in the BALF and plasma, as well as BALF total protein and total BALF cell count, were measured. Whilst only a small number of mice were used in these initial experiments (n = 2 per timepoint) and some variation between individuals was observed, consistently low levels of all inflammatory markers were detected, which did not clearly differ from T=0. In a subsequent study to investigate the ability of NMVs to potentiate an existing inflammatory response, mice were initially administered a dose of LPS, and were later administered NMVs or NMV supernatant (control). Whilst LPS generally induced a predictable inflammatory response—as measured by the same parameters as those stated above—the addition of NMVs had negligible effects on this response, neither enhancing nor reducing inflammation (fig 5.2). Again, although our study included relatively low n-numbers (4–6 mice per group), and individual variation was observed in both the LPS only and LPS + NMV groups, these results overall were consistent across all inflammatory readouts.

Previously published data from our lab (Gomez *et al.*, 2020) showed that after twice-weekly NMV administration via tail-vein injection for 6 weeks, in the same mouse strain, in atheroprone regions where NMVs preferentially adhered, increased expression of the NFκB subunit RelA (a.k.a p65) was observed; a key factor in several inflammatory pathways including in airway epithelium, neutrophils and macrophages (Isajevs *et al.*, 2011; Dorrington and Fraser, 2019; Ordoñez *et al.*, 2000). Furthermore, after just 2h *in vitro* this subunit was increased in human endothelial cells (Gomez *et al.*, 2020). Butin-Israeli et al. (2016a) showed that neutrophil-derived "microparticles"—a mixture of exosomes and NMVs pelleted at 100,000 *g*—administered by injection into a ligated intestinal loop promoted tissue injury, increased neutrophil transepithelial migration (TEM) into the intestine after just 3h of incubation and also impaired wound healing via induction of DNA double-strand breaks in

the epithelial cells (Butin-Israeli *et al.*, 2019). At 4h in our pilot study, although one of the mice had a higher BALF cell count, this seemed to be an aberration as inflammatory cytokines or total protein were not increased in this mouse at this timepoint. Further, it is not likely that the LPS-treated mice demonstrated a maximal inflammatory response which was not able to be further augmented, as a relatively low dose of LPS was used (5 μg) for this reason in our experiments. However, it would be interesting to investigate this at a shorter timepoint, and this will be examined in the 4h-treated mice used for PCLS experiments at a later date. Both Butin-Israeli and Gomez et al. found that these effects were mainly exerted via extracellular vesicle delivery of microRNAs, whilst protease activity, particularly MMP-9, also played a role in facilitating increased neutrophil TEM (Butin-Israeli *et al.*, 2016b). Although it should be noted that the method of administration and the target organ differed from that in the present study, and a mixed vesicle population was utilised, our evidence of active MMP-9 within NMVs was mirrored by Butin-Israeli et al., therefore a question remains as to why similar effects were not observed in our study. However, a limitation of the present work is lack of specific analysis and quantification of immune cell influx to the airways. Nevertheless, NMV numbers have been proven to be increased in the lungs soon after intratracheal LPS administration (Soni *et al.*, 2016), but their subsequent interactions and activity still remains unknown.

On the other hand, some authors have previously found anti-inflammatory or pro-resolving effects of NMVs in murine models of chronic inflammation. For example, NMVs from both healthy donors and patients with rheumatoid arthritis injected intra-articularly in a mouse model of arthritis were found to alter macrophage phenotype towards an M2-like state after 24h, although these vesicles were generated by TNF-α stimulation instead of fMLP used here (Rhys *et al.*, 2018). Whilst other inflammatory markers were not measured *in vivo* in that study, previous work from the same group also showed that injection of annexinA1[+] NMVs in the same model reduced cartilage degradation, likely via promoting TGF-β production from resident cells (Headland *et al.*, 2015), in contrast to the proteolytic activity found by other authors. Of interest, the same group found that LPS-induced inflammation after intrapleural injection induced protease-mediated annexin A1 cleavage, associated with increased elastase activity and decreased protease inhibitor expression, including SLPI, an endogenous inhibitor which can be found in lung tissue (Vago *et al.*, 2016). These authors identified annexin A1 as part of a pro-resolving system in their experiments, later showing than this protein was involved in host defence during pneumonia infection in mice (Machado *et al.*, 2020). NMV annexin A1 activity during lung infection could be of interest in future investigations, although NMVs did not reduce LPS-induced inflammation in our model.

The present study modelled acute lung inflammation after a single LPS administration, and this may in part explain the contrasting results found here and in the literature where chronic models of

inflammation were utilised e.g. arthritis (Headland *et al.*, 2015) and long term high-fat diet consumption (Gomez *et al.*, 2020). Additionally, the generating stimulus used for NMV production may be highly important. Methods used here were identical to those used in the publication by Gomez et al., however other publications varied in the neutrophil stimulus (e.g. TNF), time of stimulation (20 min up to 1 h), and isolation method (centrifugation speeds and processing steps), which may all significantly impact the resulting vesicle population and subsequent activity. Furthermore, the numbers of vesicles administered and method of quantification varies between publications (e.g. flow cytometry, nanoparticle tracking analysis, indirect measurement using neutrophil numbers or protein quantification). As dose-dependent effects of EVs have been demonstrated by various authors (Milani *et al.*, 2017; Tabak *et al.*, 2018; Dalli *et al.*, 2014; Genschmer *et al.*, 2019), this important factor will inevitably impact study results. Further, the number of NMVs administered intranasally in these experiments is very likely not the number reaching the lower airways, where some NMVs would have also remained in the upper airways or the pharynx. Other methods of administration, such as intratracheal, would have increased the availability of NMVs in the lower airways, and was the method of choice in the work performed by Genschmer et al. (2019).

Although we have previously shown functional effects of NMVs on lung epithelial cells *in vitro*, the magnitude of the inflammatory response to these vesicles was variable and in some cases was very low (chapter 4). The publications mentioned here all have different biological targets, however, one recent publication was the first to instil neutrophil-derived exosomes intratracheally in mice to investigate effects in the lung; Genschmer et al. (2019) found that these exosomes induced significant lung injury via elastase activity. Nevertheless, no detectable inflammatory cell infiltrate was incurred after exosome addition, as measured by histological analysis of lung sections from instilled mice, when compared with vehicle instillation. Furthermore, in a supplementary experiment, with albeit low n-numbers (n=2–3), these authors found no significant effects of neutrophil exosomes on inflammatory pathways such as MAPK or PI3K/AKT signalling or ER stress, although of note pathways related to mitochondrial dysfunction and oxidative phosphorylation were moderately altered.

Of interest in the present murine study were the changes in the lung MV population after LPS administration (fig 5.3). An expected increase in murine NMVs was detected (Ly6g$^+$ MV) by flow cytometry, as has been shown by other authors previously but at shorter time points (Soni *et al.*, 2016), it is interesting to note that this effect can still be found at 22 h. Whilst to our knowledge this has not been demonstrated previously, increased neutrophil numbers have been demonstrated in numerous studies up to approx. 72 h post-stimulus (McGrath *et al.*, 2011; Rydell-Tormanen *et al.*,

2006). Unexpectedly, the numbers of macrophage-derived MVs (MMVs; f4/80$^+$ MV) were consistently reduced to less than half that in the NMV only condition at 22 h post LPS-administration. An early peak and then return to baseline has been suggested when tracked up to 4 h by Soni et al. (2016), although in contrast, a study by Zhang et al. (2019) showed that MMVs which were positive for both f4/80 and CD11c remained almost two-fold higher than numbers in PBS-instilled mice. The dose of LPS (1 µg) used by Zhang et al. (2019) was a fifth that used in the present study—5 µg, chosen here as a relatively low dose to facilitate detection of any inflammation augmentation induced by NMVs. Whereas, that used by Soni et al. (20 µg) is four times higher than that in the present study, and likely also explains the higher numbers of immune-cell derived MVs shown by these authors in LPS-treated animals (approx. 700 and 400 MV/µl for NMVs and MMVs respectively, compared with 271.8 and 151.4 MV/µl here). It should also be noted that the volume used for BALF collection was higher in the present study (three passes with 1 ml vs. 700 µl) and could indicate a dilutional effect.

A possible explanation for the results observed in the present study whereby NMVs did not affect lung inflammation when administered intranasally may be rapid clearance of the administered NMVs by resident macrophages, precluding interaction of the NMVs with other alveolar cells. Subsequent studies confirmed that alveolar macrophages were highly effective at rapidly internalising large numbers of MVs present in the lung after just 4 h (fig 5.4 and 5.5). Indeed, Lu et al. (2018) previously showed that M2, anti-inflammatory macrophages were increased in the lung 10–24 h after intratracheal LPS administration, implying enhanced capacity for efferocytosis; this acts in a positive feedback loop to further promote the anti-inflammatory cell phenotype in a pro-resolving mechanism (Medeiros *et al.*, 2009). Of note, NMPs (mixed neutrophil exosomes and NMVs) have been shown to have similar effects (Dalli and Serhan, 2012), although anti-inflammatory action was not evidenced in the present study. Further investigation would be warranted to understand the mechanism and implication of this effect.

A limitation of this experiment was in the use of a single characteristic marker to identify each MV type, whereas other authors have used a combination of surface markers to further confirm their accurate characterisation. For example, Ly6g is considered generally as a granulocyte marker and is therefore also expressed in eosinophils, the use of further differential markers such as CD9 expressed on eosinophils (Akuthota *et al.*, 2016) but not on neutrophils (Kim *et al.*, 1997) may allow discrimination of these granulocyte-derived MVs. f4/80 is expressed on both monocytes and macrophages and therefore cannot differentiate between alveolar macrophages and recruited monocytes. Further, some non-specific staining may have been present for the anti-Ly6g antibody as NMVs were detected in the NMV only condition (where no neutrophil influx was detected) although

this cannot be confirmed since there was no vehicle only condition without NMV addition in this study. The use of an isotype control antibody or alternatively a negative control MV sample could potentially be used to further confirm the specificity of the Ly6g staining.

5.4.2 Neutrophil-derived microvesicle localisation in the lung

Despite evidence from other epithelial cell types and murine models that NMVs activate the epithelium and contribute to tissue inflammation, in our studies NMVs did not elicit or augment the lung or systemic inflammatory response. Therefore, we subsequently sought to determine the fate of NMVs in the lung to further understand their potential impact. In a pilot study using precision-cut lung slices (PCLS), despite NMVs being unable to penetrate the agarose-embedded tissue *ex vivo*, it was preliminarily observed that macrophages on the surface internalised a number of NMVs after just 1h, although no notable uptake or NMV accumulation was seen elsewhere in the tissue (fig 5.4). Subsequently, *in vitro* experiments using human monocyte-derived macrophages (MDMs) to determine an optimal time point for further investigation showed that whilst some internalisation was detectable at 2h, 4h onwards represented more notable uptake, as detected by fluorescence microscopy. Macrophages have previously been shown to internalise NMVs *in vitro* in as little as 30 min via an actin-dependent process (i.e. phagocytosis or macropinocytosis) which could be inhibited by cytochalasin D (Gasser and Schifferli, 2004). Although interpretation of these results is limited by the use of single-plane images obtained by fluorescence microscopy, these results were also confirmed by flow cytometry at 2 h (fig 5.4 (B)). The percentage of NMV-positive MDMs in our study at 2 h (24±6%) was in line with that found by others (Rhys *et al.*, 2018) where uptake was found to be time dependent, and at 1.5 h approx. 17% MDMs had internalised NMVs, measured using imaging flow cytometry. In further experiments, Rhys et al. (2018) found this uptake could be significantly inhibited by blocking NMV surface phosphatidyl-serine using annexin V, a mechanism utilised during macrophage efferocytosis (Fadok *et al.*, 1992). These authors observed anti-inflammatory effects of NMVs on activated MDMs, including reduced HLA-DR expression, however, interestingly they noted that NMVs did not exhibit all of these effects in unstimulated MDM. Importantly, Rhys et al. (2018) demonstrated that MVs had divergent activity from neutrophil exosomes, which did not impart the same anti-inflammatory effects–highlighting a key consideration for interpretation of the literature on neutrophil extracellular vesicles, and application of findings by Genschmer et al. (2019) of neutrophil exosomes in the lungs.

After determining a relevant timepoint for further investigation, mice were administered labelled NMVs by oropharyngeal aspiration, and at 4 h, PCLS were generated to determine NMV localisation. In this study macrophages were the only cells to take up these vesicles, which they did highly effectively (fig 5.5). NMVs were found mainly within the cells in the cytoplasmic portion and were

not detected freely in the lungs at this time point, or indeed anywhere in the airways, only in the alveoli. Further, these NMVs did not enter the circulation, highlighting resident alveolar macrophages as a major clearance mechanism for NMVs in the lung. Although individual NMVs that remained freely within airspaces may not have been detected due to their relatively lower signal compared with the clusters of NMVs with the cells, the large numbers of NMVs internalised by individual macrophages support the conclusion that complete or near-complete uptake was achieved. Whilst macrophages were not labelled specifically in this study, data from the pilot study (fig 5.4) along with the rounded morphology and distribution of these cells in the tissue are strongly indicative of resident alveolar macrophages, and would explain why positive cells were not detected in bronchioles or larger airways in this study.

To our knowledge, this is the first time this effect has been demonstrated in the lung tissue. However, direct NMV interaction with resident macrophages has been shown previously *in vivo* in other tissues such as in the synovium, as described above (Headland *et al.*, 2015) and uptake of other MV types, including epithelial-derived MVs has been shown previously in the lung (Lee *et al.*, 2017; Lee *et al.*, 2019). On the other hand, Genschmer at al. (2019) showed that neutrophil exosomes had long term functional impact on the lung after only a single administration, inducing significant airspace enlargement via their elastase activity. Therefore, the question of how these effects may be exerted if such an effective clearance mechanism is in place is of interest. As mentioned earlier, extrapolation of findings from neutrophil exosomes should be done with caution as divergent activities of these vesicles have been demonstrated. This method of lung imaging using PCLS has previously been well characterised for fungal particle uptake by Rudman et al. (2019), and would be a highly relevant model for further investigations of NMV fate and more in-depth exploration of uptake by alveolar macrophages. A limitation of these studies is the method of NMV administration (i.e. oropharyngeal aspiration, intranasal or intratracheal aspiration), which themselves vary the availability of NMVs in the lungs, and also differs from the *in vivo* pathological situation when an inflammatory stimulus induces neutrophil influx, and NMVs are released from migrating neutrophils and potentially access microenvironments that instilled NMVs may not be able to access. Some methods may and have been employed to inhibit MV generation *in vivo* and thereby understand their effects, including by calpeptin, a calpain inhibitor (Jorfi *et al.*, 2015), or using the Rho Kinase 1 and 2 inhibitor Y27632 (Tramontano *et al.*, 2004) which more specifically targets MV rather than exosome generation. Whilst advances are being made towards this end, particularly with therapeutic applications in mind (Kosgodage *et al.*, 2017; Catalano and O'Driscoll, 2020), currently these drugs inevitably effect other functions of the cell and are not yet cell-type specific, influencing potential study outcomes. Therefore, whilst no specific MV inhibitor yet exists, the present

administration method remains one of the best options available to investigate the role of extracellar vesicles, in isolation, in the lung.

5.5 Conclusion and future work

We have demonstrated that NMVs in the concentrations administered did not induce detectable pro- or anti-inflammatory responses in the murine lung when either administered alone or after LPS instillation. In contrast to our *in vitro* findings where NMVs were rapidly internalised by airway epithelial cells, *in vivo* resident alveolar macrophages were highly effective at taking up these NMVs in large numbers. NMVs could not be observed within other airway cells and did not transcytose into the circulation. See figure 5.7 for a summary of these results. This effect has not previously been demonstrated in the lung tissue to the best of our knowledge. Furthermore, this action of resident immune cells likely explains the lack of functional effects of these NMVs on the inflammatory parameters measured, and this process may be an important clearance mechanism in healthy individuals facilitating normal regulation of the inflammatory response. Additionally, in chronic lung conditions such as COPD or during cigarette smoking where macrophage phagocytosis and efferocytosis is impaired (Hodge *et al.*, 2003; Hodge *et al.*, 2007), NMVs may not be efficiently cleared and may therefore have differential functional activities. This could be investigated *in vitro* using MDM from COPD patients, or in further *in vivo* experiments in mice exposed to LPS in a longer-term experiment to model chronic inflammation.

In further work, lungs from mice treated with NMVs for 4 h and also 7 days with NMV will undergo histological processing and staining with haematoxylin and eosin to examine lung architecture, Picro-Sirius red for collagen distribution, and TGF-β expression to determine whether effects described in the literature, e.g. tissue damage at later time points and increased macrophage TGF-β production, apply here in the lung. In this work we aim to further delineate the functional consequences of these NMVs in order to understand whether they are beneficial or may indeed by harmful in lung inflammation, and whether protease-mediated effects are seen in the lung despite rapid vesicle clearance.

Further experiments using the present mouse model utilising PCLS would be warranted incorporating a macrophage depletion step, for example using clodronate-containing liposomes, to determine whether these vesicles may impact the lung tissue differentially in the absence of effective uptake by resident alveolar macrophages. Finally, comparing the kinetics of epithelial vs. macrophage uptake and understanding if there is a critical concentration of NMVs using

concentration-response experiments or multiple NMV administrations, and elucidating the fate of internalised NMVs at later time points would be highly interesting and relevant lines of further investigation.

Nevertheless, we have shown here that NMVs are released in the lungs in response to an inflammatory stimulus and interact with cells in the airways, contributing to our knowledge of the mechanisms of lung inflammation. Further study is warranted to understand the implications of these findings in human lung conditions.
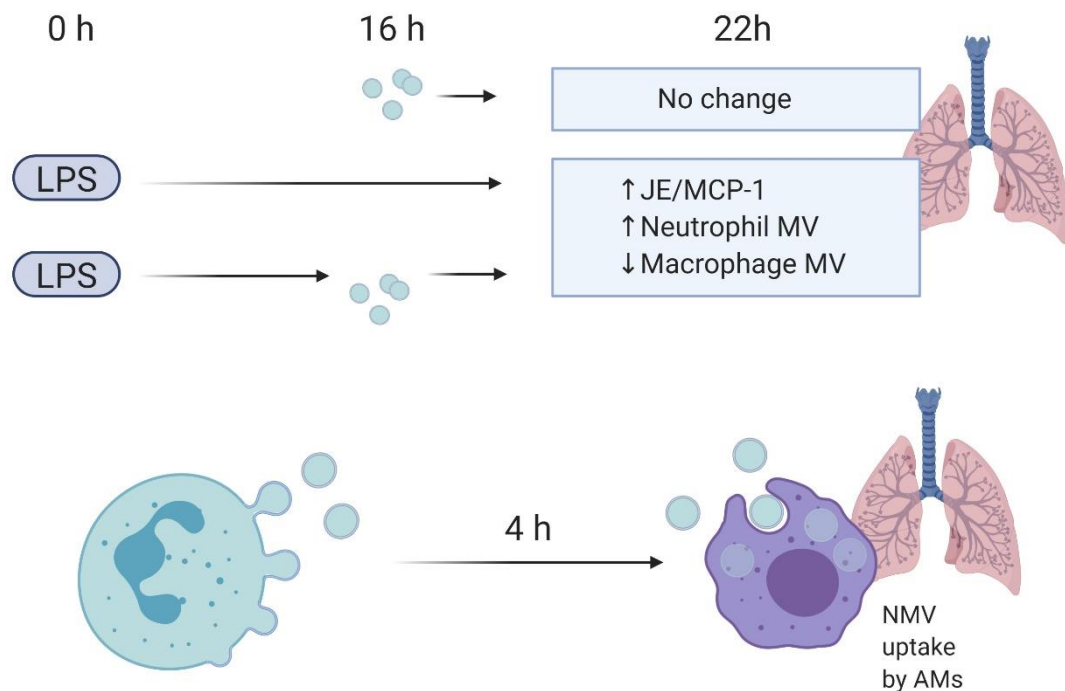
Figure 5.7 Summary of findings from Chapter 5

When neutrophil-derived microvesicles (NMVs) were administered intranasally to mice, these vesicles alone had not detectable effects lung inflammation. Administration of LPS did demonstrate increased levels of the chemokine JE (a.k.a MCP-1 or CCL-2) in the bronchoalveolar lavage fluid of these mice after 22h. Further, LPS-induced changes in the lung MV population were demonstrated: increased levels of NMVs and decreased macrophage MV concentrations were observed. LPS: lipopolysaccharide. When mice were administered fluorescently labelled NMVs by oropharyngeal aspiration, and then euthanised after 4h and precision cut lung slices generated, alveolar macrophages (AMs) were observed to have taken up many of these vesicles.

Chapter 6: General Discussion

6.1 Study Background and Summary

Despite the clear presence and widely acknowledged contributions of neutrophils in both chronic and acute inflammatory lung conditions, the exact mechanisms by which they exert their effects in the lungs are still being uncovered. In chronic obstructive pulmonary disease (COPD), persistent recruitment of neutrophils has been demonstrated in the airways and is associated with disease pathogenesis and progression (Sparrow *et al.*, 1984; Di Stefano *et al.*, 1998). Novel mechanisms of neutrophil dysfunction in the setting of such chronic inflammation are increasingly coming to light. For example, defects in neutrophil migration and its accuracy, and therefore increases in damage on the extended migratory path through the tissue have recently been shown in older individuals (Sapey *et al.*, 2011), and microenvironmental changes such as hypoxia (Hoenderdos *et al.*, 2016; Sadiku and Walmsley, 2019) and metabolite presence can dramatically alter neutrophil function to a more damaging profile (Grudzinska *et al.*, 2020). Furthermore, the possibility of neutrophil subsets with specific roles has been raised (Clemmensen *et al.*, 2012; Condamine *et al.*, 2016; Scapini *et al.*, 2016); there is certainly far more to learn about these understudied and previously underestimated cells.

As a lesser studied function of neutrophils, the release and effects of neutrophil-derived extracellular vesicles (EVs) from either outward blebbing of the cell membrane (i.e. microvesicles; MVs) or via exocytosis (exosomes) have begun to be deciphered in recent years. In particular, neutrophil EVs have been shown to possess immunomodulatory properties when internalised by other cell types (Pluskota *et al.*, 2008; Eken *et al.*, 2008; Pliyev *et al.*, 2014), and were found to have pro-inflammatory roles in the gut (Butin-Israeli *et al.*, 2019) and circulation (Gomez *et al.*, 2020), whilst others found pro-resolving and anti-inflammatory effects of these vesicles (Dalli *et al.*, 2008; Rhys *et al.*, 2018) and survival benefit in acute respiratory distress syndrome (ARDS) (Guervilly *et al.*, 2011). Further, neutrophil-derived exosomes (an EV subtype) have very recently been shown to have a destructive role in the lungs; in an article published at the end of my PhD studies, Genschmer et al. (2019) demonstrated that intratracheal administration of neutrophil exosomes in A/J mice—commonly utilised in experimentally modelling asthma (De Vooght *et al.*, 2010)—induced alveolar enlargement and reduced lung function. EVs are increasingly receiving interest in lung inflammation and disease, and key differences have already been demonstrated in EVs released in the airways, not only limited to neutrophils but also other important cell types including the epithelium; a very recent paper showed differential production, content and effects of EVs in cystic fibrosis, which had

modulatory effects on neutrophil migration (Useckaite *et al.*, 2020). Fascinatingly, Kim et al. (2017) found differences in the bacterial-derived EV population in the lungs of controls, smokers, and COPD patients, indicating the complexity and importance of EVs in the lung.

Despite this evidence, the presence of NMVs in COPD patient airways (Lacedonia *et al.*, 2016) and demonstrated NMV–epithelial cell interaction in other organs (Butin-Israeli *et al.*, 2016a), the contribution of these NMVs to COPD and lung inflammation remained relatively unexplored. Furthermore, important differences have been identified between the EV subtypes exosomes and MVs (Rhys *et al.*, 2018) and therefore individual study of these populations is needed to determine the source of differential content and effects of these vesicles. The present study aimed to understand the effects and interaction of NMVs in the airways to contribute to our knowledge of COPD pathogenesis and progression and identify potential disease biomarkers and novel therapeutic targets.

6.2 Study main findings

In the present work, COPD patient circulating microvesicles were studied, the effects of NMVs on the bronchial epithelium were evaluated *in vitro* and murine *in vivo* investigations into NMV effects and fate in the lungs were carried out. The major findings of this study were:

1. Circulating MVs were associated with significantly higher levels of the protease matrixmetalloproteinase-9 (MMP-9) in COPD patients with pulmonary hypertension, whilst immune cell, endothelial, or platelet-derived MV numbers did not differ between patients and age-matched controls.
2. Stimulated neutrophils tended to release NMVs with higher levels of active MMP-9 than unstimulated cells did, and these NMVs were capable of extracellular matrix degradation.
3. NMVs were rapidly internalised by BEAS-2B bronchial epithelial cells *in vitro*, likely via endocytic mechanisms, and had significant effects on epithelial barrier integrity, junctional protein expression and cell proliferation, with a trend towards increased levels of cell death.
4. Contrary to our original hypothesis, NMVs did not induce or augment lung inflammation in healthy mice *in vivo*, but were rapidly taken up by alveolar macrophages, where the effects of this interaction remain to be elucidated.

6.3 Future work arising from this thesis

As noted above, whilst NMVs had functional effects on the airway epithelium *in vitro*, this work did not fully support our original hypothesis, but has raised a number of important questions and suggested several further routes of enquiry including:

6.3.1 Investigation of NMV content in COPD

Data presented in this thesis demonstrated in two different COPD patient groups that levels of circulating neutrophil- or monocyte-derived MVs were not changed either during COPD exacerbations or in stable COPD with comorbid pulmonary hypertension (PH), compared with levels in matched controls. Additionally, NMV numbers generated from healthy donor neutrophils in response to a variety of stimuli such as CSE or produced spontaneously after isolation were not different. Therefore, we suggest that circulating MV numbers might not be a useful biomarker in COPD, however, COPD patient circulating MVs contained significantly higher levels of MMP-9, and healthy donor NMVs contained active MMP-9 upon stimulation, hence NMV content rather than numbers may be the most important differential factor. The presence of this protease in NMVs has been shown previously (Gasser *et al.*, 2003; Dalli *et al.*, 2013), though differential levels and activity has not been as widely explored and are a novel finding in COPD. NMV numbers may be important in some contexts and in particular in the relevant tissue micro-environment: whilst the presence of NMVs has been demonstrated in stable COPD airways (Lacedonia *et al.*, 2016), it would be expected that few to no NMVs would be present in healthy non-inflamed lungs as neutrophils are not present or present in only very small numbers. This was evidenced in our animal studies where very low levels of NMVs were detected in the BALF of mice receiving vehicle treatment, whilst LPS stimulation significantly increased these numbers. This concurs with findings reported by Soni et al. (2016) who show similar results using LPS stimulation. The utility of these numbers as a disease biomarker over much more easily quantified cell counts may be dependent on the context or disease.

Similarly, stimulation has little impact on the number of exosomes released by neutrophils, but does promote elastase-mediated effects; the latter could be abrogated by protamine sulphate (Genschmer *et al.*, 2019), currently used in humans to treat over-anticoagulation with heparin, where elastase exists on the exosome surface by electrostatic interaction and is displaced by protamine sulphate. Dalli et al. (2013) also identified differentially expressed proteins between NMVs released from adherent and suspension neutrophils. Further studies into NMV content in COPD including proteomics analysis are warranted to understand the potential differential role of these vesicles in chronic disease, providing avenues for further investigation and particularly opportunity to identify novel therapeutic targets.

 Intriguingly, Youn et al. (2019) recently proposed two different EV types with different content and function in their pre-print article; one is released from neutrophils which have arrived at an inflammatory site (NMVs) and the other is produced by migrating neutrophils (neutrophil-derived trails), both with differential content and activity. Looking further into the content of both of these

EV types would be of relevance for further study in COPD, where neutrophil migration is key to disease progression.

The systemic implications of increased circulating levels of MV-associated proteases and indeed other altered content in COPD patients, and the fate of these MVs, is of interest. In our lab it has recently been demonstrated that human coronary artery endothelial cells (HCAECs) readily internalise NMVs, inducing a pro-inflammatory response. This was further confirmed *in vivo* in a mouse model of atherosclerosis, where NMVs promoted atherogenesis (Gomez *et al.*, 2020). Other authors have shown interaction and activation in endothelial cell types including human umbilical cord cells and importantly, pulmonary microvascular endothelium (Mesri and Altieri, 1999; Tirlapur *et al.*, 2016). It is highly plausible that these circulating MVs may have differential effects in COPD, and may provide novel insight into the link between COPD and cardiovascular comorbidities. MMP-9 in particular has been shown to induce endothelial cell damage and death (Florence *et al.*, 2017) and is involved in several cardiovascular pathologies (Ramella *et al.*, 2017), and work is currently ongoing in further projects in our lab into the protease-mediated effects of NMVs on the endothelium. Furthermore, it would be interesting to determine whether NMVs had differential content in acute vs. chronic lung inflammation and the subsequent role this may have in these diseases, considering the survival benefit of NMV presence in ARDS (Guervilly *et al.*, 2011), to determine whether there may be a beneficial and harmful NMV signature, or whether these effects are simply a matter of "too much of a good thing" in chronic disease.

6.3.2 Identification of the mechanisms of NMV-induced effects on bronchial epithelial cells

The central hypothesis of this project was that NMVs would induce inflammatory activation of the bronchial epithelial cell line BEAS-2B utilised in this study. Such an effect would suggest a contribution to the cycle of inflammation, neutrophil recruitment, and tissue damage in diseases like COPD. Epithelial cells indeed rapidly internalised NMVs via a mechanism that was suggested to be endocytic since an inhibitor of actin polymerisation and low temperature modulated uptake. Whilst moderate but variable effects were observed on epithelial activation, measured by CXCL8 release, significant effects on epithelial monolayer permeability and tight junctional (TJ) protein expression were observed (Chapter 4). All of these events are consistent with observations in COPD (MacNee, 2006), however the mechanism of these effects was not pinpointed in the present work.

Beyond neutrophil granule content and beyond the scope of the present work, NMVs have been shown to contain microRNAs (miRs) important for their effects on target cells including the endothelium (Gomez *et al.*, 2020) and epithelium (Butin-Israeli *et al.*, 2019), and whether this is

differential during inflammation would open further interesting avenues of investigation. MiRs are being increasingly studied in the context of lung inflammation and have been shown to be differentially expressed in the airways of asthma (Levänen *et al.*, 2013) and COPD patients (Conickx *et al.*, 2017). Furthermore, miRs specifically associated with EVs in COPD have very recently been investigated and have potential use in differentiation between different COPD patient groups (Carpi *et al.*, 2020). The role of NMVs in the delivery of miRs in the lung could prove to be important and would be a highly relevant line of investigation. Antisense oligonucleotide (ASO) drugs are currently under investigation as therapeutic strategies to target miR activity by pharmaceutical companies including AstraZeneca for conditions such as lung cancer (Hong *et al.*, 2015); identifying the source and activity of NMV-associated miRs in COPD may have a large impact on future disease treatment.

6.3.3 Further understanding of the interaction between NMVs with alveolar macrophages

The final part of the present thesis studied the role of NMVs *in vivo* using murine models of lung inflammation. Here it was found that in normal healthy murine lungs, NMVs did not induce, augment, or reduce inflammation in the airways at the concentrations utilised, as measured by levels of inflammatory cytokines and neutrophil recruitment. Whilst these results were initially surprising, we note that in agreement, Genschmer et al. (2019) recently showed that neutrophil exosomes exerted elastase-dependent damage in the lung tissue, but did not induce any significant amount of immune cell recruitment. Further experiments using varying NMV concentrations would help to determine if there is a critical number of NMVs at which differential effects are observed, indeed, the numbers used here *in vivo* may be lower than those generated in the lungs, as discussed in Chapter 4, section 4.3.1; Lacedonia et al. (2016) showed an approximate concentration of 7000 neutrophil EVs/μL, which may actually be even higher in the airways due to dilution effects when collecting induced sputum samples as in their study. When the fate of NMVs in the lungs was further investigated in the present study utilising the novel technique of precision-cut lung slices (PCLS) to image fluorescently-labelled NMVs, we discovered that rather than being internalised by the lung epithelium, all detectable NMVs in this experimental setting were detected inside alveolar macrophages (AMs). NMV uptake by macrophages has been demonstrated previously and was found to induce immunomodulatory activity, increasing tumour growth factor-β (TGF-β) expression and reducing inflammatory gene expression (Eken *et al.*, 2010; Eken *et al.*, 2013), as well as enhancing macrophage phagocytosis (Prakash *et al.*, 2012). Further work as part of this project will determine whether TGF-β expression and extracellular matrix components were altered by NMVs in the lung tissue via histology staining.

A limitation of the present study was the use of an epithelial cell line in monoculture, which did not reflect the *in vivo* situation, where alveolar macrophages were the key missing piece here. As

discussed previously in Chapter 4, key differences also exist in epithelial cell lines which influence the response of these cells. In future work, the use of primary airway epithelial cells cultured at air–liquid interface would be a more physiologically relevant model and co-culture with macrophages, or the use of emerging 3D systems such as lung-on-chip technology recently used to investigate nanoparticle toxicity (Zhang *et al.*, 2018)—although the latter option is likely prohibitively expensive for most—would allow better understanding of the complex and multicellular environment of the lung. Further, the use of healthy human NMVs in mice is not optimal here, and although employed by other authors in recent publications (Genschmer *et al.*, 2019), those authors also validated observed effects using patient EVs isolated from BALF. Isolation of murine neutrophils and generation of NMVs or use of COPD patient NMVs would be a better experimental set up for further investigation in the present study. Alternatively, the use of PCLS generated from human lung tissue, which has been utilised by other researchers in COPD patients undergoing surgery for lung cancer by using surrounding tissue which is cancer-free (Maarsingh *et al.*, 2019), would allow human *ex vivo* study of these effects and discount effects of species mismatch. In this way, tissue effects of NMVs could be compared in these patients with and without COPD, and research into the effects of NMVs generated from healthy participant and COPD patient neutrophils on this live lung tissue would also be highly interesting.

Investigation of these effects in healthy macrophages and in the context of dysfunctional AM activity is present, as is the case in COPD and after cigarette smoke exposure (Hodge *et al.*, 2003; Hodge *et al.*, 2007), might shed light on the complex transition between acute (predominantly beneficial) inflammatory responses and detrimental chronic inflammation. Repeating the murine PCLS experiments utilising a macrophage depletion step before NMV addition would determine the localisation of NMVs in the absence of AMs and would allow investigation of AM dysfunction. In this way it could be determined whether AM activity is critical for MV clearance and what may happen in the context of chronic disease. This could also be investigated initially *in vitro* using an epithelial cell and macrophage co-culture. Further, neutrophils are also capable of rapid phagocytosis and neutrophil "cannibalism" has previously been documented (Rydell-Tormanen *et al.*, 2006). Dalli et al. (2008) previously showed that NMPs inhibited neutrophil adhesion to endothelial cells *in vitro* and also neutrophil trafficking in response to interleukin-1β *in vivo* in the lungs. Whilst we did not observe anti-inflammatory effects in our *in vivo* studies, effects of NMVs on neutrophils themselves in lung inflammation could be further examined. This would be particularly relevant as we saw increased release of CXCL8, involved in neutrophil recruitment during inflammation, when NMVs interacted with epithelial cells, which could be expected to increase neutrophil migration and presence in the lungs if NMVs were not sufficiently cleared. Indeed, repeating the *in vivo*

experiments utilised in the present study with PCLS generation after induction of lung inflammation and labelled NMV addition, followed by macrophage and neutrophil labelling using conjugated antibodies would be a straightforward way to determine whether neutrophils also take up NMVs once recruited to the lungs, as well as AMs, in an inflammatory context for further investigation of immunomodulatory properties of NMVs in the airways.

6.4 Model of possible NMV functions in COPD

NMVs are rapidly internalised by AMs in the airways, the consequences of which are currently unknown but which may be a key mechanism to protect the lung epithelium from NMV-induced damage. Such a mechanism could be compromised in diseases such as COPD where AM function is impaired, but this needs to be further studied. The complexity of the changes occurring in the airways of patients with inflammatory lung diseases like COPD make the role of NMVs in this more difficult to decipher, compounded by the challenges of accessing this tissue compartment in patients who have poor lung function and reserve. We speculate that in individuals without chronic respiratory disease during acute lung inflammation, NMVs may mainly act as neutrophil messengers delivering content to AMs and perhaps indeed other phagocytic cells like neutrophils themselves. However, in chronic disease we speculate that these events may be altered. I propose that the combination of changes in TJ expression and a possible contribution to increased cell death may be responsible for NMV-induced changes in epithelial barrier function observed here *in vitro*, and further, we found that NMVs were capable of degrading the extracellular matrix component Collagen IV, a major part of the basement membrane in the lung (Laurent, 1986), and this may contribute to the functional effects observed here on the epithelium. When key functions such as phagocytosis and efferocytosis are impaired in airway immune cells in chronic disease, NMVs, which are capable of remaining intact for more than 24h *in vitro*, may interact with other cells such as the epithelium, compromising epithelial barrier integrity and contributing to disease progression (summarised in figure 6.1).

6.5 Final conclusion

This study showed that MVs can have differential content in chronic lung diseases like COPD; these vesicles contained higher levels of inflammation-associated proteins, although circulating leukocyte-derived MV numbers were not a useful biomarker in the disease and analysis of MV content will be key going forward in extracellular vesicle research. When NMVs were applied directly, they induced airway epithelial dysfunction, a key element of COPD pathology and pathogenesis. Further, in healthy mice, NMV uptake by resident immune cells including macrophages in the alveoli prevented epithelial interaction with these vesicles, providing novel insight into neutrophil activity in lung

inflammation and highlighting a key area for further investigation which may be changed in chronic inflammation.
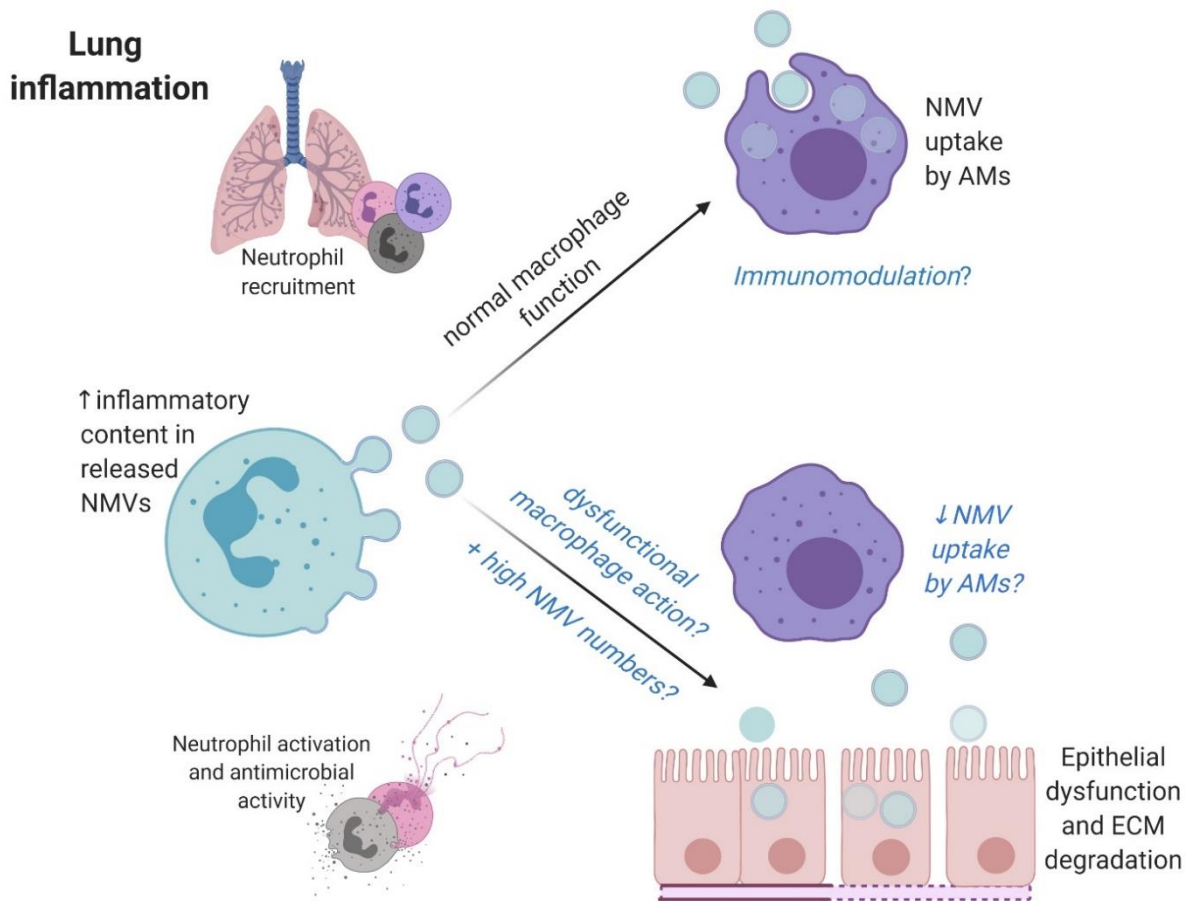
Figure 6.1 Proposed neutrophil-derived microvesicle mechanisms of action in the airways and hypothesised differences in chronic lung inflammation

Neutrophils migrate to the airways in response to chemotactic stimuli and release microvesicles (NMVs) into the airways, which have higher levels of potentially damaging content upon inflammatory activation. In healthy lung tissue, these NMVs are taken up by alveolar macrophages (MVs), effects of which may include immunomodulatory activity. When NMVs are present at higher levels due to persistent immune cell recruitment and activation, in combination with impaired AM activity in chronic lung disease, the AM-mediated clearance mechanism may be ineffective, allowing NMVs to interact with the delicate lung epithelium, reducing epithelial barrier integrity by increasing permeability and degrading the airway extracellular matrix (ECM), as observed in vitro.

Chapter 7: Bibliography

(WHO), W. H. O. (2008) *World Health Statistics Report 2008*, Geneva: World Health Organisation. Available at: http://www.who.int/whosis/whostat/EN_WHS08_Full.pdf?ua=1.

Aaron, S. D., Angel, J. B., Lunau, M., Wright, K., Fex, C., Le Saux, N. and Dales, R. E. (2001) 'Granulocyte inflammatory markers and airway infection during acute exacerbation of chronic obstructive pulmonary disease', *Am J Respir Crit Care Med,* 163(2), pp. 349-55.

Abraham, E., Carmody, A., Shenkar, R. and Arcaroli, J. (2000) 'Neutrophils as early immunologic effectors in hemorrhage- or endotoxemia-induced acute lung injury', *Am J Physiol Lung Cell Mol Physiol,* 279(6), pp. L1137-45.

Aghapour, M., Raee, P., Moghaddam, S. J., Hiemstra, P. S. and Heijink, I. H. (2018) 'Airway Epithelial Barrier Dysfunction in Chronic Obstructive Pulmonary Disease: Role of Cigarette Smoke Exposure', *Am J Respir Cell Mol Biol,* 58(2), pp. 157-169.

Agraval, H. and Yadav, U. C. S. (2019) 'MMP-2 and MMP-9 mediate cigarette smoke extract-induced epithelial-mesenchymal transition in airway epithelial cells via EGFR/Akt/GSK3β/β-catenin pathway: Amelioration by fisetin', *Chem Biol Interact,* 314, pp. 108846.

Agusti, A., Calverley, P. M., Celli, B., Coxson, H. O., Edwards, L. D., Lomas, D. A., MacNee, W., Miller, B. E., Rennard, S., Silverman, E. K., Tal-Singer, R., Wouters, E., Yates, J. C. and Vestbo, J. (2010) 'Characterisation of COPD heterogeneity in the ECLIPSE cohort', *Respir Res,* 11(1), pp. 122.

Agusti, A., Edwards, L. D., Rennard, S. I., MacNee, W., Tal-Singer, R., Miller, B. E., Vestbo, J., Lomas, D. A., Calverley, P. M., Wouters, E., Crim, C., Yates, J. C., Silverman, E. K., Coxson, H. O., Bakke, P., Mayer, R. J. and Celli, B. (2012) 'Persistent systemic inflammation is associated with poor clinical outcomes in COPD: a novel phenotype', *PLoS One,* 7(5), pp. e37483.

Ahmad, A., Shameem, M. and Husain, Q. (2013) 'Altered oxidant-antioxidant levels in the disease prognosis of chronic obstructive pulmonary disease', *Int J Tuberc Lung Dis,* 17(8), pp. 1104-9.

Ajikumar, A., Long, M. B., Heath, P. R., Wharton, S. B., Ince, P. G., Ridger, V. C. and Simpson, J. E. (2019) 'Neutrophil-Derived Microvesicle Induced Dysfunction of Brain Microvascular Endothelial Cells In Vitro', *Int J Mol Sci,* 20(20).

Akuthota, P., Carmo, L. A., Bonjour, K., Murphy, R. O., Silva, T. P., Gamalier, J. P., Capron, K. L., Tigges, J., Toxavidis, V., Camacho, V., Ghiran, I., Ueki, S., Weller, P. F. and Melo, R. C. (2016) 'Extracellular Microvesicle Production by Human Eosinophils Activated by "Inflammatory" Stimuli', *Front Cell Dev Biol,* 4, pp. 117.

Ando, K., Hasegawa, K., Shindo, K., Furusawa, T., Fujino, T., Kikugawa, K., Nakano, H., Takeuchi, O., Akira, S., Akiyama, T., Gohda, J., Inoue, J. and Hayakawa, M. (2010) 'Human lactoferrin activates NF-kappaB through the Toll-like receptor 4 pathway while it interferes with the lipopolysaccharide-stimulated TLR4 signaling', *Febs j,* 277(9), pp. 2051-66.

Anzueto, A. (2010) 'Impact of exacerbations on COPD', *Eur Respir Rev,* 19(116), pp. 113-8.

Arai, N., Kondo, M., Izumo, T., Tamaoki, J. and Nagai, A. (2010) 'Inhibition of neutrophil elastase-induced goblet cell metaplasia by tiotropium in mice', *Eur Respir J,* 35(5), pp. 1164-71.

Araki, Y. and Mimura, T. (2017) 'Matrix Metalloproteinase Gene Activation Resulting from Disordred Epigenetic Mechanisms in Rheumatoid Arthritis', *Int J Mol Sci,* 18(5).

Ardi, V. C., Kupriyanova, T. A., Deryugina, E. I. and Quigley, J. P. (2007) 'Human neutrophils uniquely release TIMP-free MMP-9 to provide a potent catalytic stimulator of angiogenesis', *Proc Natl Acad Sci U S A,* 104(51), pp. 20262-7.

Athens, J. W., Haab, O. P., Raab, S. O., Mauer, A. M., Ashenbrucker, H., Cartwright, G. E. and Wintrobe, M. M. (1961) 'Leukokinetic studies. IV. The total blood, circulating and marginal granulocyte pools and the granulocyte turnover rate in normal subjects', *J Clin Invest,* 40(6), pp. 989-95.

Atkinson, J. J., Lutey, B. A., Suzuki, Y., Toennies, H. M., Kelley, D. G., Kobayashi, D. K., Ijem, W. G., Deslee, G., Moore, C. H., Jacobs, M. E., Conradi, S. H., Gierada, D. S., Pierce, R. A., Betsuyaku, T. and Senior, R. M. (2011) 'The role of matrix metalloproteinase-9 in cigarette smoke-induced emphysema', *Am J Respir Crit Care Med,* 183(7), pp. 876-84.

Ayers, L., Kohler, M., Harrison, P., Sargent, I., Dragovic, R., Schaap, M., Nieuwland, R., Brooks, S. A. and Ferry, B. (2011) 'Measurement of circulating cell-derived microparticles by flow cytometry: sources of variability within the assay', *Thromb Res,* 127(4), pp. 370-7.

Bacha, N. C., Levy, M., Guerin, C. L., Le Bonniec, B., Harroche, A., Szezepanski, I., Renard, J. M., Gaussem, P., Israel-Biet, D., Boulanger, C. M. and Smadja, D. M. (2019) 'Treprostinil treatment decreases circulating platelet microvesicles and their procoagulant activity in pediatric pulmonary hypertension', *Pediatr Pulmonol,* 54(1), pp. 66-72.

Badesch, D. B., Champion, H. C., Sanchez, M. A., Hoeper, M. M., Loyd, J. E., Manes, A., McGoon, M., Naeije, R., Olschewski, H., Oudiz, R. J. and Torbicki, A. (2009) 'Diagnosis and assessment of pulmonary arterial hypertension', *J Am Coll Cardiol,* 54(1 Suppl), pp. S55-66.

Bafadhel, M., McKenna, S., Terry, S., Mistry, V., Reid, C., Haldar, P., McCormick, M., Haldar, K., Kebadze, T., Duvoix, A., Lindblad, K., Patel, H., Rugman, P., Dodson, P., Jenkins, M., Saunders, M., Newbold, P., Green, R. H., Venge, P., Lomas, D. A., Barer, M. R., Johnston, S. L., Pavord, I. D. and Brightling, C. E. (2011) 'Acute exacerbations of chronic obstructive pulmonary disease: identification of biologic clusters and their biomarkers', *Am J Respir Crit Care Med,* 184(6), pp. 662-71.

Bai, X., Li, Y. Y., Zhang, H. Y., Wang, F., He, H. L., Yao, J. C., Liu, L. and Li, S. S. (2017) 'Role of matrix metalloproteinase-9 in transforming growth factor-beta1-induced epithelial-mesenchymal transition in esophageal squamous cell carcinoma', *Onco Targets Ther,* 10, pp. 2837-2847.

Baker, J. R., Donnelly, L. E. and Barnes, P. J. (2020) 'Senotherapy: A New Horizon for COPD Therapy', *Chest*.

Barabutis, N., Dimitropoulou, C., Birmpas, C., Joshi, A., Thangjam, G. and Catravas, J. D. (2015) 'p53 protects against LPS-induced lung endothelial barrier dysfunction', *Am J Physiol Lung Cell Mol Physiol,* 308(8), pp. L776-87.

Barnes, P. J. (2008) 'Immunology of asthma and chronic obstructive pulmonary disease', *Nat Rev Immunol,* 8(3), pp. 183-92.

Barnes, P. J. (2016) 'Inflammatory mechanisms in patients with chronic obstructive pulmonary disease', *J Allergy Clin Immunol,* 138(1), pp. 16-27.

Barnes, P. J. (2017) 'Glucocorticosteroids', *Handb Exp Pharmacol,* 237, pp. 93-115.

Barnes, P. J., Baker, J. and Donnelly, L. E. (2019) 'Cellular Senescence as a Mechanism and Target in Chronic Lung Diseases', *Am J Respir Crit Care Med,* 200(5), pp. 556-564.

Barrecheguren, M., Esquinas, C. and Miravitlles, M. (2015) 'The asthma-chronic obstructive pulmonary disease overlap syndrome (ACOS): opportunities and challenges', *Curr Opin Pulm Med,* 21(1), pp. 74-9.

Beck-Schimmer, B., Schimmer, R. C., Warner, R. L., Schmal, H., Nordblom, G., Flory, C. M., Lesch, M. E., Friedl, H. P., Schrier, D. J. and Ward, P. A. (1997) 'Expression of lung vascular and airway ICAM-1 after exposure to bacterial lipopolysaccharide', *Am J Respir Cell Mol Biol,* 17(3), pp. 344-52.

Beck-Schimmer, B., Schwendener, R., Pasch, T., Reyes, L., Booy, C. and Schimmer, R. C. (2005) 'Alveolar macrophages regulate neutrophil recruitment in endotoxin-induced lung injury', *Respir Res,* 6(1), pp. 61.

Becker, E. L., Forouhar, F. A., Grunnet, M. L., Boulay, F., Tardif, M., Bormann, B. J., Sodja, D., Ye, R. D., Woska, J. R., Jr. and Murphy, P. M. (1998) 'Broad immunocytochemical localization of the formylpeptide receptor in human organs, tissues, and cells', *Cell Tissue Res,* 292(1), pp. 129-35.

Bergmann, S., Siekmeier, R., Mix, C. and Jaross, W. (1998) 'Even moderate cigarette smoking influences the pattern of circulating monocytes and the concentration of sICAM-1', *Respir Physiol,* 114(3), pp. 269-75.

Betsuyaku, T., Nishimura, M., Takeyabu, K., Tanino, M., Venge, P., Xu, S. and Kawakami, Y. (1999) 'Neutrophil granule proteins in bronchoalveolar lavage fluid from subjects with subclinical emphysema', *Am J Respir Crit Care Med,* 159(6), pp. 1985-91.

Bhowmik, A., Seemungal, T. A., Sapsford, R. J. and Wedzicha, J. A. (2000a) 'Relation of sputum inflammatory markers to symptoms and lung function changes in COPD exacerbations', *Thorax,* 55(2), pp. 114-20.

Bhowmik, A., Seemungal, T. A., Sapsford, R. J. and Wedzicha, J. A. (2000b) 'Relation of sputum inflammatory markers to symptoms and lung function changes in COPD exacerbations', *Thorax,* 55.

Blander, J. M. (2018) 'Regulation of the Cell Biology of Antigen Cross-Presentation', *Annu Rev Immunol,* 36, pp. 717-753.

BLF, B. L. F. (2016) *Chronic obstructive pulmonary disease (COPD) statistics: Deaths from COPD*. Available at: https://statistics.blf.org.uk/copd (Accessed: 13 Oct 2016).

Boixeda, R., Rabella, N., Sauca, G., Delgado, M., Martinez-Costa, X., Mauri, M., Vicente, V., Palomera, E., Serra-Prat, M. and Capdevila, J. A. (2012) 'Microbiological study of patients hospitalized for acute exacerbation of chronic obstructive pulmonary disease (AE-COPD) and the usefulness of analytical and clinical parameters in its identification (VIRAE study)', *Int J Chron Obstruct Pulmon Dis,* 7, pp. 327-35.

Bojarski, C., Gitter, A. H., Bendfeldt, K., Mankertz, J., Schmitz, H., Wagner, S., Fromm, M. and Schulzke, J. D. (2001) 'Permeability of human HT-29/B6 colonic epithelium as a function of apoptosis', *J Physiol,* 535(Pt 2), pp. 541-52.

Bojarski, C., Weiske, J., Schöneberg, T., Schröder, W., Mankertz, J., Schulzke, J. D., Florian, P., Fromm, M., Tauber, R. and Huber, O. (2004) 'The specific fates of tight junction proteins in apoptotic epithelial cells', *J Cell Sci,* 117(Pt 10), pp. 2097-107.

Boots, A. W., Gerloff, K., Bartholome, R., van Berlo, D., Ledermann, K., Haenen, G. R., Bast, A., van Schooten, F. J., Albrecht, C. and Schins, R. P. (2012) 'Neutrophils augment LPS-mediated pro-inflammatory signaling in human lung epithelial cells', *Biochim Biophys Acta,* 1823(7), pp. 1151-62.

Bourgeois, J. S., Jacob, J., Garewal, A., Ndahayo, R. and Paxson, J. (2016) 'The Bioavailability of Soluble Cigarette Smoke Extract Is Reduced through Interactions with Cells and Affects the Cellular Response to CSE Exposure', *PLoS One,* 11(9), pp. e0163182.

Boysen, J., Nelson, M., Magzoub, G., Maiti, G. P., Sinha, S., Goswami, M., Vesely, S. K., Shanafelt, T. D., Kay, N. E. and Ghosh, A. K. (2016) 'Dynamics of microvesicle generation in B-cell chronic lymphocytic leukemia: implication in disease progression', *Leukemia.*

Bradley, L. M., Douglass, M. F., Chatterjee, D., Akira, S. and Baaten, B. J. (2012) 'Matrix metalloprotease 9 mediates neutrophil migration into the airways in response to influenza virus-induced toll-like receptor signaling', *PLoS Pathog,* 8(4), pp. e1002641.

Brass, D. M., Hollingsworth, J. W., Cinque, M., Li, Z., Potts, E., Toloza, E., Foster, W. M. and Schwartz, D. A. (2008) 'Chronic LPS inhalation causes emphysema-like changes in mouse lung that are associated with apoptosis', *Am J Respir Cell Mol Biol,* 39(5), pp. 584-90.

Brinkmann, V., Reichard, U., Goosmann, C., Fauler, B., Uhlemann, Y., Weiss, D. S., Weinrauch, Y. and Zychlinsky, A. (2004) 'Neutrophil extracellular traps kill bacteria', *Science,* 303(5663), pp. 1532-5.

Bulut, D., Becker, V. and Mugge, A. (2011) 'Acetylsalicylate reduces endothelial and platelet-derived microparticles in patients with coronary artery disease', *Can J Physiol Pharmacol,* 89(4), pp. 239-44.

Burnett, D., Chamba, A., Hill, S. L. and Stockley, R. A. (1987) 'Neutrophils from subjects with chronic obstructive lung disease show enhanced chemotaxis and extracellular proteolysis', *Lancet,* 2(8567), pp. 1043-6.

Butin-Israeli, V., Bui, T. M., Wiesolek, H. L., Mascarenhas, L., Lee, J. J., Mehl, L. C., Knutson, K. R., Adam, S. A., Goldman, R. D., Beyder, A., Wiesmuller, L., Hanauer, S. B. and Sumagin, R. (2019) 'Neutrophil-induced genomic instability impedes resolution of inflammation and wound healing', *J Clin Invest,* 129(2), pp. 712-726.

Butin-Israeli, V., Houser, M. C., Feng, M., Thorp, E. B., Nusrat, A., Parkos, C. A. and Sumagin, R. (2016a) 'Deposition of microparticles by neutrophils onto inflamed epithelium: a new mechanism to disrupt epithelial intercellular adhesions and promote transepithelial migration', *Faseb j,* 30(12), pp. 4007-4020.

Butin-Israeli, V., Houser, M. C., Feng, M., Thorp, E. B., Nusrat, A., Parkos, C. A. and Sumagin, R. (2016b) 'Deposition of microparticles by neutrophils onto inflamed epithelium: a new mechanism to disrupt epithelial intercellular adhesions and promote transepithelial migration', *Faseb Journal,* 30(12), pp. 4007-4020.

Cai, S. X., Liu, A. R., Chen, S., He, H. L., Chen, Q. H., Xu, J. Y., Pan, C., Yang, Y., Guo, F. M., Huang, Y. Z., Liu, L. and Qiu, H. B. (2015) 'Activation of Wnt/β-catenin signalling promotes mesenchymal stem cells to repair injured alveolar epithelium induced by lipopolysaccharide in mice', *Stem Cell Res Ther,* 6(1), pp. 65.

Cain, D. W., Snowden, P. B., Sempowski, G. D. and Kelsoe, G. (2011) 'Inflammation triggers emergency granulopoiesis through a density-dependent feedback mechanism', *PLoS One,* 6(5), pp. e19957.

Carestia, A., Kaufman, T., Rivadeneyra, L., Landoni, V. I., Pozner, R. G., Negrotto, S., D'Atri, L. P., Gomez, R. M. and Schattner, M. (2016) 'Mediators and molecular pathways involved in the regulation of neutrophil extracellular trap formation mediated by activated platelets', *J Leukoc Biol,* 99(1), pp. 153-62.

Carp, H. (1982) 'Mitochondrial N-formylmethionyl proteins as chemoattractants for neutrophils', *J Exp Med,* 155(1), pp. 264-75.

Carpi, S., Polini, B., Nieri, D., Dubbini, N., Celi, A., Nieri, P. and Neri, T. (2020) 'Expression Analysis of Muscle-Specific miRNAs in Plasma-Derived Extracellular Vesicles from Patients with Chronic Obstructive Pulmonary Disease', *Diagnostics (Basel),* 10(7).

Catalano, M. and O'Driscoll, L. (2020) 'Inhibiting extracellular vesicles formation and release: a review of EV inhibitors', *J Extracell Vesicles,* 9(1), pp. 1703244.

Caudrillier, A., Kessenbrock, K., Gilliss, B. M., Nguyen, J. X., Marques, M. B., Monestier, M., Toy, P., Werb, Z. and Looney, M. R. (2012) 'Platelets induce neutrophil extracellular traps in transfusion-related acute lung injury', *J Clin Invest,* 122(7), pp. 2661-71.

Cauwe, B., Martens, E., Proost, P. and Opdenakker, G. (2009) 'Multidimensional degradomics identifies systemic autoantigens and intracellular matrix proteins as novel gelatinase B/MMP-9 substrates', *Integr Biol (Camb),* 1(5-6), pp. 404-26.

Cecere, L. M., Littman, A. J., Slatore, C. G., Udris, E. M., Bryson, C. L., Boyko, E. J., Pierson, D. J. and Au, D. H. (2011) 'Obesity and COPD: associated symptoms, health-related quality of life, and medication use', *Copd,* 8(4), pp. 275-84.

Chakrabarti, S., Zee, J. M. and Patel, K. D. (2006) 'Regulation of matrix metalloproteinase-9 (MMP-9) in TNF-stimulated neutrophils: novel pathways for tertiary granule release', *J Leukoc Biol,* 79(1), pp. 214-22.

Chakraborty, D., Zenker, S., Rossaint, J., Hölscher, A., Pohlen, M., Zarbock, A., Roth, J. and Vogl, T. (2017) 'Alarmin S100A8 Activates Alveolar Epithelial Cells in the Context of Acute Lung Injury in a TLR4-Dependent Manner', *Front Immunol,* 8, pp. 1493.

Chan, S. C., Shum, D. K., Tipoe, G. L., Mak, J. C., Leung, E. T. and Ip, M. S. (2008) 'Upregulation of ICAM-1 expression in bronchial epithelial cells by airway secretions in bronchiectasis', *Respir Med,* 102(2), pp. 287-98.

Chandler, S., Cossins, J., Lury, J. and Wells, G. (1996) 'Macrophage metalloelastase degrades matrix and myelin proteins and processes a tumour necrosis factor-alpha fusion protein', *Biochem Biophys Res Commun,* 228(2), pp. 421-9.

Chandler, W. L. (2016) 'Measurement of Microvesicle Levels in Human Blood Using Flow Cytometry', *Cytometry Part B-Clinical Cytometry,* 90(4), pp. 326-336.

Chandler, W. L., Yeung, W. and Tait, J. F. (2011) 'A new microparticle size calibration standard for use in measuring smaller microparticles using a new flow cytometer', *J Thromb Haemost,* 9(6), pp. 1216-24.

Chironi, G., Simon, A., Hugel, B., Del Pino, M., Gariepy, J., Freyssinet, J. M. and Tedgui, A. (2006) 'Circulating leukocyte-derived microparticles predict subclinical atherosclerosis burden in asymptomatic subjects', *Arterioscler Thromb Vasc Biol,* 26(12), pp. 2775-80.

Chung, K. F. and Adcock, I. M. (2008) 'Multifaceted mechanisms in COPD: inflammation, immunity, and tissue repair and destruction', *Eur Respir J,* 31(6), pp. 1334-56.

Churg, A., Wang, R., Wang, X., Onnervik, P. O., Thim, K. and Wright, J. L. (2007) 'Effect of an MMP-9/MMP-12 inhibitor on smoke-induced emphysema and airway remodelling in guinea pigs', *Thorax,* 62(8), pp. 706-13.

Chyrchel, B., Drozdz, A., Dlugosz, D., Stepien, E. L. and Surdacki, A. (2019) 'Platelet Reactivity And Circulating Platelet-Derived Microvesicles Are Differently Affected By P2Y12 Receptor Antagonists', *Int J Med Sci,* 16(2), pp. 264-275.

Clemmensen, S. N., Bohr, C. T., Rørvig, S., Glenthøj, A., Mora-Jensen, H., Cramer, E. P., Jacobsen, L. C., Larsen, M. T., Cowland, J. B., Tanassi, J. T., Heegaard, N. H., Wren, J. D., Silahtaroglu, A. N. and Borregaard, N. (2012) 'Olfactomedin 4 defines a subset of human neutrophils', *J Leukoc Biol,* 91(3), pp. 495-500.

Cleutjens, F. A., Janssen, D. J., Ponds, R. W., Dijkstra, J. B. and Wouters, E. F. (2014) 'COgnitive-pulmonary disease', *Biomed Res Int,* 2014, pp. 697825.

Comer, D. M., Kidney, J. C., Ennis, M. and Elborn, J. S. (2013) 'Airway epithelial cell apoptosis and inflammation in COPD, smokers and nonsmokers', *Eur Respir J,* 41(5), pp. 1058-67.

Condamine, T., Dominguez, G. A., Youn, J. I., Kossenkov, A. V., Mony, S., Alicea-Torres, K., Tcyganov, E., Hashimoto, A., Nefedova, Y., Lin, C., Partlova, S., Garfall, A., Vogl, D. T., Xu, X., Knight, S. C., Malietzis, G., Lee, G. H., Eruslanov, E., Albelda, S. M., Wang, X., Mehta, J. L., Bewtra, M., Rustgi, A., Hockstein, N., Witt, R., Masters, G., Nam, B., Smirnov, D., Sepulveda, M. A. and Gabrilovich, D. I. (2016) 'Lectin-type oxidized LDL receptor-1 distinguishes population of human polymorphonuclear myeloid-derived suppressor cells in cancer patients', *Sci Immunol,* 1(2).

Condliffe, A. M., Kitchen, E. and Chilvers, E. R. (1998) 'Neutrophil Priming: Pathophysiological Consequences and Underlying Mechanisms', *Clinical Science,* 94(5), pp. 461.

Conickx, G., Avila Cobos, F., van den Berge, M., Faiz, A., Timens, W., Hiemstra, P. S., Joos, G. F., Brusselle, G. G., Mestdagh, P. and Bracke, K. R. (2017) 'microRNA profiling in lung tissue and bronchoalveolar lavage of cigarette smoke-exposed mice and in COPD patients: a translational approach', *Sci Rep,* 7(1), pp. 12871.

Connor, D. E., Exner, T., Ma, D. D. and Joseph, J. E. (2010) 'The majority of circulating platelet-derived microparticles fail to bind annexin V, lack phospholipid-dependent procoagulant activity and demonstrate greater expression of glycoprotein Ib', *Thromb Haemost,* 103(5), pp. 1044-52.

Cowburn, A. S., Cadwallader, K. A., Reed, B. J., Farahi, N. and Chilvers, E. R. (2002) 'Role of PI3-kinase-dependent Bad phosphorylation and altered transcription in cytokine-mediated neutrophil survival', *Blood,* 100(7), pp. 2607-16.

Craddock, C. G., Jr., Perry, S., Ventzke, L. E. and Lawrence, J. S. (1960) 'Evaluation of marrow granulocytic reserves in normal and disease states', *Blood,* 15, pp. 840-55.

Cromwell, O., Hamid, Q., Corrigan, C. J., Barkans, J., Meng, Q., Collins, P. D. and Kay, A. B. (1992) 'Expression and generation of interleukin-8, IL-6 and granulocyte-macrophage colony-stimulating factor by bronchial epithelial cells and enhancement by IL-1 beta and tumour necrosis factor-alpha', *Immunology,* 77(3), pp. 330-7.

Culpitt, S. V., Rogers, D. F., Traves, S. L., Barnes, P. J. and Donnelly, L. E. (2005) 'Sputum matrix metalloproteases: comparison between chronic obstructive pulmonary disease and asthma', *Respiratory Medicine,* 99(6), pp. 703-710.

Curkendall, S. M., DeLuise, C., Jones, J. K., Lanes, S., Stang, M. R., Goehring, E., Jr. and She, D. (2006) 'Cardiovascular disease in patients with chronic obstructive pulmonary disease, Saskatchewan Canada cardiovascular disease in COPD patients', *Ann Epidemiol,* 16(1), pp. 63-70.

D'Armiento, J. M., Goldklang, M. P., Hardigan, A. A., Geraghty, P., Roth, M. D., Connett, J. E., Wise, R. A., Sciurba, F. C., Scharf, S. M., Thankachen, J., Islam, M., Ghio, A. J. and Foronjy, R. F. (2013) 'Increased matrix metalloproteinase (MMPs) levels do not predict disease severity or progression in emphysema', *PLoS One,* 8(2), pp. e56352.

Dalli, J., Montero-Melendez, T., Norling, L. V., Yin, X., Hinds, C., Haskard, D., Mayr, M. and Perretti, M. (2013) 'Heterogeneity in neutrophil microparticles reveals distinct proteome and functional properties', *Mol Cell Proteomics,* 12(8), pp. 2205-19.

Dalli, J., Norling, L. V., Montero-Melendez, T., Federici Canova, D., Lashin, H., Pavlov, A. M., Sukhorukov, G. B., Hinds, C. J. and Perretti, M. (2014) 'Microparticle alpha-2-macroglobulin enhances pro-resolving responses and promotes survival in sepsis', *EMBO Mol Med,* 6(1), pp. 27-42.

Dalli, J., Norling, L. V., Renshaw, D., Cooper, D., Leung, K. Y. and Perretti, M. (2008) 'Annexin 1 mediates the rapid anti-inflammatory effects of neutrophil-derived microparticles', *Blood,* 112(6), pp. 2512-9.

Dalli, J. and Serhan, C. N. (2012) 'Specific lipid mediator signatures of human phagocytes: microparticles stimulate macrophage efferocytosis and pro-resolving mediators', *Blood,* 120(15), pp. e60-72.

De Caterina, R., Sicari, R., Giannessi, D., Paggiaro, P. L., Paoletti, P., Lazzerini, G., Bernini, W., Solito, E. and Parente, L. (1993) 'Macrophage-specific eicosanoid synthesis inhibition and lipocortin-1 induction by glucocorticoids', *J Appl Physiol (1985),* 75(6), pp. 2368-75.

de Godoy, I., Donahoe, M., Calhoun, W. J., Mancino, J. and Rogers, R. M. (1996) 'Elevated TNF-alpha production by peripheral blood monocytes of weight-losing COPD patients', *Am J Respir Crit Care Med,* 153(2), pp. 633-7.

de Lucas-Ramos, P., Izquierdo-Alonso, J. L., Rodriguez-Gonzalez Moro, J. M., Frances, J. F., Lozano, P. V. and Bellon-Cano, J. M. (2012) 'Chronic obstructive pulmonary disease as a cardiovascular risk factor. Results of a case-control study (CONSISTE study)', *Int J Chron Obstruct Pulmon Dis,* 7, pp. 679-86.

De Vooght, V., Vanoirbeek, J. A., Luyts, K., Haenen, S., Nemery, B. and Hoet, P. H. (2010) 'Choice of mouse strain influences the outcome in a mouse model of chemical-induced asthma', *PLoS One,* 5(9), pp. e12581.

Decramer, M., Rennard, S., Troosters, T., Mapel, D. W., Giardino, N., Mannino, D., Wouters, E., Sethi, S. and Cooper, C. B. (2008) 'COPD as a lung disease with systemic consequences--clinical impact, mechanisms, and potential for early intervention', *Copd,* 5(4), pp. 235-56.

Dehus, O., Hartung, T. and Hermann, C. (2006) 'Endotoxin evaluation of eleven lipopolysaccharides by whole blood assay does not always correlate with Limulus amebocyte lysate assay', *J Endotoxin Res,* 12(3), pp. 171-80.

Dentener, M. A., Creutzberg, E. C., Schols, A. M., Mantovani, A., van't Veer, C., Buurman, W. A. and Wouters, E. F. (2001) 'Systemic anti-inflammatory mediators in COPD: increase in soluble interleukin 1 receptor II during treatment of exacerbations', *Thorax,* 56(9), pp. 721-6.

Deshmukh, H. S., Case, L. M., Wesselkamper, S. C., Borchers, M. T., Martin, L. D., Shertzer, H. G., Nadel, J. A. and Leikauf, G. D. (2005) 'Metalloproteinases mediate mucin 5AC expression by epidermal growth factor receptor activation', *Am J Respir Crit Care Med,* 171(4), pp. 305-14.

Devalia, J. L. and Davies, R. J. (1993) 'Airway epithelial cells and mediators of inflammation', *Respir Med: Vol. 6.* England, pp. 405-8.

Dhaliwal, K., Scholefield, E., Ferenbach, D., Gibbons, M., Duffin, R., Dorward, D. A., Morris, A. C., Humphries, D., MacKinnon, A., Wilkinson, T. S., Wallace, W. A., van Rooijen, N., Mack, M., Rossi, A. G., Davidson, D. J., Hirani, N., Hughes, J., Haslett, C. and Simpson, A. J. (2012) 'Monocytes control second-phase neutrophil emigration in established lipopolysaccharide-induced murine lung injury', *Am J Respir Crit Care Med,* 186(6), pp. 514-24.

Di Stefano, A., Capelli, A., Lusuardi, M., Balbo, P., Vecchio, C., Maestrelli, P., Mapp, C. E., Fabbri, L. M., Donner, C. F. and Saetta, M. (1998) 'Severity of airflow limitation is associated with severity of airway inflammation in smokers', *Am J Respir Crit Care Med,* 158(4), pp. 1277-85.

Dicker, A. J., Crichton, M. L., Pumphrey, E. G., Cassidy, A. J., Suarez-Cuartin, G., Sibila, O., Furrie, E., Fong, C. J., Ibrahim, W., Brady, G., Einarsson, G. G., Elborn, J. S., Schembri, S., Marshall, S. E., Palmer, C. N. A. and Chalmers, J. D. (2018) 'Neutrophil extracellular traps are associated with disease severity and microbiota diversity in patients with chronic obstructive pulmonary disease', *J Allergy Clin Immunol,* 141(1), pp. 117-127.

Dieker, J., Tel, J., Pieterse, E., Thielen, A., Rother, N., Bakker, M., Fransen, J., Dijkman, H. B., Berden, J. H., de Vries, J. M., Hilbrands, L. B. and van der Vlag, J. (2016) 'Circulating Apoptotic Microparticles in Systemic Lupus Erythematosus Patients Drive the Activation of Dendritic Cell Subsets and Prime Neutrophils for NETosis', *Arthritis Rheumatol,* 68(2), pp. 462-72.

Ding, Y., Shen, S., Lino, A. C., Curotto de Lafaille, M. A. and Lafaille, J. J. (2008) 'Beta-catenin stabilization extends regulatory T cell survival and induces anergy in nonregulatory T cells', *Nat Med,* 14(2), pp. 162-9.

Divo, M., Cote, C., de Torres, J. P., Casanova, C., Marin, J. M., Pinto-Plata, V., Zulueta, J., Cabrera, C., Zagaceta, J., Hunninghake, G. and Celli, B. (2012) 'Comorbidities and risk of mortality in patients with chronic obstructive pulmonary disease', *Am J Respir Crit Care Med,* 186(2), pp. 155-61.

Doerner, A. M., Chen, L. Y., Ye, R. D., Yong, J., Huang, S. and Pan, Z. K. (2011) 'Cell type-specific release of matrix-metallo-proteinase-9 by bacterial chemoattractant in human blood phagocytic leukocytes', *Int J Clin Exp Med,* 4(1), pp. 67-73.

Doerschuk, C. M. (2000) 'Leukocyte trafficking in alveoli and airway passages', *Respir Res,* 1(3), pp. 136-40.

Doerschuk, C. M., Beyers, N., Coxson, H. O., Wiggs, B. and Hogg, J. C. (1993) 'Comparison of neutrophil and capillary diameters and their relation to neutrophil sequestration in the lung', *J Appl Physiol (1985),* 74(6), pp. 3040-5.

Doi, M., Nakano, K., Hiramoto, T. and Kohno, N. (2003) 'Significance of pulmonary artery pressure in emphysema patients with mild-to-moderate hypoxemia', *Respir Med,* 97(8), pp. 915-20.

Dorrington, M. G. and Fraser, I. D. C. (2019) 'NF-κB Signaling in Macrophages: Dynamics, Crosstalk, and Signal Integration', *Frontiers in Immunology,* 10(705).

Dorward, D. A., Lucas, C. D., Chapman, G. B., Haslett, C., Dhaliwal, K. and Rossi, A. G. (2015) 'The role of formylated peptides and formyl peptide receptor 1 in governing neutrophil function during acute inflammation', *Am J Pathol,* 185(5), pp. 1172-84.

Downey, G. P., Worthen, G. S., Henson, P. M. and Hyde, D. M. (1993) 'NEUTROPHIL SEQUESTRATION AND MIGRATION IN LOCALIZED PULMONARY INFLAMMATION - CAPILLARY LOCALIZATION AND MIGRATION ACROSS THE INTERALVEOLAR SEPTUM', *American Review of Respiratory Disease,* 147(1), pp. 168-176.

Dragovic, R. A., Southcombe, J. H., Tannetta, D. S., Redman, C. W. and Sargent, I. L. (2013) 'Multicolor flow cytometry and nanoparticle tracking analysis of extracellular vesicles in the plasma of normal pregnant and pre-eclamptic women', *Biol Reprod,* 89(6), pp. 151.

Du, W., Liu, J., Zhou, J., Ye, D., OuYang, Y. and Deng, Q. (2018) 'Obstructive sleep apnea, COPD, the overlap syndrome, and mortality: results from the 2005-2008 National Health and Nutrition Examination Survey', *Int J Chron Obstruct Pulmon Dis,* 13, pp. 665-674.

Duffney, P. F., Embong, A. K., McGuire, C. C., Thatcher, T. H., Phipps, R. P. and Sime, P. J. (2020) 'Cigarette smoke increases susceptibility to infection in lung epithelial cells by upregulating caveolin-dependent endocytosis', *PLoS One,* 15(5), pp. e0232102.

Dye, J. A. and Adler, K. B. (1994) 'Effects of cigarette smoke on epithelial cells of the respiratory tract', *Thorax,* 49(8), pp. 825-34.

Ebaid, H. (2014) 'Neutrophil depletion in the early inflammatory phase delayed cutaneous wound healing in older rats: improvements due to the use of un-denatured camel whey protein', *Diagn Pathol,* 9, pp. 46.

Eken, C., Gasser, O., Zenhaeusern, G., Oehri, I., Hess, C. and Schifferli, J. A. (2008) 'Polymorphonuclear neutrophil-derived ectosomes interfere with the maturation of monocyte-derived dendritic cells', *J Immunol,* 180(2), pp. 817-24.

Eken, C., Martin, P. J., Sadallah, S., Treves, S., Schaller, M. and Schifferli, J. A. (2010) 'Ectosomes released by polymorphonuclear neutrophils induce a MerTK-dependent anti-inflammatory pathway in macrophages', *J Biol Chem,* 285(51), pp. 39914-21.

Eken, C., Sadallah, S., Martin, P. J., Treves, S. and Schifferli, J. A. (2013) 'Ectosomes of polymorphonuclear neutrophils activate multiple signaling pathways in macrophages', *Immunobiology,* 218(3), pp. 382-92.

Ekpenyong, A. E., Toepfner, N., Chilvers, E. R. and Guck, J. (2015) 'Mechanotransduction in neutrophil activation and deactivation', *Biochimica et Biophysica Acta (BBA) - Molecular Cell Research,* 1853(11), pp. 3105-3116.

Elbehairy, A. F., Ciavaglia, C. E., Webb, K. A., Guenette, J. A., Jensen, D., Mourad, S. M., Neder, J. A. and O'Donnell, D. E. (2015) 'Pulmonary Gas Exchange Abnormalities in Mild Chronic Obstructive Pulmonary Disease. Implications for Dyspnea and Exercise Intolerance', *Am J Respir Crit Care Med,* 191(12), pp. 1384-94.

Elliott, M. R., Chekeni, F. B., Trampont, P. C., Lazarowski, E. R., Kadl, A., Walk, S. F., Park, D., Woodson, R. I., Ostankovich, M., Sharma, P., Lysiak, J. J., Harden, T. K., Leitinger, N. and Ravichandran, K. S. (2009) 'Nucleotides released by apoptotic cells act as a find-me signal to promote phagocytic clearance', *Nature,* 461(7261), pp. 282-6.

Elwing, J. and Panos, R. J. (2008) 'Pulmonary hypertension associated with COPD', *Int J Chron Obstruct Pulmon Dis,* 3(1), pp. 55-70.

Enjeti, A. K., Lincz, L. F. and Seldon, M. (2008) 'Microparticles in health and disease', *Semin Thromb Hemost,* 34(7), pp. 683-91.

Eri, R. D., Adams, R. J., Tran, T. V., Tong, H., Das, I., Roche, D. K., Oancea, I., Png, C. W., Jeffery, P. L., Radford-Smith, G. L., Cook, M. C., Florin, T. H. and McGuckin, M. A. (2011) 'An intestinal epithelial defect conferring ER stress results in inflammation involving both innate and adaptive immunity', *Mucosal Immunol,* 4(3), pp. 354-64.

Eutamene, H., Theodorou, V., Schmidlin, F., Tondereau, V., Garcia-Villar, R., Salvador-Cartier, C., Chovet, M., Bertrand, C. and Bueno, L. (2005) 'LPS-induced lung inflammation is linked to increased epithelial permeability: role of MLCK', *Eur Respir J,* 25(5), pp. 789-96.

Fabbri, L. M. and Rabe, K. F. (2007) 'From COPD to chronic systemic inflammatory syndrome?', *Lancet,* 370(9589), pp. 797-9.

Fadok, V. A., Voelker, D. R., Campbell, P. A., Cohen, J. J., Bratton, D. L. and Henson, P. M. (1992) 'Exposure of phosphatidylserine on the surface of apoptotic lymphocytes triggers specific recognition and removal by macrophages', *J Immunol,* 148(7), pp. 2207-16.

Faille, D., El-Assaad, F., Mitchell, A. J., Alessi, M. C., Chimini, G., Fusai, T., Grau, G. E. and Combes, V. (2012) 'Endocytosis and intracellular processing of platelet microparticles by brain endothelial cells', *J Cell Mol Med,* 16(8), pp. 1731-8.

Fialkow, L., Wang, Y. and Downey, G. P. (2007) 'Reactive oxygen and nitrogen species as signaling molecules regulating neutrophil function', *Free Radic Biol Med,* 42(2), pp. 153-64.

Fink, K., Feldbrugge, L., Schwarz, M., Bourgeois, N., Helbing, T., Bode, C., Schwab, T. and Busch, H. J. (2011) 'Circulating annexin V positive microparticles in patients after successful cardiopulmonary resuscitation', *Crit Care,* 15(5), pp. R251.

Finlay, G. A., Russell, K. J., McMahon, K. J., D'arcy, E. M., Masterson, J. B., FitzGerald, M. X. and O'Connor, C. M. (1997) 'Elevated levels of matrix metalloproteinases in bronchoalveolar lavage fluid of emphysematous patients', *Thorax,* 52.

Fischer, B. M. and Voynow, J. A. (2002) 'Neutrophil elastase induces MUC5AC gene expression in airway epithelium via a pathway involving reactive oxygen species', *Am J Respir Cell Mol Biol,* 26(4), pp. 447-52.

Fitzgerald, K. A., Rowe, D. C., Barnes, B. J., Caffrey, D. R., Visintin, A., Latz, E., Monks, B., Pitha, P. M. and Golenbock, D. T. (2003) 'LPS-TLR4 signaling to IRF-3/7 and NF-kappaB involves the toll adapters TRAM and TRIF', *J Exp Med,* 198(7), pp. 1043-55.

Florence, J. M., Krupa, A., Booshehri, L. M., Allen, T. C. and Kurdowska, A. K. (2017) 'Metalloproteinase-9 contributes to endothelial dysfunction in atherosclerosis via protease activated receptor-1', *PLoS One,* 12(2), pp. e0171427.

Folkesson, M., Li, C., Frebelius, S., Swedenborg, J., Wagsater, D., Williams, K. J., Eriksson, P., Roy, J. and Liu, M. L. (2015) 'Proteolytically active ADAM10 and ADAM17 carried on membrane microvesicles in human abdominal aortic aneurysms', *Thromb Haemost,* 114(6), pp. 1165-74.

Foronjy, R., Nkyimbeng, T., Wallace, A., Thankachen, J., Okada, Y., Lemaitre, V. and D'Armiento, J. (2008) 'Transgenic expression of matrix metalloproteinase-9 causes adult-onset emphysema in mice associated with the loss of alveolar elastin', *Am J Physiol Lung Cell Mol Physiol,* 294(6), pp. L1149-57.

Forteza, R. M., Casalino-Matsuda, S. M., Falcon, N. S., Valencia Gattas, M. and Monzon, M. E. (2012) 'Hyaluronan and layilin mediate loss of airway epithelial barrier function induced by cigarette smoke by decreasing E-cadherin', *J Biol Chem,* 287(50), pp. 42288-98.

Fox, S., Leitch, A. E., Duffin, R., Haslett, C. and Rossi, A. G. (2010) 'Neutrophil apoptosis: relevance to the innate immune response and inflammatory disease', *J Innate Immun,* 2(3), pp. 216-27.

Foxman, E. F., Campbell, J. J. and Butcher, E. C. (1997) 'Multistep navigation and the combinatorial control of leukocyte chemotaxis', *J Cell Biol,* 139(5), pp. 1349-60.

Francis, N., Wong, S. H., Hampson, P., Wang, K., Young, S. P., Deigner, H. P., Salmon, M., Scheel-Toellner, D. and Lord, J. M. (2011) 'Lactoferrin inhibits neutrophil apoptosis via blockade of proximal apoptotic signaling events', *Biochimica et Biophysica Acta (BBA) - Molecular Cell Research,* 1813(10), pp. 1822-1826.

Fridman, R., Toth, M., Pena, D. and Mobashery, S. (1995) 'Activation of progelatinase B (MMP-9) by gelatinase A (MMP-2)', *Cancer Res,* 55(12), pp. 2548-55.

Friedman, G. D., Siegelaub, A. B., Seltzer, C. C., Feldman, R. and Collen, M. F. (1973) 'Smoking habits and the leukocyte count', *Arch Environ Health,* 26(3), pp. 137-43.

Friedrichs, B., Neumann, U., Schuller, J. and Peck, M. J. (2014) 'Cigarette-smoke-induced priming of neutrophils from smokers and non-smokers for increased oxidative burst response is mediated by TNF-alpha', *Toxicol In Vitro,* 28(7), pp. 1249-58.

Fujisawa, T., Velichko, S., Thai, P., Hung, L. Y., Huang, F. and Wu, R. (2009) 'Regulation of airway MUC5AC expression by IL-1beta and IL-17A; the NF-kappaB paradigm', *J Immunol,* 183(10), pp. 6236-43.

Furze, R. C. and Rankin, S. M. (2008) 'Neutrophil mobilization and clearance in the bone marrow', *Immunology,* 125(3), pp. 281-8.

Galie, N., Humbert, M., Vachiery, J. L., Gibbs, S., Lang, I., Torbicki, A., Simonneau, G., Peacock, A., Vonk Noordegraaf, A., Beghetti, M., Ghofrani, A., Gomez Sanchez, M. A., Hansmann, G., Klepetko, W., Lancellotti, P., Matucci, M., McDonagh, T., Pierard, L. A., Trindade, P. T., Zompatori, M. and Hoeper, M. (2015) '2015 ESC/ERS Guidelines for the diagnosis and treatment of pulmonary hypertension: The Joint Task Force for the Diagnosis and Treatment of Pulmonary Hypertension of the European Society of Cardiology (ESC) and the European Respiratory Society (ERS): Endorsed by: Association for European Paediatric and Congenital Cardiology (AEPC), International Society for Heart and Lung Transplantation (ISHLT)', *Eur Respir J,* 46(4), pp. 903-75.

Galluzzi, L. and Vitale, I. and Aaronson, S. A. and Abrams, J. M. and Adam, D. and Agostinis, P. and Alnemri, E. S. and Altucci, L. and Amelio, I. and Andrews, D. W. and Annicchiarico-Petruzzelli, M. and Antonov, A. V. and Arama, E. and Baehrecke, E. H. and Barlev, N. A. and Bazan, N. G. and Bernassola, F. and Bertrand, M. J. M. and Bianchi, K. and Blagosklonny, M. V. and Blomgren, K. and Borner, C. and Boya, P. and Brenner, C. and Campanella, M. and Candi, E. and Carmona-Gutierrez, D. and Cecconi, F. and Chan, F. K. and Chandel, N. S. and Cheng, E. H. and Chipuk, J. E. and Cidlowski, J. A. and Ciechanover, A. and Cohen, G. M. and Conrad, M. and Cubillos-Ruiz, J. R. and Czabotar, P. E. and D'Angiolella, V. and Dawson, T. M. and Dawson, V. L. and De Laurenzi, V. and De Maria, R. and Debatin, K. M. and DeBerardinis, R. J. and Deshmukh, M. and Di Daniele, N. and Di Virgilio, F. and Dixit, V. M. and Dixon, S. J. and Duckett, C. S. and Dynlacht, B. D. and El-Deiry, W. S. and Elrod, J. W. and Fimia, G. M. and Fulda, S. and Garcia-Saez, A. J. and Garg, A. D. and Garrido, C.

and Gavathiotis, E. and Golstein, P. and Gottlieb, E. and Green, D. R. and Greene, L. A. and Gronemeyer, H. and Gross, A. and Hajnoczky, G. and Hardwick, J. M. and Harris, I. S. and Hengartner, M. O. and Hetz, C. and Ichijo, H. and Jaattela, M. and Joseph, B. and Jost, P. J. and Juin, P. P. and Kaiser, W. J. and Karin, M. and Kaufmann, T. and Kepp, O. and Kimchi, A. and Kitsis, R. N. and Klionsky, D. J. and Knight, R. A. and Kumar, S. and Lee, S. W. and Lemasters, J. J. and Levine, B. and Linkermann, A. and Lipton, S. A. and Lockshin, R. A. and Lopez-Otin, C. and Lowe, S. W. and Luedde, T. and Lugli, E. and MacFarlane, M. and Madeo, F. and Malewicz, M. and Malorni, W. and Manic, G. and Marine, J. C. and Martin, S. J. and Martinou, J. C. and Medema, J. P. and Mehlen, P. and Meier, P. and Melino, S. and Miao, E. A. and Molkentin, J. D. and Moll, U. M. and Munoz-Pinedo, C. and Nagata, S. and Nunez, G. and Oberst, A. and Oren, M. and Overholtzer, M. and Pagano, M. and Panaretakis, T. and Pasparakis, M. and Penninger, J. M. and Pereira, D. M. and Pervaiz, S. and Peter, M. E. and Piacentini, M. and Pinton, P. and Prehn, J. H. M. and Puthalakath, H. and Rabinovich, G. A. and Rehm, M. and Rizzuto, R. and Rodrigues, C. M. P. and Rubinsztein, D. C. and Rudel, T. and Ryan, K. M. and Sayan, E. and Scorrano, L. and Shao, F. and Shi, Y. and Silke, J. and Simon, H. U. and Sistigu, A. and Stockwell, B. R. and Strasser, A. and Szabadkai, G. and Tait, S. W. G. and Tang, D. and Tavernarakis, N. and Thorburn, A. and Tsujimoto, Y. and Turk, B. and Vanden Berghe, T. and Vandenabeele, P. and Vander Heiden, M. G. and Villunger, A. and Virgin, H. W. and Vousden, K. H. and Vucic, D. and Wagner, E. F. and Walczak, H. and Wallach, D. and Wang, Y. and Wells, J. A. and Wood, W. and Yuan, J. and Zakeri, Z. and Zhivotovsky, B. and Zitvogel, L. and Melino, G. and Kroemer, G. (2018) 'Molecular mechanisms of cell death: recommendations of the Nomenclature Committee on Cell Death 2018', *Cell Death Differ,* 25(3), pp. 486-541.

Gan, W. Q., Man, S. F., Senthilselvan, A. and Sin, D. D. (2004) 'Association between chronic obstructive pulmonary disease and systemic inflammation: a systematic review and a meta-analysis', *Thorax,* 59(7), pp. 574-80.

Gao, J., Iwamoto, H., Koskela, J., Alenius, H., Hattori, N., Kohno, N., Laitinen, T., Mazur, W. and Pulkkinen, V. (2016) 'Characterization of sputum biomarkers for asthma-COPD overlap syndrome', *Int J Chron Obstruct Pulmon Dis,* 11, pp. 2457-2465.

Gasiuniene, E., Lavinskiene, S., Sakalauskas, R. and Sitkauskiene, B. (2016) 'Levels of IL-32 in Serum, Induced Sputum Supernatant, and Bronchial Lavage Fluid of Patients with Chronic Obstructive Pulmonary Disease', *Copd,* 13(5), pp. 569-75.

Gasse, P., Riteau, N., Charron, S., Girre, S., Fick, L., Petrilli, V., Tschopp, J., Lagente, V., Quesniaux, V. F., Ryffel, B. and Couillin, I. (2009) 'Uric acid is a danger signal activating NALP3 inflammasome in lung injury inflammation and fibrosis', *Am J Respir Crit Care Med,* 179(10), pp. 903-13.

Gasser, O., Hess, C., Miot, S., Deon, C., Sanchez, J. C. and Schifferli, J. A. (2003) 'Characterisation and properties of ectosomes released by human polymorphonuclear neutrophils', *Experimental Cell Research,* 285(2), pp. 243-257.

Gasser, O. and Schifferli, J. A. (2004) 'Activated polymorphonuclear neutrophils disseminate anti-inflammatory microparticles by ectocytosis', *Blood,* 104(8), pp. 2543-8.

Gebb, S. A., Graham, J. A., Hanger, C. C., Godbey, P. S., Capen, R. L., Doerschuk, C. M. and Wagner, W. W., Jr. (1995) 'Sites of leukocyte sequestration in the pulmonary microcirculation', *J Appl Physiol (1985),* 79(2), pp. 493-7.

Gelb, A. F., Gobel, P. H., Fairshter, R. and Zamel, N. (1981) 'Predominant site of airway resistance in chronic obstructive pulmonary disease', *Chest,* 79(3), pp. 273-6.

Genschmer, K. R., Russell, D. W., Lal, C., Szul, T., Bratcher, P. E., Noerager, B. D., Abdul Roda, M., Xu, X., Rezonzew, G., Viera, L., Dobosh, B. S., Margaroli, C., Abdalla, T. H., King, R. W., McNicholas, C. M., Wells, J. M., Dransfield, M. T., Tirouvanziam, R., Gaggar, A. and Blalock, J. E. (2019) 'Activated PMN Exosomes: Pathogenic Entities Causing Matrix Destruction and Disease in the Lung', *Cell,* 176(1-2), pp. 113-126.e15.

Georas, S. N. and Rezaee, F. (2014) 'Epithelial barrier function: at the front line of asthma immunology and allergic airway inflammation', *J Allergy Clin Immunol,* 134(3), pp. 509-20.

Ghosh, A., Coakley, R. D., Ghio, A. J., Muhlebach, M. S., Esther, C. R., Jr., Alexis, N. E. and Tarran, R. (2019) 'Chronic E-Cigarette Use Increases Neutrophil Elastase and Matrix Metalloprotease Levels in the Lung', *Am J Respir Crit Care Med,* 200(11), pp. 1392-1401.

GOLD, G. I. f. C. O. P. D. (2018) *Pocket Guide to COPD Diagnosis, Management, and Prevention. A Guide for Healthcare Professionals. 2018 Edition.*, goldcopd.org.

Gomez, I., Ward, B., Souilhol, C., Recarti, C., Ariaans, M., Johnston, J., Burnett, A., Mahmoud, M., Luong, L. A., West, L., Long, M., Parry, S., Woods, R., Hulston, C., Benedikter, B., Bazaz, R.,

Francis, S., Kiss-Toth, E., van Zandvoort, M., Schober, A., Hellewell, P., Evans, P. C. and Ridger, V. (2018) 'Neutrophil microvesicles drive atherosclerosis by delivering miR-155 to atheroprone endothelium', *bioRxiv*, pp. 319392.

Gomez, I., Ward, B., Souilhol, C., Recarti, C., Ariaans, M., Johnston, J., Burnett, A., Mahmoud, M., Luong, L. A., West, L., Long, M., Parry, S., Woods, R., Hulston, C., Benedikter, B., Niespolo, C., Bazaz, R., Francis, S., Kiss-Toth, E., van Zandvoort, M., Schober, A., Hellewell, P., Evans, P. C. and Ridger, V. (2020) 'Neutrophil microvesicles drive atherosclerosis by delivering miR-155 to atheroprone endothelium', *Nat Commun,* 11(1), pp. 214.

Gouin, K., Peck, K., Antes, T., Johnson, J. L., Li, C., Vaturi, S. D., Middleton, R., de Couto, G., Walravens, A. S., Rodriguez-Borlado, L., Smith, R. R., Marbán, L., Marbán, E. and Ibrahim, A. G. (2017) 'A comprehensive method for identification of suitable reference genes in extracellular vesicles', *J Extracell Vesicles,* 6(1), pp. 1347019.

Grabiec, A. M. and Hussell, T. (2016) 'The role of airway macrophages in apoptotic cell clearance following acute and chronic lung inflammation', *Semin Immunopathol,* 38(4), pp. 409-23.

Gresele, P., Dottorini, M., Selli, M. L., Iannacci, L., Canino, S., Todisco, T., Romano, S., Crook, P., Page, C. P. and Nenci, G. G. (1993) 'Altered platelet function associated with the bronchial hyperresponsiveness accompanying nocturnal asthma', *J Allergy Clin Immunol,* 91(4), pp. 894-902.

Grommes, J. and Soehnlein, O. (2011) 'Contribution of neutrophils to acute lung injury', *Mol Med,* 17(3-4), pp. 293-307.

Gross, J. C., Chaudhary, V., Bartscherer, K. and Boutros, M. (2012) 'Active Wnt proteins are secreted on exosomes', *Nat Cell Biol,* 14(10), pp. 1036-45.

Grudzinska, F. S., Brodlie, M., Scholefield, B. R., Jackson, T., Scott, A., Thickett, D. R. and Sapey, E. (2020) 'Neutrophils in community-acquired pneumonia: parallels in dysfunction at the extremes of age', *Thorax,* 75(2), pp. 164-171.

Guervilly, C., Lacroix, R., Forel, J.-M., Roch, A., Camoin-Jau, L., Papazian, L. and Dignat-George, F. (2011) 'High levels of circulating leukocyte microparticles are associated with better outcome in acute respiratory distress syndrome', *Critical Care,* 15(1).

Gunay, E., Sarinc Ulasli, S., Akar, O., Ahsen, A., Gunay, S., Koyuncu, T. and Unlu, M. (2014) 'Neutrophil-to-lymphocyte ratio in chronic obstructive pulmonary disease: a retrospective study', *Inflammation,* 37(2), pp. 374-80.

Guo, L., Wang, T., Wu, Y., Yuan, Z., Dong, J., Li, X., An, J., Liao, Z., Zhang, X., Xu, D. and Wen, F. Q. (2016) 'WNT/beta-catenin signaling regulates cigarette smoke-induced airway inflammation via the PPARdelta/p38 pathway', *Lab Invest,* 96(2), pp. 218-29.

Guo, W., Wang, P., Liu, Z. H. and Ye, P. (2018) 'Analysis of differential expression of tight junction proteins in cultured oral epithelial cells altered by Porphyromonas gingivalis, Porphyromonas gingivalis lipopolysaccharide, and extracellular adenosine triphosphate', *Int J Oral Sci,* 10(1), pp. e8.

Guthrie, L. A., McPhail, L. C., Henson, P. M. and Johnston, R. B., Jr. (1984) 'Priming of neutrophils for enhanced release of oxygen metabolites by bacterial lipopolysaccharide. Evidence for increased activity of the superoxide-producing enzyme', *J Exp Med,* 160(6), pp. 1656-71.

Guzik, K., Skret, J., Smagur, J., Bzowska, M., Gajkowska, B., Scott, D. A. and Potempa, J. S. (2011) 'Cigarette smoke-exposed neutrophils die unconventionally but are rapidly phagocytosed by macrophages', *Cell Death Dis,* 2, pp. e131.

Hackett, T. L. (2012) 'Epithelial-mesenchymal transition in the pathophysiology of airway remodelling in asthma', *Curr Opin Allergy Clin Immunol,* 12(1), pp. 53-9.

Hamacher, J., Sadallah, S., Schifferli, J. A., Villard, J. and Nicod, L. P. (1998) 'Soluble complement receptor type 1 (CD35) in bronchoalveolar lavage of inflammatory lung diseases', *Eur Respir J,* 11(1), pp. 112-9.

Headland, S. E., Jones, H. R., Norling, L. V., Kim, A., Souza, P. R., Corsiero, E., Gil, C. D., Nerviani, A., Dell'Accio, F., Pitzalis, C., Oliani, S. M., Jan, L. Y. and Perretti, M. (2015) 'Neutrophil-derived microvesicles enter cartilage and protect the joint in inflammatory arthritis', *Sci Transl Med,* 7(315), pp. 315ra190.

Heijink, I. H., Brandenburg, S. M., Postma, D. S. and van Oosterhout, A. J. (2012) 'Cigarette smoke impairs airway epithelial barrier function and cell-cell contact recovery', *Eur Respir J,* 39(2), pp. 419-28.

Heijink, I. H., Kies, P. M., Kauffman, H. F., Postma, D. S., van Oosterhout, A. J. and Vellenga, E. (2007) 'Down-regulation of E-cadherin in human bronchial epithelial cells leads to epidermal growth factor receptor-dependent Th2 cell-promoting activity', *J Immunol,* 178(12), pp. 7678-85.

Heijink, I. H., Noordhoek, J. A., Timens, W., van Oosterhout, A. J. and Postma, D. S. (2014) 'Abnormalities in airway epithelial junction formation in chronic obstructive pulmonary disease', *Am J Respir Crit Care Med,* 189(11), pp. 1439-42.

Hellewell, P. G., Young, S. K., Henson, P. M. and Worthen, G. S. (1994) 'Disparate role of the beta 2-integrin CD18 in the local accumulation of neutrophils in pulmonary and cutaneous inflammation in the rabbit', *Am J Respir Cell Mol Biol,* 10(4), pp. 391-8.

Hendershot, L. M. (2004) 'The ER function BiP is a master regulator of ER function', *Mt Sinai J Med,* 71(5), pp. 289-97.

Henke, M. O., John, G., Rheineck, C., Chillappagari, S., Naehrlich, L. and Rubin, B. K. (2011) 'Serine proteases degrade airway mucins in cystic fibrosis', *Infect Immun,* 79(8), pp. 3438-44.

Hess, C., Sadallah, S., Hefti, A., Landmann, R. and Schifferli, J. A. (1999) 'Ectosomes released by human neutrophils are specialized functional units', *J Immunol,* 163(8), pp. 4564-73.

Hiemstra, P. S., McCray, P. B., Jr. and Bals, R. (2015) 'The innate immune function of airway epithelial cells in inflammatory lung disease', *Eur Respir J,* 45(4), pp. 1150-62.

Higham, A., Rattray, N. J., Dewhurst, J. A., Trivedi, D. K., Fowler, S. J., Goodacre, R. and Singh, D. (2016) 'Electronic cigarette exposure triggers neutrophil inflammatory responses', *Respir Res,* 17(1), pp. 56.

Hodge, S., Hodge, G., Ahern, J., Jersmann, H., Holmes, M. and Reynolds, P. N. (2007) 'Smoking alters alveolar macrophage recognition and phagocytic ability: implications in chronic obstructive pulmonary disease', *Am J Respir Cell Mol Biol,* 37(6), pp. 748-55.

Hodge, S., Hodge, G., Holmes, M. and Reynolds, P. N. (2005) 'Increased airway epithelial and T-cell apoptosis in COPD remains despite smoking cessation', *Eur Respir J,* 25(3), pp. 447-54.

Hodge, S., Hodge, G., Scicchitano, R., Reynolds, P. N. and Holmes, M. (2003) 'Alveolar macrophages from subjects with chronic obstructive pulmonary disease are deficient in their ability to phagocytose apoptotic airway epithelial cells', *Immunol Cell Biol,* 81(4), pp. 289-96.

Hoenderdos, K., Lodge, K. M., Hirst, R. A., Chen, C., Palazzo, S. G., Emerenciana, A., Summers, C., Angyal, A., Porter, L., Juss, J. K., O'Callaghan, C., Chilvers, E. R. and Condliffe, A. M. (2016) 'Hypoxia upregulates neutrophil degranulation and potential for tissue injury', *Thorax,* 71(11), pp. 1030-1038.

Hoeper, M. M., Bogaard, H. J., Condliffe, R., Frantz, R., Khanna, D., Kurzyna, M., Langleben, D., Manes, A., Satoh, T., Torres, F., Wilkins, M. R. and Badesch, D. B. (2013) 'Definitions and diagnosis of pulmonary hypertension', *J Am Coll Cardiol,* 62(25 Suppl), pp. D42-50.

Hoeper, M. M., Humbert, M., Souza, R., Idrees, M., Kawut, S. M., Sliwa-Hahnle, K., Jing, Z. C. and Gibbs, J. S. (2016) 'A global view of pulmonary hypertension', *Lancet Respir Med,* 4(4), pp. 306-22.

Hofman, P., d'Andrea, L., Guzman, E., Selva, E., Le Negrate, G., Far, D. F., Lemichez, E., Boquet, P. and Rossi, B. (1999) 'Neutrophil F-actin and myosin but not microtubules functionally regulate transepithelial migration induced by interleukin 8 across a cultured intestinal epithelial monolayer', *Eur Cytokine Netw,* 10(2), pp. 227-36.

Hogg, J. C., Chu, F., Utokaparch, S., Woods, R., Elliott, W. M., Buzatu, L., Cherniack, R. M., Rogers, R. M., Sciurba, F. C., Coxson, H. O. and Pare, P. D. (2004) 'The nature of small-airway obstruction in chronic obstructive pulmonary disease', *N Engl J Med,* 350(26), pp. 2645-53.

Hollingsworth, J. W., Chen, B. J., Brass, D. M., Berman, K., Gunn, M. D., Cook, D. N. and Schwartz, D. A. (2005) 'The critical role of hematopoietic cells in lipopolysaccharide-induced airway inflammation', *Am J Respir Crit Care Med,* 171(8), pp. 806-13.

Hong, D., Kurzrock, R., Kim, Y., Woessner, R., Younes, A., Nemunaitis, J., Fowler, N., Zhou, T., Schmidt, J., Jo, M., Lee, S. J., Yamashita, M., Hughes, S. G., Fayad, L., Piha-Paul, S., Nadella, M. V., Mohseni, M., Lawson, D., Reimer, C., Blakey, D. C., Xiao, X., Hsu, J., Revenko, A., Monia, B. P. and MacLeod, A. R. (2015) 'AZD9150, a next-generation antisense oligonucleotide inhibitor of STAT3 with early evidence of clinical activity in lymphoma and lung cancer', *Sci Transl Med,* 7(314), pp. 314ra185.

Hong, J. S., Greenlee, K. J., Pitchumani, R., Lee, S. H., Song, L. Z., Shan, M., Chang, S. H., Park, P. W., Dong, C., Werb, Z., Bidani, A., Corry, D. B. and Kheradmand, F. (2011) 'Dual protective mechanisms of matrix metalloproteinases 2 and 9 in immune defense against Streptococcus pneumoniae', *J Immunol,* 186(11), pp. 6427-36.

Hong, Y., Eleftheriou, D., Hussain, A. A., Price-Kuehne, F. E., Savage, C. O., Jayne, D., Little, M. A., Salama, A. D., Klein, N. J. and Brogan, P. A. (2012) 'Anti-neutrophil cytoplasmic antibodies stimulate release of neutrophil microparticles', *J Am Soc Nephrol,* 23(1), pp. 49-62.

Hosseinzadeh, S., Noroozian, M., Mortaz, E. and Mousavizadeh, K. (2018) 'Plasma microparticles in Alzheimer's disease: The role of vascular dysfunction', *Metab Brain Dis,* 33(1), pp. 293-299.

Houghton, A. M. (2015) 'Matrix metalloproteinases in destructive lung disease', *Matrix Biol,* 44-46, pp. 167-74.

Houghton, A. M., Quintero, P. A., Perkins, D. L., Kobayashi, D. K., Kelley, D. G., Marconcini, L. A., Mecham, R. P., Senior, R. M. and Shapiro, S. D. (2006) 'Elastin fragments drive disease progression in a murine model of emphysema', *J Clin Invest,* 116(3), pp. 753-9.

Houssaini, A., Breau, M., Kebe, K., Abid, S., Marcos, E., Lipskaia, L., Rideau, D., Parpaleix, A., Huang, J., Amsellem, V., Vienney, N., Validire, P., Maitre, B., Attwe, A., Lukas, C., Vindrieux, D., Boczkowski, J., Derumeaux, G., Pende, M., Bernard, D., Meiners, S. and Adnot, S. (2018) 'mTOR pathway activation drives lung cell senescence and emphysema', *JCI Insight,* 3(3).

Hsieh, M. M., Everhart, J. E., Byrd-Holt, D. D., Tisdale, J. F. and Rodgers, G. P. (2007) 'Prevalence of neutropenia in the U.S. population: age, sex, smoking status, and ethnic differences', *Ann Intern Med,* 146(7), pp. 486-92.

Hughes, J. E., Stewart, J., Barclay, G. R. and Govan, J. R. (1997) 'Priming of neutrophil respiratory burst activity by lipopolysaccharide from Burkholderia cepacia', *Infect Immun,* 65(10), pp. 4281-7.

Hung, L. Y., Sen, D., Oniskey, T. K., Katzen, J., Cohen, N. A., Vaughan, A. E., Nieves, W., Urisman, A., Beers, M. F., Krummel, M. F. and Herbert, D. R. (2019) 'Macrophages promote epithelial proliferation following infectious and non-infectious lung injury through a Trefoil factor 2-dependent mechanism', *Mucosal Immunol,* 12(1), pp. 64-76.

Hurst, J. R., Perera, W. R., Wilkinson, T. M., Donaldson, G. C. and Wedzicha, J. A. (2006) 'Systemic and upper and lower airway inflammation at exacerbation of chronic obstructive pulmonary disease', *Am J Respir Crit Care Med,* 173(1), pp. 71-8.

Huynh, M. L., Fadok, V. A. and Henson, P. M. (2002) 'Phosphatidylserine-dependent ingestion of apoptotic cells promotes TGF-beta1 secretion and the resolution of inflammation', *J Clin Invest,* 109(1), pp. 41-50.

Hwang, J. W., Kim, J. H., Kim, H. J., Choi, I. H., Han, H. M., Lee, K. J., Kim, T. H. and Lee, S. H. (2019) 'Neutrophil extracellular traps in nasal secretions of patients with stable and exacerbated chronic rhinosinusitis and their contribution to induce chemokine secretion and strengthen the epithelial barrier', *Clin Exp Allergy,* 49(10), pp. 1306-1320.

Ilumets, H., Rytila, P., Demedts, I., Brusselle, G. G., Sovijarvi, A., Myllarniemi, M., Sorsa, T. and Kinnula, V. L. (2007) 'Matrix metalloproteinases -8, -9 and -12 in smokers and patients with stage 0 COPD', *Int J Chron Obstruct Pulmon Dis,* 2(3), pp. 369-79.

Imai, K., Mercer, B. A., Schulman, L. L., Sonett, J. R. and D'Armiento, J. M. (2005) 'Correlation of lung surface area to apoptosis and proliferation in human emphysema', *Eur Respir J,* 25(2), pp. 250-8.

Isajevs, S., Taivans, I., Svirina, D., Strazda, G. and Kopeika, U. (2011) 'Patterns of inflammatory responses in large and small airways in smokers with and without chronic obstructive pulmonary disease', *Respiration,* 81(5), pp. 362-71.

Jackson, P. L., Xu, X., Wilson, L., Weathington, N. M., Clancy, J. P., Blalock, J. E. and Gaggar, A. (2010) 'Human neutrophil elastase-mediated cleavage sites of MMP-9 and TIMP-1: implications to cystic fibrosis proteolytic dysfunction', *Mol Med,* 16(5-6), pp. 159-66.

Jagels, M. A., Chambers, J. D., Arfors, K. E. and Hugli, T. E. (1995) 'C5a- and tumor necrosis factor-alpha-induced leukocytosis occurs independently of beta 2 integrins and L-selectin: differential effects on neutrophil adhesion molecule expression in vivo', *Blood,* 85(10), pp. 2900-9.

Jasper, A. E., McIver, W. J., Sapey, E. and Walton, G. M. (2019) 'Understanding the role of neutrophils in chronic inflammatory airway disease', *F1000Res,* 8.

Jenne, C. N., Wong, C. H., Zemp, F. J., McDonald, B., Rahman, M. M., Forsyth, P. A., McFadden, G. and Kubes, P. (2013) 'Neutrophils recruited to sites of infection protect from virus challenge by releasing neutrophil extracellular traps', *Cell Host Microbe,* 13(2), pp. 169-80.

Jiang, B., Guan, Y., Shen, H. J., Zhang, L. H., Jiang, J. X., Dong, X. W., Shen, H. H. and Xie, Q. M. (2018) 'Akt/PKB signaling regulates cigarette smoke-induced pulmonary epithelial-mesenchymal transition', *Lung Cancer,* 122, pp. 44-53.

Jimenez, J. J., Jy, W., Mauro, L. M., Soderland, C., Horstman, L. L. and Ahn, Y. S. (2003) 'Endothelial cells release phenotypically and quantitatively distinct microparticles in activation and apoptosis', *Thromb Res,* 109(4), pp. 175-80.

Johnson, B. L., 3rd, Goetzman, H. S., Prakash, P. S. and Caldwell, C. C. (2013) 'Mechanisms underlying mouse TNF-alpha stimulated neutrophil derived microparticle generation', *Biochem Biophys Res Commun,* 437(4), pp. 591-6.

Johnson, B. L., III, Kuethe, J. W. and Caldwell, C. C. (2014) 'Neutrophil Derived Microvesicles: Emerging Role of a Key Mediator to the Immune Response', *Endocrine Metabolic & Immune Disorders-Drug Targets,* 14(3), pp. 210-217.

Johnson, R. M. and Vinetz, J. M. (2020) 'Dexamethasone in the management of covid -19', *Bmj,* 370, pp. m2648.

Jones, J. G., Minty, B. D., Lawler, P., Hulands, G., Crawley, J. C. and Veall, N. (1980) 'Increased alveolar epithelial permeability in cigarette smokers', *Lancet,* 1(8159), pp. 66-8.

Jorfi, S., Ansa-Addo, E. A., Kholia, S., Stratton, D., Valley, S., Lange, S. and Inal, J. (2015) 'Inhibition of microvesiculation sensitizes prostate cancer cells to chemotherapy and reduces docetaxel dose required to limit tumor growth in vivo', *Sci Rep,* 5, pp. 13006.

Juncadella, I. J., Kadl, A., Sharma, A. K., Shim, Y. M., Hochreiter-Hufford, A., Borish, L. and Ravichandran, K. S. (2013) 'Apoptotic cell clearance by bronchial epithelial cells critically influences airway inflammation', *Nature,* 493(7433), pp. 547-51.

Kalra, H., Drummen, G. P. and Mathivanan, S. (2016) 'Focus on Extracellular Vesicles: Introducing the Next Small Big Thing', *Int J Mol Sci,* 17(2), pp. 170.

Kanada, M., Bachmann, M. H., Hardy, J. W., Frimannson, D. O., Bronsart, L., Wang, A., Sylvester, M. D., Schmidt, T. L., Kaspar, R. L., Butte, M. J., Matin, A. C. and Contag, C. H. (2015) 'Differential fates of biomolecules delivered to target cells via extracellular vesicles', *Proc Natl Acad Sci U S A,* 112(12), pp. E1433-42.

Kang, J. H., Hwang, S. M. and Chung, I. Y. (2015) 'S100A8, S100A9 and S100A12 activate airway epithelial cells to produce MUC5AC via extracellular signal-regulated kinase and nuclear factor-kappaB pathways', *Immunology,* 144(1), pp. 79-90.

Karlsson, A., Markfjall, M., Stromberg, N. and Dahlgren, C. (1995) 'Escherichia coli-induced activation of neutrophil NADPH-oxidase: lipopolysaccharide and formylated peptides act synergistically to induce release of reactive oxygen metabolites', *Infect Immun,* 63(12), pp. 4606-12.

Kasahara, Y., Tuder, R. M., Cool, C. D., Lynch, D. A., Flores, S. C. and Voelkel, N. F. (2001) 'Endothelial cell death and decreased expression of vascular endothelial growth factor and vascular endothelial growth factor receptor 2 in emphysema', *Am J Respir Crit Care Med,* 163(3 Pt 1), pp. 737-44.

Keck, T., Balcom, J. H. t., Fernández-del Castillo, C., Antoniu, B. A. and Warshaw, A. L. (2002) 'Matrix metalloproteinase-9 promotes neutrophil migration and alveolar capillary leakage in pancreatitis-associated lung injury in the rat', *Gastroenterology,* 122(1), pp. 188-201.

Kelley, J. M., Monach, P. A., Ji, C., Zhou, Y., Wu, J., Tanaka, S., Mahr, A. D., Johnson, S., McAlear, C., Cuthbertson, D., Carette, S., Davis, J. C., Jr., Dellaripa, P. F., Hoffman, G. S., Khalidi, N., Langford, C. A., Seo, P., St Clair, E. W., Specks, U., Stone, J. H., Spiera, R. F., Ytterberg, S. R., Merkel, P. A., Edberg, J. C. and Kimberly, R. P. (2011) 'IgA and IgG antineutrophil cytoplasmic antibody engagement of Fc receptor genetic variants influences granulomatosis with polyangiitis', *Proc Natl Acad Sci U S A,* 108(51), pp. 20736-41.

Kenche, H., Baty, C. J., Vedagiri, K., Shapiro, S. D. and Blumental-Perry, A. (2013) 'Cigarette smoking affects oxidative protein folding in endoplasmic reticulum by modifying protein disulfide isomerase', *Faseb j,* 27(3), pp. 965-77.

Kenche, H., Ye, Z. W., Vedagiri, K., Richards, D. M., Gao, X. H., Tew, K. D., Townsend, D. M. and Blumental-Perry, A. (2016) 'Adverse Outcomes Associated with Cigarette Smoke Radicals Related to Damage to Protein-disulfide Isomerase', *J Biol Chem,* 291(9), pp. 4763-78.

Kerst, J. M., Slaper-Cortenbach, I. C., von dem Borne, A. E., van der Schoot, C. E. and van Oers, R. H. (1992) 'Combined measurement of growth and differentiation in suspension cultures of purified human CD34-positive cells enables a detailed analysis of myelopoiesis', *Exp Hematol,* 20(10), pp. 1188-93.

Kessenbrock, K., Krumbholz, M., Schonermarck, U., Back, W., Gross, W. L., Werb, Z., Grone, H. J., Brinkmann, V. and Jenne, D. E. (2009) 'Netting neutrophils in autoimmune small-vessel vasculitis', *Nat Med,* 15(6), pp. 623-5.

Kessler, R., Faller, M., Fourgaut, G., Mennecier, B. and Weitzenblum, E. (1999) 'Predictive factors of hospitalization for acute exacerbation in a series of 64 patients with chronic obstructive pulmonary disease', *Am J Respir Crit Care Med,* 159(1), pp. 158-64.

Kessler, R., Faller, M., Weitzenblum, E., Chaouat, A., Aykut, A., Ducolone, A., Ehrhart, M. and Oswald-Mammosser, M. (2001) '"Natural history" of pulmonary hypertension in a series of 131 patients with chronic obstructive lung disease', *Am J Respir Crit Care Med,* 164(2), pp. 219-24.

Ketterer, M. R., Shao, J. Q., Hornick, D. B., Buscher, B., Bandi, V. K. and Apicella, M. A. (1999) 'Infection of primary human bronchial epithelial cells by Haemophilus influenzae:

macropinocytosis as a mechanism of airway epithelial cell entry', *Infect Immun,* 67(8), pp. 4161-70.

Khoshnoodi, J., Pedchenko, V. and Hudson, B. G. (2008) 'Mammalian collagen IV', *Microsc Res Tech,* 71(5), pp. 357-70.

Kielgast, F., Schmidt, H., Braubach, P., Winkelmann, V. E., Thompson, K. E., Frick, M., Dietl, P. and Wittekindt, O. H. (2016) 'Glucocorticoids Regulate Tight Junction Permeability of Lung Epithelia by Modulating Claudin 8', *Am J Respir Cell Mol Biol,* 54(5), pp. 707-17.

Kim, H. J., Kim, Y. S., Kim, K. H., Choi, J. P., Kim, Y. K., Yun, S., Sharma, L., Dela Cruz, C. S., Lee, J. S., Oh, Y. M., Lee, S. D. and Lee, S. W. (2017) 'The microbiome of the lung and its extracellular vesicles in nonsmokers, healthy smokers and COPD patients', *Exp Mol Med,* 49(4), pp. e316.

Kim, J. T., Gleich, G. J. and Kita, H. (1997) 'Roles of CD9 molecules in survival and activation of human eosinophils', *J Immunol,* 159(2), pp. 926-33.

Kim, M. H., Bae, C. H., Choi, Y. S., Na, H. G., Song, S. Y. and Kim, Y. D. (2019) 'Endoplasmic Reticulum Stress Induces MUC5AC and MUC5B Expression in Human Nasal Airway Epithelial Cells', *Clin Exp Otorhinolaryngol,* 12(2), pp. 181-189.

Klein, J. B., Buridi, A., Coxon, P. Y., Rane, M. J., Manning, T., Kettritz, R. and McLeish, K. R. (2001) 'Role of extracellular signal-regulated kinase and phosphatidylinositol-3 kinase in chemoattractant and LPS delay of constitutive neutrophil apoptosis', *Cell Signal,* 13(5), pp. 335-43.

Kleniewska, A., Walusiak-Skorupa, J., Piotrowski, W., Nowakowska-Świrta, E. and Wiszniewska, M. (2016) 'Comparison of biomarkers in serum and induced sputum of patients with occupational asthma and chronic obstructive pulmonary disease', *J Occup Health,* 58(4), pp. 333-9.

Klinke, A., Berghausen, E., Friedrichs, K., Molz, S., Lau, D., Remane, L., Berlin, M., Kaltwasser, C., Adam, M., Mehrkens, D., Mollenhauer, M., Manchanda, K., Ravekes, T., Heresi, G. A., Aytekin, M., Dweik, R. A., Hennigs, J. K., Kubala, L., Michaëlsson, E., Rosenkranz, S., Rudolph, T. K., Hazen, S. L., Klose, H., Schermuly, R. T., Rudolph, V. and Baldus, S. (2018) 'Myeloperoxidase aggravates pulmonary arterial hypertension by activation of vascular Rho-kinase', *JCI Insight,* 3(11).

Knauper, V., Smith, B., Lopez-Otin, C. and Murphy, G. (1997) 'Activation of progelatinase B (proMMP-9) by active collagenase-3 (MMP-13)', *Eur J Biochem,* 248(2), pp. 369-73.

Kornmann, L. M., Zernecke, A., Curfs, D. M., Janssen, B. J., Weber, C., de Winther, M. P., Reneman, R. S., Hoeks, A. P. and Reesink, K. D. (2015) 'Echogenic perfluorohexane-loaded macrophages adhere in vivo to activated vascular endothelium in mice, an explorative study', *Cardiovasc Ultrasound,* 13, pp. 1.

Kosgodage, U. S., Trindade, R. P., Thompson, P. R., Inal, J. M. and Lange, S. (2017) 'Chloramidine/Bisindolylmaleimide-I-Mediated Inhibition of Exosome and Microvesicle Release and Enhanced Efficacy of Cancer Chemotherapy', *Int J Mol Sci,* 18(5).

Kruger, P., Saffarzadeh, M., Weber, A. N., Rieber, N., Radsak, M., von Bernuth, H., Benarafa, C., Roos, D., Skokowa, J. and Hartl, D. (2015) 'Neutrophils: Between host defence, immune modulation, and tissue injury', *PLoS Pathog,* 11(3), pp. e1004651.

Kubo, H., Doyle, N. A., Graham, L., Bhagwan, S. D., Quinlan, W. M. and Doerschuk, C. M. (1999) 'L- and P-selectin and CD11/CD18 in intracapillary neutrophil sequestration in rabbit lungs', *Am J Respir Crit Care Med,* 159(1), pp. 267-74.

Kuebler, W. M., Borges, J., Sckell, A., Kuhnle, G. E., Bergh, K., Messmer, K. and Goetz, A. E. (2000) 'Role of L-selectin in leukocyte sequestration in lung capillaries in a rabbit model of endotoxemia', *Am J Respir Crit Care Med,* 161(1), pp. 36-43.

Kuravi, S. J., Harrison, P., Rainger, G. E. and Nash, G. B. (2019) 'Ability of Platelet-Derived Extracellular Vesicles to Promote Neutrophil-Endothelial Cell Interactions', *Inflammation,* 42(1), pp. 290-305.

Kurie, J. M., Shin, H. J., Lee, J. S., Morice, R. C., Ro, J. Y., Lippman, S. M., Hittelman, W. N., Yu, R., Lee, J. J. and Hong, W. K. (1996) 'Increased epidermal growth factor receptor expression in metaplastic bronchial epithelium', *Clin Cancer Res,* 2(10), pp. 1787-93.

Lacedonia, D., Carpagnano, G. E., Trotta, T., Palladino, G. P., Panaro, M. A., Zoppo, L. D., Foschino Barbaro, M. P. and Porro, C. (2016) 'Microparticles in sputum of COPD patients: a potential biomarker of the disease?', *Int J Chron Obstruct Pulmon Dis,* 11, pp. 527-33.

Lacroix, R., Robert, S., Poncelet, P., Kasthuri, R. S., Key, N. S. and Dignat-George, F. (2010) 'Standardization of platelet-derived microparticle enumeration by flow cytometry with calibrated beads: results of the International Society on Thrombosis and Haemostasis SSC Collaborative workshop', *J Thromb Haemost,* 8(11), pp. 2571-4.

Lahousse, L., van den Bouwhuijsen, Q. J., Loth, D. W., Joos, G. F., Hofman, A., Witteman, J. C., van der Lugt, A., Brusselle, G. G. and Stricker, B. H. (2013) 'Chronic obstructive pulmonary disease and lipid core carotid artery plaques in the elderly: the Rotterdam Study', *Am J Respir Crit Care Med,* 187(1), pp. 58-64.

Lahoz-Beneytez, J., Elemans, M., Zhang, Y., Ahmed, R., Salam, A., Block, M., Niederalt, C., Asquith, B. and Macallan, D. (2016) 'Human neutrophil kinetics: modeling of stable isotope labeling data supports short blood neutrophil half-lives', *Blood,* 127(26), pp. 3431-8.

Larangeira, A. P., Silva, A. R., Gomes, R. N., Penido, C., Henriques, M. G., Castro-Faria-Neto, H. C. and Bozza, P. T. (2001) 'Mechanisms of allergen- and LPS-induced bone marrow eosinophil mobilization and eosinophil accumulation into the pleural cavity: a role for CD11b/CD18 complex', *Inflamm Res,* 50(6), pp. 309-16.

Lashin, H. M. S., Nadkarni, S., Oggero, S., Jones, H. R., Knight, J. C., Hinds, C. J. and Perretti, M. (2018) 'Microvesicle Subsets in Sepsis Due to Community Acquired Pneumonia Compared to Faecal Peritonitis', *Shock,* 49(4), pp. 393-401.

Laurell, C. B. and Eriksson, S. (2013) 'The electrophoretic alpha1-globulin pattern of serum in alpha1-antitrypsin deficiency. 1963', *Copd,* 10 Suppl 1, pp. 3-8.

Laurent, G. J. (1986) 'Lung collagen: more than scaffolding', *Thorax,* 41(6), pp. 418-28.

Lazaar, A. L., Miller, B. E., Donald, A. C., Keeley, T., Ambery, C., Russell, J., Watz, H. and Tal-Singer, R. (2020) 'CXCR2 antagonist for patients with chronic obstructive pulmonary disease with chronic mucus hypersecretion: a phase 2b trial', *Respir Res,* 21(1), pp. 149.

Lee, A. S. (2005) 'The ER chaperone and signaling regulator GRP78/BiP as a monitor of endoplasmic reticulum stress', *Methods,* 35(4), pp. 373-81.

Lee, H., Groot, M., Pinilla-Vera, M., Fredenburgh, L. E. and Jin, Y. (2019) 'Identification of miRNA-rich vesicles in bronchoalveolar lavage fluid: Insights into the function and heterogeneity of extracellular vesicles', *J Control Release,* 294, pp. 43-52.

Lee, H., Zhang, D., Wu, J., Otterbein, L. E. and Jin, Y. (2017) 'Lung Epithelial Cell-Derived Microvesicles Regulate Macrophage Migration via MicroRNA-17/221-Induced Integrin beta1 Recycling', *J Immunol,* 199(4), pp. 1453-1464.

Lee, Y., El Andaloussi, S. and Wood, M. J. (2012) 'Exosomes and microvesicles: extracellular vesicles for genetic information transfer and gene therapy', *Hum Mol Genet,* 21(R1), pp. R125-34.

Levänen, B., Bhakta, N. R., Torregrosa Paredes, P., Barbeau, R., Hiltbrunner, S., Pollack, J. L., Sköld, C. M., Svartengren, M., Grunewald, J., Gabrielsson, S., Eklund, A., Larsson, B. M., Woodruff, P. G., Erle, D. J. and Wheelock Å, M. (2013) 'Altered microRNA profiles in bronchoalveolar lavage fluid exosomes in asthmatic patients', *J Allergy Clin Immunol,* 131(3), pp. 894-903.

Ley, K., Laudanna, C., Cybulsky, M. I. and Nourshargh, S. (2007) 'Getting to the site of inflammation: the leukocyte adhesion cascade updated', *Nat Rev Immunol,* 7(9), pp. 678-89.

Lindberg, C. A., Engström, G., de Verdier, M. G., Nihlén, U., Anderson, M., Forsman-Semb, K. and Svartengren, M. (2012) 'Total desmosines in plasma and urine correlate with lung function', *Eur Respir J,* 39(4), pp. 839-45.

Linder, R., Ronmark, E., Pourazar, J., Behndig, A., Blomberg, A. and Lindberg, A. (2015) 'Serum metalloproteinase-9 is related to COPD severity and symptoms - cross-sectional data from a population based cohort-study', *Respir Res,* 16, pp. 28.

Liou, T. G. and Campbell, E. J. (1996) 'Quantum proteolysis resulting from release of single granules by human neutrophils: a novel, nonoxidative mechanism of extracellular proteolytic activity', *J Immunol,* 157(6), pp. 2624-31.

Liu, B., Jiang, T., Hu, X., Liu, Z., Zhao, L., Liu, H. and Ma, L. (2018) 'Downregulation of microRNA-30a in bronchoalveolar lavage fluid from idiopathic pulmonary fibrosis patients', *Mol Med Rep,* 18(6), pp. 5799-5806.

Liu, S., Zhou, Y., Wang, X., Wang, D., Lu, J., Zheng, J., Zhong, N. and Ran, P. (2007) 'Biomass fuels are the probable risk factor for chronic obstructive pulmonary disease in rural South China', *Thorax,* 62(10), pp. 889-97.

Lodge, K. (2018) *Hypoxia induces selective neutrophil degranulation to promote endothelial damage in COPD.* Doctor of Philosophy, University of Cambridge.

Lokwani, R., Wark, P. A., Baines, K. J., Fricker, M., Barker, D. and Simpson, J. L. (2019) 'Blood Neutrophils In COPD But Not Asthma Exhibit A Primed Phenotype With Downregulated CD62L Expression', *Int J Chron Obstruct Pulmon Dis,* 14, pp. 2517-2525.

Lorincz, A. M., Timar, C. I., Marosvari, K. A., Veres, D. S., Otrokocsi, L., Kittel, A. and Ligeti, E. (2014) 'Effect of storage on physical and functional properties of extracellular vesicles derived from neutrophilic granulocytes', *J Extracell Vesicles,* 3, pp. 25465.

Lowe, G. D. and Pepys, M. B. (2006) 'C-reactive protein and cardiovascular disease: weighing the evidence', *Curr Atheroscler Rep,* 8(5), pp. 421-8.

Maarsingh, H., Bidan, C. M., Brook, B. S., Zuidhof, A. B., Elzinga, C. R. S., Smit, M., Oldenburger, A., Gosens, R., Timens, W. and Meurs, H. (2019) 'Small airway hyperresponsiveness in COPD: relationship between structure and function in lung slices', *Am J Physiol Lung Cell Mol Physiol,* 316(3), pp. L537-l546.

Machado, M. G., Tavares, L. P., Souza, G. V. S., Queiroz-Junior, C. M., Ascenção, F. R., Lopes, M. E., Garcia, C. C., Menezes, G. B., Perretti, M., Russo, R. C., Teixeira, M. M. and Sousa, L. P. (2020) 'The Annexin A1/FPR2 pathway controls the inflammatory response and bacterial dissemination in experimental pneumococcal pneumonia', *Faseb j,* 34(2), pp. 2749-2764.

MacNee, W. (1990) 'Pulmonary neutrophil kinetics', *Clin Phys Physiol Meas,* 11 Suppl A, pp. 133-9.

MacNee, W. (2006) 'Pathology, pathogenesis, and pathophysiology', *BMJ,* 332(7551), pp. 1202-1204.

Maduskuie, T. P., Jr., McNamara, K. J., Ru, Y., Knabb, R. M. and Stouten, P. F. (1998) 'Rational design and synthesis of novel, potent bis-phenylamidine carboxylate factor Xa inhibitors', *J Med Chem,* 41(1), pp. 53-62.

Majo, J., Ghezzo, H. and Cosio, M. G. (2001) 'Lymphocyte population and apoptosis in the lungs of smokers and their relation to emphysema', *Eur Respir J,* 17(5), pp. 946-53.

Malik, M., Bakshi, C. S., McCabe, K., Catlett, S. V., Shah, A., Singh, R., Jackson, P. L., Gaggar, A., Metzger, D. W., Melendez, J. A., Blalock, J. E. and Sellati, T. J. (2007) 'Matrix metalloproteinase 9 activity enhances host susceptibility to pulmonary infection with type A and B strains of Francisella tularensis', *J Immunol,* 178(2), pp. 1013-20.

Mannino, D. M., Ford, E. S. and Redd, S. C. (2003) 'Obstructive and restrictive lung disease and markers of inflammation: data from the Third National Health and Nutrition Examination', *Am J Med,* 114(9), pp. 758-62.

Marquis, K., Maltais, F., Duguay, V., Bezeau, A. M., LeBlanc, P., Jobin, J. and Poirier, P. (2005) 'The metabolic syndrome in patients with chronic obstructive pulmonary disease', *J Cardiopulm Rehabil: Vol. 4.* United States, pp. 226-32; discussion 233-4.

McGovern, N. N., Cowburn, A. S., Porter, L., Walmsley, S. R., Summers, C., Thompson, A. A., Anwar, S., Willcocks, L. C., Whyte, M. K., Condliffe, A. M. and Chilvers, E. R. (2011) 'Hypoxia selectively inhibits respiratory burst activity and killing of Staphylococcus aureus in human neutrophils', *J Immunol,* 186(1), pp. 453-63.

McGrath, E. E., Marriott, H. M., Lawrie, A., Francis, S. E., Sabroe, I., Renshaw, S. A., Dockrell, D. H. and Whyte, M. K. (2011) 'TNF-related apoptosis-inducing ligand (TRAIL) regulates inflammatory neutrophil apoptosis and enhances resolution of inflammation', *J Leukoc Biol,* 90(5), pp. 855-65.

Mecklenburgh, K. I., Walmsley, S. R., Cowburn, A. S., Wiesener, M., Reed, B. J., Upton, P. D., Deighton, J., Greening, A. P. and Chilvers, E. R. (2002) 'Involvement of a ferroprotein sensor in hypoxia-mediated inhibition of neutrophil apoptosis', *Blood,* 100(8), pp. 3008-16.

Medeiros, A. I., Serezani, C. H., Lee, S. P. and Peters-Golden, M. (2009) 'Efferocytosis impairs pulmonary macrophage and lung antibacterial function via PGE2/EP2 signaling', *J Exp Med,* 206(1), pp. 61-8.

Mesri, M. and Altieri, D. C. (1998) 'Endothelial cell activation by leukocyte microparticles', *J Immunol,* 161(8), pp. 4382-7.

Mesri, M. and Altieri, D. C. (1999) 'Leukocyte microparticles stimulate endothelial cell cytokine release and tissue factor induction in a JNK1 signaling pathway', *J Biol Chem,* 274(33), pp. 23111-8.

Milani, G., Lana, T., Bresolin, S., Aveic, S., Pastò, A., Frasson, C. and Te Kronnie, G. (2017) 'Expression Profiling of Circulating Microvesicles Reveals Intercellular Transmission of Oncogenic Pathways', *Mol Cancer Res,* 15(6), pp. 683-695.

Millichip, M. I., Dallas, D. J., Wu, E., Dale, S. and McKie, N. (1998) 'The metallo-disintegrin ADAM10 (MADM) from bovine kidney has type IV collagenase activity in vitro', *Biochem Biophys Res Commun,* 245(2), pp. 594-8.

Min, T., Bodas, M., Mazur, S. and Vij, N. (2011) 'Critical role of proteostasis-imbalance in pathogenesis of COPD and severe emphysema', *J Mol Med (Berl),* 89(6), pp. 577-93.

Mittal, M., Siddiqui, M. R., Tran, K., Reddy, S. P. and Malik, A. B. (2014) 'Reactive oxygen species in inflammation and tissue injury', *Antioxid Redox Signal,* 20(7), pp. 1126-67.

Mock, J. R., Garibaldi, B. T., Aggarwal, N. R., Jenkins, J., Limjunyawong, N., Singer, B. D., Chau, E., Rabold, R., Files, D. C., Sidhaye, V., Mitzner, W., Wagner, E. M., King, L. S. and D'Alessio, F.

R. (2014) 'Foxp3+ regulatory T cells promote lung epithelial proliferation', *Mucosal Immunol,* 7(6), pp. 1440-51.

Mohning, M. P., Thomas, S. M., Barthel, L., Mould, K. J., McCubbrey, A. L., Frasch, S. C., Bratton, D. L., Henson, P. M. and Janssen, W. J. (2018) 'Phagocytosis of microparticles by alveolar macrophages during acute lung injury requires MerTK', *Am J Physiol Lung Cell Mol Physiol,* 314(1), pp. L69-L82.

Monaco, S., Sparano, V., Gioia, M., Sbardella, D., Di Pierro, D., Marini, S. and Coletta, M. (2006) 'Enzymatic processing of collagen IV by MMP-2 (gelatinase A) affects neutrophil migration and it is modulated by extracatalytic domains', *Protein Sci,* 15(12), pp. 2805-15.

Mondal, A., Ashiq, K. A., Phulpagar, P., Singh, D. K. and Shiras, A. (2019) 'Effective Visualization and Easy Tracking of Extracellular Vesicles in Glioma Cells', *Biol Proced Online,* 21, pp. 4.

Moon, J. Y., Leitao Filho, F. S., Shahangian, K., Takiguchi, H. and Sin, D. D. (2018) 'Blood and sputum protein biomarkers for chronic obstructive pulmonary disease (COPD)', *Expert Rev Proteomics,* 15(11), pp. 923-935.

Moore, K. L., Patel, K. D., Bruehl, R. E., Li, F., Johnson, D. A., Lichenstein, H. S., Cummings, R. D., Bainton, D. F. and McEver, R. P. (1995) 'P-selectin glycoprotein ligand-1 mediates rolling of human neutrophils on P-selectin', *J Cell Biol,* 128(4), pp. 661-71.

Moraes, T. J., Chow, C. W. and Downey, G. P. (2003) 'Proteases and lung injury', *Crit Care Med,* 31(4 Suppl), pp. S189-94.

Morelli, A. E., Larregina, A. T., Shufesky, W. J., Sullivan, M. L., Stolz, D. B., Papworth, G. D., Zahorchak, A. F., Logar, A. J., Wang, Z., Watkins, S. C., Falo, L. D., Jr. and Thomson, A. W. (2004) 'Endocytosis, intracellular sorting, and processing of exosomes by dendritic cells', *Blood,* 104(10), pp. 3257-66.

Mori, K., Kurihara, N., Hayashida, S., Tanaka, M. and Ikeda, K. (2002) 'The intrauterine expression of surfactant protein D in the terminal airways of human fetuses compared with surfactant protein A', *Eur J Pediatr,* 161(8), pp. 431-4.

Mullen, J. B., Wright, J. L., Wiggs, B. R., Pare, P. D. and Hogg, J. C. (1985) 'Reassessment of inflammation of airways in chronic bronchitis', *Br Med J (Clin Res Ed),* 291(6504), pp. 1235-9.

Mullerova, H., Chigbo, C., Hagan, G. W., Woodhead, M. A., Miravitlles, M., Davis, K. J. and Wedzicha, J. A. (2012) 'The natural history of community-acquired pneumonia in COPD patients: a population database analysis', *Respir Med,* 106(8), pp. 1124-33.

Murray, J., Barbara, J. A., Dunkley, S. A., Lopez, A. F., Van Ostade, X., Condliffe, A. M., Dransfield, I., Haslett, C. and Chilvers, E. R. (1997) 'Regulation of neutrophil apoptosis by tumor necrosis factor-alpha: requirement for TNFR55 and TNFR75 for induction of apoptosis in vitro', *Blood,* 90(7), pp. 2772-83.

Nadel, J., Takeyama, K. and Agusti, C. (1999) 'Role of neutrophil elastase in hypersecretion in asthma', *European Respiratory Journal,* 13(1), pp. 190-196.

Naeije, R. (2005) 'Pulmonary hypertension and right heart failure in chronic obstructive pulmonary disease', *Proc Am Thorac Soc,* 2(1), pp. 20-2.

Nahum, A., Chamberlin, W. and Sznajder, J. I. (1991) 'Differential activation of mixed venous and arterial neutrophils in patients with sepsis syndrome and acute lung injury', *Am Rev Respir Dis,* 143(5 Pt 1), pp. 1083-7.

Nakamura, H., Yoshimura, K., McElvaney, N. G. and Crystal, R. G. (1992) 'Neutrophil elastase in respiratory epithelial lining fluid of individuals with cystic fibrosis induces interleukin-8 gene expression in a human bronchial epithelial cell line', *J Clin Invest,* 89(5), pp. 1478-84.

Negewo, N. A., McDonald, V. M. and Gibson, P. G. (2015) 'Comorbidity in chronic obstructive pulmonary disease', *Respir Investig,* 53(6), pp. 249-58.

Neumeier, A. and Keith, R. (2020) 'Clinical Guideline Highlights for the Hospitalist: The GOLD and NICE Guidelines for the Management of COPD', *J Hosp Med,* 15(2), pp. e1-e2.

Newton, K. and Dixit, V. M. (2012) 'Signaling in innate immunity and inflammation', *Cold Spring Harb Perspect Biol,* 4(3).

Newton, R., Holden, N. S., Catley, M. C., Oyelusi, W., Leigh, R., Proud, D. and Barnes, P. J. (2007) 'Repression of inflammatory gene expression in human pulmonary epithelial cells by small-molecule IkappaB kinase inhibitors', *J Pharmacol Exp Ther,* 321(2), pp. 734-42.

Noda, N., Matsumoto, K., Fukuyama, S., Asai, Y., Kitajima, H., Seki, N., Matsunaga, Y., Kan, O. K., Moriwaki, A., Morimoto, K., Inoue, H. and Nakanishi, Y. (2013) 'Cigarette smoke impairs phagocytosis of apoptotic neutrophils by alveolar macrophages via inhibition of the histone deacetylase/Rac/CD9 pathways', *Int Immunol,* 25(11), pp. 643-50.

Noguera, A., Batle, S., Miralles, C., Iglesias, J., Busquets, X., MacNee, W. and Agusti, A. G. (2001) 'Enhanced neutrophil response in chronic obstructive pulmonary disease', *Thorax,* 56(6), pp. 432-7.

Noguera, A., Busquets, X., Sauleda, J., Villaverde, J. M., MacNee, W. and Agusti, A. G. (1998) 'Expression of adhesion molecules and G proteins in circulating neutrophils in chronic obstructive pulmonary disease', *Am J Respir Crit Care Med,* 158(5 Pt 1), pp. 1664-8.

Nolan, S., Dixon, R., Norman, K., Hellewell, P. and Ridger, V. (2008) 'Nitric oxide regulates neutrophil migration through microparticle formation', *Am J Pathol,* 172(1), pp. 265-73.

Nunes, G. L., Simoes, A., Dyszy, F. H., Shida, C. S., Juliano, M. A., Juliano, L., Gesteira, T. F., Nader, H. B., Murphy, G., Chaffotte, A. F., Goldberg, M. E., Tersariol, I. L. and Almeida, P. C. (2011) 'Mechanism of heparin acceleration of tissue inhibitor of metalloproteases-1 (TIMP-1) degradation by the human neutrophil elastase', *PLoS One,* 6(6), pp. e21525.

Nuutila, J. and Lilius, E. M. (2005) 'Flow cytometric quantitative determination of ingestion by phagocytes needs the distinguishing of overlapping populations of binding and ingesting cells', *Cytometry A,* 65(2), pp. 93-102.

Obeidat, M., Li, X., Burgess, S., Zhou, G., Fishbane, N., Hansel, N. N., Bosse, Y., Joubert, P., Hao, K., Nickle, D. C., van den Berge, M., Timens, W., Cho, M. H., Hobbs, B. D., de Jong, K., Boezen, M., Hung, R. J., Rafaels, N., Mathias, R., Ruczinski, I., Beaty, T. H., Barnes, K. C., Pare, P. D. and Sin, D. D. (2017) 'Surfactant protein D is a causal risk factor for COPD: results of Mendelian randomisation', *Eur Respir J,* 50(5).

Ofir-Birin, Y., Abou Karam, P., Rudik, A., Giladi, T., Porat, Z. and Regev-Rudzki, N. (2018) 'Monitoring Extracellular Vesicle Cargo Active Uptake by Imaging Flow Cytometry', *Front Immunol,* 9, pp. 1011.

Ogata, Y., Enghild, J. J. and Nagase, H. (1992) 'Matrix metalloproteinase 3 (stromelysin) activates the precursor for the human matrix metalloproteinase 9', *J Biol Chem,* 267(6), pp. 3581-4.

Oldenburger, A., Poppinga, W. J., Kos, F., de Bruin, H. G., Rijks, W. F., Heijink, I. H., Timens, W., Meurs, H., Maarsingh, H. and Schmidt, M. (2014) 'A-kinase anchoring proteins contribute to loss of E-cadherin and bronchial epithelial barrier by cigarette smoke', *Am J Physiol Cell Physiol,* 306(6), pp. C585-97.

Olivera, D., Knall, C., Boggs, S. and Seagrave, J. (2010) 'Cytoskeletal modulation and tyrosine phosphorylation of tight junction proteins are associated with mainstream cigarette smoke-induced permeability of airway epithelium', *Exp Toxicol Pathol,* 62(2), pp. 133-43.

Ordoñez, C. L., Shaughnessy, T. E., Matthay, M. A. and Fahy, J. V. (2000) 'Increased neutrophil numbers and IL-8 levels in airway secretions in acute severe asthma: Clinical and biologic significance', *Am J Respir Crit Care Med,* 161(4 Pt 1), pp. 1185-90.

Osei, E. T., Noordhoek, J. A., Hackett, T. L., Spanjer, A. I., Postma, D. S., Timens, W., Brandsma, C. A. and Heijink, I. H. (2016) 'Interleukin-1α drives the dysfunctional cross-talk of the airway epithelium and lung fibroblasts in COPD', *Eur Respir J,* 48(2), pp. 359-69.

Oswald-Mammosser, M., Weitzenblum, E., Quoix, E., Moser, G., Chaouat, A., Charpentier, C. and Kessler, R. (1995) 'Prognostic factors in COPD patients receiving long-term oxygen therapy. Importance of pulmonary artery pressure', *Chest,* 107(5), pp. 1193-8.

Ott, I., Neumann, F. J., Gawaz, M., Schmitt, M. and Schomig, A. (1996) 'Increased neutrophil-platelet adhesion in patients with unstable angina', *Circulation,* 94(6), pp. 1239-46.

Oudijk, E. J., Lammers, J. W. and Koenderman, L. (2003) 'Systemic inflammation in chronic obstructive pulmonary disease', *Eur Respir J Suppl,* 46, pp. 5s-13s.

Owen, C. A., Campbell, M. A., Sannes, P. L., Boukedes, S. S. and Campbell, E. J. (1995) 'Cell surface-bound elastase and cathepsin G on human neutrophils: a novel, non-oxidative mechanism by which neutrophils focus and preserve catalytic activity of serine proteinases', *J Cell Biol,* 131(3), pp. 775-89.

Owen, C. A., Hu, Z., Barrick, B. and Shapiro, S. D. (2003) 'Inducible expression of tissue inhibitor of metalloproteinases-resistant matrix metalloproteinase-9 on the cell surface of neutrophils', *Am J Respir Cell Mol Biol,* 29(3 Pt 1), pp. 283-94.

Paone, G., Conti, V., Leone, A., Schmid, G., Puglisi, G., Giannunzio, G. and Terzano, C. (2011) 'Human neutrophil peptides sputum levels in symptomatic smokers and COPD patients', *Eur Rev Med Pharmacol Sci,* 15(5), pp. 556-62.

Papakonstantinou, E., Karakiulakis, G., Batzios, S., Savic, S., Roth, M., Tamm, M. and Stolz, D. (2015) 'Acute exacerbations of COPD are associated with significant activation of matrix metalloproteinase 9 irrespectively of airway obstruction, emphysema and infection', *Respiratory Research,* 16(1), pp. 78.

Papi, A., Bellettato, C. M., Braccioni, F., Romagnoli, M., Casolari, P., Caramori, G., Fabbri, L. M. and Johnston, S. L. (2006) 'Infections and airway inflammation in chronic obstructive pulmonary disease severe exacerbations', *Am J Respir Crit Care Med,* 173(10), pp. 1114-21.

Park, I., Kim, M., Choe, K., Song, E., Seo, H., Hwang, Y., Ahn, J., Lee, S. H., Lee, J. H., Jo, Y. H., Kim, K., Koh, G. Y. and Kim, P. (2019) 'Neutrophils disturb pulmonary microcirculation in sepsis-induced acute lung injury', *Eur Respir J,* 53(3).

Parkos, C. A. (2016) 'Neutrophil-Epithelial Interactions: A Double-Edged Sword', *Am J Pathol,* 186(6), pp. 1404-16.

Pascoe, S. J., Papi, A., Midwinter, D., Lettis, S. and Barnes, N. (2019) 'Circulating neutrophils levels are a predictor of pneumonia risk in chronic obstructive pulmonary disease', *Respir Res,* 20(1), pp. 195.

Pasquet, J. M., Dachary-Prigent, J. and Nurden, A. T. (1996) 'Calcium influx is a determining factor of calpain activation and microparticle formation in platelets', *Eur J Biochem,* 239(3), pp. 647-54.

Patel, I. S., Seemungal, T. A., Wilks, M., Lloyd-Owen, S. J., Donaldson, G. C. and Wedzicha, J. A. (2002) 'Relationship between bacterial colonisation and the frequency, character, and severity of COPD exacerbations', *Thorax,* 57.

Peleman, R. A., Rytila, P. H., Kips, J. C., Joos, G. F. and Pauwels, R. A. (1999) 'The cellular composition of induced sputum in chronic obstructive pulmonary disease', *Eur Respir J,* 13(4), pp. 839-43.

Perretti, M. and D'Acquisto, F. (2009) 'Annexin A1 and glucocorticoids as effectors of the resolution of inflammation', *Nat Rev Immunol,* 9(1), pp. 62-70.

Petecchia, L., Sabatini, F., Varesio, L., Camoirano, A., Usai, C., Pezzolo, A. and Rossi, G. A. (2009) 'Bronchial airway epithelial cell damage following exposure to cigarette smoke includes disassembly of tight junction components mediated by the extracellular signal-regulated kinase 1/2 pathway', *Chest,* 135(6), pp. 1502-1512.

Pilecki, B., Wulf-Johansson, H., Støttrup, C., Jørgensen, P. T., Djiadeu, P., Nexøe, A. B., Schlosser, A., Hansen, S. W. K., Madsen, J., Clark, H. W., Nielsen, C. H., Vestbo, J., Palaniyar, N., Holmskov, U. and Sorensen, G. L. (2018) 'Surfactant Protein D Deficiency Aggravates Cigarette Smoke-Induced Lung Inflammation by Upregulation of Ceramide Synthesis', *Front Immunol,* 9, pp. 3013.

Pillay, J., den Braber, I., Vrisekoop, N., Kwast, L. M., de Boer, R. J., Borghans, J. A., Tesselaar, K. and Koenderman, L. (2010) 'In vivo labeling with 2H2O reveals a human neutrophil lifespan of 5.4 days', *Blood,* 116(4), pp. 625-7.

Pipoly, D. J. and Crouch, E. C. (1987) 'Degradation of native type IV procollagen by human neutrophil elastase. Implications for leukocyte-mediated degradation of basement membranes', *Biochemistry,* 26(18), pp. 5748-54.

Pitanga, T. N., de Aragao Franca, L., Rocha, V. C., Meirelles, T., Borges, V. M., Goncalves, M. S., Pontes-de-Carvalho, L. C., Noronha-Dutra, A. A. and dos-Santos, W. L. (2014a) 'Neutrophil-derived microparticles induce myeloperoxidase-mediated damage of vascular endothelial cells', *BMC Cell Biol,* 15, pp. 21.

Pitanga, T. N., Franca, L. d. A., Junqueira Rocha, V. C., Meirelles, T., Borges, V. M., Goncalves, M. S., Pontes-de-Carvalho, L. C., Noronha-Dutra, A. A. and Conrado dos-Santos, W. L. (2014b) 'Neutrophil-derived microparticles induce myeloperoxidase-mediated damage of vascular endothelial cells', *Bmc Cell Biology,* 15.

Pliyev, B. K., Kalintseva, M. V., Abdulaeva, S. V., Yarygin, K. N. and Savchenko, V. G. (2014) 'Neutrophil microparticles modulate cytokine production by natural killer cells', *Cytokine,* 65(2), pp. 126-9.

Pluskota, E., Woody, N. M., Szpak, D., Ballantyne, C. M., Soloviev, D. A., Simon, D. I. and Plow, E. F. (2008) 'Expression, activation, and function of integrin alphaMbeta2 (Mac-1) on neutrophil-derived microparticles', *Blood,* 112(6), pp. 2327-35.

Poncelet, P., Robert, S., Bouriche, T., Bez, J., Lacroix, R. and Dignat-George, F. (2016) 'Standardized counting of circulating platelet microparticles using currently available flow cytometers and scatter-based triggering: Forward or side scatter?', *Cytometry A,* 89(2), pp. 148-58.

Prakash, P. S., Caldwell, C. C., Lentsch, A. B., Pritts, T. A. and Robinson, B. R. H. (2012) 'Human microparticles generated during sepsis in patients with critical illness are neutrophil-derived and modulate the immune response', *Journal of Trauma and Acute Care Surgery,* 73(2), pp. 401-406.

Preston, R. A., Jy, W., Jimenez, J. J., Mauro, L. M., Horstman, L. L., Valle, M., Aime, G. and Ahn, Y. S. (2003) 'Effects of severe hypertension on endothelial and platelet microparticles', *Hypertension,* 41(2), pp. 211-7.

Rahman, I. and Adcock, I. M. (2006) 'Oxidative stress and redox regulation of lung inflammation in COPD', *Eur Respir J,* 28(1), pp. 219-42.

Rahman, I., Morrison, D., Donaldson, K. and MacNee, W. (1996) 'Systemic oxidative stress in asthma, COPD, and smokers', *Am J Respir Crit Care Med,* 154(4 Pt 1), pp. 1055-60.

Rainard, P., Riollet, C., Poutrel, B. and Paape, M. J. (2000) 'Phagocytosis and killing of Staphylococcus aureus by bovine neutrophils after priming by tumor necrosis factor-alpha and the des-arginine derivative of C5a', *Am J Vet Res,* 61(8), pp. 951-9.

Ramella, M., Boccafoschi, F., Bellofatto, K., Follenzi, A., Fusaro, L., Boldorini, R., Casella, F., Porta, C., Settembrini, P. and Cannas, M. (2017) 'Endothelial MMP-9 drives the inflammatory response in abdominal aortic aneurysm (AAA)', *Am J Transl Res,* 9(12), pp. 5485-5495.

Ramos-DeSimone, N., Hahn-Dantona, E., Sipley, J., Nagase, H., French, D. L. and Quigley, J. P. (1999) 'Activation of matrix metalloproteinase-9 (MMP-9) via a converging plasmin/stromelysin-1 cascade enhances tumor cell invasion', *J Biol Chem,* 274(19), pp. 13066-76.

Raposo, G. and Stoorvogel, W. (2013) 'Extracellular vesicles: exosomes, microvesicles, and friends', *J Cell Biol,* 200(4), pp. 373-83.

Rascon-Aguilar, I. E., Pamer, M., Wludyka, P., Cury, J. and Vega, K. J. (2011) 'Poorly treated or unrecognized GERD reduces quality of life in patients with COPD', *Dig Dis Sci,* 56(7), pp. 1976-80.

Reeves, E. P., Lu, H., Jacobs, H. L., Messina, C. G., Bolsover, S., Gabella, G., Potma, E. O., Warley, A., Roes, J. and Segal, A. W. (2002) 'Killing activity of neutrophils is mediated through activation of proteases by K+ flux', *Nature,* 416(6878), pp. 291-7.

Reid, L. (1960) 'Measurement of the bronchial mucous gland layer: a diagnostic yardstick in chronic bronchitis', *Thorax,* 15, pp. 132-41.

Ren, Y., Xie, Y., Jiang, G., Fan, J., Yeung, J., Li, W., Tam, P. K. and Savill, J. (2008) 'Apoptotic cells protect mice against lipopolysaccharide-induced shock', *J Immunol,* 180(7), pp. 4978-85.

Reutershan, J., Basit, A., Galkina, E. V. and Ley, K. (2005) 'Sequential recruitment of neutrophils into lung and bronchoalveolar lavage fluid in LPS-induced acute lung injury', *Am J Physiol Lung Cell Mol Physiol,* 289(5), pp. L807-15.

Reutershan, J., Morris, M. A., Burcin, T. L., Smith, D. F., Chang, D., Saprito, M. S. and Ley, K. (2006) 'Critical role of endothelial CXCR2 in LPS-induced neutrophil migration into the lung', *J Clin Invest,* 116(3), pp. 695-702.

Rhys, H. I., Dell'Accio, F., Pitzalis, C., Moore, A., Norling, L. V. and Perretti, M. (2018) 'Neutrophil Microvesicles from Healthy Control and Rheumatoid Arthritis Patients Prevent the Inflammatory Activation of Macrophages', *EBioMedicine,* 29, pp. 60-69.

Ridger, V. C., Boulanger, C. M., Angelillo-Scherrer, A., Badimon, L., Blanc-Brude, O., Bochaton-Piallat, M. L., Boilard, E., Buzas, E. I., Caporali, A., Dignat-George, F., Evans, P. C., Lacroix, R., Lutgens, E., Ketelhuth, D. F. J., Nieuwland, R., Toti, F., Tunon, J., Weber, C. and Hoefer, I. E. (2017) 'Microvesicles in vascular homeostasis and diseases. Position Paper of the European Society of Cardiology (ESC) Working Group on Atherosclerosis and Vascular Biology', *Thromb Haemost,* 117(7), pp. 1296-1316.

Ridger, V. C., Wagner, B. E., Wallace, W. A. and Hellewell, P. G. (2001) 'Differential effects of CD18, CD29, and CD49 integrin subunit inhibition on neutrophil migration in pulmonary inflammation', *J Immunol,* 166(5), pp. 3484-90.

Rittirsch, D., Flierl, M. A., Day, D. E., Nadeau, B. A., McGuire, S. R., Hoesel, L. M., Ipaktchi, K., Zetoune, F. S., Sarma, J. V., Leng, L., Huber-Lang, M. S., Neff, T. A., Bucala, R. and Ward, P. A. (2008) 'Acute lung injury induced by lipopolysaccharide is independent of complement activation', *J Immunol,* 180(11), pp. 7664-72.

Roderfeld, M., Graf, J., Giese, B., Salguero-Palacios, R., Tschuschner, A., Muller-Newen, G. and Roeb, E. (2007) 'Latent MMP-9 is bound to TIMP-1 before secretion', *Biol Chem,* 388(11), pp. 1227-34.

Roos, D., Weening, R. S., Wyss, S. R. and Aebi, H. E. (1980) 'Protection of Human Neutrophils by Endogenous Catalase: STUDIES WITH CELLS FROM CATALASE-DEFICIENT INDIVIDUALS', *Journal of Clinical Investigation,* 65(6), pp. 1515-1522.

Rosales, C. (2018) 'Neutrophil: A Cell with Many Roles in Inflammation or Several Cell Types?', *Front Physiol,* 9, pp. 113.

Rose, F., Hattar, K., Gakisch, S., Grimminger, F., Olschewski, H., Seeger, W., Tschuschner, A., Schermuly, R. T., Weissmann, N., Hanze, J., Sibelius, U. and Ghofrani, H. A. (2003) 'Increased neutrophil mediator release in patients with pulmonary hypertension--suppression by inhaled iloprost', *Thromb Haemost,* 90(6), pp. 1141-9.

Rossaint, J., Kuhne, K., Skupski, J., Van Aken, H., Looney, M. R., Hidalgo, A. and Zarbock, A. (2016) 'Directed transport of neutrophil-derived extracellular vesicles enables platelet-mediated innate immune response', *Nat Commun,* 7, pp. 13464.

Rudman, J., Marriott, H. M., Carlin, L. M. and Johnston, S. A. (2019) 'The mouse lung early cellular innate immune response is not sufficient to control fungal infection with Cryptococcus neoformans. Pre-Print', *bioRxiv,* 679274; doi: https://doi.org/10.1101/679274.

Rutgers, S. R., Timens, W., Kaufmann, H. F., van der Mark, T. W., Koeter, G. H. and Postma, D. S. (2000) 'Comparison of induced sputum with bronchial wash, bronchoalveolar lavage and bronchial biopsies in COPD', *Eur Respir J,* 15(1), pp. 109-15.

Rydell-Tormanen, K., Uller, L. and Erjefalt, J. S. (2006) 'Neutrophil cannibalism--a back up when the macrophage clearance system is insufficient', *Respir Res,* 7, pp. 143.

Sadallah, S., Eken, C. and Schifferli, J. A. (2011) 'Ectosomes as immunomodulators', *Semin Immunopathol,* 33(5), pp. 487-95.

Sadiku, P. and Walmsley, S. R. (2019) 'Hypoxia and the regulation of myeloid cell metabolic imprinting: consequences for the inflammatory response', *EMBO Rep,* 20(5).

Saetta, M., Di Stefano, A., Turato, G., Facchini, F. M., Corbino, L., Mapp, C. E., Maestrelli, P., Ciaccia, A. and Fabbri, L. M. (1998) 'CD8+ T-lymphocytes in peripheral airways of smokers with chronic obstructive pulmonary disease', *Am J Respir Crit Care Med,* 157(3 Pt 1), pp. 822-6.

Saetta, M., Turato, G., Baraldo, S., Zanin, A., Braccioni, F., Mapp, C. E., Maestrelli, P., Cavallesco, G., Papi, A. and Fabbri, L. M. (2000) 'Goblet cell hyperplasia and epithelial inflammation in peripheral airways of smokers with both symptoms of chronic bronchitis and chronic airflow limitation', *Am J Respir Crit Care Med,* 161(3 Pt 1), pp. 1016-21.

Saetta, M., Turato, G., Facchini, F. M., Corbino, L., Lucchini, R. E., Casoni, G., Maestrelli, P., Mapp, C. E., Ciaccia, A. and Fabbri, L. M. (1997) 'Inflammatory cells in the bronchial glands of smokers with chronic bronchitis', *Am J Respir Crit Care Med,* 156(5), pp. 1633-9.

Saffarzadeh, M., Aslam, M., Juenemann, C. and Preissner, K. T. (2011) 'The Role Of Neutrophil Extracellular Trap (NET) In Lung Epithelial Cell Cytotoxicity And Permeability', ***American Journal of Respiratory and Critical Care Medicine*** **183:A2894**

Sand, J. M., Leeming, D. J., Byrjalsen, I., Bihlet, A. R., Lange, P., Tal-Singer, R., Miller, B. E., Karsdal, M. A. and Vestbo, J. (2016) 'High levels of biomarkers of collagen remodeling are associated with increased mortality in COPD - results from the ECLIPSE study', *Respir Res,* 17(1), pp. 125.

Sapey, E., Greenwood, H., Walton, G., Mann, E., Love, A., Aaronson, N., Insall, R. H., Stockley, R. A. and Lord, J. M. (2014) 'Phosphoinositide 3-kinase inhibition restores neutrophil accuracy in the elderly: toward targeted treatments for immunosenescence', *Blood,* 123(2), pp. 239-48.

Sapey, E., Stockley, J. A., Greenwood, H., Ahmad, A., Bayley, D., Lord, J. M., Insall, R. H. and Stockley, R. A. (2011) 'Behavioral and structural differences in migrating peripheral neutrophils from patients with chronic obstructive pulmonary disease', *Am J Respir Crit Care Med,* 183(9), pp. 1176-86.

Sawant, K. V., Xu, R., Cox, R., Hawkins, H., Sbrana, E., Kolli, D., Garofalo, R. P. and Rajarathnam, K. (2015) 'Chemokine CXCL1-Mediated Neutrophil Trafficking in the Lung: Role of CXCR2 Activation', *J Innate Immun,* 7(6), pp. 647-58.

Scapini, P., Marini, O., Tecchio, C. and Cassatella, M. A. (2016) 'Human neutrophils in the saga of cellular heterogeneity: insights and open questions', *Immunol Rev,* 273(1), pp. 48-60.

Schneider, D. J., Speth, J. M., Penke, L. R., Wettlaufer, S. H., Swanson, J. A. and Peters-Golden, M. (2017) 'Mechanisms and modulation of microvesicle uptake in a model of alveolar cell communication', *J Biol Chem,* 292(51), pp. 20897-20910.

Schnell, K., Weiss, C. O., Lee, T., Krishnan, J. A., Leff, B., Wolff, J. L. and Boyd, C. (2012) 'The prevalence of clinically-relevant comorbid conditions in patients with physician-diagnosed COPD: a cross-sectional study using data from NHANES 1999-2008', *BMC Pulm Med,* 12, pp. 26.

Schols, A. M., Buurman, W. A., Staal van den Brekel, A. J., Dentener, M. A. and Wouters, E. F. (1996) 'Evidence for a relation between metabolic derangements and increased levels of inflammatory mediators in a subgroup of patients with chronic obstructive pulmonary disease', *Thorax,* 51(8), pp. 819-24.

Schulz, C., Farkas, L., Wolf, K., Kratzel, K., Eissner, G. and Pfeifer, M. (2002) 'Differences in LPS-induced activation of bronchial epithelial cells (BEAS-2B) and type II-like pneumocytes (A-549)', *Scand J Immunol,* 56(3), pp. 294-302.

Segura-Valdes, L., Pardo, A., Gaxiola, M., Uhal, B. D., Becerril, C. and Selman, M. (2000) 'Upregulation of gelatinases A and B, collagenases 1 and 2, and increased parenchymal cell death in COPD', *Chest,* 117.

Segura-Valdez, L., Pardo, A., Gaxiola, M., Uhal, B. D., Becerril, C. and Selman, M. (2000) 'Upregulation of gelatinases A and B, collagenases 1 and 2, and increased parenchymal cell death in COPD', *Chest,* 117(3), pp. 684-94.

Selvarajah, S., Todd, I., Tighe, P. J., John, M., Bolton, C. E., Harrison, T. and Fairclough, L. C. (2016) 'Multiple Circulating Cytokines Are Coelevated in Chronic Obstructive Pulmonary Disease', *Mediators Inflamm,* 2016, pp. 3604842.

Sha, Q., Truong-Tran, A. Q., Plitt, J. R., Beck, L. A. and Schleimer, R. P. (2004) 'Activation of airway epithelial cells by toll-like receptor agonists', *Am J Respir Cell Mol Biol,* 31(3), pp. 358-64.

Shao, M. X. and Nadel, J. A. (2005) 'Neutrophil elastase induces MUC5AC mucin production in human airway epithelial cells via a cascade involving protein kinase C, reactive oxygen species, and TNF-alpha-converting enzyme', *J Immunol,* 175(6), pp. 4009-16.

Sharafkhaneh, A., Hanania, N. A. and Kim, V. (2008) 'Pathogenesis of emphysema: from the bench to the bedside', *Proc Am Thorac Soc,* 5(4), pp. 475-7.

Shimizu, K., Konno, S., Ozaki, M., Umezawa, K., Yamashita, K., Todo, S. and Nishimura, M. (2012) 'Dehydroxymethylepoxyquinomicin (DHMEQ), a novel NF-kappaB inhibitor, inhibits allergic inflammation and airway remodelling in murine models of asthma', *Clin Exp Allergy,* 42(8), pp. 1273-81.

Shoemark, A., Cant, E., Carreto, L., Smith, A., Oriano, M., Keir, H. R., Perea, L., Canto, E., Terranova, L., Vidal, S., Moffitt, K., Aliberti, S., Sibila, O. and Chalmers, J. D. (2019) 'A point-of-care neutrophil elastase activity assay identifies bronchiectasis severity, airway infection and risk of exacerbation', *Eur Respir J,* 53(6).

Sidney, S., Sorel, M., Quesenberry, C. P., Jr., DeLuise, C., Lanes, S. and Eisner, M. D. (2005) 'COPD and incident cardiovascular disease hospitalizations and mortality: Kaiser Permanente Medical Care Program', *Chest,* 128(4), pp. 2068-75.

Siganaki, M., Koutsopoulos, A. V., Neofytou, E., Vlachaki, E., Psarrou, M., Soulitzis, N., Pentilas, N., Schiza, S., Siafakas, N. M. and Tzortzaki, E. G. (2010) 'Deregulation of apoptosis mediators' p53 and bcl2 in lung tissue of COPD patients', *Respir Res,* 11, pp. 46.

Silva, M. T., Silva, M. N. and Appelberg, R. (1989) 'Neutrophil-macrophage cooperation in the host defence against mycobacterial infections', *Microb Pathog,* 6(5), pp. 369-80.

Simon, D. I., Chen, Z., Xu, H., Li, C. Q., Dong, J., McIntire, L. V., Ballantyne, C. M., Zhang, L., Furman, M. I., Berndt, M. C. and Lopez, J. A. (2000a) 'Platelet glycoprotein ibalpha is a counterreceptor for the leukocyte integrin Mac-1 (CD11b/CD18)', *J Exp Med,* 192(2), pp. 193-204.

Simon, H. U., Haj-Yehia, A. and Levi-Schaffer, F. (2000b) 'Role of reactive oxygen species (ROS) in apoptosis induction', *Apoptosis,* 5(5), pp. 415-8.

Sinden, N. J. and Stockley, R. A. (2010) 'Systemic inflammation and comorbidity in COPD: a result of 'overspill' of inflammatory mediators from the lungs? Review of the evidence', *Thorax,* 65(10), pp. 930-6.

Skeppholm, M., Mobarrez, F., Malmqvist, K. and Wallen, H. (2012) 'Platelet-derived microparticles during and after acute coronary syndrome', *Thromb Haemost,* 107(6), pp. 1122-9.

Slater, T. W., Finkielsztein, A., Mascarenhas, L. A., Mehl, L. C., Butin-Israeli, V. and Sumagin, R. (2017) 'Neutrophil Microparticles Deliver Active Myeloperoxidase to Injured Mucosa To Inhibit Epithelial Wound Healing', *J Immunol,* 198(7), pp. 2886-2897.

Smith, J. A. (1994) 'Neutrophils, host defense, and inflammation: a double-edged sword', *J Leukoc Biol,* 56(6), pp. 672-86.

Smith, M. C. and Wrobel, J. P. (2014) 'Epidemiology and clinical impact of major comorbidities in patients with COPD', *Int J Chron Obstruct Pulmon Dis,* 9, pp. 871-88.

Song, J. S., Cho, K. S., Yoon, H. K., Moon, H. S. and Park, S. H. (2005) 'Neutrophil elastase causes MUC5AC mucin synthesis via EGF receptor, ERK and NF-kB pathways in A549 cells', *Korean J Intern Med,* 20(4), pp. 275-83.

Soni, S., Wilson, M. R., O'Dea, K. P., Yoshida, M., Katbeh, U., Woods, S. J. and Takata, M. (2016) 'Alveolar macrophage-derived microvesicles mediate acute lung injury', *Thorax,* 71(11), pp. 1020-1029.

Soong, G., Martin, F. J., Chun, J., Cohen, T. S., Ahn, D. S. and Prince, A. (2011) 'Staphylococcus aureus protein A mediates invasion across airway epithelial cells through activation of RhoA GTPase signaling and proteolytic activity', *J Biol Chem,* 286(41), pp. 35891-8.

Sparrow, D., Glynn, R. J., Cohen, M. and Weiss, S. T. (1984) 'The relationship of the peripheral leukocyte count and cigarette smoking to pulmonary function among adult men', *Chest,* 86(3), pp. 383-6.

Stackowicz, J., Jönsson, F. and Reber, L. L. (2019) 'Mouse Models and Tools for the in vivo Study of Neutrophils', *Front Immunol,* 10, pp. 3130.

Stamenkovic, I. (2003) 'Extracellular matrix remodelling: the role of matrix metalloproteinases', *J Pathol,* 200(4), pp. 448-64.

Stanescu, D., Sanna, A., Veriter, C., Kostianev, S., Calcagni, P. G., Fabbri, L. M. and Maestrelli, P. (1996) 'Airways obstruction, chronic expectoration, and rapid decline of FEV1 in smokers are associated with increased levels of sputum neutrophils', *Thorax,* 51(3), pp. 267-71.

Starkey, P. M. (1977) 'The effect of human neutrophil elastase and cathepsin G on the collagen of cartilage, tendon, and cornea', *Acta Biol Med Ger,* 36(11-12), pp. 1549-54.

Staunton, D. E., Merluzzi, V. J., Rothlein, R., Barton, R., Marlin, S. D. and Springer, T. A. (1989) 'A cell adhesion molecule, ICAM-1, is the major surface receptor for rhinoviruses', *Cell,* 56(5), pp. 849-53.

Stein, J. M. and Luzio, J. P. (1991) 'Ectocytosis caused by sublytic autologous complement attack on human neutrophils. The sorting of endogenous plasma-membrane proteins and lipids into shed vesicles', *Biochem J,* 274 (Pt 2), pp. 381-6.

Steinberg, K. P., Milberg, J. A., Martin, T. R., Maunder, R. J., Cockrill, B. A. and Hudson, L. D. (1994) 'Evolution of bronchoalveolar cell populations in the adult respiratory distress syndrome', *Am J Respir Crit Care Med,* 150(1), pp. 113-22.

Stolz, D., Leeming, D. J., Kristensen, J. H. E., Karsdal, M. A., Boersma, W., Louis, R., Milenkovic, B., Kostikas, K., Blasi, F., Aerts, J., Sand, J. M. B., Wouters, E. F. M., Rohde, G., Prat, C., Torres, A., Welte, T., Roth, M., Papakonstantinou, E. and Tamm, M. (2017) 'Systemic Biomarkers of Collagen and Elastin Turnover Are Associated With Clinically Relevant Outcomes in COPD', *Chest,* 151(1), pp. 47-59.

Summers, C., Rankin, S. M., Condliffe, A. M., Singh, N., Peters, A. M. and Chilvers, E. R. (2010a) 'Neutrophil kinetics in health and disease', *Trends Immunol,* 31(8), pp. 318-24.

Summers, C., Rankin, S. M., Condliffe, A. M., Singh, N., Peters, A. M. and Chilvers, E. R. (2010b) 'Neutrophil kinetics in health and disease', *Trends in Immunology,* 31(8), pp. 318-324.

Summers, C., Singh, N. R., White, J. F., Mackenzie, I. M., Johnston, A., Solanki, C., Balan, K. K., Peters, A. M. and Chilvers, E. R. (2014) 'Pulmonary retention of primed neutrophils: a novel protective host response, which is impaired in the acute respiratory distress syndrome', *Thorax,* 69(7), pp. 623-9.

Sun, X. and Whittaker, G. R. (2007) 'Role of the actin cytoskeleton during influenza virus internalization into polarized epithelial cells', *Cell Microbiol,* 9(7), pp. 1672-82.

Tabak, S., Schreiber-Avissar, S. and Beit-Yannai, E. (2018) 'Extracellular vesicles have variable dose-dependent effects on cultured draining cells in the eye', *J Cell Mol Med,* 22(3), pp. 1992-2000.

Takafuji, S., Ishida, A., Miyakuni, Y. and Nakagawa, T. (2003) 'Matrix metalloproteinase-9 release from human leukocytes', *J Investig Allergol Clin Immunol,* 13(1), pp. 50-5.

Takeyama, K., Jung, B., Shim, J. J., Burgel, P. R., Dao-Pick, T., Ueki, I. F., Protin, U., Kroschel, P. and Nadel, J. A. (2001) 'Activation of epidermal growth factor receptors is responsible for mucin synthesis induced by cigarette smoke', *Am J Physiol Lung Cell Mol Physiol,* 280(1), pp. L165-72.

Tardif, M. R., Chapeton-Montes, J. A., Posvandzic, A., Pagé, N., Gilbert, C. and Tessier, P. A. (2015) 'Secretion of S100A8, S100A9, and S100A12 by Neutrophils Involves Reactive Oxygen Species and Potassium Efflux', *J Immunol Res,* 2015, pp. 296149.

Tate, M. D., Deng, Y. M., Jones, J. E., Anderson, G. P., Brooks, A. G. and Reading, P. C. (2009) 'Neutrophils ameliorate lung injury and the development of severe disease during influenza infection', *J Immunol,* 183(11), pp. 7441-50.

Tatsuta, M., Kan, O. K., Ishii, Y., Yamamoto, N., Ogawa, T., Fukuyama, S., Ogawa, A., Fujita, A., Nakanishi, Y. and Matsumoto, K. (2019) 'Effects of cigarette smoke on barrier function and tight junction proteins in the bronchial epithelium: protective role of cathelicidin LL-37', *Respir Res,* 20(1), pp. 251.

Thabut, G., Dauriat, G., Stern, J. B., Logeart, D., Levy, A., Marrash-Chahla, R. and Mal, H. (2005) 'Pulmonary hemodynamics in advanced COPD candidates for lung volume reduction surgery or lung transplantation', *Chest,* 127(5), pp. 1531-6.

Theander, K., Hasselgren, M., Luhr, K., Eckerblad, J., Unosson, M. and Karlsson, I. (2014) 'Symptoms and impact of symptoms on function and health in patients with chronic

obstructive pulmonary disease and chronic heart failure in primary health care', *Int J Chron Obstruct Pulmon Dis,* 9, pp. 785-94.

Theilgaard-Monch, K., Knudsen, S., Follin, P. and Borregaard, N. (2004) 'The transcriptional activation program of human neutrophils in skin lesions supports their important role in wound healing', *J Immunol,* 172(12), pp. 7684-93.

Thery, C. and Witwer, K. W. and Aikawa, E. and Alcaraz, M. J. and Anderson, J. D. and Andriantsitohaina, R. and Antoniou, A. and Arab, T. and Archer, F. and Atkin-Smith, G. K. and Ayre, D. C. and Bach, J. M. and Bachurski, D. and Baharvand, H. and Balaj, L. and Baldacchino, S. and Bauer, N. N. and Baxter, A. A. and Bebawy, M. and Beckham, C. and Bedina Zavec, A. and Benmoussa, A. and Berardi, A. C. and Bergese, P. and Bielska, E. and Blenkiron, C. and Bobis-Wozowicz, S. and Boilard, E. and Boireau, W. and Bongiovanni, A. and Borras, F. E. and Bosch, S. and Boulanger, C. M. and Breakefield, X. and Breglio, A. M. and Brennan, M. A. and Brigstock, D. R. and Brisson, A. and Broekman, M. L. and Bromberg, J. F. and Bryl-Gorecka, P. and Buch, S. and Buck, A. H. and Burger, D. and Busatto, S. and Buschmann, D. and Bussolati, B. and Buzas, E. I. and Byrd, J. B. and Camussi, G. and Carter, D. R. and Caruso, S. and Chamley, L. W. and Chang, Y. T. and Chen, C. and Chen, S. and Cheng, L. and Chin, A. R. and Clayton, A. and Clerici, S. P. and Cocks, A. and Cocucci, E. and Coffey, R. J. and Cordeiro-da-Silva, A. and Couch, Y. and Coumans, F. A. and Coyle, B. and Crescitelli, R. and Criado, M. F. and D'Souza-Schorey, C. and Das, S. and Datta Chaudhuri, A. and de Candia, P. and De Santana, E. F. and De Wever, O. and Del Portillo, H. A. and Demaret, T. and Deville, S. and Devitt, A. and Dhondt, B. and Di Vizio, D. and Dieterich, L. C. and Dolo, V. and Dominguez Rubio, A. P. and Dominici, M. and Dourado, M. R. and Driedonks, T. A. and Duarte, F. V. and Duncan, H. M. and Eichenberger, R. M. and Ekstrom, K. and El Andaloussi, S. and Elie-Caille, C. and Erdbrugger, U. and Falcon-Perez, J. M. and Fatima, F. and Fish, J. E. and Flores-Bellver, M. and Forsonits, A. and Frelet-Barrand, A. and Fricke, F. and Fuhrmann, G. and Gabrielsson, S. and Gamez-Valero, A. and Gardiner, C. and Gartner, K. and Gaudin, R. and Gho, Y. S. and Giebel, B. and Gilbert, C. and Gimona, M. and Giusti, I. and Goberdhan, D. C. and Gorgens, A. and Gorski, S. M. and Greening, D. W. and Gross, J. C. and Gualerzi, A. and Gupta, G. N. and Gustafson, D. and Handberg, A. and Haraszti, R. A. and Harrison, P. and Hegyesi, H. and Hendrix, A. and Hill, A. F. and Hochberg, F. H. and Hoffmann, K. F. and Holder, B. and Holthofer, H. and Hosseinkhani, B. and Hu, G. and Huang, Y. and Huber, V. and Hunt, S. and Ibrahim, A. G. and Ikezu, T. and Inal, J. M. and Isin, M. and Ivanova, A. and Jackson, H. K. and Jacobsen, S. and Jay, S. M. and Jayachandran, M. and Jenster, G. and Jiang, L. and Johnson, S. M. and Jones, J. C. and Jong, A. and Jovanovic-Talisman, T. and Jung, S. and Kalluri, R. and Kano, S. I. and Kaur, S. and Kawamura, Y. and Keller, E. T. and Khamari, D. and Khomyakova, E. and Khvorova, A. and Kierulf, P. and Kim, K. P. and Kislinger, T. and Klingeborn, M. and Klinke, D. J., 2nd and Kornek, M. and Kosanovic, M. M. and Kovacs, A. F. and Kramer-Albers, E. M. and Krasemann, S. and Krause, M. and Kurochkin, I. V. and Kusuma, G. D. and Kuypers, S. and Laitinen, S. and Langevin, S. M. and Languino, L. R. and Lannigan, J. and Lasser, C. and Laurent, L. C. and Lavieu, G. and Lazaro-Ibanez, E. and Le Lay, S. and Lee, M. S. and Lee, Y. X. F. and Lemos, D. S. and Lenassi, M. and Leszczynska, A. and Li, I. T. and Liao, K. and Libregts, S. F. and Ligeti, E. and Lim, R. and Lim, S. K. and Line, A. and Linnemannstons, K. and Llorente, A. and Lombard, C. A. and Lorenowicz, M. J. and Lorincz, A. M. and Lotvall, J. and Lovett, J. and Lowry, M. C. and Loyer, X. and Lu, Q. and Lukomska, B. and Lunavat, T. R. and Maas, S. L. and Malhi, H. and Marcilla, A. and Mariani, J. and Mariscal, J. and Martens-Uzunova, E. S. and Martin-Jaular, L. and Martinez, M. C. and Martins, V. R. and Mathieu, M. and Mathivanan, S. and Maugeri, M. and McGinnis, L. K. and McVey, M. J. and Meckes, D. G., Jr. and Meehan, K. L. and Mertens, I. and Minciacchi, V. R. and Moller, A. and Moller Jorgensen, M. and Morales-Kastresana, A. and Morhayim, J. and Mullier, F. and Muraca, M. and Musante, L. and Mussack, V. and Muth, D. C. and Myburgh, K. H. and Najrana, T. and Nawaz, M. and Nazarenko, I. and Nejsum, P. and Neri, C. and Neri, T. and Nieuwland, R. and Nimrichter, L. and Nolan, J. P. and Nolte-'t Hoen, E. N. and Noren Hooten, N. and O'Driscoll, L. and O'Grady, T. and O'Loghlen, A. and Ochiya, T. and Olivier, M. and Ortiz, A. and Ortiz, L. A. and Osteikoetxea, X. and Ostergaard, O. and Ostrowski, M. and Park, J. and Pegtel, D. M. and Peinado, H. and Perut, F. and Pfaffl, M. W. and Phinney, D. G. and Pieters, B. C. and Pink, R. C. and Pisetsky, D. S. and Pogge von Strandmann, E. and Polakovicova, I. and Poon, I. K. and Powell, B. H. and Prada, I. and Pulliam, L. and Quesenberry, P. and Radeghieri, A. and Raffai, R. L. and Raimondo, S. and Rak, J. and Ramirez, M. I. and Raposo, G. and Rayyan, M. S. and Regev-Rudzki, N. and Ricklefs, F. L.

and Robbins, P. D. and Roberts, D. D. and Rodrigues, S. C. and Rohde, E. and Rome, S. and Rouschop, K. M. and Rughetti, A. and Russell, A. E. and Saa, P. and Sahoo, S. and Salas-Huenuleo, E. and Sanchez, C. and Saugstad, J. A. and Saul, M. J. and Schiffelers, R. M. and Schneider, R. and Schoyen, T. H. and Scott, A. and Shahaj, E. and Sharma, S. and Shatnyeva, O. and Shekari, F. and Shelke, G. V. and Shetty, A. K. and Shiba, K. and Siljander, P. R. and Silva, A. M. and Skowronek, A. and Snyder, O. L., 2nd and Soares, R. P. and Sodar, B. W. and Soekmadji, C. and Sotillo, J. and Stahl, P. D. and Stoorvogel, W. and Stott, S. L. and Strasser, E. F. and Swift, S. and Tahara, H. and Tewari, M. and Timms, K. and Tiwari, S. and Tixeira, R. and Tkach, M. and Toh, W. S. and Tomasini, R. and Torrecilhas, A. C. and Tosar, J. P. and Toxavidis, V. and Urbanelli, L. and Vader, P. and van Balkom, B. W. and van der Grein, S. G. and Van Deun, J. and van Herwijnen, M. J. and Van Keuren-Jensen, K. and van Niel, G. and van Royen, M. E. and van Wijnen, A. J. and Vasconcelos, M. H. and Vechetti, I. J., Jr. and Veit, T. D. and Vella, L. J. and Velot, E. and Verweij, F. J. and Vestad, B. and Vinas, J. L. and Visnovitz, T. and Vukman, K. V. and Wahlgren, J. and Watson, D. C. and Wauben, M. H. and Weaver, A. and Webber, J. P. and Weber, V. and Wehman, A. M. and Weiss, D. J. and Welsh, J. A. and Wendt, S. and Wheelock, A. M. and Wiener, Z. and Witte, L. and Wolfram, J. and Xagorari, A. and Xander, P. and Xu, J. and Yan, X. and Yanez-Mo, M. and Yin, H. and Yuana, Y. and Zappulli, V. and Zarubova, J. and Zekas, V. and Zhang, J. Y. and Zhao, Z. and Zheng, L. and Zheutlin, A. R. and Zickler, A. M. and Zimmermann, P. and Zivkovic, A. M. and Zocco, D. and Zuba-Surma, E. K. (2018) 'Minimal information for studies of extracellular vesicles 2018 (MISEV2018): a position statement of the International Society for Extracellular Vesicles and update of the MISEV2014 guidelines', *J Extracell Vesicles,* 7(1), pp. 1535750.

Thulborn, S. J., Cane, J. L., Connolly, C., Borg, C., Moffitt, K. L., Ribeiro, D., Robb, C., Russell, R. E. K. and Bafadhel, M. (2020) 'Evaluating the sensitivity and specificity of NEATstik(R) technology compared to an activity-based immunoassay in sputum samples from participants with chronic obstructive pulmonary disease', *Eur Respir J.*

Thulborn, S. J., Mistry, V., Brightling, C. E., Moffitt, K. L., Ribeiro, D. and Bafadhel, M. (2019) 'Neutrophil elastase as a biomarker for bacterial infection in COPD', *Respir Res,* 20(1), pp. 170.

Timar, C. I., Lorincz, A. M., Csepanyi-Komi, R., Valyi-Nagy, A., Nagy, G., Buzas, E. I., Ivanyi, Z., Kittel, A., Powell, D. W., McLeish, K. R. and Ligeti, E. (2013) 'Antibacterial effect of microvesicles released from human neutrophilic granulocytes', *Blood,* 121(3), pp. 510-8.

Tirlapur, N., O'Dea, K. P. and Takata, M. (2016) 'Human Neutrophil-Derived Microvesicles Activate Pulmonary Endothelial Cells In An In Vitro Model Of Pulmonary Microvascular Inflammation', *American Journal of Respiratory and Critical Care Medicine,* 193.

Tokes-Fuzesi, M., Ruzsics, I., Rideg, O., Kustan, P., Kovacs, G. L. and Molnar, T. (2018) 'Role of microparticles derived from monocytes, endothelial cells and platelets in the exacerbation of COPD', *Int J Chron Obstruct Pulmon Dis,* 13, pp. 3749-3757.

Tosi, M. F., Stark, J. M., Smith, C. W., Hamedani, A., Gruenert, D. C. and Infeld, M. D. (1992) 'Induction of ICAM-1 expression on human airway epithelial cells by inflammatory cytokines: effects on neutrophil-epithelial cell adhesion', *Am J Respir Cell Mol Biol,* 7(2), pp. 214-21.

Toussaint, M., Jackson, D. J., Swieboda, D., Guedán, A., Tsrououktsoglou, T. D., Ching, Y. M., Radermecker, C., Makrinioti, H., Aniscenko, J., Bartlett, N. W., Edwards, M. R., Solari, R., Farnir, F., Papayannopoulos, V., Bureau, F., Marichal, T. and Johnston, S. L. (2017) 'Host DNA released by NETosis promotes rhinovirus-induced type-2 allergic asthma exacerbation', *Nat Med,* 23(6), pp. 681-691.

Touyz, R. M. (2005) 'Reactive oxygen species as mediators of calcium signaling by angiotensin II: implications in vascular physiology and pathophysiology', *Antioxid Redox Signal,* 7(9-10), pp. 1302-14.

Tramontano, A. F., O'Leary, J., Black, A. D., Muniyappa, R., Cutaia, M. V. and El-Sherif, N. (2004) 'Statin decreases endothelial microparticle release from human coronary artery endothelial cells: implication for the Rho-kinase pathway', *Biochem Biophys Res Commun,* 320(1), pp. 34-8.

Traves, S. L., Culpitt, S. V., Russell, R. E., Barnes, P. J. and Donnelly, L. E. (2002) 'Increased levels of the chemokines GROalpha and MCP-1 in sputum samples from patients with COPD', *Thorax,* 57(7), pp. 590-5.

Travis, J., Pike, R., Imamura, T. and Potempa, J. (1994) 'The role of proteolytic enzymes in the development of pulmonary emphysema and periodontal disease', *Am J Respir Crit Care Med,* 150(6 Pt 2), pp. S143-6.

Tregay, N., Begg, M., Cahn, A., Farahi, N., Povey, K., Madhavan, S., Simmonds, R., Gillett, D., Solanki, C., Wong, A., Maison, J., Lennon, M., Bradley, G., Jarvis, E., de Groot, M., Wilson, F., Babar, J., Peters, A. M., Hessel, E. M. and Chilvers, E. R. (2019) 'Use of autologous (99m)Technetium-labelled neutrophils to quantify lung neutrophil clearance in COPD', *Thorax,* 74(7), pp. 659-666.

Tsiligianni, I. G., Kosmas, E., Van der Molen, T. and Tzanakis, N. (2013) 'Managing comorbidity in COPD: a difficult task', *Curr Drug Targets,* 14(2), pp. 158-76.

Tuck, S. (2011) 'Extracellular vesicles: budding regulated by a phosphatidylethanolamine translocase', *Curr Biol,* 21(24), pp. R988-90.

Tuder, R. M., Petrache, I., Elias, J. A., Voelkel, N. F. and Henson, P. M. (2003) 'Apoptosis and emphysema: the missing link', *Am J Respir Cell Mol Biol,* 28(5), pp. 551-4.

Turturici, G., Tinnirello, R., Sconzo, G. and Geraci, F. (2014) 'Extracellular membrane vesicles as a mechanism of cell-to-cell communication: advantages and disadvantages', *Am J Physiol Cell Physiol,* 306(7), pp. C621-33.

Useckaite, Z., Ward, M. P., Trappe, A., Reilly, R., Lennon, J., Davage, H., Matallanas, D., Cassidy, H., Dillon, E. T., Brennan, K., Doyle, S. L., Carter, S., Donnelly, S., Linnane, B., McKone, E. F., McNally, P. and Coppinger, J. A. (2020) 'Increased extracellular vesicles mediate inflammatory signalling in cystic fibrosis', *Thorax,* 75(6), pp. 449-458.

Uysal, P. and Uzun, H. (2019) 'Relationship Between Circulating Serpina3g, Matrix Metalloproteinase-9, and Tissue Inhibitor of Metalloproteinase-1 and -2 with Chronic Obstructive Pulmonary Disease Severity', *Biomolecules,* 9(2).

Vachon, E., Martin, R., Plumb, J., Kwok, V., Vandivier, R. W., Glogauer, M., Kapus, A., Wang, X., Chow, C. W., Grinstein, S. and Downey, G. P. (2006) 'CD44 is a phagocytic receptor', *Blood,* 107(10), pp. 4149-58.

Vago, J. P., Tavares, L. P., Sugimoto, M. A., Lima, G. L., Galvão, I., de Caux, T. R., Lima, K. M., Ribeiro, A. L., Carneiro, F. S., Nunes, F. F., Pinho, V., Perretti, M., Teixeira, M. M. and Sousa, L. P. (2016) 'Proresolving Actions of Synthetic and Natural Protease Inhibitors Are Mediated by Annexin A1', *J Immunol,* 196(4), pp. 1922-32.

Van den Steen, P. E., Proost, P., Wuyts, A., Van Damme, J. and Opdenakker, G. (2000) 'Neutrophil gelatinase B potentiates interleukin-8 tenfold by aminoterminal processing, whereas it degrades CTAP-III, PF-4, and GRO-alpha and leaves RANTES and MCP-2 intact', *Blood,* 96(8), pp. 2673-81.

van Houwelingen, A. H., Weathington, N. M., Verweij, V., Blalock, J. E., Nijkamp, F. P. and Folkerts, G. (2008) 'Induction of lung emphysema is prevented by L-arginine-threonine-arginine', *Faseb j,* 22(9), pp. 3403-8.

Van Overveld, F. J., Demkow, U., Gorecka, D., De Backer, W. A. and Zielinski, J. (2006) 'Differences in responses upon corticosteroid therapy between smoking and non-smoking patients with COPD', *J Physiol Pharmacol,* 57 Suppl 4, pp. 273-82.

van Rijt, S. H., Keller, I. E., John, G., Kohse, K., Yildirim, A., Eickelberg, O. and Meiners, S. (2012) 'Acute cigarette smoke exposure impairs proteasome function in the lung', *Am J Physiol Lung Cell Mol Physiol,* 303(9), pp. L814-23.

Vandivier, R. W., Fadok, V. A., Hoffmann, P. R., Bratton, D. L., Penvari, C., Brown, K. K., Brain, J. D., Accurso, F. J. and Henson, P. M. (2002) 'Elastase-mediated phosphatidylserine receptor cleavage impairs apoptotic cell clearance in cystic fibrosis and bronchiectasis', *J Clin Invest,* 109(5), pp. 661-70.

Vandivier, R. W., Henson, P. M. and Douglas, I. S. (2006) 'Burying the dead: the impact of failed apoptotic cell removal (efferocytosis) on chronic inflammatory lung disease', *Chest,* 129(6), pp. 1673-82.

Vargas, A., Roux-Dalvai, F., Droit, A. and Lavoie, J. P. (2016) 'Neutrophil-Derived Exosomes: A New Mechanism Contributing to Airway Smooth Muscle Remodeling', *Am J Respir Cell Mol Biol,* 55(3), pp. 450-61.

Veranth, J. M., Cutler, N. S., Kaser, E. G., Reilly, C. A. and Yost, G. S.

Verjans, E., Kanzler, S., Ohl, K., Rieg, A. D., Ruske, N., Schippers, A., Wagner, N., Tenbrock, K., Uhlig, S. and Martin, C. (2018) 'Initiation of LPS-induced pulmonary dysfunction and its recovery occur independent of T cells', *BMC Pulm Med,* 18(1), pp. 174.

Vermeer, P. D., Denker, J., Estin, M., Moninger, T. O., Keshavjee, S., Karp, P., Kline, J. N. and Zabner, J. (2009) 'MMP9 modulates tight junction integrity and cell viability in human airway epithelia', *Am J Physiol Lung Cell Mol Physiol,* 296(5), pp. L751-62.

Vernooy, J. H., Bracke, K. R., Drummen, N. E., Pauwels, N. S., Zabeau, L., van Suylen, R. J., Tavernier, J., Joos, G. F., Wouters, E. F. and Brusselle, G. G. (2010) 'Leptin modulates innate

and adaptive immune cell recruitment after cigarette smoke exposure in mice', *J Immunol,* 184(12), pp. 7169-77.

Vernooy, J. H., Dentener, M. A., van Suylen, R. J., Buurman, W. A. and Wouters, E. F. (2001) 'Intratracheal instillation of lipopolysaccharide in mice induces apoptosis in bronchial epithelial cells: no role for tumor necrosis factor-alpha and infiltrating neutrophils', *Am J Respir Cell Mol Biol,* 24(5), pp. 569-76.

Vestbo, J., Anderson, W., Coxson, H. O., Crim, C., Dawber, F., Edwards, L., Hagan, G., Knobil, K., Lomas, D. A., MacNee, W., Silverman, E. K. and Tal-Singer, R. (2008) 'Evaluation of COPD Longitudinally to Identify Predictive Surrogate End-points (ECLIPSE)', *Eur Respir J,* 31(4), pp. 869-73.

Vestbo, J., Hurd, S. S., Agusti, A. G., Jones, P. W., Vogelmeier, C., Anzueto, A., Barnes, P. J., Fabbri, L. M., Martinez, F. J., Nishimura, M., Stockley, R. A., Sin, D. D. and Rodriguez-Roisin, R. (2013) 'Global strategy for the diagnosis, management, and prevention of chronic obstructive pulmonary disease: GOLD executive summary', *Am J Respir Crit Care Med,* 187(4), pp. 347-65.

Vlahos, R., Wark, P. A., Anderson, G. P. and Bozinovski, S. (2012) 'Glucocorticosteroids differentially regulate MMP-9 and neutrophil elastase in COPD', *PLoS One,* 7(3), pp. e33277.

Vogelmeier, C., Hubbard, R. C., Fells, G. A., Schnebli, H. P., Thompson, R. C., Fritz, H. and Crystal, R. G. (1991) 'Anti-neutrophil elastase defense of the normal human respiratory epithelial surface provided by the secretory leukoprotease inhibitor', *J Clin Invest,* 87(2), pp. 482-8.

Volckaert, T., Campbell, A. and De Langhe, S. (2013) 'c-Myc regulates proliferation and Fgf10 expression in airway smooth muscle after airway epithelial injury in mouse', *PLoS One,* 8(8), pp. e71426.

von Vietinghoff, S. and Ley, K. (2008) 'Homeostatic regulation of blood neutrophil counts', *Journal of immunology (Baltimore, Md. : 1950),* 181(8), pp. 5183-5188.

Voynow, J. A. and Rubin, B. K. (2009) 'Mucins, mucus, and sputum', *Chest,* 135(2), pp. 505-12.

Walmsley, S. R., Print, C., Farahi, N., Peyssonnaux, C., Johnson, R. S., Cramer, T., Sobolewski, A., Condliffe, A. M., Cowburn, A. S., Johnson, N. and Chilvers, E. R. (2005) 'Hypoxia-induced neutrophil survival is mediated by HIF-1alpha-dependent NF-kappaB activity', *J Exp Med,* 201(1), pp. 105-15.

Wang, H., Li, Z. Y., Liu, Y., Persson, J., Beyer, I., Möller, T., Koyuncu, D., Drescher, M. R., Strauss, R., Zhang, X. B., Wahl, J. K., 3rd, Urban, N., Drescher, C., Hemminki, A., Fender, P. and Lieber, A. (2011) 'Desmoglein 2 is a receptor for adenovirus serotypes 3, 7, 11 and 14', *Nat Med,* 17(1), pp. 96-104.

Wang, L., Luo, H., Chen, X., Jiang, Y. and Huang, Q. (2014) 'Functional characterization of S100A8 and S100A9 in altering monolayer permeability of human umbilical endothelial cells', *PLoS One,* 9(3), pp. e90472.

Wang, M., Wey, S., Zhang, Y., Ye, R. and Lee, A. S. (2009) 'Role of the unfolded protein response regulator GRP78/BiP in development, cancer, and neurological disorders', *Antioxid Redox Signal,* 11(9), pp. 2307-16.

Wang, Q., Teder, P., Judd, N. P., Noble, P. W. and Doerschuk, C. M. (2002a) 'CD44 deficiency leads to enhanced neutrophil migration and lung injury in Escherichia coli pneumonia in mice', *Am J Pathol,* 161(6), pp. 2219-28.

Wang, X., Moser, C., Louboutin, J. P., Lysenko, E. S., Weiner, D. J., Weiser, J. N. and Wilson, J. M. (2002b) 'Toll-like receptor 4 mediates innate immune responses to Haemophilus influenzae infection in mouse lung', *J Immunol,* 168(2), pp. 810-5.

Wark, P. A., Johnston, S. L., Moric, I., Simpson, J. L., Hensley, M. J. and Gibson, P. G. (2002) 'Neutrophil degranulation and cell lysis is associated with clinical severity in virus-induced asthma', *Eur Respir J,* 19(1), pp. 68-75.

Watanabe, J., Marathe, G. K., Neilsen, P. O., Weyrich, A. S., Harrison, K. A., Murphy, R. C., Zimmerman, G. A. and McIntyre, T. M. (2003) 'Endotoxins stimulate neutrophil adhesion followed by synthesis and release of platelet-activating factor in microparticles', *J Biol Chem,* 278(35), pp. 33161-8.

Weathington, N. M., van Houwelingen, A. H., Noerager, B. D., Jackson, P. L., Kraneveld, A. D., Galin, F. S., Folkerts, G., Nijkamp, F. P. and Blalock, J. E. (2006) 'A novel peptide CXCR ligand derived from extracellular matrix degradation during airway inflammation', *Nat Med,* 12(3), pp. 317-23.

Weiss, S. J. (1989) 'Tissue destruction by neutrophils', *N Engl J Med,* 320(6), pp. 365-76.

Weiss, S. J., Peppin, G., Ortiz, X., Ragsdale, C. and Test, S. T. (1985) 'Oxidative autoactivation of latent collagenase by human neutrophils', *Science,* 227(4688), pp. 747-9.

Wells, J. M., Parker, M. M., Oster, R. A., Bowler, R. P., Dransfield, M. T., Bhatt, S. P., Cho, M. H., Kim, V., Curtis, J. L., Martinez, F. J., Paine, R., 3rd, O'Neal, W., Labaki, W. W., Kaner, R. J., Barjaktarevic, I., Han, M. K., Silverman, E. K., Crapo, J. D., Barr, R. G., Woodruff, P., Castaldi, P. J. and Gaggar, A. (2018) 'Elevated circulating MMP-9 is linked to increased COPD exacerbation risk in SPIROMICS and COPDGene', *JCI Insight,* 3(22).

Wen, Y., Reid, D. W., Zhang, D., Ward, C., Wood-Baker, R. and Walters, E. H. (2010) 'Assessment of airway inflammation using sputum, BAL, and endobronchial biopsies in current and ex-smokers with established COPD', *Int J Chron Obstruct Pulmon Dis,* 5, pp. 327-34.

Werner, N., Wassmann, S., Ahlers, P., Kosiol, S. and Nickenig, G. (2006) 'Circulating CD31+/annexin V+ apoptotic microparticles correlate with coronary endothelial function in patients with coronary artery disease', *Arterioscler Thromb Vasc Biol,* 26(1), pp. 112-6.

WHO, W. H. O. (2017) *Chronic obstructive pulmonary disease (COPD)* COPD Factsheet. Available at: https://www.who.int/news-room/fact-sheets/detail/chronic-obstructive-pulmonary-disease-(copd) (Accessed: 15/04 2020).

Wisgrill, L., Lamm, C., Hartmann, J., Preissing, F., Dragosits, K., Bee, A., Hell, L., Thaler, J., Ay, C., Pabinger, I., Berger, A. and Spittler, A. (2016) 'Peripheral blood microvesicles secretion is influenced by storage time, temperature, and anticoagulants', *Cytometry A,* 89(7), pp. 663-72.

Wolf, P. (1967) 'The nature and significance of platelet products in human plasma', *Br J Haematol,* 13(3), pp. 269-88.

Wong, S. L., Demers, M., Martinod, K., Gallant, M., Wang, Y., Goldfine, A. B., Kahn, C. R. and Wagner, D. D. (2015) 'Diabetes primes neutrophils to undergo NETosis, which impairs wound healing', *Nat Med,* 21(7), pp. 815-9.

Wright, J. L., Tai, H., Wang, R., Wang, X. and Churg, A. (2007) 'Cigarette smoke upregulates pulmonary vascular matrix metalloproteinases via TNF-alpha signaling', *Am J Physiol Lung Cell Mol Physiol,* 292(1), pp. L125-33.

Yago, T., Shao, B., Miner, J. J., Yao, L., Klopocki, A. G., Maeda, K., Coggeshall, K. M. and McEver, R. P. (2010) 'E-selectin engages PSGL-1 and CD44 through a common signaling pathway to induce integrin alphaLbeta2-mediated slow leukocyte rolling', *Blood,* 116(3), pp. 485-94.

Yanai, M., Sekizawa, K., Ohrui, T., Sasaki, H. and Takishima, T. (1992) 'Site of airway obstruction in pulmonary disease: direct measurement of intrabronchial pressure', *J Appl Physiol (1985),* 72(3), pp. 1016-23.

Yende, S., Waterer, G. W., Tolley, E. A., Newman, A. B., Bauer, D. C., Taaffe, D. R., Jensen, R., Crapo, R., Rubin, S., Nevitt, M., Simonsick, E. M., Satterfield, S., Harris, T. and Kritchevsky, S. B. (2006) 'Inflammatory markers are associated with ventilatory limitation and muscle dysfunction in obstructive lung disease in well functioning elderly subjects', *Thorax,* 61(1), pp. 10-6.

Yi, X., Wang, Y. and Yu, F. S. (2000) 'Corneal epithelial tight junctions and their response to lipopolysaccharide challenge', *Invest Ophthalmol Vis Sci,* 41(13), pp. 4093-100.

Yıldız, A., Kaya, H., Ertaş, F., Oylumlu, M., Bilik, M. Z., Yüksel, M., Polat, N., Akil, M. A., Atılgan, Z. and Ulgen, M. S. (2013) 'Association between neutrophil to lymphocyte ratio and pulmonary arterial hypertension', *Turk Kardiyol Dern Ars,* 41(7), pp. 604-9.

Yipp, B. G., Petri, B., Salina, D., Jenne, C. N., Scott, B. N., Zbytnuik, L. D., Pittman, K., Asaduzzaman, M., Wu, K., Meijndert, H. C., Malawista, S. E., de Boisfleury Chevance, A., Zhang, K., Conly, J. and Kubes, P. (2012) 'Infection-induced NETosis is a dynamic process involving neutrophil multitasking in vivo', *Nat Med,* 18(9), pp. 1386-93.

Yokohori, N., Aoshiba, K. and Nagai, A. (2004) 'Increased levels of cell death and proliferation in alveolar wall cells in patients with pulmonary emphysema', *Chest,* 125(2), pp. 626-32.

Yoshida, K., Kondo, R., Wang, Q. and Doerschuk, C. M. (2006) 'Neutrophil cytoskeletal rearrangements during capillary sequestration in bacterial pneumonia in rats', *Am J Respir Crit Care Med,* 174(6), pp. 689-98.

Youn, Y.-J., Shrestha, S., Kim, J.-K., Lee, Y.-B., Lee, J. H., Hur, K., Mali, N. M., Nam, S.-W., Kim, S.-H., Song, D.-K., Jin, H. K., Bae, J.-s. and Hong, C.-W. (2019) 'Neutrophil-derived extracellular vesicles: proinflammatory trails and anti-inflammatory microvesicles', *bioRxiv*, pp. 583435.

Young, R. P., Hopkins, R. and Eaton, T. E. (2007) 'Forced expiratory volume in one second: not just a lung function test but a marker of premature death from all causes', *Eur Respir J,* 30(4), pp. 616-22.

Yu, Q. and Stamenkovic, I. (1999) 'Localization of matrix metalloproteinase 9 to the cell surface provides a mechanism for CD44-mediated tumor invasion', *Genes Dev,* 13(1), pp. 35-48.

Zariffard, M. R., Anastos, K., French, A. L., Munyazesa, E., Cohen, M., Landay, A. L. and Spear, G. T. (2015) 'Cleavage/alteration of interleukin-8 by matrix metalloproteinase-9 in the female lower genital tract', *PLoS One,* 10(1), pp. e0116911.

Zeki, A. A., Schivo, M., Chan, A., Albertson, T. E. and Louie, S. (2011) 'The Asthma-COPD Overlap Syndrome: A Common Clinical Problem in the Elderly', *J Allergy (Cairo),* 2011, pp. 861926.

Zhang, D., Lee, H., Wang, X., Groot, M., Sharma, L., Dela Cruz, C. S. and Jin, Y. (2019) 'A potential role of microvesicle-containing miR-223/142 in lung inflammation', *Thorax,* 74(9), pp. 865-874.

Zhang, M., Xu, C., Jiang, L. and Qin, J. (2018) 'A 3D human lung-on-a-chip model for nanotoxicity testing', *Toxicol Res (Camb),* 7(6), pp. 1048-1060.

Zhao, F. and Klimecki, W. T. (2015) 'Culture conditions profoundly impact phenotype in BEAS-2B, a human pulmonary epithelial model', *J Appl Toxicol,* 35(8), pp. 945-51.

Zhou, Y., Zou, Y., Li, X., Chen, S., Zhao, Z., He, F., Zou, W., Luo, Q., Li, W., Pan, Y., Deng, X., Wang, X., Qiu, R., Liu, S., Zheng, J., Zhong, N. and Ran, P. (2014) 'Lung function and incidence of chronic obstructive pulmonary disease after improved cooking fuels and kitchen ventilation: a 9-year prospective cohort study', *PLoS Med,* 11(3), pp. e1001621.

Zorzetto, M., Russi, E., Senn, O., Imboden, M., Ferrarotti, I., Tinelli, C., Campo, I., Ottaviani, S., Scabini, R., von Eckardstein, A., Berger, W., Brandli, O., Rochat, T., Luisetti, M. and Probst-Hensch, N. (2008) 'SERPINA1 gene variants in individuals from the general population with reduced alpha1-antitrypsin concentrations', *Clin Chem,* 54(8), pp. 1331-8.

Zou, W., Zou, Y., Zhao, Z., Li, B. and Ran, P. (2013) 'Nicotine-induced epithelial-mesenchymal transition via Wnt/beta-catenin signaling in human airway epithelial cells', *Am J Physiol Lung Cell Mol Physiol,* 304(4), pp. L199-209.

Zwaal, R. F., Comfurius, P. and Bevers, E. M. (2005) 'Surface exposure of phosphatidylserine in pathological cells', *Cell Mol Life Sci,* 62(9), pp. 971-88.